ISAS - INTERNATIONAL SCHOOL FOR ADVANCED STUDIES

Statistical Properties of the Large–Scale Distribution of Matter and Velocity Fields in the Universe

Doctor Philosophiæ

CANDIDATE

Paolo Catelan

SUPERVISOR

Prof. Dennis W. Sciama

Academic Year 1992-1993

Astrophysics Sector

TRIESTE

SISSA - SCUOLA INTERNAZIONALE SUPERIORE DI STUDI AVANZATI

TRIESTE
Strada Costiera 11

a Elena

Le Stelle

Si suona il flauto per dichiarare l'amore o per annunziare il ritorno dei cacciatori. Gli indios waiwai convocano col flauto i loro invitati. Per i tukano il flauto piange; e per i kalina il flauto parla, mentre il corno grida.

Sulle rive del Río Negro, il flauto assicura agli uomini il potere. I flauti sacri sono tenuti nascosti e ogni donna che si avvicina merita la morte.

In tempi molto remoti, quando le donne possedevano i flauti sacri, gli uomini raccoglievano la legna e l'acqua e preparavano il pane di manioca.

Narrano gli uomini che il Sole si indignò alla vista di un mondo nel quale erano le donne a regnare. Il Sole scese nella selva e fecondò una vergine, spruzzandole succo di foglie.

Così nacque Jurupari.

Jurupari rubò i flauti sacri e li consegnò agli uomini. Insegnò loro a nasconderli e a difenderli e a celebrare feste rituali senza donne. Raccontò loro, inoltre, i segreti che dovevano trasmettere ai figli maschi sussurrandoli all'orecchio.

Quando sua madre scoprì il nascondiglio dei flauti sacri, Jurupari la condannò a morte; e con i brandelli del suo corpo fece le stelle del cielo.

Eduardo Galeano

Memoria del Fuoco

Abstract

The study of the statistical distribution of the matter and velocity fields in the universe may be a way to address fundamental issues such as the origin and the formation of structures on large scales.

Most theories of galaxy formation assume that galaxies and other large–scale structures grew by gravitational instability from initially small stochastic perturbations to the energy density of the Universe. The simplest and most usually accepted hypothesis is that the very early distribution is Gaussian. In such a case, the higher–order connected correlation functions are zero. However, even if the primordial fluctuations are Gaussian, the non–linear time evolution will ensure that the mass density fluctuations become highly non–Gaussian. We analyse the dependence of the gravitationally–induced skewness and kurtosis of density and velocity fields from the initial power spectrum of fluctuation. We show that by accurate measurements of skewness and kurtosis it is possible to deduce important informations about the primordial spectral index n and then to constrain the mechanism for the generation of cosmological large–scale structure.

However, the galaxy formation is such a complicated process that it is extremely difficult to deduce the correct form of the matter distribution from the observed galaxy distribution. In models of biased galaxy formation, the luminous objects like galaxies and clusters do not fairly trace the underlying mass distribution. In most of biased scenarios, one is able to relate luminous matter and dark matter by involving a very specific form of bias.

We consider a new weighted biasing scheme for galaxy clustering. This differs from previous treatments in the fact that the biased density field coincides with the background mass–density whenever the latter exceeds a given threshold value. Calculations of the correlation properties of the high–density regions are performed. We explain how different classes of objects could be biased in different ways with respect to the underlying density distribution but still have $b = 1$. This could also be the reason why the correlation function of galaxies in groups does not differ substantially from the correlation function of all galaxies.

We have also reanalysed the QDOT survey in order to investigate the convergence properties of the estimated dipole and the consequent reliability of the derived value of density parameter $\Omega_o^{0.6}/b$. We find that there is no compelling evidence that the QDOT dipole has converged within the limits of reliable determination and completeness.

Acknowledgments

Cosmology is not a science in which one can enter alone.

It is a pleasure to acknowledge my supervisor Dennis Sciama for his help, guidance and financial support throughout these three years at SISSA–ISAS. Without Dennis' patience and willingness, it would have been impossible for me to conclude this thesis.

I am very grateful to Francesco Lucchin and Sabino Matarrese. Since many years Francesco and Sabino have continuously inspired me and have followed my efforts in trying to understand cosmology.

There are no words to thank (Zio)Lauro Moscardini, with whom I collaborated during the last year: Lauro's pignatta is boiling without interrumption since many months to steal some nontrivial numbers from my (wrong?) integral expressions.

Manolis Plionis personally followed my work at SISSA since the beginning, and during his militar service by telephone, calling from Greece. Manolis maked me convinced that to measure Ω_0 is a bit difficult!

My gratitude to Robert "Bob" Scherrer for his very kind hospitality during my visit at the Ohio State University; many of the ideas explored in this work have originated during (rapid) conversations with him.

The scientific collaboration with Peter Coles has been very fruitful and interesting. I hope to continue working with him in England. Billiard–tables are waiting there.

Enzo Branchini has been involved continuosly in my research activity. During our discussions, his deep cosmological intuition always yielded remarkable insights about my calculations, that sometime I do not understand myself.

Many other people divided with me SISSA space–time (and often OSMIZA space–time): Ugo Aglietti, Josè Carlos de Araujo, Marco Atzori, Elsye and Zyomara Carphio

Mariño, Miguel Chavez de Agostino, Stefano Borgani, Li–Cai Deng, Pietro Donatis, Annamaria Ferrari, Gaetano "Profesor" Fiore, Francesco Haardt, Giona di Giacomi, Luigi Guzzo, Bruce Hoeneisen, Aurora, Daniele, Francesca and Antonio Lanza, Hugo Morales Tecotl, Ornella Pantano, Joseph "Joe" Pesce, Elena "πan" Pian, Antonio Riotto, Rita Sambruna, Francesca and Giuseppe "Bepi" Tormen, Aldo Treves, Riccardo Valdarnini, thank you all for everything.

Thanks to George Efstathiou for inviting me to work at Oxford for the next two years.

GRACIAS to José "Pepe" Guillermo Lorenzana .

Gisselle Carphio Mariño has been really a compañera during the last years: this work is hers too.

CONTENTS

INTRODUCTION

In this Thesis I review some topics of modern cosmology I am interested in; I also present some original results about the large–scale distribution of matter and velocity fields in the Universe. The layout of this work is as follows.

In Chapter I, I summarize the fundamental assumptions of physical cosmology, then fixing basic concepts and notation. The link between matter fluctuations and metric fluctuations in Newtonian approximation and the role of the comoving coordinates in describing the dynamics of particles in an expanding Universe are discussed. The Newtonian theory is accurate for cosmological perturbations with sizes that are very much smaller than the Hubble radius.

Most theories of galaxy formation assume that galaxies and other large–scale structures grew by gravitational instability from initially small *stochastic* perturbations δ to the energy density of the Universe. An important point is that no cosmological theory attempts to predict the initial conditions $\delta(\mathrm{x}, t)$ exactly. A "complete" theory might predict e.g. the mean abundance of clusters and of galaxies and the mean distance of galaxies, but not the specific locations of galaxies and clusters in our Universe. In other words, theories predict only the *statistical* properties of $\delta(\mathrm{x}, t)$, in particular the *spatial* statistical properties.

The statistical predictions about large scale structures in the Universe are commented in Chapter II, where the concept of "random field" is introduced. The Gaussian and non–Gaussian nature of primordial density distribution are compared. Technical aspects of Gaussian random fields can be found in Appendix A, while the strong theoretical reasons for analyzing generic non–Gaussian density fields are reviewed in Section II.4.

Quantifying the large scale structures of the Universe is a difficult task and a variety of techniques have been developed to approach it. In Chapter III, I describe in some detail the most commonly used statistical measurements of galaxy clustering, the correlation functions and their Fourier transform, the power spectra; if someone is interested in, the cumulant expansion theorem is presented in Appendix B.

The most largely accepted scenario to approach the structure formation is the so called gravitational instability scenario, which treats essentially noise amplification, ie. linear (small) perturbations at some early time grow to non linearity under their own self gravitation. I describe in Chapter IV the fundamental equations governing the growth of matter perturbations. Linear solutions are discussed in detail. The Eulerian and Lagrangian formulations of the dynamical evolution of density fluctuations are reviewed. The Zel'dovich approximation is derived directly from the equations of motion in Lagrangian framework, but a formulation in terms of the gravitational potential is also presented.

Measuring the mass content of the Universe is one of the most important tasks in observational cosmology, but it is not easy at all. In Chapter V, I review dynamical techniques for estimating the density parameter Ω_o. The missing mass problem and non baryonic universes are discussed.

In Appendix D, the QDOT survey is analysed in order to investigate the convergence properties of the estimated dipole and the consequent reliability of the derived value of Ω_o. It is found that there is no compelling evidence that the QDOT dipole has converged within the limits of reliable determination and completeness. Therefore the value of Ω_o derived by Rowan-Robinson *et al.* (1990) should be considered only as an upper limit. Furthermore, it is found strong evidence that the shell between 140 and 160 h^{-1} Mpc does contribute significantly to the total dipole anisotropy and therefore to the motion of the Local Group with respect to the Cosmic Microwave Background. This shell contains the Shapley concentration, but it is argued that this concentration itself cannot explain all the gravitational acceleration

produced by it; there must exist a coherent anisotropy which includes this structure, but extends greatly beyond it. With the QDOT data alone, it is impossible to determine precisely the magnitude of any such anisotropy but any contribution to the Local Group motion from large scales would favour a value of $\Omega_o^{0.6}/b_{IRAS} \leq 0.6$, smaller than previous extimates based on IRAS galaxies; such a result would be consistent with the dipole measured from samples of rich clusters, which are much more complete at large depths (Plionis, Coles & Catelan 1993).

Until fairly recently cosmologists tacitly assumed that the luminous matter traces the matter distribution ie. the mass-to-light ratios M/L of different cosmic structures were the same. However, there is a great deal of observational and theoretical evidence that this is not the case (Chapter V).

Such an evidence leads in a natural way to the concept of " biased" galaxy formation i.e. galaxy formation (or, more in general, cosmic structure formation) occuring in such a way that galaxies do not fairly trace the underlying mass distribution. In most biased scenarios, one is able to relate luminous matter and "dark matter" by involving a very specific form of bias, although such a prescription is not unique. In Chapter VI, I talk about the motivations for biasing the galaxy distribution, possible physical mechanisms and the types of bias expected in various cosmological scenarios.

Since the Kaiser's suggestion (1984) that the prominent structures in the Universe formed in correspondence of the high peaks of the primordial fluctuation field, the biased approach characterized the way with which cosmologists analyze the structure formation in the Universe, although the relation between light and matter has become sometimes obscure. In Section VI.9 I propose and explore a new "weighted" biasing scheme for galaxy clustering. Contrary to previous treatments, the biased density field coincides with the background mass–density whenever the latter exceeds a given threshold. All the observables in this approach can be continuously defined down to the unbiased case. The two-point function of biased objects – computed for underlying Gaussian density fluctuations – turns out to be quite different from that obtained in previous treatments even at large distances and

for high thresholds. There is some physical motivation for this scheme and it is in better accord with intuitive ideas than models based on the Kaiser (1984) analysis of the clustering of rich clusters. I explain how different classes of object could be biased in different ways with respect to the underlying density distribution but still have $b = 1$. I also show that if one applies the weighted scheme consistently a weak dependence of b upon density can be implied. This could also be the reason why the correlation function of galaxies in groups does not differ substantially from the correlation function of all galaxies (Catelan *et al.* 1993; Appendix E).

Developing or applying (semi–) analytical approaches to the clustering of the "peaks" of the density fluctuation field has been one of the main source of cosmological papers during the last decade. The Chapter VII is essentially divided in two parts. In the first part we review how to calculate, in the framework of the Kaiser biased model of galaxy clustering (Kaiser 1984), exact formulae for the probability that mass density – at a randomly given point – lies above a certain threshold and for the N–point correlation functions among the points above the same threshold, in the most general case of non–Gaussian underlying matter distribution (Matarrese, Lucchin & Bonometto 1986). Even though the final expressions are rather difficult to handle directly, it is shown that in the high–threshold limit, which is the limit of physical interest, fairly simple expressions for the N–point excursion correlation functions may be obtained. These relations generalyze the results obtained by Politzer & Wise (1984) and Grinstein & Wise (1986) for underlying Gaussian density distributions. We restrict the analysis to the excursion regions above a fixed threshold, since the statistical description is much more simple. Rigorously, in the biased theory the observed objects coincide with density local maxima (peaks) exceeding some threshold. We consider this more complicated case in the second part of the Chapter VII. The complications arise because the field quantities that must be specified at a point $\mathbf{r}_{pk}$ for it to be the site of a peak of the (smoothed) density field δ_R are the gradient $\nabla\delta_R$ which must vanish, and the second derivative tensor $\nabla\nabla\delta_R$ which must be negative definite. Peak theory applied to cosmological

models has been first developed by Doroshkevich (1970) and Doroshkevich and Shandarin (1978a, b) for models with a natural filter such as adiabatic hot dark matter models in which large structures form first (and galaxies form out of a highly nonlinear fragmentation process), and for hierarchical models such as the cold dark matter model by Peacock and Heavens (1985) and Bardeen et al. (1986). We review how to derive fundamental statistics such as the mean number peak density and the genus of the density countours in the case of underlying Gaussian density fields. We shall demonstrate that in the very high threshold limit the density profiles are simply connected and in a one–to–one correspondence with the local maxima of the background Gaussian density field. A generalization of these Gaussian results to the non–Gaussian case may be found in Appendix C of the thesis (Catelan, Lucchin & Matarrese 1988a, b).

The linear growth laws discussed in Chapter IV hold until $\delta \approx 1$. When the perturbation amplitudes approach unity, nonlinear gravitational effects become important. The evolution of linear perturbations of FRW models has been discussed by a large number of authors and little of this material is controversial. In contrast, the evolution of non-linear cosmological perturbations is still poorly understood despite the existence of a large literature on the topic. After reviewing the recent literature on the subject, though this is changing too rapidly to make such an enterprise worthwile, I analyze in Chapter VIII second and third perturbative order equations of motion for density and velocity fields. New cosmological observables are considered, like skewness and kurtosis of density and velocity fields.

Gaussian fields have zero skewness by definition, but the presence of a non-zero skewness in the e.g. IRAS data, does not necessarily imply non-Gaussian initial conditions: even if the initial probability distribution of the mass density contrast δ is Gaussian then symmetric, an asymmetry will inevitably develop later, as a second order effect, under the influence of gravity. Indeed, δ can grow indefinitely in regions where it was initially positive, whereas in the voids it can never decrease below -1.

I review how gravity can induce skewness in an initially Gaussian distribution, computing the second order solutions of the equations of motion for matter. Next, the skewness in density field, assumed Gaussian at early time (e.g. at recombination), is calculated, also suggesting how to work out the skewness in the more general case in which δ is non–Gaussian at the beginning. I discuss how the observations can be used to distinguish "conventional" models from an intrinsically non–Gaussian alternative.

In Section VIII.3 it is studied the non–linear growth of the excess kurtosis parameter of the smoothed density fluctuation field δ, namely

$$S_4 \equiv \frac{\langle \delta^4 \rangle - 3\langle \delta^2 \rangle^2}{\langle \delta^2 \rangle^3} ,$$

in an Einstein–de Sitter universe. I assume Gaussian primordial density fluctuations with scale–free power spectrum $P(k) \propto k^n$ and analyze the dependence of S_4 on primordial spectral index n, after smoothing with a Gaussian filter. I apply up to third–order perturbative calculations. As already known for the skewness ratio S_3, the kurtosis parameter is a *decreasing function* of n, both in exact perturbative theory and in the Zel'dovich approximation. The parameter S_4 provides a powerful statistics to test different cosmological scenarios (Catelan & Moscardini 1993a; Appendix F).

In a similar fashion, in Section VIII.4, I discuss the non–linear growth of the kurtosis of the smoothed peculiar velocity field (along an arbitrary direction $\widehat{\alpha}$), namely the parameter

$$S_{4,v} \equiv \frac{\langle v_\alpha^4 \rangle - 3\,\langle v_\alpha^2 \rangle^2}{\langle v_\alpha^2 \rangle^2\,\langle \delta^2 \rangle} ,$$

in an Einstein–de Sitter universe. Again, I assume Gaussian primordial density fluctuations δ with scale–free power spectrum $P(k) \propto k^n$ and analyze the dependence of $S_{4,v}$ on primordial spectral index n, after smoothing with a Gaussian filter. According to very preliminary results, the velocity kurtosis is a *decreasing function* of n in exact perturbative theory but it is constant and consistent with zero in the Zel'dovich approximation (Catelan & Moscardini 1993b; Appendix G).

The Zel'dovich approximation breaks down after the first–generation of collapsing objects since it forces that particles sail through pancakes and clusters unperturbed. This failure is particularly problematic for modelling hierarchical scenarios, in which the primordial density fluctuations have power on all scales and small structures collapse early (see Section IV.4). In the Chapter IX , I review a particular implementation of the Zel'dovich approximation, namely the *adhesion approximation* where an artificial addition of a tiny amount of viscosity to the Euler equation – converting it into a three–dimensional generalization of the well known Burgers' equation – stops the matter particles at the pancakes. Furthermore, after reviewing the Frozen–Flow approximation (FFA), we anticipate the first few calculations leading to a new approximation scheme, named *Local–Flow approximation* – LFA – (Catelan *et al.* 1993a). In this approximation the peculiar velocity field $\mathbf{u}$ is considered up to the second–order contribution as given by the standard perturbative theory, expanding in series the gravitational potential ϕ and the velocity potential Φ. An advantage of this approach is that we can easily work out the higher order velocity contributions $\mathbf{v}^{(n)}$ in a manifestly irrotational form in Eulerian configuration space [all the previous irrotational expressions for $\mathbf{v}^{(n)}$ were obtained in Fourier space (see Goroff *et al.* 1986)]. The importance of having explicit irrotational expressions for the velocity field at any perturbative order lies on the fact that a collisionless gravitating fluid cannot generate vorticity (before orbit mixing) and that the conservation of circulation is applicable well beyond the linear regime. In LFA one still solves exactly the continuity equation, but the local flow is no longer stationary, since the local acceleration is taken into account. Considering a dynamical instead of a stationary flow is expected to partially solve the lack of merging processes of the first generation of pancakes which is the main difficulty of the FFA.

Finally, in Appendix H, I anticipate very preliminary analysis of the large–scale velocity field in a special class of intrinsically non–Gaussian models, in which the initial inhomogeneities are stimulated by a primordial population of *seeds*, e.g. cosmic string loops (e.g. Vilenkin 1985) or global textures (Turok 1989), and the final linear matter fluctuations

may not be described by a Gaussian distribution. A method to detect the non–Gaussian behaviour of the matter distribution is to examine the large–scale peculiar velocity field, which is, in linear regime i.e. large scales, directly related to the density field (Peebles 1980). The problem has been addressed by Scherrer (1992). Here we extend the previous analysis of Scherrer.

In particular, we calculate the skewness of the parallel component of the velocity difference distribution $p[v_{\|}(\mathbf{x}_1) - v_{\|}(\mathbf{x}_2)]$ for global textures in an $\Omega = 1$ Cold Dark Matter (CDM) model, demonstrating that the distribution of velocity differences is a good method for detecting intrinsic non–Gaussian behaviour (Catelan & Scherrer 1993).

To avoid an excess of mathematical contorsions in the text, technical appendices may be found at the end of some chapter. Furthermore, I prudently marked with a star ($\star$) those chapters or sections I consider particularly cumbersome, which may be possibly omitted in a first reading.

CHAPTER I

Background Cosmology

We summarize here the fundamental assumptions of standard cosmology:

- The observable part of our Universe may be approximated as part of a homogeneous and isotropic Friedmann–Robertson–Walker (FRW) universe. The assumptions of large–scale homogeneity and isotropy is often called the *COSMOLOGICAL PRINCIPLE.*
- To describe the evolution and structure of space time we apply General Relativity Theory, mainly in its Newtonian approximation.
- We live in a *perturbed* FRW Universe: the metric fluctuations are small within our horizon, although density fluctuations are not necessarily small.

Three main tested observational facts support the so called Hot "Big Bang" Cosmological model (Gamow 1946):

- THE UNIVERSE IS EXPANDING. During the thirties, Hubble discovered that (distant) galaxies are receding from us according to the Hubble's law

$$v = Hr \ , \tag{1.1}$$

where v is the recession velocity, H is the Hubble constant, r is the estimated distance of the galaxy. This expansion corresponds to a true geometrical space–time expansion (see Hubble 1934; 1936).

- THE MICROWAVE BACKGROUND. Penzias and Wilson (1965) discovered the cosmic microwave background radiation (CBR, MWB), measured as an excess antenna temperature in the first experimental studies for the Telstar project. Soon it was realized that this could be relic blackbody radiation left by a primeval fire ball (Dicke *et al.* 1965). This has been definitively confirmed by the recent measurement of COBE (Mather *et al.* 1990; Smoot *et al.* 1991).

- LIGHT ELEMENT COSMIC ABUNDANCES. The hot big bang model predicts the nucleosynthesis of the light elements (e.g. Wagoner 1973) with abundances which are remarkably close to the estimates obtained from observations (Yang *et al.* 1984; Walker *et al.* 1991).

The synthesis of the light elements is determined by (nuclear) events occuring in the epoch from $\sim 1\,s$ to $\sim 1000\,s$ in the history of the Universe, when temperatures varied from $\sim 10^{10}\,K$ or higher ($\gtrsim 1\,MeV$) to $\sim 10^{9}\,K$ or higher ($\gtrsim 0.1\,MeV$): thus the observed abundances offer a probe of the Universe at epoch far earlier than those probed by CBR ($t \sim 10^{5}\,yr$; $T \sim 10^{4}\,K \sim 1\,eV$) (see e.g. Weinberg 1972).

The zeroth–order Hubble expansion is described by the cosmic scale factor $a(t)$ that satisfies the Friedmann equation

$$H^2 \equiv \left(\frac{\dot{a}}{a}\right)^2 = \frac{8\pi}{3} G\,\rho_b(t) - \frac{c^2 k}{a^2}\,. \tag{1.2}$$

Here $\rho_b(t)$ is the background total mean density in the Universe; k is the curvature constant. The Hubble parameter has present value $H_\circ = 100\,h$ km/s/Mpc, where almost certainly $0.5 \lesssim h \lesssim 1$; several recent determinations favor $h \approx 0.8$ (Jacoby, Ciardullo & Ford 1990; Tonry 1991; see Huchra 1992). The present value of a is indicated by $a_\circ \equiv a(t_\circ)$. The Eq.(1.2) is the most important equation in cosmology; solving for k we get

$$k = (\Omega_\circ - 1) c^{-2} H_\circ^2 a_\circ^2\,, \tag{1.3}$$

where $\Omega_o \equiv \Omega(t_o)$, $\Omega(t)$ being the density parameter, defined by

$$\Omega(t) \equiv \frac{8\pi G\,\rho_b(t)}{3\,H(t)^2} \equiv \frac{\rho_b(t)}{\rho_{cr}(t)}\,, \tag{1.4}$$

and ρ_{cr} is called the critical density. $\rho_b(t)$ is the sum of the matter, radiation and vacuum energy contributions. It satisfies the energy equation

$$\frac{d\rho_b}{dt} = -3\left(\rho_b + \frac{p_b}{c^2}\right)\frac{\dot{a}}{a}\,, \tag{1.5}$$

where p is the pressure (subscripts refer to the background). The equation of state $p = p(\rho)$ relates p versus ρ (see Weinberg 1972). The Eqs.(1.2), (1.5) together with the equation of state $p = p(\rho)$ allow to calculate the time evoluton of the scale factor $a(t)$.

If the Universe is dominated by non relativistic matter, for which $p \ll \rho c^2$, like in the late stages of the expansion of the Universe, when the matter is the only dynamically important constituent, its adiabatic expansion dilutes the mass density inversely with volume ie.

$$\rho_b = \rho_o \left(\frac{a}{a_o}\right)^{-3} \qquad \text{(matter era)}\,, \tag{1.6}$$

where

$$\rho_o \equiv 1.88 \times 10^{-29}\,\Omega_o\,h^2\,g\,cm^{-3} \tag{1.7}$$

is the present mean density; Ω_o lies in the range (see e.g. Peebles 1986)

$$0 < \Omega_o < \text{few}\,. \tag{1.8}$$

Some preliminary aspects of the evolution of the model might be noted; for instance from (1.2) and (1.6) we get

$$\frac{1-\Omega(t)}{\Omega(t)} = \frac{a(t)}{a_o}\,\frac{1-\Omega_o}{\Omega_o}\,, \tag{1.9}$$

therefore we see that $\Omega = 1$ is an unstable fixed point during the evolution of the Universe: as $a(t)$ increases, Ω increasingly deviates from $\Omega = 1$; if $\Omega \equiv 1$ at the beginning, then $\Omega_o = 1$ (a very interesting kinematical analysis of the behaviour of the parameter $\Omega(t)$ is given in Madsen & Ellis (1988)). The Einstein–de Sitter model has $\Omega = 1$ and $p = 0$ (= Λ = cosmological constant); in such a model we have

$$a \propto t^{2/3}\,, \tag{1.10}$$

$$6\pi G\rho_b t^2 = 1\ , \tag{1.11}$$

that we shall use often. The Einstein–de Sitter model is a favored model among cosmologists, above all the inflationary ones (Guth 1981): in fact inflation predicts $\Omega = 1$ with great precision (however, see Ellis 1988); anyway, both the open ($\Omega_\circ < 1$) and closed ($\Omega_\circ > 1$) very early universes expand like the Einstein–de Sitter solution, $a \propto t^{2/3}$.

The curvature constant k appears in the expression of the Robertson–Walker metric (RW); it can be obtained directly starting from the homogeneity and isotropy hypothesis (see Weinberg 1972)

$$\begin{aligned} ds^2 &= g_{\mu\nu}\, dx^\mu\, dx^\nu \\ &= c^2dt^2 - a^2\left[(1-kx^2/c^2)^{-1}dx^2 + x^2(d\theta^2 + \sin^2\theta d\varphi^2)\right]\ . \end{aligned} \tag{1.12}$$

The coordinates x, θ and φ are comoving, fixed to fluid elements: we obtain a proper distance r multiplying the comoving distance x by the scale factor $a(t)$.

The effects of curvature are negligible in correspondence of scales much smaller than the Hubble length $cH_\circ^{-1} = 3000\,h^{-1}Mpc$, which is a convenient measure of the distance to the horizon (about the distance that free photons have travelled since the big bang): because of (1.3) and (1.8), the condition $r \ll cH_\circ^{-1}$ implies $kx^2/c^2 \ll 1$; typically the Universe is well sampled only on scales much smaller than the Hubble length (an all-sky redshift survey of galaxies detected by IRAS has been used to map the Universe out to $\sim 140\,h^{-1}Mpc$ (Saunders *et al.* 1991)), and if we restrict ourselves to structures much smaller than this, the curvature term may be neglected in the RW metric (1.12) (but not necessarily in the dynamical Friedmann equation); the RW line element reduces to the simplified form $ds^2 = c^2dt^2 - a^2\, d\mathbf{x}\cdot d\mathbf{x}$, $\mathbf{x} = (x_1,\ x_2,\ x_3)$ being Cartesian comoving coordinates.

The proper position will be denoted by

$$\mathbf{r} = a(t)\,\mathbf{x}\ . \tag{1.13}$$

Sometimes in cosmology the *conformal time* is introduced

$$\tau \equiv \int_0^t \frac{dt}{a(t)} \,. \tag{1.14}$$

Transforming t in τ reduces (1.12) to a conformally equivalent metric ie.

$$ds^2 = a(\tau)^2 \left[c^2 d\tau^2 - (1 - kx^2/c^2)^{-1} dx^2 - x^2(d\theta^2 + \sin^2\theta d\varphi^2)\right] \,, \tag{1.15}$$

which is flat in the limit of small scales ($kx^2/c^2 \ll 1$); adopting this metric, the equations of motion for the matter have a very simple form, as we shall see. We indicate there τ by the usual symbol t, unless differently indicated.

During the matter–dominated epoch (post–recombination universe: below $4000\,K$ the atomic H is almost completely formed) the large–scale structures are developing, so the fluctuations in the background radiation (and any other possible relativistic components, as neutrinos) are negligible with respect to the non relativistic density fluctuations, the only dynamically significant; these load to fluctuations in the metric, which can be described just by one scalar field, the Newtonian gravitational potential ϕ; we know indeed that, solving the Einstein equations to first order in ϕ/c^2 we get $g_{00} = 1 + 2\,\phi/c^2$ (see e.g. Weinberg 1972); in the conformal Newtonian gauge we have

$$ds^2 = a(\tau)^2 \left[(1 + 2\,\phi/c^2)\, c^2 d\tau^2 - (1 - 2\,\phi/c^2)\, d\mathbf{x} \cdot d\mathbf{x}\right] \,. \tag{1.16}$$

This form of the metric highlights the metric fluctuations induced by a non perfectly homogeneous and isotropic distribution of matter, at least at small scales. Note that the metric fluctuations are small even if the matter density fluctuations are not so small: $\delta M \sim \phi$ (see below).

The coordinate velocity of a matter particle in conformal time is just the peculiar velocity ie. the velocity measured by an observer at the particle position and at fixed $\mathbf{x}$:

$$\mathbf{v} \equiv \frac{d\mathbf{x}}{d\tau} = a\frac{d\mathbf{x}}{dt} = \frac{d\mathbf{r}}{dt} - H\mathbf{r} \,. \tag{1.17}$$

Note that, of course, the Hubble velocity is subtracted; also, the proper velocity of a particle relative to the origin can be written, from Eq.(1.17), as

$$\frac{d\mathbf{r}}{dt} = a\,\dot{\mathbf{x}} + \dot{a}\,\mathbf{x}\,, \tag{1.18}$$

where dot indicates time derivatives d/dt.

The gradient of the gravitational potential perturbation in the metric (1.16) corresponds to the Newtonian gravitational force. The geodesics in this metric correspond to the equations of motion. For a massive test particle m (see Peebles 1980, §7)

$$\mathbf{p} = m\,a^2\,\dot{\mathbf{x}}\,, \tag{1.19}$$

$$\frac{d\mathbf{p}}{dt} = -m\nabla\phi\,, \tag{1.20}$$

where the gradient is with respect to $\mathbf{x}$. According to (1.19) and (1.20),

$$\frac{d\mathbf{v}}{dt} = -\frac{\dot{a}}{a}\,\mathbf{v} - \frac{\nabla\phi}{a}\,. \tag{1.21}$$

The extra "Hubble drag" term $-\dot{a}\,\mathbf{v}/a$ arises because we are using comoving coordinates and it is not due to some cosmic force: if $\phi \equiv 0$, $\mathbf{p}$ is constant, but $\mathbf{v} \propto a^{-1}$ because of the Hubble expansion.

The zero–zero component of the Einstein equation for an ideal fluid is, to first order in ϕ/c^2 (see Peebles 1980, §7)

$$\nabla^2\phi = 4\pi G\,a^2\,[\rho(\mathbf{x},t) - \rho_b(t)]\,, \tag{1.22}$$

where $\rho(\mathbf{x},t)$ is the mass density at the point $(\mathbf{x},t)$. Eq.(1.22) is known as the (comoving) Poisson equation. We stress the fact that the source for ϕ is always the fluctuating part of the non relativistic matter density. Also note that (1.16), obtained from the standard weak field approximation (see e.g. Landau & Lifshitz 1979, Eq. (105.9)), does not assume that $\delta\rho \equiv \rho - \rho_b$ is small. The reason is just that we assumed $\phi \ll c^2$: if a region of scale λ contains a mass $M \sim \rho_b\,\lambda^3$, where the density ρ_b is roughly uniform, the condition

$\phi \ll c^2$ implies that $G\rho_b \lambda^2 \ll c^2$; in the Friedmann-Lemaitre models Hubble constant is $H \sim (G\rho_b)^{1/2}$ (see Eq.(1.11)); therefore in the Newtonian approximation we are neglecting terms of order $(\lambda H/c)^2$ ie. we assume that perturbation are small with respect to the Hubble scale; more in detail, the source of ϕ is the fluctuation $\delta\rho$, then $\phi/c^2 \sim (H\lambda/c)^2\, \delta\rho/\rho_b$ and, on scales much smaller than the horizon, ϕ/c^2 may be small even though $\delta\rho/\rho_b$ is very large.

Apart from the baryonic matter, the Universe contains a homogeneous sea of black body radiation, with temperature (e.g. Weinberg 1972; Mather *et al.* 1990; see also Gush, Halpern & Wishnow 1990)

$$T(t) = T_\circ (1+z)\,, \tag{1.23}$$

$$T_\circ = 2.735 \pm 0.06\, K\,, \tag{1.24}$$

where z is the cosmological redshift (because expansion)

$$\lambda_\circ = \frac{a(t_\circ)}{a(t)}\,\lambda = (1+z)\,\lambda\,. \tag{1.25}$$

$\lambda_\circ$ is the wavelength observed now ($t_\circ$), of radiation emitted at epoch t at wavelength λ by an object comoving with the fluid; the redshift z often is used as a label of an epoch, just because

$$z = a_\circ\, a^{-1} - 1\,. \tag{1.26}$$

The Hubble law, $\dot{r} = Hr$, gives the redshift of an object at proper distance $r \ll cH_\circ^{-1}$:

$$z \approx H_\circ\, r/c\,, \tag{1.27}$$

which is a good approximation for $z \ll 1$.

The mean mass density in the radiation is

$$E_b(t) = E_\circ\,(1+z)^4\,, \tag{1.28}$$

$$E_\circ = a_s\, T_\circ^4/c^2 = 4.5 \times 10^{-34}\, g\, cm^{-3}\,. \tag{1.29}$$

At the beginning, the Universe is radiation dominated; instead of (1.10) and (1.11), during the radiative–era we have

$$a \propto t^{1/2}\,, \tag{1.30}$$

$$\frac{32}{3}\pi G\rho_b t^2 = 1 \,, \tag{1.31}$$

in an Einstein–de Sitter universe; (1.6) is substituted by

$$\rho_b \propto a^{-4} \qquad \text{(radiation era)} \,. \tag{1.32}$$

The crossover between the matter era and radiation era occurs at the equivalence epoch, a_{eq}, when $\rho_r \equiv \rho_m$; detailed calculations show that $z_{eq} \approx 10^4$. The other important cosmological epoch is that of recombination, z_{rec}, after the temperature has fallen below $4000\,K$, the baryonic matter is essentially unionized and the matter and radiation therefore decouple.

After reviewing some basics in standard cosmology, we start to enter more in detail in that branch of modern cosmology in which we are interested in, the statistical analysis of the large–scale matter distribution in the Universe.

CHAPTER II

Statistical Predictions of Large Scale Structures

Most theories of galaxy formation assume that galaxies and other large–scale structures grew by gravitational instability from initially small stochastic perturbations δ to the energy density of the Universe (Chapter IV).

An important point is that no cosmological theory attempts to predict the initial conditions $\delta(\mathrm{x}, t)$ exactly. A "complete" theory might predict e.g. the mean abundance of clusters and of galaxies and the mean distance of galaxies, but not the specific locations of galaxies and clusters in our Universe. In other words, theories predict only the *statistical* properties of $\delta(\mathrm{x}, t)$, in particular the *spatial* statistical properties and, for this reason, the temporal parameter t is commonly understood, all statistical computations being made at a given cosmic time t.

2.1 Random Fields

In the statistical description of the matter distribution on large–scales, the energy–density fluctuation field in the Universe

$$\delta(\mathrm{x}) \equiv \frac{\rho(\mathrm{x}) - \langle\rho(\mathrm{x})\rangle}{\langle\rho(\mathrm{x})\rangle} , \qquad (2.1)$$

is treated as a *random field* ie. a set of random variables, one for each point x in the three dimensional real space, defined by the set of finite–dimensional *joint probability distribution*

function

$$P_N[\delta(\mathbf{x}_1), \delta(\mathbf{x}_2), \ldots, \delta(\mathbf{x}_N)]\, d\delta(\mathbf{x}_1)\, d\delta(\mathbf{x}_2) \cdots d\delta(\mathbf{x}_N) \tag{2.2}$$

(Here, forcing the notation, $\delta(\mathbf{x})$ also indicates the *value* of the *field* $\delta(\mathbf{x})$ at the point $\mathbf{x}$). This is the probability that the function $\delta(\mathbf{x})$ has values in the range $[\delta(\mathbf{x}_i), \delta(\mathbf{x}_i) + d\delta(\mathbf{x}_i)]$, with $i = 1, 2, \ldots, N$, N an arbitrary integer and $\mathbf{x}_1, \mathbf{x}_2, \ldots, \mathbf{x}_N$ are N arbitrary points in the euclidean space (Kac & Logan 1979; Adler 1981; Vanmarcke 1983; Bardeen *et al.* 1986 (BBKS)).

By *random* process we mean that $\delta(\mathbf{x})$ for our Universe is just a *random* realization from a statistical *ensemble* of universes.

The assumption that the Universe is homogeneous and isotropic on average implies that the density field $\rho(\mathbf{x})$, ie. $\delta(\mathbf{x})$, is a homogeneous and isotropic random process (sometimes called *stationary* ; see e.g. Fall 1979). So, the averages over the ensemble in (2.1), $\langle \cdot \rangle$, are invariant with respect to spatial translations and rotations. Observations probe only the spatial distribution in one realization of $\delta(\mathbf{x})$. On the other hand, theory specifies the probability distribution over an ensemble.

2.2 Ergodic Hypothesis

Actually implicit in all theoretical discussions is the *Ergodic Hypothesis* : ensemble averages equal spatial averages taken over one realization of the random field. The Ergodic Hypothesis has been demonstrated for a Gaussian random field (see Appendix A) *iff* its power spectrum (see §3.3) is continuous as a function of k (Adler 1981; see also BBKS). Essentially, the Ergodic Hypothesis requires spatial correlations (§ 3.1) to decay sufficiently rapidly with increasing separation so that there exist many statistically independent volumes in one realization. These conditions are satisfied in a large class of theories of primordial

scenarios, including quantum fluctuations produced during inflation (Brandenberger 1985). If the Ergodic Hypothesis is assumed valid, then all the information is available from a single sample of $\delta(\mathbf{x})$ over all space, and we have to hope that by measuring $\delta(\mathbf{x})$ over a sufficiently large volume arbitrarily precise tests of theories can be made.

2.3 Path–Integral Approach

An alternative approach, which has been extensively explored in recent years, is to apply the *path-integral approach* of Feynman & Hibbs (1965). More in general, the random field $\delta(\mathbf{x})$ is fully described by the joint probability distribution *functional* $P[\delta(\mathbf{x})]$ with measure

$$P[\delta(\mathbf{x})]\,[d\delta(\mathbf{x})]\,, \tag{2.3}$$

which is obtained from (2.2) for $N \to \infty$, with the points $\mathbf{x}_i$ covering the whole Universe; the limit may be made well-defined (see Bertschinger 1992), the corresponding measure is called a Wiener measure. By the assumption of statistical homogeneity, even though $\delta(\mathbf{x})$ is not constant, the distribution $P[\delta(\mathbf{x})]$ is independent of position $\mathbf{x}$. One recovers the n-point distribution by

$$\begin{aligned} P_N(\alpha_1,\ldots,\alpha_N)\,d\alpha_1\cdots d\alpha_N &= \langle \prod_{h=1}^{N} \delta_D(\delta(\mathbf{x}_h)-\alpha_h) \rangle \\ &= \int [d\delta] \prod_{h=1}^{N} \delta_D(\delta(\mathbf{x}_h)-\alpha_h)\, P[\delta]\,. \end{aligned} \tag{2.4}$$

This approach is not necessary for any of the applications we are interested in, but it surely permits us to develop in a relatively simple formalism a statistical study of the field $\delta(\mathbf{x})$, obtaining results that may not be easily worked out using the classical prescription, above all in the case in which the density distribution is a generic *non–Gaussian* type distribution. (see Fry 1984; Politzer & Wise 1986; Matarrese, Lucchin & Bonometto 1986; Goroff *et al.* 1987; Bertschinger 1988; Cline *et al.* 1988; Catelan, Lucchin & Matarrese 1988a; see also 1988b; Coles 1988; Lucchin, Matarrese & Vittorio 1988; Scherrer & Bertschinger 1991).

In particular, the path–integral technique we shall be applied to calculate the weighted–peak correlation functions (Section VI.9), the N–point correlation functions of excursion regions (Chapter VIII) and peak–number density of underlying non–Gaussian density fields (Appendix C).

2.4 Nature of Density Distribution

One of the most challenging and interesting problems to solve is to establish the nature of the distribution (2.3).

In the last decade of studies of cosmological large–scale structures, attention has been focused mainly on the two–point galaxy correlation function (§ 3.1) and on the analysis of the primordial *Gaussian* distributed density fluctuations (we briefly discuss the technical aspects of Gaussian fields in Appendix A).

Indeed the simplest and more usually accepted hypothesis is that the distribution (2.3) is Gaussian.

A reason justifying this is a *principle of simplicity*, according to which all the *complications* should arise during the non–linear evolution of the perturbations after the recombination (see e.g. Primack 1984; Chapter VII). If we had to translate this statement into the language of field theory, we could say that the density fluctuation field was initially free, and all its interactions are due to the subsequent action of gravity. Stated in such a manner, it appears as a quantitative formulation of our intuitive idea that the gravitational interaction has to play the main dynamical role on large scales. Furthermore, it is known that a Gaussian distribution provides us many practical advantages.

The *Central Limit Theorem*, which tells us that the probability distribution of the sum, or mean, of many random variables, being both (nearly) independent and (nearly)

identically distributed, tends to a Gaussian distribution (see e.g. Feller 1971; Adler 1981; Vanmarcke 1983), is largely used to justify such a restrictive hypothesis. Also, the Gaussian functional distribution, being exponential of a quadratic form, involves extremely simple analytical calculations; this is due to the fact that a Gaussian distribution is completely determined by its power spectrum (see below) ie. by its 2–point correlation function (which corresponds to the Green's function of a free scalar field): a possible definition of Gaussian distribution is indeed when all the reduced or connected correlations (see Appendix B) of order higher than second are *zero* [1].

There exist many usually invoked arguments asserting that, during the linear phase of evolution of perturbations, the second order correlations constitute all that is necessary to know. During the most part of the primordial history of the Universe, the clustering process is negligible, as one observes in correspondence of the largest scales, and the connected correlations of higher order are assumed be negligibly small (however see e.g. Baumgart & Fry 1991). Furthermore, the inflationary model (see e.g. Kolb & Turner 1990) predicts the existence of scale–free primordial Gaussian density fluctuations ie. fluctuations that cross the horizon with constant scale–independent mass variance (§3.3; Bardeen, Steinhardt & Turner 1983).

However, non–Gaussian fluctuations for structure formation have been advocated by numerous cosmologists.

Peebles (1983; 1987) has suggested that the distribution of galaxies is not adequately described by a Gaussian process: actually the distribution of galaxies is surely non–Gaussian on small scales (as confirmed, for instance, by detection of low order connected galaxy correlations; see §3.2; Saunders *et al.* 1991) and, from a certain moment onwards, we must think that the assumption of Gaussian distribution is inadequate; we could deduce that such moment corresponds to the beginning of the non–linear regime, but there exist

[1] There exists only *one* positive definite density probability $p(x)$ with only a mean and a variance, the Gaussian distribution (see Fry 1985).

many indications asserting that it could be very antecedent to that phase (Fry 1984; 1985; Baumgart & Fry 1991).

Non–Gaussian distributed perturbations can be assumed to be the most general starting point for computing a number of cosmological observables, such as spatial correlation functions (Matarrese, Lucchin & Bonometto 1986), expected size and frequency of high density regions (Catelan, Lucchin & Matarrese 1988) and of fine–scale hotspots and coldspots in the microwave background distribution on the sky (Coles & Barrow 1987).

A strong theoretical reason for analyzing non–Gaussian probabilities is that the fractional density enhancement $\delta(\mathbf{x})$ must satisfy the fundamental constraint

$$\delta(\mathbf{x}) \geq -1 \tag{2.5}$$

everywhere, because the semipositivity of the mass density $\rho(\mathbf{x})$. The normal distribution cannot allow for this constraint, because it predicts a finite chance that δ assumes a value smaller than -1 (the consequences of this are particularly relevant in the 'weighted' biased scheme presented in § 6.9; Catelan *et al.* 1992). Since cosmological perturbations can only be assumed normally distributed during the very linear stage of their evolution, this latter problem is commonly disregarded. In this stage the probability of getting one of these "negative mass" events is negligibly small; one can recall the Chebyshev inequality (e.g. Feller 1971), stating that, given any distribution function $p(\delta)$, the *a priori* probability that $\delta < -1$, in a randomly chosen point, is not larger than the mean square fluctuation σ^2, where linearity implies $\sigma^2 \ll 1$.

Variations of the inflation model which yields to *non–Gaussian* primordial fluctuations which are basically scale–invariant have been recently widely discussed (Matarrese, Ortolan & Lucchin 1988; Barrow & Coles 1990; Salopek & Bond 1991; Mollerach *et al.* 1991; Salopek 1992). In the context of inflationary models, Allen, Grinstein & Wise (1987) and Kofman & Linde (1987) constructed axion models with non–Gaussian fluctuations. Late–time phase transitions (Hill, Schramm & Fry 1989), cosmic string models (Vilenkin 1981; Turok 1984; Scherrer, Melott & Bertschinger 1989) and global textures (Turok 1989; Turok

& Spergel 1990; 1991) are additional models whose statistics may not be described by a Gaussian distribution (Scherrer & Bertschinger 1991; Scherrer 1992). The importance of the high order moments of density distribution for the final destiny of the large scale structures has been recently analyzed in a series of N–body simulations by Messina *et al.* (1990; 1992), Moscardini *et al.* (1991), Matarrese *et al.* (1991) and Weinberg & Cole (1992).

Particular non–Gaussian random fields are usually defined e.g. by performing a nonlinear transformation on an underlying Gaussian random field; a possible statistics obtained in this way is the *lognormal distribution*, the prototype for multiplicative processes, which has been widely analyzed in cosmological framework (Coles & Barrow 1987; Lucchin & Matarrese 1988; Coles 1989; Coles & Jones 1990); negative mass events are not allowed in this statistics.

CHAPTER III

Statistical Measures of Galaxy Distribution

We now review some of the statistics usually applied by cosmologists to describe the spatial distribution of galaxies and clusters.

The first systematic analyses of galaxies surveys concentrated on the measurement of low order galaxy correlation functions for two–dimensional sky surveys (Totsuji & Kihara 1969; Peebles 1980; Sharp, Bonometto & Lucchin 1984). The same methods have been applied to the CfA survey (Shanks *et al.* 1983; Davis & Peebles 1983), the Abell cluster catalogue (Bahcall and Soneira 1983; Klypin and Kopilov 1983; Postman, Huchra & Geller 1992) and to the recent new catalogues e.g. the APM galaxy survey (Maddox *et al.* 1990; Dalton *et al.* 1992; Efstathiou *et al.* 1992). The cross correlations of galaxies and rich clusters have also been studied (Lilje & Efstathiou 1983)

A simple linear integral equation, Limber's equation (Limber 1953), provides us with the ability to obtain the *angular* correlations starting from the knowledge of the spatial correlations and/or viceversa (for a thorough exposition see Peebles 1980; for the inversion of Limber's equation see also: Fall & Tremaine 1977; Bonometto & Lucchin 1978).

3.1 Definitions

The probability that an object (galaxy, cluster of galaxies) is found in the infinitesimal volume δV chosen at random is defined by

$$\delta P = n\,\delta V\ , \tag{3.1}$$

where the mean number density n is independent from the position; this is an average on the ensemble. The probability of finding more than one object in δV is an infinitesimal of higher order if we assume, in the cases of practical interest, that the objects do not cluster in arbitrarily dense regions.

The two–point correlation function $\xi^{(2)}$ is defined in such a way that

$$\delta P = n^2\,\left[1+\xi^{(2)}(r_{12})\right]\,\delta V_1 \delta V_2 \tag{3.2}$$

is the *joint probability* of finding (two) objects in the volumes δV_1 and δV_2, chosen at random and separated by the distance r_{12}. Consistently with the assumption of homogeneity and isotropy, $\xi^{(2)}$ has been written like a function of spatial separation. For a purely random process, the probabilities of finding objects in δV_1 and δV_2 are independent, so that the joint probability is the product of the single point probabilities

$$\delta P = n^2\,\delta V_1 \delta V_2\ , \tag{3.3}$$

In this case $\xi^{(2)} \equiv 0$; if the positions of the objects are correlated, $\xi^{(2)} > 0$; if the positions are anticorrelated, $-1 \leq \xi^{(2)} < 0$. $\xi^{(2)}$ is the excess or the defect of probability with respect to a purely random distribution (Poisson distribution).

An equivalent way to introduce the correlations is possible when the distribution of objects can be (approximately) described by a *continuous* density function, $\rho(\mathrm{x})$. A link relating discrete and continuous distributions is given, for example, defining the number density field for a point–like process as a sum over Dirac delta function:

$$\rho(\mathbf{r}) = \sum_i \delta_D(\mathbf{r}-\mathbf{x}_i)\ , \tag{3.4}$$

with mean over the statistical ensemble of point processes

$$\langle \rho(\mathbf{r}) \rangle \equiv n \ . \tag{3.5}$$

The two–point function is then introduced as

$$\xi^{(2)}(r) \equiv \langle [\rho(\mathbf{x}) - \langle \rho \rangle] [\rho(\mathbf{x}+\mathbf{r}) - \langle \rho \rangle] \rangle / \langle \rho \rangle^2 = \langle \delta(\mathbf{x}) \, \delta(\mathbf{x}+\mathbf{r}) \rangle \ . \tag{3.6}$$

We stress the fact that $\xi^{(2)}(r)$ has a *different* meaning in this case: in the continuous case, $\xi^{(2)}(r)$ is the *autocorrelation function* of the field $\delta(\mathbf{r})$ ie. a measure of the degree of spatial correlation of the density fluctuation $\delta(\mathbf{r})$; in the discrete case, we repeat, correlations are defined in term of probabilities of finding discrete objects at specified points.

If, viceversa, one is interested in generating a discrete distribution from a continuous one, the simplest method is to employ the *Poisson model* : given the continuous realization $\rho(\mathbf{x})$, one randomly places *one* particle in each volume $\delta V \equiv d\mathbf{x}$ with probability $\rho(\mathbf{x})d\mathbf{x}$ and independent probabilities for all volume elements. Correlations are built into the point process by correlations in the density field $\rho(\mathbf{x})$; for instance, the result of discretizing the continuous process $\delta(\mathbf{x})$ writes

$$\langle \delta(\mathbf{x}_1) \delta(\mathbf{x}_2) \rangle_{(d)} = \xi^{(2)}(r_{12}) + n^{-1} \delta_D(\mathbf{x}_1 - \mathbf{x}_2) \ , \tag{3.7}$$

where the Dirac delta function contribution to the correlation arises from discreteness, and it is not present in the continuous case; the outcome is a double random process, with one level of stochasticity coming from the random field $\rho(\mathbf{x})$ and a second from the Poisson sampling (see Peebles 1980, §33; Fry 1985a; Scherrer & Bertschinger 1991).

According to (3.6), it is possible to write

$$1 + \xi^{(2)}(r) = \langle \rho(\mathbf{x}) \, \rho(\mathbf{x}+\mathbf{r}) \rangle / \langle \rho \rangle^2 \ , \tag{3.8}$$

and we can see that $\xi^{(2)}$ is the *connected* part of the *complete* two–point correlation function $\langle \rho(\mathbf{x}) \rho(\mathbf{x}+\mathbf{r}) \rangle / \langle \rho \rangle^2$.

In a similar fashion, the three–point function $\xi^{(3)}(r_{12}, r_{23}, r_{13}) \equiv \zeta$ is such that

$$\delta P = n^3 \left[1 + \xi^{(2)}(12) + \xi^{(2)}(23) + \xi^{(2)}(13) + \xi^{(3)}(12, 23, 13)\right] \delta V_1 \delta V_2 \delta V_3 \,, \qquad (3.9)$$

is the joint probability of finding (three) objects in the volume elements δV_1, δV_2, δV_3, separated by the distances r_{12}, r_{23}, r_{13}. The assumption of the homogeneity and isotropy of the Universe on large scales means that $\xi^{(3)}$ depends on the absolute value of the separations only, and it is a symmetric function of the three separations. If the distribution of the objects is described by a continuous density function, we have that

$$\xi^{(3)}(r, s, |\mathbf{r} - \mathbf{x}|) = \langle \delta(\mathbf{x})\, \delta(\mathbf{x} + \mathbf{r})\, \delta(\mathbf{x} + \mathbf{s}) \rangle \qquad (3.10)$$

ie.

$$1 + \xi^{(2)}(r_{12}) + \xi^{(2)}(r_{23}) + \xi^{(2)}(r_{13}) + \xi^{(3)}(r_{12}, r_{23}, r_{13}) = \langle \rho(\mathbf{x}_1)\, \rho(\mathbf{x}_2)\, \rho(\mathbf{x}_3) \rangle / \langle \rho \rangle^3 \,, \qquad (3.11)$$

where $r_{ij} \equiv |\mathbf{x}_i - \mathbf{x}_j|$. $\xi^{(3)}$ is the *connected* part of the *complete* 3–point function (3.11), which is zero if the density distribution is Gaussian.

In general, by supposing that the distribution is approximately continuous, the N–point correlation function is defined by

$$\delta P = \langle \prod_{h=1}^{N} \rho(\mathbf{x}_h) \rangle \prod_{h=1}^{N} \delta V_h \,, \qquad (3.12)$$

and the N–point joint probability contains all the *connected* correlations until order N, different from zero only for non–Gaussian distributions (we discuss in Appendix B the role of the reduced or connected moments in describing a general probability distribution).

As we shall see, the only galaxy correlation functions actually estimated are not beyond the fourth order; those higher than fourth order are undetermined because the scarcity of the available data (see Sharp, Bonometto & Lucchin 1984; Baumgart & Fry 1991).

3.2 Observational Data

One of the main observational tests of the large scale matter distribution is supplied by the analysis of the two point correlations of different sets of objects (from galaxies to superclusters). The relation

$$\xi_i^{(2)}(r) \approx (r/r_i)^{-1.8} \tag{3.13}$$

sufficiently interpolates the 2–point correlation functions for all classes of objects, each one characterized by a correlation length r_i and by an interval of distances where (3.13) holds. Moreover, there are indications that r_i increases with the richness of the system (Davis & Peebles 1983; Bahcall & Soneira 1983; Klypin & Kopilov 1983; Schectman 1985; Bahcall & Burgett 1986; Plionis & Borgani 1991).

Galaxies

The observed 2–point correlation function for the galaxies has the form (see e.g. Peebles 1980)

$$\xi_g^{(2)}(r) = (r/r_g)^{-\gamma} , \tag{3.14}$$

$$\gamma = 1.77 \pm 0.4 , \tag{3.15}$$

$$r_g = 5.4 \pm 0.1\, h^{-1} Mpc , \tag{3.16}$$

with $0.1\, h^{-1} Mpc \lesssim r \lesssim 10\, h^{-1} Mpc$ and $\xi_g^{(2)}(r) \ll 1$.

Hierarchical (CDM) models reproduce this reasonably well in N–body simulations (Frenk *et al.* 1983; Davies *et al.* 1985; White *et al.* 1987; Frenk *et al.* 1988). The Durham deep–redshift sample (Shanks *et al.* 1989) indicates a correlation function with scale length $\sim 7\, h^{-1} Mpc$, beyond which a break in the slope appears. There is persistent evidence that the correlation function is not a power law, but has a "shoulder" on scales $\sim 2 \div 5\, h^{-1} Mpc$ (see also Dekel & Aarseth 1984; Guzzo *et al.* 1991), although this could arise because the data are in redshift space rather than true position (Kaiser 1987). There is also persistent evidence that the correlation function becomes negative at $20\, h^{-1} Mpc$ never turning positive

again, but this may be because the survey appears to avoid notable galaxy clusters; the newly compiled APM catalogue of more than 2 million galaxies reveals a strictly positive $\xi_g^{(2)}$ up to $\sim 50 \div 100\, h^{-1} Mpc$, which is unexpected within the popular (biased) CDM model (Chapter VI). Peacock and Nicholson (1991), using an all–sky sample of *radio* galaxies at redshifts $z \leq 0.1$, find $\xi \approx (r/11\, h^{-1} Mpc)^{-1.8}$ on scales up to several hundred Mpc; this strength of clustering is hardly surprising, since radio galaxies are elliptical and tend to reside in clusters.

In the case of the higher order galaxy correlation function, the results are essentially relative to 2–dimensional catalogs and they have pointed out an approximately hierarchical form for the connected correlations, in the sense that $\xi_g^{(3)}$ and $\xi_g^{(4)}$ can be expressed as sums of products of $N-1$ ($N = 3, 4$) 2–point correlation functions; respectively (Groth & Peebles 1977; Fry and Peebles 1978; see also Peebles 1980)

$$\xi_g^{(3)}(1,2,3) \approx Q \left[\xi_g^{(2)}(12)\,\xi_g^{(2)}(23) + \xi_g^{(2)}(12)\,\xi_g^{(2)}(13) + \xi_g^{(2)}(13)\,\xi_g^{(2)}(23)\right] , \tag{3.17}$$

$$Q \approx 1.29 \pm 0.21 , \tag{3.18}$$

$$\xi_g^{(4)}(1,2,3,4) \approx \sum_{ijkl} \left[R_a\, \xi_g^{(2)}(ij)\,\xi_g^{(2)}(jk)\,\xi_g^{(2)}(kl) + R_b\, \xi_g^{(2)}(ij)\,\xi_g^{(2)}(ik)\,\xi_g^{(2)}(il)\right] , \tag{3.19}$$

$$R_a \approx 2.5 \pm 0.6 ; \qquad R_b \approx 4.3 \pm 1.2 . \tag{3.20}$$

Note that these hierarchical forms are symmetric in their arguments and go to zero if one or more objects are far from those remaining .

Fry (1984) showed that the above forms are originated by nonlinear evolution starting from Gaussian primordial conditions. The form of Eq.(3.17) appears in hydrodynamics, where the complete three–point correlation function is given by the Kirkwood superposition relation (Huang 1963; Ichimaru 1974; see Chapter VIII). Melott & Fry (1986) extract a reasonable value of ζ from a big N–body simulation. Szalay (1988), in the biased scenario, computed the scaling coefficient Q in terms of the Hermite expansion of a general non linear thresholding function.

It has been attempted to obtain from the Zwicky Catalogue the 5–point correlation function, but with poor success, because the errors have the tendency to become comparable with the measurable quantities (Sharp, Bonometto & Lucchin 1984).

Clusters

Since the first quantitative analysis of (rich) cluster correlations (Hauser & Peebles 1973), showing that clusters are clumped on scales at least as large as $\sim 25\,h^{-1}Mpc$ and possibly larger, it was known that the 2–point correlation function for the rich Abell clusters (number of galaxies $N_g > 65$) has the form (Bahcall & Soneira 1983; Klypin & Kopilov 1983; Postman, Geller & Huchra 1986)

$$\xi_c^{(2)}(r) \approx \left(\frac{r}{25\,h^{-1}Mpc}\right)^{-1.8}, \tag{3.21}$$

out to separations of order $\sim 100\,h^{-1}Mpc$, although this upper limit is controversial (Olivier *et al.* 1990; Sutherland & Efstathiou 1991). Note that this implies that $\xi_c^{(2)} \approx 20\,\xi_g^{(2)}$ and the rich clusters of galaxies are observed to have greater amplitude than could be expected for the galaxy distribution on the same large scales.

Recently many controversies have grown about the first thought well established clustering of Abell clusters. Firstly, the Bahcall & Soneira sample (1983) is very small (only 104 clusters) and the statistical uncertainties are correspondingly large. A realistic analysis of the likely errors is given in Ling, Frenk & Barrow (1986). Secondly, there are considerable doubts as to the reliability of Abell's catalogue; in particular the visual method used to obtain the richness classes of clusters can lead to large systematic effects (Lucey 1983; Efstathiou *et al.* 1992). A careful analysis of a larger three dimensional cluster catalogue (Struble & Rood 1987) has, moreover, revealed clear evidence for projection effects in the Abell catalogue (Sutherland 1988) that, once allowed, reduce the amplitude of $\xi_c^{(2)}$ to ~ 1 at $14\,h^{-1}Mpc$ rather than $25\,h^{-1}Mpc$ (see also Dekel, Blumenthal & Primack 1988)

$$\xi_c^{(2)}(r) \approx \left(\frac{r}{14\,h^{-1}Mpc}\right)^{-1.8}. \tag{3.22}$$

This trend seems confirmed also by recent determinations of cluster correlation for the new APM cluster catalogue (Dalton *et al.* 1992; Efstathiou *et al.* 1992; see also Postman, Huchra & Geller 1992) and for ACO catalog (Mc Gill & Couchman 1989; Batuski *et al.* 1989).

In addition, the correlation length for the Abell clusters increases with cluster richness (Bahcall & Soneira 1983; Bahcall, Soneira & Burgett 1986). This can be understood qualitatively just because the richer clusters are rarer. Shectman (1985) determined the 2–point correlation function for the identified poor clusters for the Lick catalog and confirmed the previous results: richer and more luminous systems are more strongly correlated (see also Plionis & Borgani 1991).

The Kirkwood relation for the spatial three–point correlation function for the rich clusters has been analitically obtained by Politzer & Wise (1984) and, in a more general way, Matarrese, Lucchin & Bonometto (1986). The problem of estimating the 3–point correlation function of galaxy clusters has been recently addressed by several authors, considering angular samples (Jing & Zhang 1989; Toth, Hollosi & Szalay 1989), three dimensional samples (Jing & Valdarnini 1991) and numerical simulations (Gott, Gao & Park 1991). All these analyses converge to indicate that the hierarchical model of Eq.(3.17) is consistent with data. However, although similar values of Q are worked out from such analyses, remarkably different estimates of the relative uncertainties were given, according to the different method used for the correlation and error analysis; these problems are summarized and addressed in Borgani, Jing & Plionis (1992).

Superclusters

Analyses like these have been extended to the supercluster scale. Bahcall & Burgett (1986) have studied the Supercluster Sample of Bahcall & Soneira (1984) and they found a positive correlation on scales of the order of $\gtrsim 10\, h^{-1} Mpc$. If this correlation is quantified

by the usual power law,

$$\xi_{sc}^{(2)}(r) \approx \left(\frac{r}{r_{sc}}\right)^{-\gamma} , \tag{3.23}$$

one has $r_{sc} \approx 60\, h^{-1} Mpc$ (Bahcall & Burgett 1986), higher than r_c. The law (3.23) holds in the range $50\, h^{-1} Mpc \lesssim r \lesssim 150\, h^{-1} Mpc$.

These results, even more than those relative to the clusters, must be considered with caution, because of the smallness and the peculiarity of the statistical samples examined.

Richness–Correlation Relation

As suggested above, there exists a tendency for the correlation between homogeneous systems of rising richness and scale (galaxies, clusters and superclusters) to increase. This fact is shown e.g. in Fig.1 and Fig.2 in Bahcall & Burgett (1986). A universally accepted theoretical justification of this does not exist, but some authors have attempted to explain such a tendency in the framework of the biased galaxy formation scenario (classical references are e.g.: Kaiser 1984; Politzer & Wise 1984; Schaeffer & Silk 1985; Fry 1986; BBKS 1986; Jensen & Szalay 1986; Matarrese, Lucchin & Bonometto 1986), where high peaks of the mass density field are taken as the sites where bright galaxies or rich clusters of galaxies form. The consequences of such a hypothesis are discussed in Chapter VI.

3.3 Power Spectra

Cosmological information is stored not only in the N–point correlation functions, but also, in a complementary way, in their Fourier transform, the *power spectra* (see e.g. Baumgart & Fry 1991; Peacock 1991).

Furthermore, to follow the ultimate gravitational collapse into condensed systems of initially small (Gaussian) perturbations, one must first determine an initial spectrum for density perturbations in the very early Universe.

The main physical observable connected with density perturbations, indeed, is the root–mean–square relative mass fluctuation $\sigma_M = \sqrt{\langle \delta_M^2 \rangle}$ inside a sphere of radius R; cosmologists estimate it by e.g. the r.m.s. fluctuation in galaxy counts, $(\delta N/N)_g$. Such an observable can be expressed in terms of the density perturbation $\tilde{\delta}(\mathbf{k})$ in Fourier space, which in turn can be expressed in terms of the 2–point correlation function

$$\sigma_M^2 = \frac{\langle M^2 \rangle - \langle M \rangle^2}{\langle M \rangle^2} = \frac{1}{2\pi^2} \int_0^\infty dk\, k^2 \langle\, |\tilde{\delta}(\mathbf{k})|^2 \rangle\, \widetilde{W}^2(kR)\,, \tag{3.24}$$

where $M \equiv \frac{4}{3}\pi\rho R^3$ is the mass inside the R–sphere and $\widetilde{W}(y) \equiv 3\,(\sin y - y\cos y)/y^3$, which is zero if $y \gg 1$ and one if $y \ll 1$: essentially all the perturbations with wavelength $\lambda \approx k^{-1} > R$ contribute to the variance σ_M^2. Another important physical observable is the rms peculiar velocity on a given scale R (e.g. Peebles 1980)

$$\sigma_v^2(R) = \langle\, v(R)^2 \rangle = \frac{H^2 f(\Omega)^2 a^2}{2\pi^2} \int_0^\infty dk\, \langle\, |\tilde{\delta}(\mathbf{k})|^2 \rangle\, \widetilde{W}^2(kR)\,, \tag{3.25}$$

where $f(\Omega) \approx \Omega^{0.6}$ (see §4.1).

The *power spectrum* can be defined from the expectation value of the two–point function in Fourier space, as follows (see e.g. Fry 1986; Bertschinger 1991)

$$\langle \tilde{\delta}(\mathbf{k}_1)\, \tilde{\delta}(\mathbf{k}_2) \rangle \equiv (2\pi)^3\, \delta_D(\mathbf{k}_1 + \mathbf{k}_2)\, P(k_1)\,. \tag{3.26}$$

If we assume that the density field is continuous, $P(k)$ is the Fourier transform of the 2–point correlation function $\xi(r)$ (Wiener–Kintchine theorem)

$$P(k) = \int d\mathbf{r}\, \xi(r)\, \mathrm{e}^{i\,\mathbf{k}\cdot\mathbf{r}} = 4\pi \int_0^\infty dr\, r^2\, \xi(r)\, \frac{\sin kr}{kr}\,, \tag{3.27}$$

$$\xi(r) = \frac{1}{(2\pi)^3} \int d\mathbf{k}\, P(k)\, \mathrm{e}^{-i\,\mathbf{k}\cdot\mathbf{r}} = \frac{1}{2\pi^2} \int_0^\infty dk\, k^2 P(k)\, \frac{\sin kr}{kr}\,. \tag{3.28}$$

Once $\xi(r)$ is given, (3.27) can be considered another definition of $P(k)$; the Dirac delta function is required because of translational invariance: it is reminiscent of the "momentum conservation" in QFT Green's function. Similarly, isotropy implies that $P(k)$ depends only on the magnitude of the wavevector k. Instead of (3.24) and (3.25), we can write

$$\sigma_M^2 = \frac{1}{(2\pi)^3} \int d\mathbf{k}\, P(k)\, \widetilde{W}^2(kR)\,, \tag{3.29}$$

$$\sigma_v^2 = \frac{H^2 f^2 a^2}{(2\pi)^3} \int d\mathbf{k}\, \frac{P(k)}{k^2}\, \widetilde{W}^2(kR)\ . \tag{3.30}$$

We see here one of the several reasons for the importance of the power spectrum: apart from the presence of $\widetilde{W}$ ($\widetilde{W} = 1$ for any $\mathbf{k}$ if the density field is not smoothed out), we see that $P(k)d\mathbf{k}$ is the contribution to the variance of δ_M from modes with wavevectors in the volume element $d\mathbf{k}$ around $\mathbf{k}$.

Another way to say that is that $d\sigma_M^2/d\ln k = (1/2\pi^2)k^3 P(k)$ is the contribution to the variance of δ_M per logarithmic interval of k. Moreover, $d\sigma_v^2/d\ln k = (1/2\pi^2)(aHf)^2 k P(k)$. If the power spectrum is peaked at some scale k_{max}, we can say that more energy is injected in correspondence of that scale, and

$$\sigma_M^2 \approx (1/2\pi^2)\, k_{max}^3\, P(k_{max})\ ,$$

$$\sigma_v^2 \approx (1/2\pi^2)(aHf)^2\, k_{max}\, P(k_{max})\ .$$

Another reason for the importance of the power spectrum is that it completely specifies the statistics of a Gaussian random field (Appendix A; B).

As cosmologists are increasingly realizing (Baumgart & Fry 1991; Peacock 1991; Park 1991), $P(k)$ is a powerful *direct* statistic for describing both large–scale and small–scale structure.

Smoothing

For doing comparisons between observational data and theory, it is *necessary* to filter the fluctuation field $\delta(\mathbf{x})$ by means of a *window function* $W_R(x)$, $x \equiv |\mathbf{x}|$,

$$\delta_R(\mathbf{x}) \equiv \int dy\, \delta(\mathbf{y})\, W_R(|\mathbf{x}-\mathbf{y}|) = \int dy\, \delta(\mathbf{x}-\mathbf{y})\, W_R(y)\ . \tag{3.31}$$

The windowing convolution averages the fluctuation δ over the points $\mathbf{y}$ in a volume $\sim R^3$, where one has no interest in the substructure, filtering out the high frequencies corresponding to scales inside this volume: the physical information on scale $\lambda < R$ is completely lost.

The characteristic of $W_R(x)$ is to be essentially constant for $x \lesssim R$ and practically zero otherwise, with $\int dx\, W_R(x) = 1$. The introduction of this cut–off is moreover justified by the fact that the high frequency content of the spectrum $P(k)$ can be overlooked, since the microscale fluctuations ($k \gg R^{-1}$) are not observable and also not relevant in cosmology (see e.g. BBKS).

Usually one assumes R as the typical size of the proto–object considered, and it is related to the mass M of the proto–object through $M(R) = 4\pi\langle\rho\rangle \int_0^\infty dx\, x^2\, W_R(x) = c_W \langle\rho\rangle R^3$, c_W being a number that depends on the particular choice of the window function.

The result in (3.24) can be now understood in another manner: $\widetilde{W}(y) = 3\,(\sin y - y\cos y)/y^3$ is the Fourier transform of the "top–hat" window function $W_R(x) = 3\,\theta(x - R)/4\pi R^3$, introduced just because of the definition of mass given there, $M_{TH} = \frac{4}{3}\pi\langle\rho\rangle R_{TH}^3$. This is not necessarily realistic, an observational sample has indeed a complicated boundary determined by observational selection; moreover galaxies and clusters of galaxies do not have sharp edges.

An alternative assumption is that of a Gaussian window (see BBKS)

$$W_R(x) = (2\pi R^2)^{-3/2} \exp\left(-\frac{x^2}{2R^2}\right) , \tag{3.32}$$

$$\widetilde{W}(kR) = \exp\left(-\frac{R^2k^2}{2}\right) , \tag{3.33}$$

for which $M_G = (2\pi)^{3/2}\langle\rho\rangle\, R_G^3$; $M_{TH} = M_G$ if $R_G = 0.64\, R_{TH}$.

The arbitrariness of the smoothing procedure means one must be cautious about making quantitative predictions, particularly when these are sensitive to R. However, the filtering is not only a purely formal concept, but it can correspond to real physical processes (see Peebles 1980; BBKS).

All properties of $\delta(\mathbf{x})$ are inherited by $\delta_R(\mathbf{x})$ and for each observable relative to $\delta(\mathbf{x})$, there exists the correspondent relative to $\delta_R(\mathbf{x})$. In such a manner, the 2–point correlation

function of the filtered density field $\delta_R(\mathbf{x})$ is

$$\xi_R^{(2)}(\mathbf{x}_1 - \mathbf{x}_2) \equiv \langle \delta_R(\mathbf{x}_1)\delta_R(\mathbf{x}_2)\rangle = \int\int \Big\{ \prod_{h=1}^{2} d\mathbf{y}_h \, W_R(|\mathbf{x}_h - \mathbf{y}_h|) \Big\} \, \xi^{(2)}(\mathbf{y}_1 - \mathbf{y}_2) \, . \tag{3.34}$$

The Wiener–Kintchine relation reads

$$\xi_R^{(2)}(r) = \frac{1}{2\pi^2} \int_0^\infty dk \, k^2 \, \frac{\sin kr}{kr} \, P(k) \, \widetilde{W}_R^2(k) \, . \tag{3.35}$$

One can say that

$$P_R(k) \equiv P(k) \, \widetilde{W}_R^2(k) \tag{3.36}$$

is the power spectrum of the fluctuation $\delta_R(\mathbf{x})$. In this context, δ_R represents the mass fluctuation in a volume of radius R, suitably smoothed by the chosen W_R. The relation (3.29) can be written in the more general form as

$$\sigma_o^2(R) = \xi_R^{(2)}(0) \, . \tag{3.37}$$

Origin

The most common choice of the wave–number analytical dependence of $P(k)$ is

$$P(k) \propto k^n \, . \tag{3.38}$$

n is the *primordial spectral index*, where $n > -3$ to provide convergence of the rms density fluctuation as $k \to 0$ (ie. asymptotic homogeneity) and $n < 4$ is imposed by the discretness of matter (*minimal spectrum*; see Peebles 1980; Peacock 1991). The power–law form is chosen because we have no *a priori* physical reason for picking out any characteristic scale: it is therefore a statement of our ignorance more than anything else.

The assumption (3.38) can be written in terms of primordial mass variance on scale M as

$$\sigma_M \propto M^{-(n+3)/6} \tag{3.39}$$

changing, because of evolution, to $\sigma_M \propto M^{-(n-1)/6}$ upon first coming within the horizon (see e.g. Peebles 1980): the *Harrison–Zel'dovich* $n = 1$ spectrum is characterized by a constant variance at the horizon crossing, independent of the scale; it is the most natural primordial

power spectrum (Harrison 1970; Peebles & Yu 1970; Zel'dovich 1972), predicted in inflationary models too (Brandenberger 1985, 1990; Mukhanov, Feldman & Brandenberger 1992 and references therein). The Zel'dovich spectrum also arises automatically if the fluctuations are due to cosmic strings (Zel'dovich 1980; Vilenkin 1981; see however Albrecht & Stebbins 1992) or to the global textures (see Cen *et al.* 1991; Gooding *et al.* 1991). Other nomenclature which is worth mentioning is the *flicker–noise* spectrum ($n = -3$), and the *white–noise* spectrum ($n = 0$). Spectra with $n < 0$ ($n > 0$) imply more power on large (small) scale.

Evolution of the fluctuations after the inflation epoch modifies the spectrum. While the fluctuations are still linear the modification is simply a linear filtering, with transfer function $T(k,a) = P(k,a)/P(k,a_i)$. For a discussion of the transfer function in various cosmological models see Efstathiou (1990).

With a power–law model

$$P(k) = Ak^n \, \mathrm{e}^{-k/k_c} \, , \tag{3.40}$$

where k_c is a short wavelength cut–off that is necessary if $n \geq 0$ (see Peebles 1980, § 42), some insights into $\xi(r)$ are obtained.

The autocorrelation function simplifies to

$$\xi(r) = \frac{A\,\Gamma(3+n)}{2\pi^2\,(2+n)} \sin\left(\frac{(2+n)\pi}{2}\right) r^{-(3+n)} \, . \tag{3.41}$$

For $0 < n < 2$, ξ becomes anticorrelated at large r, approaching zero as r^{-3-n}, and first becomes negative at

$$r_\circ = k_c^{-1} \, \mathrm{tg}\left(\frac{\pi}{2+n}\right) \, . \tag{3.42}$$

Therefore, sign and slope of ξ_{gg} on linear scales should provide direct information about the power spectrum there.

Normalization

Although inflation generically predicts the slope of the initial power spectrum, the overall amplitude is effectively a free parameter that cannot be calculated with any confidence

because it is highly model dependent: it is usually assumed to be fixed by observations. However, there are, as yet, no observations that can be related unambiguously to the amplitude of linear fluctuations in the density field. Two prescriptions for fixing the normalization have been applied relatively widely.

The first is based on the second moment of the mass correlation function

$$J_3(R) \equiv \int_0^R dr\, r^2\, \xi(r) = \frac{R^3}{6\pi^2} \int d\mathrm{k}\, P(k)\, \widetilde{W}^2(kR)\,, \tag{3.43}$$

compared with estimates from galaxy redshift surveys. There are several problems with this type of comparison (see e.g. Efstathiou 1990). By an analysis of the spatial correlation function from the CfA redshift survey (Huchra *et al.* 1983), Davis & Peebles (1983) find $J_3(10\,h^{-1}Mpc) = 277\,(h^{-1}Mpc)^3$ and $J_3(25\,h^{-1}Mpc) = 780\,(h^{-1}Mpc)^3$, although $10\,h^{-1}Mpc$ is about the largest scale on which a reliable estimate of J_3 can be derived from the CfA survey (see Efstathiou 1990).

Another prescription for matching theoretical power spectrum with observations is similar and involves the variance of the galaxy distribution when sampled with randomly placed spheres of radius R (see Eq.(3.24)). Normalization now corresponds to specifying σ_R for some R. For $R = 8\,h^{-1}Mpc$, the rms relative mass fluctuation is also denoted σ_8. Galaxy number counts give $\sigma_8 \approx 1$ (Peebles 1982); if galaxies trace mass on scales of several Mpc and if nonlinear effects do not modify σ_8 appreciably, then $\sigma_8 = 1$ is reasonable. In practice, this method of normalizing theoretical spectra is similar to the J_3 method.

If instead of assuming that galaxies accurately trace the mass distribution we adopt the less restrictive assumption that fluctuations in the galaxy distribution are proportional to fluctuations in the mass distribution, $(\delta\rho/\rho)_g = b\,(\delta\rho/\rho)$, $b = \text{const.} > 1$, then $\xi_g \approx \xi_\rho$ (see Kaiser 1984) and $\sigma_8 = b^{-1}$. In the $\Omega = 1$ adiabatic CDM model, which we discuss in detail in § 5.3, a "biasing" parameter of $b \approx 1.5$ is required for consistency with the observed peculiar velocities of galaxies and then the mass density fluctuations on scales $\gtrsim 8\,h^{-1}Mpc$ are expected to be linear.

Other normalization prescriptions are based on measurements of peculiar velocity fields (see Eq.(3.25)) and of fluctuations of the microwave background radiation (Peebles 1982; Abbott & Wise 1984; Smoot *et al.* 1992).

High Order Spectra

We can also evaluate higher order spectra. The *bispectrum* B is defined by the irreducible part of the 3–point correlation function in Fourier space

$$\left\langle \tilde{\delta}(\mathbf{k}_1)\,\tilde{\delta}(\mathbf{k}_2)\,\tilde{\delta}(\mathbf{k}_3)\right\rangle_c \equiv (2\pi)^3\,\delta_D(\mathbf{k}_1+\mathbf{k}_2+\mathbf{k}_3)\,B(k_1,k_2) \tag{3.44}$$

ie.

$$B(k_1,k_2) = \int d\mathbf{r}\,ds\,\zeta(\mathbf{r},\mathbf{s})\,\mathrm{e}^{i\,\mathbf{k}_1\cdot\mathbf{r}+i\,\mathbf{k}_2\cdot\mathbf{s}}\ , \tag{3.45}$$

where, in the continuous case, ζ is the connected three point correlation function.

Fry & Seldner (1982) showed that if the three–point function is of hierarchical form (see Eq.(3.17)), then the bispectrum

$$B(k_1,k_2,k_3) = Q\,[P(k_1)\,P(k_2) + P(k_1)\,P(k_3) + P(k_2)\,P(k_3)]\ , \tag{3.46}$$

with the same value of Q, which can be also estimated by the simple gravitational instability picture in perturbative theory (Fry 1984; Chapter VIII).

Similarly, for the fourth moment we have

$$\left\langle \tilde{\delta}(\mathbf{k}_1)\,\tilde{\delta}(\mathbf{k}_2)\,\tilde{\delta}(\mathbf{k}_3)\tilde{\delta}(\mathbf{k}_4)\right\rangle_c \equiv (2\pi)^3\,\delta_D\Big(\sum_i \mathbf{k}_i\Big)\,T(k_1,k_2,k_3) \tag{3.47}$$

where, by extension, T is the *trispectrum*

$$T(k_1,k_2,k_3) = \int d\mathbf{r}\,ds\,dz\;\eta(\mathbf{r},\mathbf{s},\mathbf{z})\,\mathrm{e}^{i\,\mathbf{k}_1\cdot\mathbf{r}+i\,\mathbf{k}_2\cdot\mathbf{s}+i\,\mathbf{k}_3\cdot\mathbf{z}}\ , \tag{3.48}$$

and η is the connected 4–point correlation function. In the hierachical model (see Eq.(3.18)), the trispectrum is the product of three power spectra

$$\begin{aligned} T(k_1,k_2,k_3,k_4) &= R_a\,[P(k_1)\,P(|\mathbf{k}_1+\mathbf{k}_2|)\,P(k_3) + \text{c.p. (12 terms)}] \\ &+ R_b\,[P(k_1)\,P(k_2)\,P(k_3) + \text{c.p. (4 terms)}]\ . \end{aligned} \tag{3.49}$$

Recently, Baumgart & Fry (1991) claimed a strong detection of a third moment from CfA catalogue data (Huchra *et al.* 1983) and from a compilation of galaxy redshifts in the Perseus–Pisces supercluster region (Giovanelli & Haynes 1985; Giovanelli, Haynes & Chincarini 1986; Haynes *et al.* 1988). The observed bispectrum obeys the hierarchical pattern. The trispectrum, though weakly detected at best, still follows the hierarchical pattern.

Nonvanishing higher order ($N \geq 3$) moments imply that the galaxy distribution is decidedly non Gaussian, even on those large scales where correlations are very weak. This should not be surprising: in a nonlinear theory, even an initially Gaussian primordial distribution soon develops higher order correlations (Chapter VIII).

CHAPTER IV

Growth of Perturbations

Cosmologists reasonably believe that observed structures grew from general small perturbations of the homogeneous and isotropic background in the energy density of the universe at early times.

The most largely accepted scenario to approach the structure formation is the so called *gravitational instability scenario*, which treats essentially noise amplification; ie. linear (small) perturbations at some early time grow to non linearity under their own self gravitation.

Since the beginning of modern cosmology, the role of gravity in developing the departures from homogeneity into structures like galaxies and clusters of galaxies has been at the center of exciting discussions (Einstein 1917; Jeans 1928; Lemaitre 1933a; 1933b; 1934). Curiously, Lifshitz, who developed the general analysis of linear perturbation in a Friedmann–Lemaitre model (Lifshitz 1946a; 1946b), stated that "we can apparently conclude that gravitational instability is not the source of condensation of matter into separate nebulae" (Lifshitz 1946b). Why Lifshitz's statement was not quite correct was first pointed out by Novikov (1964a; 1964b).

Another problem is to understand the physical mechanism which could generate these fluctuations. Peebles (1980, §17) takes in consideration primeval magnetic fields, perhaps present at the time of the big bang, as possible sources of mass density fluctuations.

At present, cosmologists tend to solve the problem of the *origin* of the primordial fluctuations by accepting inflation: perturbations are generated during the epoch of vacuum energy domination, when the Universe is in an accelerated expansion; primordial scalar fields driving inflation exhibit quantum fluctuations, which generate perturbations to the matter density (Bardeen 1980; Guth & Pi 1982; Hawking 1982; Starobinsky 1982; Bardeen, Steinhardt & Turner 1983; Abbott & Wise 1984; Brandenberger 1985; Mukhanov, Feldman & Branderberger 1992).

These quantum fluctuations manifest themselves as *curvature fluctuations* with a constant amplitude on the horizon scale as long as the inflation persists. Therefore it is a "natural" prediction of the inflationary model that the Universe should contain primordial fluctuations of scale–invariant form, as apparently confirmed by the more recent COBE measurements (Smoot *et al.* 1992).

Because these were generated by fluctuations in spatial curvature, they are *adiabatic* in nature, affecting the matter density and radiation density fluctuations equally, namely

$$\delta_r = \frac{4}{3}\,\delta_m \ . \tag{4.1}$$

A solution orthogonal to curvature fluctuation is conceivable: it is termed *isocurvature fluctuation.* This mode results from isothermal initial conditions, in which the matter density is perturbed, but not the radiation density

$$\delta_r = -\,\frac{\rho_m}{\rho_r}\,\delta_m \ , \tag{4.2}$$

where, in the radiation–dominated era, $\rho_m \ll \rho_r$: this generates no perturbations in the curvature, just because matter is a negligible constituent of the very early universe, instead modifying the number of photons per particle (entropy per baryon), leading to the alternative name of *entropy perturbations.*

It is more natural to produce adiabatic fluctuations than isocurvature fluctuations, namely any GUT model, in which the baryon asymmetry of the Universe is generated via baryon number violation, will produce a constant entropy per baryon (Kolb & Turner 1990). Models have been suggested in which later phase transitions (e.g. quark–hadron transition)

generate entropy fluctuations, but there is not clear evidence for them to be scale–invariant. Moreover, isothermal fluctuations generate adiabatic perturbations of the same magnitude, at horizon crossing time; this point has been further clarified by careful investigation of isothermal fluctuations through the epoch of decoupling (Suto, Sato & Kodama 1985): even initially isothermal perturbations give rise to temperature fluctuations in later stages comparable with those of initially adiabatic perturbations. This seems to rule out isothermal perturbations as a solution to the galaxy formation problem, but the possibility for them should not be rejected (Barrow & Turner 1981; Bond, Kolb & Silk 1982; Kofman & Linde 1987). For a detailed discussion of isocurvature perturbations using general relativity, see Kodama & Sasaki (1986). A recent review on cosmological perturbations is given by Mukhanov, Feldman & Brandenberger (1992).

4.1 Equations of Motion for Matter

We want now to describe in some detail the motion of nonrelativistic matter in the Universe; galaxies and clusters of galaxies are possibly tracing it now. Namely we present here the fundamental equations describing the growth of matter perturbations. We assume the (adiabatic) instability scenario: perturbations generated somehow in the early stages of the Universe start to grow when (nonrelativistic) matter begins to dominate the density of the Universe; we assume the existence of post–recombination density fluctuations in nonrelativistic components of matter; it contains nucleonic matter as well as a collisionless dark matter component clustered around galaxies and clusters of galaxies.

We treat the matter as a pressureless ($p \equiv 0$) ideal fluid, ie. the particles' paths do not cross. The standard equations for an ideal fluid are the classical Poisson equation, Euler equation and continuity equation, ie. respectively, in Eulerian formulation

$$\nabla^2 \phi = 4\pi G\, a^2 \left(\rho - \rho_b\right) , \tag{4.3}$$

$$\frac{\partial \mathbf{v}}{\partial t} + \frac{1}{a}(\mathbf{v}\cdot\nabla)\mathbf{v} + \frac{\dot{a}}{a}\mathbf{v} = -\frac{1}{a}\nabla\phi\,, \tag{4.4}$$

$$\frac{\partial \rho}{\partial t} + 3\frac{\dot{a}}{a}\rho + \frac{1}{a}\nabla\cdot\rho\mathbf{v} = 0\,. \tag{4.5}$$

All the observables, potential ϕ, peculiar velocity $\mathbf{v}$ and density ρ are functions of the comoving coordinates $\mathbf{x} = \mathbf{r}/a(t)$; the cosmic scale factor is not an unknown here, it is solution of the Friedmann equation (1.2).

The Poisson equation (4.3) states that (matter) density fluctuations originate, and are originated by, metric perturbations given by the Newtonian gravitational potential ϕ. The Euler equation (4.4) and the continuity equation (4.5) state respectively the momentum and the energy conservation during the evolution of the perturbations.

If we define the (mass) fluctuation $\delta(\mathbf{x},t)$ as

$$\rho(\mathbf{x},t) \equiv \rho_b(t)\,[1+\delta(\mathbf{x},t)]\,, \tag{4.6}$$

the previous system of equations takes the more familiar form in the literature

$$\nabla^2\phi = 4\pi G\,\rho_b\,a^2\,\delta\,, \tag{4.7}$$

$$\frac{\partial \mathbf{v}}{\partial t} + \frac{1}{a}(\mathbf{v}\cdot\nabla)\mathbf{v} + \frac{\dot{a}}{a}\mathbf{v} = -\frac{1}{a}\nabla\phi\,, \tag{4.8}$$

$$\frac{\partial \delta}{\partial t} + \frac{1}{a}\nabla\cdot(1+\delta)\,\mathbf{v} = 0\,. \tag{4.9}$$

Essentially any relativistic component contributes negligibly to the density fluctuations, therefore *fluctuations* means *mass fluctuations.*

Sometimes, looking for δ solutions, a second order differential equation is introduced, obtained combining (4.8) and (4.9); explicitly it is given by (see e.g. Peebles 1980, § 9; Fry 1984)

$$\partial_\circ^2\delta + 2\dot{a}a^{-1}\partial_\circ\delta = a^{-2}\left[\partial_\alpha(1+\delta)\,\partial_\alpha\phi + \partial_\alpha\partial_\beta\,(1+\delta)v^\alpha v^\beta\right]\,, \tag{4.10}$$

ie., from (4.7)

$$\partial_\circ^2\delta + 2\dot{a}a^{-1}\partial_\circ\delta - 4\pi G\rho_b\,\delta =$$

$$= 4\pi G\rho_b\,\delta^2 + a^{-2}\partial_\alpha\delta\,\partial_\alpha\phi + a^{-2}\partial_\alpha\partial_\beta\,(1+\delta)v^\alpha v^\beta\,, \tag{4.11}$$

where $\partial_o \equiv \partial/\partial t$, $\partial_\alpha \equiv \partial/\partial x^\alpha$ and summation over repeated indices is understood.

The Eulerian fluid equations may also be derived by taking velocity moments of the Vlasov equation for the time evolution of the phase space distribution function $f(\mathrm{x}, \mathrm{v}, t)$: the streaming velocity of the fluid is defined as the local mean momentum per unit mass of the particles (for this alternative approach see Peebles 1980, §9A).

We stress that the comoving Euler and continuity equations hold *even* for large δ; to apply Eq. (4.11) one must find some technique for dealing with the right–hand side term: in the *linear* approximation such a term is just dropped.

Linear Solutions

The lowest order solutions of the fluid equations are recovered linearizing (4.7), (4.8) and (4.9): we assume that the amplitude of the matter fluctuations is very small ($\delta \ll 1$), so that the rms particle velocity about the zeroth–order Hubble flow solution is small too. The main reason for looking for linear solutions is that surely at early times $\delta \ll 1$ (because of CBR constraints), or, in other words, the linear description may be good for describing the large scale phenomena, even if $\delta \gg 1$ on small scales.

(i) Linear δ Solution

δ is solution of the equation (just dropping the right hand side of (4.11))

$$\partial_o^2 \delta + 2\dot{a}a^{-1}\partial_o \delta - 4\pi G \rho_b \, \delta = 0 \; . \tag{4.12}$$

This equation has been discussed at lenght (Meszaros 1974; Groth & Peebles 1975).

The general growing mode (the decaying mode disappears rapidly: we shall not consider it) is given by

$$\delta(\mathrm{x}, t) = \delta_1(\mathrm{x})\, D(t). \tag{4.13}$$

Therefore the δ solution is *self–similar* in the linear regime (in fact the Eq. (4.12) does not depend on spatial derivatives): δ evolves only in amplitude, preserving their original shape. Thus in the linear regime *structure retains a memory of its origin.*

The function $D(t)$, which satisfies the ordinary equation corresponding to (4.12)

$$\ddot{D} + 2\dot{a}a^{-1}\dot{D} - 4\pi G\,\rho_b\,D = 0\ , \tag{4.14}$$

takes different forms depending on the model of Universe. For instance, in an Einstein–de Sitter universe ($\Omega = 1,\ \Lambda = 0$), we have $a \propto t^{2/3}$ and $4\pi G\rho_b = 2/3t^2$; therefore (4.14) reduces to

$$\ddot{D} + \frac{4}{3t}\dot{D} = \frac{2}{3t^2}D\ . \tag{4.15}$$

One finds

$$\delta(\mathbf{x},t) = \delta_1(\mathbf{x})\,t^{2/3}\ . \tag{4.16}$$

Solutions for open or closed universes are given in Peebles (1980, § 11): usually they are much more complicated.

We stress the fact that the solution (4.16) is *local* even though the peculiar gravitational field $\mathbf{g}$ depends on an integral over the mass distribution

$$\phi(\mathbf{x},t) = -Ga^2\rho_b \int d\mathbf{x}'\,\frac{\delta(\mathbf{x}',t)}{|\mathbf{x}'-\mathbf{x}|}\ , \tag{4.17}$$

$$\begin{aligned}\mathbf{g}(\mathbf{x},t) = -\frac{1}{a}\nabla\phi &= Ga\,\rho_b \int d\mathbf{x}'\,\delta(\mathbf{x}',t)\,\frac{\mathbf{x}'-\mathbf{x}}{|\mathbf{x}'-\mathbf{x}|^3} \\ &= Ga \int d\mathbf{x}'\,\rho(\mathbf{x}',t)\,\frac{\mathbf{x}'-\mathbf{x}}{|\mathbf{x}'-\mathbf{x}|^3}\ ;\end{aligned} \tag{4.18}$$

in fact, what is relevant is the divergence of $\mathbf{g}$ ($\nabla\cdot\mathbf{g} \propto \nabla^2\phi$), which of course depends on local density.

The evolution of δ is non–local i.e. non–selfsimilar to second order perturbation expansion.

(ii) Linear $\mathbf{v}$ *Solution*

In the linear regime, the peculiar velocity field satisfies the equations

$$\partial_\circ(a\,\mathbf{v}) = a\,\mathbf{g}\ , \tag{4.19}$$

$$\nabla\cdot\mathbf{v} = -a\,\partial_\circ\delta\ . \tag{4.20}$$

By solving the last equation

$$\mathbf{v} = a\,\partial_\circ \left(\frac{\mathbf{g}}{4\pi G \rho_b\, a} \right) , \tag{4.21}$$

which, once substituted in (4.19), gives us

$$\partial_\circ \left(a^2\, \partial_\circ \frac{\mathbf{g}}{\rho_b\, a} \right) = 4\pi G a\, \mathbf{g} . \tag{4.22}$$

This is another form of the Eq.(4.12). The growing mode of the velocity field $\mathbf{v}$ corresponds to the growing mode of the density field in (4.16):

$$\mathbf{v} = \frac{\mathbf{g}}{4\pi G \rho_b} \frac{d \ln D}{dt} . \tag{4.23}$$

In an Einstein–de Sitter universe we recover the classical $\mathbf{v} = \mathbf{g}\, t$ ($\sim t^{1/3}$). Eq.(4.23) is usually known in the form (e.g. Peebles 1980, Eq.(14.8))

$$\mathbf{v} = \frac{H f}{4\pi G \rho_b} \mathbf{g} = \frac{2f}{3H\Omega} \mathbf{g} , \tag{4.24}$$

where

$$f = f(\Omega) \equiv \frac{d \ln D}{d \ln a} \tag{4.25}$$

is the logarithmic growth rate. The approximation $f(\Omega) \approx \Omega^{0.6}$ is commonly used (Peebles 1980); more accurately, the leading term near $\Omega = 1$ is $f(\Omega) = \Omega^{4/7}$ (Lightman & Schecter 1990; actually the first one to work out this result was Fry, in a not well known paper (Fry 1985b)). We stress the fact that $\mathbf{v}$ is parallel to the acceleration $\mathbf{g}$ (since (4.19)).

Eq.(4.24) is extremely important in observational cosmology; it offers the possibility of determining the density parameter Ω: this is usually done by measuring the infall velocity of the Local Group towards the Local Supercluster (see Davis & Peebles 1983).

We shall often use alternative expressions of the linear velocity; defining the Newtonian potential

$$\triangle \equiv \frac{\phi}{4\pi G \rho_b\, a^2} = -\frac{1}{4\pi} \int d\mathbf{x}' \, \frac{\delta(\mathbf{x}', t)}{|\mathbf{x}' - \mathbf{x}|} , \tag{4.26}$$

for which

$$\nabla^2 \triangle = \delta \,, \tag{4.27}$$

$$\mathbf{g} = -4\pi G \rho_b \, a \, \nabla \triangle \,, \tag{4.28}$$

we get

$$\mathbf{v} = -\frac{1}{4\pi G \rho_b \, a} \frac{\dot{D}}{D} \nabla \phi = -a \, \partial_\circ \nabla \triangle = -a \frac{\dot{D}}{D} \nabla \triangle \,. \tag{4.29}$$

It is evident from these expressions that $\mathbf{v}$ has zero vorticity.

It is often convenient, especially for instance when going to higher orders in perturbation theory, to work in k–space, where one wins simplicity, since derivatives become simple algebraic operations.

The linear (growing) solutions of the equations of matter in k–space look, respectively

$$-\, k^2 \, \tilde{\triangle}(\mathbf{k}) = \tilde{\delta}(\mathbf{k}) \,, \tag{4.30}$$

$$\tilde{v}^\alpha(\mathbf{k}) = i \, a \frac{\dot{D}}{D} \tilde{\delta}(\mathbf{k}) \frac{k^\alpha}{k^2} \,. \tag{4.31}$$

This simplification is not obtained at no cost, however; for instance the simple products in x–space ($\cdot$) become *convolutions* ($*$) in the transform formulation

$$F\left(\prod_{h=1}^{N} f_h(\mathbf{x})\right) \equiv \Big(*\Big)_{h=1}^{N} \tilde{f}_h(\mathbf{k}_h) =$$

$$\frac{1}{(2\pi)^{3N}} \int d\mathbf{k}_1 \cdots \int d\mathbf{k}_N \left[(2\pi)^3 \, \delta_D\Big(\sum_{h=1}^{N} \mathbf{k}_h - \mathbf{k}\Big)\right] \prod_{h=1}^{N} \tilde{f}_h(\mathbf{k}_h) \,.$$

Typical Scales: Critical Jeans Length

We have seen how the matter perturbations in an expanding universe grow; effectively, processes other than gravity can modify our simple description. Competing effects of gravity and pressure gradient force are in fact important before the recombination or in correspondence of small scales: the more important result of taking into account the radiation

pressure is that not all the matter perturbations are destined to grow, but only those above a precise scale.

Before recombination, matter is Compton radiation dragged and the matter plus radiation fluid can be treated as an ideal fluid.

Modifying the Euler equation to consider the pressure contribution, one finds that perturbation amplitudes of comoving wavelength $\lambda/a = 2\pi/k$ are described by a linear acoustic wave equation with Hubble dragging and gravitational driving terms (Peebles 1980)

$$\partial_\circ^2 \tilde{\delta}(\mathbf{k},t) + 2\dot{a}a^{-1}\partial_\circ \tilde{\delta}(\mathbf{k},t) = 4\pi G\rho_b \left[1 - \frac{\lambda_J}{\lambda}\right] \tilde{\delta}(\mathbf{k},t) \,. \tag{4.32}$$

At very long wavelengths (very large scales), $\lambda \to \infty$, this equation reduces to the zero pressure case discussed previously; but, at small scales, $\lambda \to 0$, the pressure term is dominant and the primordial plasma simply oscillates just like an acoustic wave. The balance between tha pure gravitational regime and the acoustic regime occurs at the scale

$$\lambda = \lambda_J \equiv c_s\sqrt{\pi/G\rho_b} \,, \tag{4.33}$$

$c_s^2 = dp/d\rho$ being the square of the adiabatic sound speed. λ_J is called the *Jeans length* ; it defines equivalently the *Jeans mass*

$$M_J = \frac{4}{3}\pi\,\rho_b \left(\frac{\lambda_J}{2}\right)^3 = \frac{\pi}{6}\,\rho_b\,\lambda_J^3 \,. \tag{4.34}$$

M_J (ie. λ_J) fixes the smallest scale on which gravitational instability can be expected. At the recombination z_{rec}, M_J drops from its highest value $\approx 2.2 \times 10^{17}\,(\Omega h)^{-2} M_\odot$ to the much smaller $\approx 1.27 \times 10^6\,(\Omega h)^{-1/2} M_\odot$, just because c_s drops from $c/\sqrt{3}$ to $\sqrt{5k_BT/3m_p}$ ($\approx 10\,km\,s^{-1}$), then $M_J \propto a^{-3/2}$ as the temperature falls down.

We know that the perturbations with $\lambda > \lambda_J$ grow as a power t^α of the cosmic time t (in a flat universe); those with $\lambda < \lambda_J$ behave like oscillating waves: in the limit $p \ll \rho c^2$ the cosmic expansion damps their amplitude (but not in the case $p = \rho c^2/3$) according to the law

$$\delta \sim [c_s(t)\,a(t)]^{-1/2}\, \mathrm{e}^{-i\int^t dt\, c_s k/a} \,. \tag{4.35}$$

We could reconstruct at this point the history and the fate of a relevant sized fluctuation, say on a galaxy scale $M_G \sim 10^{11} M_\odot$, but the picture is effectively complicated by another process that we have not considered, the *Silk damping* (Silk 1968): the photon diffusion indeed damps out very efficiently the adiabatic baryon fluctuations below the Silk scale during the radiative era. The Silk scale can be estimated as follows. The photon mean free path is given by $l \sim (\sigma_T n_e)^{-1}$, where σ_T is the Thomson scattering cross–section and n_e is the number density of electrons. A photon diffuses a distance λ in the time $\tau_d(\lambda) \sim \lambda^2/lc$; the Silk damping scale is found if we equal $\tau_d(\lambda)$ to the Hubble time t ie. $\lambda_S \sim (lct)^{1/2}$, and the Silk mass is defined by

$$M_S = \frac{\pi}{6} \rho_m \lambda_S^3 \,. \tag{4.36}$$

Detailed calculations show that, at recombination (Silk 1968; Peebles & Yu 1970; Bonometto & Lucchin 1976; Press & Vishniac 1980; Wilson & Silk 1981; Peebles 1980; 1981)

$$M_S \approx 10^{12} (\Omega h^2)^{-5/4} \,. \tag{4.37}$$

All the fluctuations $\lambda < \lambda_S$ are damped by photon diffusion, since $\tau_d < t$; the damping rate, determined also by the fractional ionization of the hydrogen, increases for decreasing scales.

Depending on the spectrum of the primordial perturbation, the cutoff at M_S may fix the size of the first generation of objects to form after recombination. If $\Omega h^2 = 1$, $M_S \approx 10^{12} M_\odot$; if $\Omega h^2 = 0.03$, $M_S \approx 10^{14} M_\odot$ and it is very interesting that one can find a reasonable interpretation for either of these numbers: the mass in the visible parts of the largest galaxies is $\sim 10^{12} M_\odot$ and the nominal mass in a rich cluster is $\sim 10^{14} M_\odot$. Thus, typical galaxies, $\sim 10^{11} M_\odot$, can form only by *fragmentation* of larger collapsed perturbations. This opens another problem. The value of the Silk cutoff, extrapolated to the present epoch is

$$\lambda_S \approx 2/(0.036 + \Omega h^2)\, Mpc \,, \tag{4.38}$$

which is uncomfortably large for any acceptable baryonic universe: if the amplitude at recombination is large enough to make bound systems of size M_S form, then we should also see density fluctuations of large amplitude on the scale λ_S. This *strongly* contradicts

the observations that the galaxy 2–point correlation function is less than unity at $r \gtrsim r_0 \sim 4\,h^{-1}\,Mpc$.

A way to solve the problem is to consider the isocurvature modes. In such a case, there is no Silk damping, just because the radiation is smoothed, and fluctuations on scales below the baryon Jeans mass (now $10^6\,M_\odot$) can grow after recombination: in this picture, the larger structures form by hierarchical merging of sub smaller scale structures. This scenario, popular in the 1970's, is not actually so favoured, mainly because of small scale anisotropy constraints from CBR (Bond & Efstathiou 1984; Vittorio & Silk 1984), detailed N—body studies (Frenk 1986) and, overall, the requirement that Ω should take the value unity: this can occur only in non–baryonic dark matter universes, as we shall discuss in a next section.

4.2 Density Evolution Via Gravitational Potential *

An equivalent way to describe the dynamical evolution of density fluctuations is directly in terms of gravitational potential ϕ. Unlike the density fluctuation field, the gravitational potential is required neither to have zero mean (since only its *gradient* is physically meaningful), nor to satisfy the positive–mass constraint (see Eq.(2.5)). Furthermore, in linear approximation, density and velocity fields may be described in terms of the same gravitational potential ϕ, which practically does not change in time during the linear regime. In this section, we assume a matter dominated Einstein–de Sitter Universe. We derive a particular form of the equations governing the evolution of the gravitational potential ϕ and the velocity potential Φ which allows us to cancel out *automatically* the rotational part of the velocity field. An advantage of this is that we can easily work out the higher–order velocity contributions $\mathbf{v}^{(n)}$ (see Chapters VII and VIII) in a manifestly irrotational form in Eulerian configuration space [all the previous irrotational expressions for $\mathbf{v}^{(n)}$ were obtained in Fourier space (see Goroff *et al.* 1986)]. The importance of having explicit irrotational

expressions for the velocity field at any perturbative order lies on the fact that a collisionless gravitating fluid cannot generate vorticity (before orbit mixing) and that the conservation of circulation is applicable well beyond the linear regime. I anticipate here some calculations of a forthcoming work (Catelan *et al.* 1993a).

The potential ϕ defines the mass fluctuation δ via the Poisson Equation

$$\delta = Aa\nabla^2\phi \ , \qquad A \equiv \frac{3}{2} \ . \tag{4.39}$$

In particular, we may think that δ contains only the growing mode $D(t)\delta_1$.

We introduce a new comoving velocity

$$\mathbf{u} \equiv \frac{d\mathbf{x}}{da} = \frac{\mathbf{v}}{a\,\dot{a}} \ . \tag{4.40}$$

In this notation, the time variable is $a(t)$ instead of t. The continuity equation and the Euler equation become

$$\frac{\partial\delta}{\partial a} + \nabla\cdot(1+\delta)\mathbf{u} = 0 \tag{4.41}$$

$$\frac{\partial\mathbf{u}}{\partial a} + (\mathbf{u}\cdot\nabla)\mathbf{u} + \frac{3}{2a}\mathbf{u} = -\frac{3A}{2a}\nabla\phi \ , \tag{4.42}$$

or, if

$$\frac{d}{da} \equiv \frac{\partial}{\partial a} + (\mathbf{u}\cdot\nabla) \ , \tag{4.43}$$

alternative forms are

$$\frac{d\delta}{da} + (1+\delta)\nabla\cdot\mathbf{u} = 0 \ , \tag{4.44}$$

$$\frac{d\mathbf{u}}{da} = -\frac{3}{2a}(\mathbf{u} + A\nabla\phi) \ . \tag{4.45}$$

Outside regions of orbit mixing (initially irrotational flow), we can define the velocity potential $\Phi_u = \Phi(\mathbf{x}, a) \equiv \Phi$

$$\mathbf{u} = \nabla\Phi \ . \tag{4.46}$$

From Eq.(4.42), we obtain

$$\frac{\partial\nabla\Phi}{\partial a} + (\nabla\Phi\cdot\nabla)\nabla\Phi = -\frac{3}{2a}(\nabla\Phi + A\nabla\phi) \ .$$

Since

$$(\mathbf{e}\cdot\nabla)\mathbf{e} = \frac{1}{2}(\nabla\mathbf{e})^2 - \mathbf{e}\wedge(\nabla\wedge\mathbf{e})\,,$$

we have

$$\frac{\partial\Phi}{\partial a} + \frac{1}{2}(\nabla\Phi)^2 = -\frac{3}{2a}(\Phi + A\phi)\,. \tag{4.47}$$

This equation is known as *Bernoulli Equation* for a cosmological pressureless potential flow: it relates the velocity potential Φ to the gravitational one. Nusser and Dekel (1992) used this differential equation in the Zel'dovich approximation (Zel'dovich 1970; see Section IV.4) to recover the growing mode of the initial fluctuations of a cosmological gravitating system from the present large–scale peculiar velocity and density field.

From Eqs.(4.24) and (4.46), in linear regime, we have

$$\Phi^{(1)} = -A\phi^{(1)}\,, \tag{4.48}$$

and the Bernoulli equation reduces to

$$\frac{\partial\Phi^{(1)}}{\partial a} = 0\,, \tag{4.49}$$

ie. the linear gravitational potential is constant in time, as can be directly deduced from Eq.(4.39), since $\delta \propto a$.

Furthermore, from Eq.(4.41), one gets

$$\frac{\partial}{\partial a}(Aa\nabla^2\phi) + \nabla\cdot(1 + Aa\nabla^2\phi)\nabla\Phi = 0\,, \tag{4.50}$$

ie.

$$\nabla\cdot\left[\frac{\partial}{\partial a}(Aa\nabla\phi) + (1 + Aa\nabla^2\phi)\nabla\Phi\right] = 0\,. \tag{4.51}$$

To summarize:

the fundamental equations for the potentials Φ and ϕ are

$$\begin{cases} A\nabla^2\phi = \dfrac{\delta}{a} \;; \qquad \nabla\Phi = \mathbf{u} \;, \\ \\ \dfrac{\partial\Phi}{\partial a} + \dfrac{1}{2}(\nabla\Phi)^2 = -\dfrac{3}{2a}(\Phi + A\phi) \;, \\ \\ \nabla\cdot\left[\dfrac{\partial}{\partial a}(Aa\nabla\phi) + (1 + Aa\nabla^2\phi)\nabla\Phi\right] = 0 \;. \end{cases} \tag{4.52}$$

A general solution of the last of the previous equations is

$$\frac{\partial}{\partial a}(Aa\nabla\phi) + (1 + Aa\nabla^2\phi)\nabla\Phi = \nabla\wedge\mathbf{F} \;. \tag{4.53}$$

The last term in the l.h.s of this equation may be written as (apart of an additional harmonic function)

$$(Aa\nabla^2\phi)\nabla\Phi = \delta\mathbf{u} \equiv \nabla f + \nabla\wedge\mathbf{F} \;, \tag{4.54}$$

in such a manner that the rotational part in Eq.(4.53) is canceled out:

$$\frac{\partial}{\partial a}(Aa\nabla\phi) + \nabla\Phi + \nabla f = 0 \;. \tag{4.55}$$

The function f satisfies the differential equation

$$\nabla^2 f = \nabla\cdot(\delta\mathbf{u}) = \delta\nabla^2\Phi + \nabla\delta\cdot\nabla\Phi \;. \tag{4.56}$$

We can rewrite the set of equation for the cosmological potentials as (Catelan *et al.* 1993a)

$$\begin{cases} \dfrac{\partial}{\partial a}(Aa\phi) + \Phi + f = 0 \;, \\ \\ \dfrac{\partial\Phi}{\partial a} + \dfrac{1}{2}(\nabla\Phi)^2 = -\dfrac{3}{2a}(\Phi + A\phi) \;, \\ \\ \nabla^2 f = Aa\nabla\cdot[\nabla^2\phi\nabla\Phi] = Aa\left[\nabla^2\phi\nabla^2\Phi + \nabla\nabla^2\phi\cdot\nabla\Phi\right] \;. \end{cases} \tag{4.57}$$

We stress the fact that the function f is by construction at least a second–order quantity;

the first order form of the set of equations (4.57) is therefore

$$\begin{cases} A\phi^{(1)} + \Phi^{(1)} = 0 \,, \\ \\ \dfrac{\partial \Phi^{(1)}}{\partial a} = 0 \,. \end{cases} \tag{4.58}$$

already known. We shall show in Section IV.4 how some approximations of the nonlinear evolution of density fluctuation, e.g. the Zel'dovich approximation or the frozen–flow approximation (see Section VIII.2), may be described in terms of the gravitational potential ϕ. Furthermore, we shall look for perturbative solutions of the set of equations (4.57) to improve the frozen–flow approximation in a new scheme named *Local–Flow approximation* (Catelan *et al.* 1993a).

4.3 Lagrangian Picture *

In the previous sections, the equations of motion are formulated in the Eulerian picture, namely the motion of the fluid is considered relative to some frame of reference (coordinate system) which is unattached to the fluid. An opposite point of view is the so called *Lagrangian* formulation, in which the paths of each particle or fluid element are followed during the evolution. In this case, each particle is labeled by e.g. its initial (comoving) coordinate. Therefore, at the beginning, say $t = t_0$, Eulerian and Lagrangian coordinates coincide, $\mathbf{q} = \mathbf{x}(a_0)$, where $a_0 \equiv a(t_0)$ (we are using the scale factor a as temporal parameter). In the Lagrangian space, the particle's paths are described by the maps from $\mathbf{q}$ to $\mathbf{x}(\mathbf{q}, a)$, which are now constructed as a new vectorial field (the variables $\mathbf{x}$ are instead independent in the Eulerian picture). If we restrict to the case of a collisionless dust in which the particles interact only by gravity, then the equations of motion are the geodesic equations. Namely

the velocity $\mathbf{u}$ and the gravitational field strength $d^2\mathbf{x}/da^2$ are expressed as follows

$$\frac{d\,\mathbf{x}(\mathbf{q},a)}{da} = \mathbf{u}(\mathbf{q},a)\,, \tag{4.59}$$

$$\frac{d^2\mathbf{x}(\mathbf{q},a)}{da^2} = -\frac{3}{2a}\Big(\mathbf{u}[\mathbf{x}(\mathbf{q},a),a] + A\nabla\phi[\mathbf{x}(\mathbf{q},a),a]\Big)\,, \tag{4.60}$$

where $A = 3/2$ [see Eq.(4.45)]. The time derivatives are all taken at fixed $\mathbf{q}$, precisely $\frac{d}{da} \equiv \partial_a|_{\mathbf{x}} + \mathbf{u}\cdot\nabla_{\mathbf{x}} \equiv \partial_a|_{\mathbf{q}}$ is the usual convective Lagrangian time derivative, which follows the element of fluid. The gravitational potential ϕ is related to the density fluctuation δ via the Poisson equation. To find the solution δ of continuity equation in Lagrangian formulation, we can merely apply the conservation of mass ie.

$$\rho[\mathbf{x}(\mathbf{q},a),a]\,d\mathbf{x} = \rho_b(a)\,d\mathbf{q}\,, \tag{4.61}$$

where ρ_b is the Lagrangian density ie. the background mean density. The density contrast $\eta \equiv 1 + \delta[\mathbf{x}(\mathbf{q},a),a] \equiv \eta_c$ is therefore given by

$$\eta_c = \left\|\frac{\partial\mathbf{x}}{\partial\mathbf{q}}\right\|^{-1}\,, \tag{4.62}$$

where $\|\partial\mathbf{x}/\partial\mathbf{q}\|$ is the determinant of the Jacobian J of the map $\mathbf{q} \to \mathbf{x}(\mathbf{q},a)$. Eqs.(4.59) and (4.60) are just the definitions of the velocity and acceleration fields, and Eq.(4.62) gives the general solution of the Eulerian continuity equation [see e.g. Eq.(4.41)] determining the density field in terms of the derivatives of the field of trajectories [1]. Therefore, in the Lagrangian framework, all the Eulerian fields can be represented in terms of a single dynamical field $\mathbf{x}(\mathbf{q},a)$ tracing the trajectories of fluid elements. The Lagrangian system of equations describing a collisionless fluid is given by the equations (4.59) and (4.60) for the field $\mathbf{x}(\mathbf{q},a)$, the mass conservation relation (4.61) and the Poisson equation (4.39).

The mass conservation relation (4.62) implicitely assumes that there is a one–to–one correspondence between the Eulerian coordinate $\mathbf{x}$ and the Lagrangian one $\mathbf{q}$ ie. particle trajectories do not intersect. It can be compared with the formal solution of the continuity

[1] We have to use the identity $\frac{d}{da}\|J\| = \|J\|\nabla_{\mathbf{x}}\cdot\mathbf{u}$ to obtain $\frac{d}{da}\eta = \eta\nabla_{\mathbf{x}}\cdot\mathbf{u} \Longrightarrow \frac{d}{da}[\eta\|J\|] = 0 \Longleftrightarrow \eta = \|J\|^{-1}$. Therefore, irrespectively of *any* equation which the trajectories $\mathbf{x}$ obey, mass conservation is guaranteed.

equation (4.44) ie.

$$\eta[\mathbf{x}(\mathbf{q},a),a] = \eta_0\, \mathrm{e}^{\left\{-\int_{a_0}^{a} da' \nabla\cdot\mathbf{u}[\mathbf{x}(\mathbf{q},a'),a']\right\}} \,. \tag{4.63}$$

Before the particle trajectories start to intersect (shell–crossing or caustic formation) equations (4.62) and (4.63) concide, but the advantage of using Eq.(4.63) instead of Eq.(4.62) is that the former can be continued after the first caustic formation, since the integration is just along the particle trajectory $\mathbf{x}(a)$. The canonical mass conservation (4.63) has been used in some recent approximation scheme of the non–linear evolution of the large scale structures, namely the frozen–flow approximation, in which the Euler equation is linearized (Matarrese *et al.* 1992; see Chapter VIII) and the LEP approximation, in which the gravitational potential is assumed to remain constant up to the present (Brainerd, Scherrer & Villumsen 1993). Both these approximation schemes may be considered as an improvement with respect to the classical Zel'dovich approximation (Zel'dovich 1970), which can be recovered if one takes the linear perturbative approximation of the Lagrangian trajectories. We follow a review by Bertschinger (1992).

4.4 Zel'dovich approximation *

When the density perturbations are small ($\delta^2 \ll 1$), one can describe the deformation of the field $\mathbf{x}(\mathbf{q},a)$ as follow

$$\mathbf{x}(\mathbf{q},a) = \mathbf{q} + \mathbf{S}^{(1)}(\mathbf{q},a) + \mathbf{S}^{(2)}(\mathbf{q},a) + \cdots \,, \tag{4.64}$$

where higher order terms are taken to be rapidly diminishing. In practice the method is to seek perturbative solutions within the Lagrangian framework [2]. In the same manner, one can expand density and gravitational potential fields. Taking up to the first order of the

[2]While the Eulerian perturbative theory has been extensively discussed (see Chapter VII and references therein), the Lagrangian perturbative method is relatively unexplored (Buchert 1992; Bouchet *et al.* 1992; Gramann 1993a, b; Lachieze–Rey 1993a, b).

Lagrangian expansion (4.64), the mass conservation (4.62) may be written as

$$\delta_c = \left\| I + \frac{\partial \mathbf{S}^{(1)}}{\partial \mathbf{q}} \right\|^{-1} - 1 \,, \tag{4.65}$$

and, evaluating the mass density to first order, one gets

$$\delta^{(1)}[\mathbf{x}, a] = -\nabla_{\mathbf{q}} \cdot \mathbf{S}^{(1)}(\mathbf{q}, a) \,. \tag{4.66}$$

The Poisson equation (4.39) may be now expressed in terms of the displacement field S. If we decompose $\mathbf{S}^{(1)}(\mathbf{q}, a)$ into its longitudinal and transverse parts, specifically $\mathbf{S}^{(1)} \equiv \mathbf{S}^{(1)}_{\parallel} + \mathbf{S}^{(1)}_{\perp}$, such that

$$\nabla_{\mathbf{q}} \cdot \mathbf{S}^{(1)}_{\perp} = 0 \;\; ; \qquad \nabla_{\mathbf{q}} \wedge \mathbf{S}^{(1)}_{\parallel} = \mathbf{0} \,, \tag{4.67}$$

it results that only the longitudinal (irrotational) part originates a gravitational perturbation ie. a density perturbation

$$A \nabla_{\mathbf{q}} \phi^{(1)} = -\frac{\mathbf{S}^{(1)}_{\parallel}}{a} \,. \tag{4.68}$$

From the equation of motion (4.60) we get the partial differential equation for $\mathbf{S}^{(1)}$,

$$\frac{\partial^2 \mathbf{S}^{(1)}}{\partial a^2} + \frac{3}{2a} \frac{\partial \mathbf{S}^{(1)}}{\partial a} = \frac{3}{2a^2} \mathbf{S}^{(1)}_{\parallel} \,. \tag{4.69}$$

The transverse part of this equation gives the *rotational* perturbation modes (we are not interested on such modes, since we shall essentially treat only collisionless gravitating fluids, without any tangential stresses such as e.g. magnetic stresses). The longitudinal part is equivalent to the linear equation (4.12) for the Eulerian density perturbation δ in the limit of collisionless fluid. The solution may be looked in the form $D(a)\mathbf{S}(\mathbf{q})$. One gets, to first order

$$\mathbf{x}(\mathbf{q}, a) = \mathbf{q} + a\, \mathbf{S}(\mathbf{q}) \,, \tag{4.70}$$

where now $\mathbf{S}(\mathbf{q})$ is a longitudinal vector field which we shall call, following Bertschinger (1992), *linear growing-mode displacement field.* Because $\mathbf{S}(\mathbf{q})$ is considered a first-order quantity, we may change the argument from $\mathbf{q}$ to $\mathbf{x}$; from Eq.(4.66) we get

$$\delta^{(1)} = -\, a\, \nabla \cdot \mathbf{S} \,, \tag{4.71}$$

and from Eq.(4.59)

$$\mathbf{u}(\mathbf{q},a) = \mathbf{S}(\mathbf{x}) = a^{-1}\,(\mathbf{x}-\mathbf{q})\,. \tag{4.72}$$

We see therefore that the linear displacement field $\mathbf{S}$ corresponds to the velocity field $\mathbf{u}$ or $\mathbf{S}(\mathbf{q}) = \nabla\Phi(\mathbf{q}) = \nabla\Phi(\mathbf{x},0)$. The *Zel'dovich approximation* (Zel'dovich 1970) corresponds to the non–linear solution obtained by extrapolating the straight paths of Eq.(4.70) *beyond* the linear regime of strict applicability, then computing exactly the density using the continuity equation [see Eq.(4.63)]. Let us define the *deformation tensor* with components $\mathcal{D}_{hj} \equiv \partial^2\Phi(\mathbf{q})/\partial q_h \partial q_j$. Since the displacement field is longitudinal, the deformation tensor is symmetric and may be (locally) diagonalized. In the principal axes frame the eigenvectors are orthogonal and let be $\lambda_1(\mathbf{q}), \lambda_2(\mathbf{q}), \lambda_3(\mathbf{q})$ the eigenvalues. The expression (4.62) for the density field may be written as

$$1 + \delta_c(\mathbf{q},a) = ||I + a\,\mathcal{D}||^{-1} = \frac{1}{[1+a\,\lambda_1]\,[1+a\,\lambda_2]\,[1+a\,\lambda_3]}\,. \tag{4.73}$$

According to the latter expression, collapse to infinite density (caustic) may occur at those points in Lagrangian space where the deformation tensor has (at least one) negative eigenvalues. Collapse first occur along the eigenvector direction corresponding to the most negative eigenvalue. In the most general case, in which e.g. $\lambda_1 < \lambda_2 < \lambda_3$, this one–dimensional collapse leads to two–dimensional surfaces ("pancakes"); collapse after that continues along the direction corresponding to the second most negative eigenvalue (where it does exist), compressing the matter in the plane of the pancake and leading to a filament. Finally, collapse occurs along the last direction, forming a knot i.e. a cluster–like configuration. Such a qualitative description is essentially confirmed by numerical calculations of gravitational instability. A very fine review may be found in Shandarin and Zel'dovich (1989). More in detail, according to Doroshkevich (1970) and Shandarin and Zel'dovich (1984) if Φ is a Gaussian random field, there is a 42% chance to have one negative and two positive eigenvalue and 42% to have the opposite situation. In the 8% of the cases all three eigenvalues are negative. The remaining 8% is the case of three positive eigenvalues, corresponding to the expansion of a void (i.e. regions where $\delta < 0$). The actual shape of the final configurations

just depends on the precise λ_h/λ_j ratios.

Zel'dovich Approximation in terms of the Gravitational Potential

We want now to show as the Zel'dovich approximation may be formulated in terms of an equation for gravitational potential. According to the results of Section IV.2, the fondamental equations for the potentials Φ and ϕ, where $A\nabla^2\phi = \delta/a$ and $\nabla\Phi = \mathbf{u}$, are

$$\begin{cases} \dfrac{\partial\Phi}{\partial a} + \dfrac{1}{2}(\nabla\Phi)^2 = -\dfrac{3}{2a}(\Phi + A\phi) \,, \\ \\ \nabla\cdot\left[\dfrac{\partial}{\partial a}(Aa\nabla\phi) + (1 + Aa\nabla^2\phi)\nabla\Phi\right] = 0 \,. \end{cases} \tag{4.74}$$

Substituting ϕ from the first equation to the second we may reduce the problem even to a single equation for the field Φ. In the one–dimensional case, the exact solution of the previous set of equations is

$$\phi = -A^{-1}\Phi \,, \tag{4.75}$$

where

$$\frac{\Phi}{\partial a} + \frac{1}{2}(\nabla\Phi)^2 = 0 \,. \tag{4.76}$$

In the three–dimensional physical case and in the *linear* regime, this solution also satisfies the basic equations. The ansatz leading to the Zel'dovich approximation consists to extend the relations (4.75) and (4.76) *beyond* the range of applicability, namely in the nonlinear regime too. Indeed, it is not difficult to show that the solution of Eq.(4.76) (e.g. Kofman 1991)

$$\Phi(\mathbf{x}, a) = \Phi(\mathbf{q}) + \frac{(\mathbf{x} - \mathbf{q})^2}{2a} \,, \tag{4.77}$$

leads to the

$$\mathbf{x} = \mathbf{q} + a\nabla\Phi(\mathbf{q}) \,, \tag{4.78}$$

which is just the already obtained Eq.(4.70). The relation (4.78) allow a simple geometrical description of the Zel'dovich approximation. If one inserts the osculating paraboloid $\mathcal{P} = \frac{(\mathbf{q}-\mathbf{x})^2}{2a} - \Phi(\mathbf{x}, a)$ between the hypersurface of the initial linear gravitational potential $\phi =$

$-A^{-1}\Phi(\mathbf{q})$ at the point $\mathbf{q}$, then the Eulerian coordinate $\mathbf{x}$ at the given time $a(t)$ is just the projection of the apex of $\mathcal{P}$. The internal inconsistency of extrapolating the condition (4.75) beyond the linear regime may be seen in the following way. Inserting the ansatz $\phi = -A^{-1}\Phi$ into the Poisson equation, one gets an alternative expression for the density fluctuation field $\delta_{dyn} = -a\nabla\cdot\mathbf{u}$, which is nothing but the linear relation between peculiar velocity and density perturbation. This point has been discussed by Nusser et al. (1991) who indicate δ_{dyn} as *dynamical* density, to distinguish it from the continuity density in Eq.(4.73). Substituting the dynamical density δ_{dyn} in the conservation equation Eq.(4.44)

$$1 + \delta_{dyn} = \frac{1}{1 + a[\lambda_1 + \lambda_2 + \lambda_3]} \,. \tag{4.79}$$

This relation shows that the Zel'dovich ansatz is exact in one dimension or for one–dimensional perturbations, in that equations (4.73) and (4.79) coincide; however, in the general three–dimensional case it fails. As shown by Nusser *et al.* (1991), the dynamical density contrast tends to overestimate the "correct" result, whereas δ_c typically underestimates it; they also argue that the mean value $(\delta_c + \delta_{dyn})/2$ provides a better approximation to the actual value of the evolved density field δ. Very recently, Gramann (1993) applying a *second*–order Lagrangian perturbative theory [the Zel'dovich approximation corresponding to the first–order; see Eq.(4.64)] showed that it is possible to satisfy simultaneously the requirements of mass conservation and momentum conservation, and for flat models ($\Omega = 1$) the consistency between the second–order dynamical and continuity density is exact. Finally, it is worth to mention that an *Eulerian* expression for the comoving density can be obtained by starting from the phase–space distribution of particles which move according to the Zel'dovich approximation (Grinstein & Wise 1987; a discussion of this representation of the Zel'dovich approximation is reported in Chapter VII).

4.5 An Application of Linear Theory: The Local Group Motion

The strongest evidence for a peculiar motion of the Local Group (LG) of galaxies is provided by the observations of the CBR.

Since the first convincing detection of anisotropy in the CBR (Fabbri *et al.* 1980), it was realized that a dipole anisotropy characterizes the microwave sky map: the dipole, amplitude $\triangle T/T \approx 1.2 \times 10^{-3}$, points roughly towards 45° away from the Virgo Cluster (namely, in galactic coordinates: $l = 268°$, $b = 27°$). The usual interpretation is that such a dipole is not a cosmological phenomenum, instead it is originated by the fact that the Earth is moving with respect the CBR rest frame. The recent spectacular COBE measurements confirm that $\triangle T/T = 1.2 \pm 0.03 \times 10^{-3}$ and $v_{LG} = 622 \pm 20\, km\, s^{-1}$ towards $(l, b) = (277° \pm 2°, 30° \pm 2°)$ (Smoot *et al.* 1991).

Using determinations of solar motion relative to the LG (Yahil, Tamman & Sandage 1977), Davis and Peebles (1983) quantified one component of the LG velocity, precisely the LG infall velocity towards the Virgo Cluster, located roughly at the center of the Local Supercluster ($\sim 10\, h^{-1} Mpc$ far from us). Knowing this, Davis and Peebles (1983) did the first determination of Ω_o from large scale dynamics. Adopting a simple spherical model, the LG infall velocity at distance R from the Virgo Cluster is related to the excess of mass δM located there by the linear equation (4.24)

$$v_V = \frac{2\, G\, f(\Omega_o)}{3\, H_o R^2\, \Omega_o}\, \delta M \ , \tag{4.80}$$

or

$$v_V = \frac{1}{3}\, H_o\, R\, \Omega_o^{0.6}\, \frac{\delta M}{M} \ . \tag{4.81}$$

Assuming the Local Supercluster to be a fair indicator of the distribution of matter ie. estimating $\delta M/M = \delta N/N = \delta$, where $\delta N/N$ is the concentration of bright galaxies in the LSC, one obtains

$$\Omega_o^{0.6} = 3 \left(\frac{v_V}{v_H}\right) \delta \ , \tag{4.82}$$

$v_H = H_o\, r$ being the Hubble flow velocity. Measurements in the LSC give $\delta N/N = 2.2 \pm 0.3$; $v_V = 400 \pm 60\, km\, s^{-1}$ and (Davis & Peebles 1983)

$$\Omega_{o,LSC} \approx 0.2 \,. \tag{4.83}$$

The uncertainty on $\Omega_{o,LSC}$ is essentially due to the uncertainty in v_V; on the other hand, a simple spherical model does not seem quite adequate, in view of the fact that the LG peculiar motion with respect to the rest frame of the MWB has other components besides v_V.

Many efforts are actually devoted to understanding the peculiar motion of the LG and its origin. Further modifications of the smooth Hubble flow have been revealed, and there is evidence that the LG motion is shared by the whole local volume within $30 \div 40\, h^{-1} Mpc$ (Staveley–Smith & Davies 1987; 1988).

An innovative suggestion has been advanced that the local galaxy bulk motions are caused by enormous mass concentrations just beyond $\approx 40\, h^{-1} Mpc$ (Dressler *et al.* 1987; Burstein 1989; Kaiser 1990a; Dressler 1991), this opening the era of the huge "attractors" (see e.g. Scaramella *et al.* 1989).

Another open question is the determination of Ω_o from large scales. Among others, an elegant technique consists in calculating the peculiar acceleration acting on the LG from the distribution of objects like galaxies and clusters of galaxies, as sampled by flux–limited catalogues (optical, IRAS, Abell, ACO, etc.): applying Eq.(4.80) one can obtain, in principle, estimates of Ω_o, namely $\Omega_o^{0.6}/b$, where b is a linear "bias" factor (see Chapter VI), from the deepest depths until now sampled (e.g. $\approx 300\, h^{-1} Mpc$ in Scaramella, Vettolani & Zamorani (1991)). All these analyses seem to suggest the existence of a huge mass concentration towards the Centaurus region at $\sim 150\, h^{-1} Mpc$, which could contribute to originate the LG motion, but the reliability of the estimated Ω_o value is controversial, both for the biasing scheme dependence and/or statistical incompleteness of the available catalogues; moreover, the clustering pattern in redshift space may be strongly distorted by peculiar velocities (Kaiser 1987; Mc Gill 1990; Strauss *et al.* 1992).

The existence of a large scale anisotropy towards Centaurus is confirmed by a recent analysis (Plionis, Coles & Catelan 1993) of the all–sky QDOT–IRAS redshift survey of galaxies (see Kaiser 1990b), where the questions of biasing dependence, statistical catalogue incompleteness and redshift distortion in doing Ω_o determinations are discussed; the text of the paper may be found in Appendix D.

In the next chapter we shall review other techniques with which it is possible to estimate the value of the density parameter Ω_o.

CHAPTER V

The Mean Mass Density in the Universe

Measuring the mass density of the Universe is one of the most important tasks in observational cosmology, but it is not easy at all. In the previous section we showed how the value of the density parameter Ω_o can be estimated by the Local Group infall to Virgo. Here we review other dynamical techniques for estimating Ω_o (a fine review is in Peebles 1986). The missing mass problem is then discussed.

5.1 Dark Matter in Spiral Galaxies

From the fact that the rotation curves of spiral galaxies are flat (but see Persic & Salucci 1991 and references therein) from few kpc to distances well beyond the point where the light emission ceases (by observing the rare stars or 21–cm emission from neutral H, or HI, gas clouds; see e.g. Bosma 1981) it follows that the mass of *dark* halos is much larger than the entire visible mass. In particular, the mass–to–light ratio M/L can increase by a factor 100 in $10\,kpc$ (Faber & Gallagher 1979; Carignan & Freeman 1985). From dynamical studies of the Milky Way's satellites (see Primack 1984), it is possible to set lower limits of $r_{halo} \gtrsim 70\,kpc$ and correspondingly $M/M_{lum} \gtrsim 10$ and $M \gtrsim 2 \times 10^{12}\,M_\odot$ for our own Galaxy. This mass is comparable to that suggested by studies of the dynamics of the LG of galaxies (Einasto, Koasik & Sear 1974).

A dark matter component is present also in large cosmic structures, like Abell

clusters and superclusters; moreover the DM fraction increases with the scale. Indeed, the first one to show the presence of DM in the Universe was Zwicky (1933; 1937); analyzing the velocity dispersion of galaxies in Coma Cluster, Zwicky demonstrated that $M_{COMA,dyn}/M_{COMA,lum} \gtrsim 100$.

The presence of DM in spiral galaxies translates into a DM contribution to Ω_o.

To quantify it, we remember that the observed galaxy luminosity density is roughly (see e.g. Peebles 1980)

$$\langle L \rangle \approx 1.8 \times 10^8 \, h \, L_\odot \, Mpc^{-3} \, , \tag{5.1}$$

where $L_\odot = 3.83 \times 10^{33} \, erg \, s^{-1}$. With this, we can evaluate the mean mass–to–light ratio of the Universe

$$M/L = \Omega \rho_c / \langle L \rangle \approx 1500 \, \Omega h \, M_\odot / L_\odot \, . \tag{5.2}$$

Typically, in the central regions of galaxies (Efstathiou & Silk 1983)

$$M/L \approx 14 \, h \, M_\odot / L_\odot \, , \tag{5.3}$$

then

$$\Omega_{gal} = \rho_{gal}/\rho_c \approx 0.02 \, , \tag{5.4}$$

if we take into account the entire visible mass.

On the other hand, if the *dynamical* galactic mass, including that of the halo, is about ten times greater, as previously discussed, then

$$\Omega_{dyn} = \rho_{dyn}/\rho_c \approx 0.2 \, . \tag{5.5}$$

This is the strongest evidence that the *observed* Universe is open and that 90% of the dynamical mass in the Universe is *dark*.

Remembering that hot big bang primordial nucleosynthesis and the observed light element cosmic abundances constrain the baryonic contribution Ω_b of the matter density (Yang *et al.* 1984; Walker *et al.* 1991)

$$\Omega_b \lesssim 0.1 \, , \tag{5.6}$$

we conclude that essentially all the dynamical mass can be in baryonic form. However, an Einstein–de Sitter (or inflationary) $\Omega = 1$ Universe cannot be baryonic.

5.2 Correlation Analysis

Galaxy correlation data, combined with estimates of the relative *peculiar* velocity between pairs of galaxies, can be used to give dynamical estimates of Ω. In order to use these data to estimate the mean content of matter in the Universe, it is fundamental to assume that the luminous matter distribution coincides with the underlying mass distribution. However this is not the case; it is known that the rich clusters are more correlated than galaxies (Kaiser 1984), therefore they cannot *both* be good tracers of the mass, perhaps neither are. For the moment we ignore the problem (however it will come up again in Chapter VI), and assume that the galaxies are good tracers of the mass, with $\delta\rho/\bar{\rho} \sim \xi_g(r) = \xi(r)$ (Efstathiou & Silk 1983).

Peculiar Galaxy Dynamics

According to Peebles (1980), the rms of the peculiar velocity field $\mathbf{v}_{12} \equiv \mathbf{v}_1 - \mathbf{v}_2$ of a pair of galaxies at comoving separation $\mathbf{x} = \mathbf{x}_1 - \mathbf{x}_2$ is

$$\langle v_{12}^2(r) \rangle = \frac{6\,G\,\rho_b}{\xi^{(2)}(r)} \int_r^\infty \frac{dr}{r} \int d\mathbf{z}\, \frac{\mathbf{r}\cdot\mathbf{z}}{z^3}\, \xi^{(3)}(r, z, |\mathbf{r}-\mathbf{z}|)\,, \tag{5.7}$$

where $\mathbf{r} = a(t)\mathbf{u}$, $\mathbf{z}$ is a fixed position relative to the pair of galaxies. By Eqs.(3.14) and (3.17), the previous relation reduces to the form (Peebles 1980)

$$\langle v_{12}^2(r) \rangle = \frac{6\pi G \rho_b\, Q\, r_g\, J(\gamma)}{(\gamma-1)(2-\gamma)(4-\gamma)}\, r^{2-\gamma}\,, \tag{5.8}$$

where $J(1.8) = 3.70$. Eq.(5.8) is known as the *Cosmic Virial Theorem*. It can be understood also remembering that the mass of a typical aggregation of matter with $r \ll r_g$ is

$$M(r) \approx \rho\, r^3 \approx \rho_b\, \xi_g^{(2)}(r)\, r^3 \approx \rho_b\, r_g^\gamma\, r^{3-\gamma} \tag{5.9}$$

and therefore the currents on scale r are

$$v(r)^2 \approx GM(r)\, r^{-1} \approx G\rho_b\, r_g^{\gamma}\, r^{2-\gamma}\ ; \tag{5.10}$$

we observe that $\langle v_{12}^2(r)\rangle$ is the sum of the contributions of motions on all the scales $\lesssim r$ interior to the subclusters. Since $\gamma < 2$, the main contribution to this sum is given by the currents in correspondence of the scale r, so that Eq.(5.10) coincides with Eq.(5.8).

We can rewrite Eq.(5.8) as

$$\Omega \equiv \rho_b/\rho_c \approx Q^{-1} \left(\frac{\sqrt{\langle v_{12}^2(r)\rangle}}{800\, km\, s^{-1}} \right)^2 \left(\frac{1\, h^{-1} Mpc}{r} \right)^{2-\gamma} . \tag{5.11}$$

Observationally, from estimates of redshifts (Davis & Peebles 1983; Bean *et al.* 1983)

$$\sqrt{\langle v_{12}^2\rangle} = 300 \pm 50\, km\, s^{-1} \tag{5.12}$$

on scales $\sim 1\, h^{-1} Mpc$, with a slight dependence on r compatible with Eq.(5.8). By the Cosmic Virial Theorem with $Q \approx 0.7 \div 1.3$, one has

$$\Omega \approx 0.1 \div 0.2\ . \tag{5.13}$$

Cosmic Energy Equation

Another estimate of Ω can be obtained by applying the *Cosmic Energy Equation* (Layzer 1963; 1964; Dmitriev & Zel'dovich 1964; Irvine 1965)

$$\frac{d}{dt}(T+W) + \frac{1}{a}\frac{da}{dt}(2T+W) = 0\ . \tag{5.14}$$

Eq.(5.14) relates the cosmic potential energy per unit mass W with the cosmic kinetic energy per unit mass T due to the gravitational interaction with the rest of the Universe. In particular, Eq.(5.14) relates the velocity dispersion along a fixed direction, say $\overline{v}_p$, of a galaxy, with the potential energy stored in the mass fluctuations (see Peebles 1980).

The differential equation (5.14) can be approximated by an algebraic relation (Davis & Peebles 1983)

$$\overline{v}_p^2 \approx \frac{2}{7} H_o^2\, J_2(\infty)\, \Omega\ , \tag{5.15}$$

where $J_2(\infty) = \int_0^r d\tilde{r}\, \xi_g^{(2)}(\tilde{r})$ and $H_\circ$ is the Hubble constant. If $\xi_g^{(2)}$ is negligible at $r \gtrsim 20\, h^{-1} Mpc$ one has $J_2(\infty)h^2 \approx 150\, Mpc^2$, from which

$$\Omega \approx \left(\frac{\overline{v}_p}{660\, km/s}\right)^2 , \approx 0.25 , \tag{5.16}$$

where $\overline{v}_p \approx 330\, kms^{-1}$ (Davis & Peebles 1983).

Statistical Equilibrium

An estimate of Ω due to Davis & Peebles (1983) is based on the assumption that the matter clustering on scales less than $1\, h^{-1} Mpc$ is statistically stable, ie. the Hubble flow and the processes of gravitational collapse are compensated *on average*. This condition can be written as

$$\sigma_v(r)^2 \approx 4.13\, Q\, (H_\circ r)^2\, \xi_g^{(2)}(r)\, \Omega , \tag{5.17}$$

where $\sigma_v(r)$ is the line of sight rms fluctuation of the difference of the peculiar velocities of correlated pairs of galaxies at separation r; such a quantity is measured precisely on scales $hr < 5\, Mpc$:

$$\sigma(r) = \sigma_\circ \left(\frac{hr}{1\, Mpc}\right)^{(0.13 \pm 0.04)} km\, s^{-1} , \tag{5.18}$$

$$\sigma_\circ = 340 \pm 40\, km\, s^{-1} , \tag{5.19}$$

$$10\, kpc \lesssim hr \lesssim 1\, Mpc . \tag{5.20}$$

Finally we obtain

$$\Omega \approx Q^{-1} \left(\frac{\sigma_\circ}{900\, km\, s^{-1}}\right)^2 = 0.20\, e^{\pm 0.4} , \tag{5.21}$$

compatible with previous results.

We have to stress that all these methods, estimating the mean mass clustered on scale $\sim 1\, h^{-1} Mpc$, are insensitive to a possible component of dark matter that is not clustered on such a small scales, but instead distributed rather uniformly in the Universe (see Dekel & Rees 1987). The 'biased' galaxy formation scenario, according to which the galaxies

form where the high peaks of the field $\delta\rho/\rho$ are, can reconcile the observed value of Ω with the larger theoretical value.

Conclusions:

The accurate measurement of the cosmological density parameter is difficult, but it probably lies in the range $0.1 \lesssim \Omega \lesssim$ few. Large Ω, such as the Einstein–de Sitter value $\Omega = 1$, are excluded, unless mass density is distributed considerably more broadly than luminosity.

Arguments for $\Omega = 1$

As we have seen, the value of Ω is of course an observational question. Despite of the dynamical estimates of Ω, we review some theoretical arguments which have been advanced in support of $\Omega = 1$. A more detailed discussion is given in Peebles (1986 and references therein).

- (i) In inflation model (Guth 1984; Kolb & Turner 1989), the expansion of the Universe can be traced back to a phase transition before which the energy density would have had a large nearly constant term (which behaves like a large Λ–term) that would have caused space to expand as an exponential function of time (instead of the power–law expansion of the usual models). If this exponential *inflationary* phase lasted long enough, it could have stretched all characteristic lengths. This implies that the curvature term in Friedmann equation (Eq.(1.2)) is negligibly small. This brings us to $\Omega = 1$.

- (ii) Galaxy formation seems to be easier to understand if $\Omega = 1$. Actually in a purely baryonic universe, $\Omega = \Omega_b \approx 10^{-1}$, the adiabatic perturbations cannot collapse in cosmic proto–objects without violation of the CBR isotropy: indeed at recombination their amplitudes should be $\delta_b(z_{rec}) \gtrsim (\Omega z_{rec})^{-1} \gtrsim 10^{-2}$. On the contrary, if $10^{-1} \approx$

$\Omega_b < \Omega = 1$ then $\delta_b(z_{rec}) \approx 10^{-3}$ compatible with the CBR constraints $\delta T/T < 10^{-4}$ (Bond & Efsthatiou 1984; Vittorio & Silk 1984).

- (iii) Galaxy biased clustering (Chapter VI).

The amount of (dark) matter in the Universe is strictly related to the age of the Universe. If one assumes the existence of a non baryonic component weakly interacting with the other components and closing the Universe, formed by (unspecified) massive particle, say X , such that $\Omega_b < \Omega_X \approx \Omega \approx 1$, it is possible to fix the following constraint.

Remembering that, for a matter dominated model with $\Omega = 1$, the age of the Universe is given by

$$t_\circ = \frac{2}{3} H_\circ^{-1} \approx 6.5\, h^{-1} Gyr \ , \tag{5.22}$$

and, since the oldest stars in globular clusters formed at least $10 \div 13\, Gyr$ ago, it must be that $h \lesssim 0.5 \div 0.65$, from which

$$\Omega_X h^2 \lesssim 0.25 \div 0.425 \ . \tag{5.23}$$

We remember that the parameter Ωh^2 is very often present in the cosmological expressions. We stress that, if a cosmological term is absent, the values $\Omega = 1$ and $H_\circ = 100\, km\, s^{-1} Mpc^{-1}$, which is the maximum value of $H_\circ$, are incompatible, since for a such a type of universe $t_\circ \approx 6.5\, Gyr$; instead, it must be $H_\circ \lesssim 60\, km\, s^{-1} Mpc^{-1}$ ie. $h \lesssim 0.6$. Standard CDM model assumes $\Omega = 1$ and $h = 0.5$.

5.3 Non Baryonic Dark Matter in the Universe

The particle candidates to constitute the cosmological dark matter are essentially divided in three classes: Hot, Warm and Cold DM particles. The classification has been introduced by Bond, Primack & Blumenthal (Primack & Blumenthal 1983; Primack 1984), in terms of the *free–streaming* of the DM particles. The free–streaming distance is the mean

distance covered by the DM particles, since the decoupling with the other components of the primordial plasma to the moment in which they are not longer relativistic. Collisionless particles, as the DM particles, rapidly dissipate the fluctuations with wavelength below the free–streaming distance. Essentially, the fluctuations on a typical galactic scale ($\approx 10^{11}\, M_{\odot}$) are dissipated by hot particles, but preserved with warm particles; all the cosmologically significative fluctuations survive in universes dominated by cold dark particles.

Of course, there is the possibilty that the dark matter is a mixture of, for instance, "jupiters" plus neutrinos (Schramm & Steigman 1981). Some models even include unstable DM that decays into relativistic particles (Sciama 1990a; 1990b; Splinter & Melott 1992).

For brevity, we shall consider in more detail the cosmological implications of two types of particles, the hot and cold DM particles, since these seem the more promising scenarios. The WDM scenario shows considerable intrinsic difficulties; for instance, there is at present no obvious warm DM candidate elementary particle, in contrast to the hot and cold DM cases.

Hot Dark Matter (HDM)

'Hot' dark matter is any form of non–baryonic dark matter that has a relativistic velocity at the time of equal matter and radiation ($z \sim 10^4$). The standard candidate is the massive neutrino, which has to have a mass $m_{\nu} \approx 30\, eV$ for being cosmologically important (Gershtein & Zel'dovich 1966; Bond, Efstathiou & Silk 1980). There is no conclusive evidence that there actually exists a species of neutrino with the required mass.

The important fact about neutrinos (or other HDM particles) is that they are expected to be relativistic at decoupling, with neutrino decoupling temperature $T_{d,\nu} \approx M_{Pl}^{-1/3} G_F^{-2/3} \approx 1\, MeV$, where the Planck mass $M_{Pl} = 1.22 \times 10^{19}\, GeV$ and the Fermi constant $G_F \approx 10^{-5}\, GeV^{-2}$; they remain relativistic until the matter temperature drops to $\approx m_{\nu}$. During this interval of time, the neutrinos stream freely over a distance $\lambda_{\nu} = \lambda_h(T = m_{\nu}) \sim M_{Pl}\, m_{\nu}^{-2}$, where $\lambda_h \sim (G\rho)^{-1/2} \sim M_{Pl}\, T^{-2}$. In order to survive this free streaming, a neutrino fluctuation must have linear size $> \lambda_{\nu}$. Correspondingly, the minimun mass in

neutrinos of a surviving fluctuation is $M_{J,\nu} \approx \lambda_\nu^3 \, m_\nu \, n_\nu(T = m_\nu) \approx M_{Pl}^3 \, m_\nu^{-2}$. Thus, even collisionless particles effectively exhibit a Jeans mass (*free–streaming Jeans mass*). Careful calculations (Bond, Efstathiou & Silk 1980; Bond & Szalay 1984) give

$$\lambda_\nu = 41 \left(\frac{m_\nu}{30\,eV}\right)^{-1} (1+z)^{-1} \, Mpc \, , \tag{5.24}$$

or $\lambda_\nu = 41\,(m_\nu/30\,eV)\,Mpc$ in *comoving coordinates.* The corresponding neutrino Jeans mass is

$$M_J = 1.77\, M_{Pl}^3 \, m_\nu^{-2} = 3.2 \times 10^{15}\,(m_\nu/30\,eV)^{-2}\, M_\odot \, , \tag{5.25}$$

which is the mass scale of superclusters; objects of this size are the first to form in a ν–dominated universe, so that galaxies must form by fragmentation of early larger structures.

Note that when a fluctuation of total mass $\approx 10^{15}\, M_\odot$ enters the horizon at the equivalence epoch $z \approx 10^4$, the photon–baryon fluid perturbations cease growing, starting to oscillate as an acoustic wave, while those of the massive neutrinos continue to grow linearly with rate $(1+z)^{-1}$. At recombination, $z \approx 10^3$, $\delta_{r-m}/\delta_\nu \lesssim 10^{-1}$, with an eventual additional suppression of δ_{r-m} by Silk damping (see Primack 1984, Fig. 3.4). Thus the hot DM scheme with adiabatic primordial fluctuations predicts small–angle fluctuations in the CBR somewhat below observational limits (Uson & Wilkinson 1984). Similar arguments apply in the CDM scenario (Bond & Efstathiou 1984; Vittorio & Silk 1984).

There exist however a number of problems with the neutrino dominated universe.

- (i) From dynamical studies of non–linear clustering, $\lambda \lesssim 10\, Mpc$, and bulk velocities in the linear regime, the supercluster formation is not an ancient event: $z_{SC} < 2$ in any case (Frenk, White & Davis 1983; Kaiser 1983). On the other hand, limits on galaxy ages from globular clusters (Faber 1984), and determinations of high redshift quasars (Warren *et al.* 1987) and radio sources (Lilly 1988; Chambers, Miley & van Breugel 1990), indicate that $z_{GF} \gtrsim 3$. This *timing–scaling problem* has severe implications for the neutrino pancake model. However, since a recent radio detection of neutral H at

redshift $z = 3.4$ (Uson, Bagri & Cornwell 1991), claimed as the first observational evidence of a Zel'dovich pancake, the timing–scaling problem could be not so acute.

- (ii) Another problem regards the ratio mass *vs.* baryonic mass at small and large scales. Large clusters ($\geq 10^{14}\, M_\odot$) should contain a larger amount of neutrinic component than the galaxies ($\approx 10^{12}\, M_\odot$), and M/M_b should increase by a factor ~ 5 from galactic scale to supercluster scale (Bond, Szalay & White 1983). Such a trend is not observed.

- (iii) Both theoretical arguments related to the dwarf spheroidal (dS) galaxies around the Milky Way (Faber & Lin 1983) and data on Draco, Carina and Ursa Minor (Aaronson 1983; Aaronson & Olszewski 1988) imply that dark matter is present in exceptionally large amounts in these systems. The phase–space constraint (Tremaine & Gunn 1979) then sets a lower limit $m_\nu > 500\, eV$ (Lin & Faber 1983), which is completely incompatible with the cosmological constraints (Gershtein & Zel'dovich 1966). Viceversa, for reasonable neutrino mass, ($\approx 30\, eV$), phase–space limits would then require very large core radii ($\sim 10\, kpc$) and masses ($\sim 4 \times 10^{11}\, M_\odot$: objects of such enormous masses would have spiraled into and merged with the Milky Way long ago (Gerhard & Spergel 1992).

The general problem with HDM is that it may possess too little power on small scales, just due to its own free streaming scale. One possible way to correct that problem is to produce density fluctuations not from inflation but from *seed* perturbations. Seeded hot dark matter models have been recently studied by a large numbers of people (Scherrer, Melott & Berschinger 1989; Villumsen, Scherrer & Bertschinger 1991; Cen *et al.* 1991). Traditionally, in these studies the seeded perturbations have been taken to be either primordial black holes, cosmic strings or global textures, and have been quite successful at improving the small scale power relative to the standard hot dark matter models.

Cold Dark Matter (CDM)

Whereas HDM is characterised by a free–streaming mass $M_J \sim 10^{15}\, M_\odot$, cold dark matter has a free streaming mass very much smaller than the mass of a galaxy ($< 10^8\, M_\odot$), since the CDM particles decouple and become non relativistic much earlier than the hot particles. There are a host of plausible particle physics candidates for CDM including *axions* of mass $\sim 10^{-5}$ eV (Weinberg 1978; Wilczek 1978; Ipser & Sikivie 1983; Sikivie 1983); a heavy, weakly interacting, stable *photino*, with a mass $\gtrsim \frac{1}{2}$ GeV (Goldberg 1983; Ellis *et al.* 1984); and *primordial black holes* with $10^{17} g \lesssim M \lesssim M_\odot$ (Carr 1978; Stecker & Shafi 1983; Freese, Price & Schramm 1983; Mac Gibbon 1987).These and other CDM candidates are reviewed in e.g. Primack (1984). None of these candidates has yet been detected, although experiments are capable of detecting cosmological abundances of some of them (Smith 1988; Ellis 1991).

Assuming that the primordial fluctuations are adiabatic, when the Universe is radiation–dominated, the perturbations in the CDM grow as $\delta \sim a^2$ on scales larger than the horizon. When a fluctuation crosses the horizon in this era, the photons and charged particles oscillate as an acoustic wave and the neutrinos, assumed to be massless in this scenario, stream away. This means that the driving term for the growth of the CDM perturbations disappears and the growth consequently *stagnates* until we reach the transition to matter–domination at $z \approx 10^4$ (Blumenthal *et al.* 1984), after which all linear modes grow with the same rate; as a consequence, the fluctuation power spectrum has a discontinuity at the horizon scale. The detailed growth of fluctuations in this scenario must be handled essentially numerically , although it is possible to make substantial analytic progresses (Peebles 1982a; 1982b; Vittorio & Silk 1984; Bond & Efstathiou 1984; Efstathiou 1990 and references therein). The detailed solutions are obviously complicated, but they are characterized by limiting forms. The initial power spectrum $P(k) \propto k^n$ is modified so that

$$P(k) \propto k^{n-4}\,, \tag{5.26}$$

for small scales ($k \to -\infty$). Thus, for mass scales much less than the horizon mass at the

matter–radiation equivalence ($M_{eq} \approx 10^{15}\, M_{\odot}$), we get

$$\frac{\delta M}{M} \sim (\ln M)^{3/2}\ , \tag{5.27}$$

so that the spectrum is rather flat for $M \ll M_{eq}$. If $n = 1$, the spectrum steepens to

$$\frac{\delta M}{M} \sim M^{-2/3}\ , \tag{5.28}$$

for $M \gg M_{eq}$. A more detailed discussion of the growth of perturbations in this scenario is given in a fine review by Blumenthal *et al.* (1984).

In this scenario, as in the HDM case, the CDM perturbations can start to grow *before* the baryons decouple from the radiation. After recombination ($z \approx 10^3$), the baryon fluctuations grow rapidly to match the CDM fluctuations (they tend to fall into the potential well created by the CDM perturbations): in this model the first structures to form will be of the order of the baryon Jeans mass after recombination, $\sim 10^6\, M_{\odot}$ ("bottom–up" scenario).

The CDM model has been considered, during the last years, the most successful theory for the formation of structure in the Universe (Davis *et al.* 1992). However it has recently suffered some setbacks from observational evidence suggesting that there is more large–scale power than it can explain.

The most serious of these observational challenges has come from statistical studies of the galaxy distribution on large scales ($\gtrsim 10\, h^{-1} Mpc$). The recent APM catalogue of more than 2 million galaxies reveals indeed more large–scale structure than predicted by simple versions of the theory (Maddox *et al.* 1990). Further evidence has come from infrared galaxies detected with the IRAS satellite (Efstathiou *et al.* 1990; Saunders *et al.* 1991), from clusters of galaxies (Bahcall & Soneira 1983) and from radio galaxies (Peacock & Nicholson 1991).

Possible fixes for the CDM model involve decaying particles or departures from the scale–invariant fluctuations predicted by simple inflationary models. For instance, the predictions for large–scale structures can be boosted if 17–keV neutrinos (Simpson 1985; Hime & Jelley 1991) really do exist (in addition to CDM) and decay on a timescale of

$\sim 1 \div 5$ years (Bond & Efstathiou 1991). Alternatively, one can construct models of inflation that are tuned (for example, by involving multiple scalar fields) to produce seed fluctuations with a large–scale characteristic length (Salopek, Bond & Bardeen 1989). A third possibility is that primordial fluctuations do not arise from quantum processes during inflation, but rather reflect the gravitational effect of topological defects generated at a different phase transition. Recent work, however, indicates that the cosmic string model, for a long time the most promising of its kind, actually produces less large–scale structure than standard CDM (Albrecht & Stebbins 1992)! Cosmic textures, a type of topological knot that unties itself as it shrinks, may provide a more successful model (Turok 1991). Notice that each of these proposals requires both CDM and a flat universe; the *only* differences from the standard theory concern the nature of the seeding perturbations.

After the COBE measurement (Smoot *et al.* 1992), a further burst of activity has resulted. The standard ($n = 1$ and $\Omega = 1$) CDM model, normalized at ultra–large ($\approx 10^3 h^{-1}$ Mpc) scales to COBE, predicts too much power on small scales ($\approx 1 h^{-1}$ Mpc) which is inconsistent with the observed pairwise galaxy velocity dispersion (Davis & Peebles 1983). Other possible variations of the "standard" CDM model have been thus proposed. Each of these variations introduces a new physical parameter, which is different from its fixed value in the standard CDM model, namely: 1. CDM with a non scale–free primordial fluctuation spectrum. The so called "tilted" model ($n < 1$) arises in some version of inflation (Cen *et al.* 1992; Lucchin, Matarrese & Mollerach 1992; Adams *et al.* 1992). 2. Mixed dark matter scenarios. In addition to the cold component, a relevant fraction of total density is composed of a massive (muon) neutrino (Davis, Summers & Schlegel 1992; Klypin *et al.* 1993). 3. Low density CDM with a non–vanishing cosmological constant (Efstathiou, Sutherland & Maddox; Turner 1991; Kofman, Gnedin & Bahcall 1993).

There may be less exotic ways of producing extra large–scale structures, which require nothing more than low–energy astrophysics. As we shall note in the next chapter the relation between the distribution of galaxies and mass is uncertain and is poorly constrained by current observations; although it is a *convenient* model, the "high–peak" biasing scheme

may be a poor representation of where galaxies actually form. Possibly, the galaxy formation process could itself introduce structure in the galaxy distribution on large scales (Bower *et al.* 1992).

CHAPTER VI

Biased Galaxy Formation

Until fairly recently cosmologists tacitly assumed that the luminous matter traces the matter distribution ie. the mass-to-light ratios M/L of different cosmic structures were the same. However, there is a great deal of observational and theoretical evidence that this is not the case. Such a evidence leads in a natural way to the concept of *biased* galaxy formation ie. galaxy formation (or, more in general, cosmic structure formation) occuring in such a way that galaxies do not fairly trace the underlying mass distribution. In most of biased scenarios, one is able to relate luminous matter and *dark matter* by involving a very specific form of bias (Kaiser 1984), although such a prescription is not unique (Bower *et al.* 1993; Catelan *et al.* 1993).

In this section we review the motivations for biasing the galaxy distribution, possible physical mechanisms and the types of bias expected in various cosmological scenarios. A more detailed discussion is e.g. in Dekel & Rees (1986).

6.1 Missing Mass Problem: Can the Universe Be Flat?

Mass estimates on very large scales are obtained using knowledge of the statistical properties of galaxy clustering and/or linear theory of overdensities, using galaxy counts to estimate the overdensity (§ 4.5). If one assumes that galaxies trace mass, on the scale r (Eq.(5.8))

$$\Omega \approx \rho_c^{-1} G^{-1} \xi(r)^{-1} \left(\frac{v(r)}{r} \right)^2 , \tag{6.1}$$

where $\xi(r)$ is the two-point correlation function , v is the mean pair-velocity and/or (Eq.(4.82))

$$\Omega \approx \delta^{-1.7} \left(\frac{3v}{Hr}\right)^{1.7} , \tag{6.2}$$

where δ is the density enhancement within the LG radius r, and v is the infall velocity at r. The results apparently suggest $\Omega \approx 0.2$. The crucial point is that they are obtained using observables corresponding to *galaxies*: their number overdensity δ_g or the galaxy-galaxy correlation function $\xi_g(r)$. If, indeed, the galaxies cluster more than the underlying matter, such that $\delta_g = b\,\delta$ ie. $\xi_g(r) = b^2\xi(r)$, the real value of Ω, as obtained by (6.1) and (6.2) is larger by a factor $b^{1.7} \div b^2$. The data would be compatible with $\Omega = 1$ if the degree of bias corresponds to $b \approx 2 \div 3$.

6.2 Voids

"Voids" $\sim 50\,h^{-1}Mpc$ in diameter in the galaxy distribution are actually quite common (Hoffman, Salpeter & Wasserman 1982; De Lapparent, Geller & Huchra 1986; Oemler 1987; Geller 1987). It is difficult to reconcile the existence of such a voids with the CBR isotropy, if the galaxy formation is not biased. The number density of bright galaxies in these "voids" is typically less than 10% of the mean, and, according to spherical model (Hoffman, Salpeter & Wasserman 1982), such an underdensity in the mass distribution corresponds, at decoupling z_{dec}, to $|\delta| \leq 10^{-2}$ if $\Omega \approx 1$, and to $|\delta| \leq 5 \times 10^{-2}$ if $\Omega \approx 0.1$, evidently too large. The existence of void-regions so large (like the Great Void in Böotes) contradicts the results of large scale N-body simulations too; even in the "pancake" scenario (White, Frenk & Davis 1983; Centrella & Melott 1983; Dekel & Aarseth 1984) such large regions are never found with an underdensity less than 25% of the mean. Moreover, voids cannot be dynamically so evacuated (by the only gravity), even harder if $\Omega < 1$.

For estimating the real mass in the voids, let consider a simple model of universe in

which superclusters and voids have uniform density, both in luminous and dark matter, and

$$\left(\frac{\delta_g}{\delta_{DM}}\right)_{void} = \left(\frac{\delta_g}{\delta_{DM}}\right)_{SuperCluster} = b\,. \tag{6.3}$$

If we assume that structures like the Local SuperCluster (LSC) and the Böotes Void (BV) are quite common, we can adopt the corresponding observed values for the *galaxies* $\delta_{g,SC} \approx \delta_{g,LSC} \approx 2.5$ and $\delta_{g,V} \approx \delta_{g,BV} \approx -0.9$. On the other hand, if $\Omega = 1$ ($b = 3$), we get, from the previous relations $\delta_{DM,SC} \approx \delta_{DM,LCS} \approx 0.85$ and $\delta_{DM,V} \approx \delta_{DM,BV} \approx -0.32$. It is not difficult to see that the fractional volume of voids is 0.73 and the fractional mass in voids is 0.5. The obtained mass densities in superclusters and in voids are both compatible with $|\delta| \approx 10^{-3}$, at z_{dec}, which corresponds to $\delta_T \approx 3.5 \times 10^{-5}\,(\Omega h^{-1})$, if most of the dark matter is non-baryonic, which is compatible with the observed isotropy constraints if $\Omega h^2 = 1$. An open universe with $\Omega \approx 0.2$ ($b = 1$) would require a real mass underdensity of $\sim 10\%$ in the voids ie. $\delta_T \approx 5 \times 10^{-3}$, too large.

6.3 Difficulties in Cosmogonic Scenarios

Simulations of the two most popular scenarios (see e.g. Primack 1984), in which the Universe is either dominated by "cold" DM or by massive neutrinos, have led to the conclusion that (if $\Omega \approx 1$) neither can reproduce the observed large-scale distribution of galaxies unless galaxy formation is biased.

- CDM. The CDM N-body simulations of Davis *et al.* (1985) are not compatible with the observed Universe unless bright galaxies formed at the top of high peaks of matter distribution. Assuming that light traces mass, Davis *et al.* (1985) found that $r_g = 1.27\,h^{-2}Mpc$ in an Einstein-de Sitter universe, too small if compared directly with the $r_o = 5\,h^{-2}Mpc$ observed for galaxies, except for the case $h = 0.25$. The specific scenario of CDM with $\Omega = 1$ would require an enhanced clustering of the galaxies relative to CDM such that $\xi_g(r) = 5 \div 20\,\xi(r)$, $h = 0.5 \div 1$, which is consistent with

the values of b deduced above from more general considerations.

- HDM. In the case of $30\,eV$ neutrinos, N-body simulations (Centrella & Melott 1983; White, Frenk & Davis 1983) show that the neutrino correlation length is $r \approx 8\,(\Omega h^2)^{-1}$, too large in comparison with r_0 unless $\Omega h^2 > 1$. If the galaxies form only in the collapsed regions, these constraints become even tighter, so the bias required here is of an opposite sense: the galaxies should somehow be less clustered than the neutrinos. This seems to make a "biased" neutrino model rather difficult to accept: we require an anti-bias to get the correct $\xi_{gg}(r)$, but a positive bias to resolve the problems of missing mass and voids.

To summarize:

- (i) A large-scale segregation between galaxies and the dominant mass seems inevitable.
- (ii) Large regions of low density as observed in the "voids" cannot form by the present, especially if $\Omega < 1$.
- (iii) If $\Omega = 1$, as favoured by theory, most of the (non-baryonic) mass must hide in the "voids" to escape detection in clusters and superclusters.
- (iv) Neither the CDM scenario nor the HDM scenario can match the observed large-scale galaxy distribution unless galaxy formation is biased ie. restricted to the peaks of the density field.

6.4 Physical Bias Mechanism

We review here some physical mechanisms that could originate galaxies in correspondence of high peaks of density field. Such a type of bias mechanism could be classified in three general types (see e.g. Rees 1985).

- (i) The voids may be filled with a *uniform* component of 'missing-mass' of a different nature from the clustered DM.

- (ii) There is one important kind of DM, but the baryonic component is segregated from the non-baryonic DM even on scales $\sim 30\,h^{-1}Mpc$, providing supply for galaxy formation only in certain regions (density peaks).

- (iii) The large-scale baryon distribution traces the DM on scales $> 1\,h^{-1}Mpc$, but the efficiency with which baryons turn into luminous galaxies is sensitive to other enviromental effects.

In particular the bias mechanism could be *autonomously* determined in each protogalaxy, when the intrinsic properties of a protogalactic perturbation determine its final state (galaxy or no galaxy), or it may be a result of feedback interaction, not only gravitational, among more galaxies. The result might be destructive, suppressing galaxy formation locally (causing underclustering) or far away, but it could also be constructive, enhancing galaxy formation in the neighborhood of other galaxies (e.g. explosions).

Recently, Bower *et al.* (1993) have considered a feedback biased model, in which galaxy formation occurs at high peaks of the mass density field, as in the standard biased picture, but is further enhanced by the presence of nearby galaxies. Such a modification produces enough additional clustering to fit the angular correlation function of the APM galaxy survey (Maddox *et al.* 1991).

6.5 Uniform Component

A hypothesis that might hopefully ease the voids problem previously discussed is to suppose that the Universe is dynamically dominated by a uniform unclustered component of dark matter with different properties than the clustered dark matter. For example, the spread DM may be non baryonic and the clumped DM all baryonic.

One way that this could happen is in an Universe dominated by 'ultra-hot' dark matter particles which are still relativistic today, or at least they have velocity $> 10^3\, km\, s^{-1}$, the estimated peculiar velocity among clusters (Bahcall 1988), and therefore do not cluster at all. Hoffman & Bludman (1984) have shown that if such particles formed at an early stage of the evolution of the Universe, they would always be dynamically dominant over the baryons, and would have prevented any gravitational clustering. This would also yield an unacceptably fast expansion timescale during nucleosynthesis. Further possibilities are that the particles are generated by the decay of heavy particles with lifetimes comparable to the age of the Universe (Turner, Steigman & Krauss 1984; Gelmini, Schramm & Valle 1984; Olive, Seckel & Vishniac 1985; Daly 1987; 1988).

Apart from the *ad hoc* fine-tuning of particle lifetimes in these scenarios, the main observational constraints on such models arise from the isotropy of the microwave background and from the effects of the decay on the dynamics of structures (Turner 1985; Efstathiou 1985). For instance, Flores *et al.* (1986) find that the galactic rotation curves would not have remained flat if the Universe were dominated by relativistic decay products.

6.6 High Peak Biasing

An enhanced clustering of galaxies or rich clusters over the background matter can arise in a 'bottom-up' scenario if galaxies formed only from *high peaks* of the density distribution smoothed on galactic scales or cluster scales; peaks are characterized by an overdensity δ above a threshold $\nu\sigma_\circ$, where $\sigma_\circ^2 \equiv \langle\delta^2\rangle$. Kaiser (1984) showed that, in the case where the density field is Gaussian distributed, in correspondence of scales where $\xi \ll 1$, the enhanced correlation function of high ν-peaks is approximated by

$$\xi_\nu^{(2)}(r) \approx \left(\frac{\exp(-\nu^2/2)}{\int_\nu^\infty dx\, \exp(-x^2/2)}\right)^2 \frac{\xi^{(2)}(r)}{\xi^{(2)}(0)} \approx \left(\frac{\nu}{\sigma_\circ}\right)^2 \xi^{(2)}(r)\,. \qquad (6.4)$$

This relation shows that, while $\xi_\nu^{(2)}$ has the same form of $\xi^{(2)}$, higher peaks (ie. richer systems) have an *amplified* autocorrelation.

The result (6.4), which determines precisely the bias parameter b, suggests a *statistical* interpretation of the clustering properties of rich Abell clusters (we'll rederive it in a detailed manner in another section; see Chapter VII).

This suggestion motivated a number of detailed mathematical analyses of the properties of high level regions in Gaussian random field (e.g. BBKS 1986; Couchman 1987a; 1987b) following previous discussions in a rather different context (Rice 1954; Cartwright & Longuet-Higgins 1956; Doroshkevich 1970; Adler 1981; Vanmarcke 1983).

It is argued that for rich clusters this form of biasing is very natural: clusters form very recently in bottom-up models and they are clearly very rare; they are plausibly identified with high peaks. The lower peaks on cluster scales either have not yet collapsed or have collapsed but have not produced a final object identified as a rich cluster.

The crucial question one has to answer for applying this idea to *galaxies* is what astrophysical mechanism prevents lower-amplitude peaks from turning into galaxies as well? Such a mechanism would produce a fairly sharp *cut off* in the efficiency of (bright) galaxy formation at $\nu \approx 2 \div 3$, the number density of such peaks being comparable to that of bright galaxies (see the papers by Bardeen, Kaiser and White, 1986).

The most obvious thing about high ν peaks is that they could collapse earlier and have a higher turn around density than the typical fluctuations on a given mass scale [1]. Rees (1985) argue that, in principle, this might be enough to create the biasing if star formation were highly sensitive to, for instance, the ratio of the cooling time, $\tau_{cool} \sim \rho^{-1}$, to the collapse time, $\tau_{coll} \sim \rho^{-1/2}$; collapse and fragmentation of gas clouds to form stars are faster when this ratio is small. If high ν peaks collapse at $z \geq 10$, Compton scattering off MWB photons

[1]The height of the peak is correlated with the time of collapse. Modeled as a spherical, uniform density "top-hat" with a density excess δ_{TH} extrapolated to the present by linear perturbation theory, the peak collapses to infinite density at a redshift z_c such that

$$1 + z_c = \delta/1.68 \, .$$

A threshold in δ corresponds to a threshold in time, in that only peaks which collapse before a certain time (above a certain redshift) form the galaxy or cluster.

would produce very efficient cooling. If lower peaks form after this time, Compton cooling would be unimportant and cooling much less efficient. It is still an open question if these effects can produce a cutoff sharp enough at ν.

The bias may result from processes *intrinsic* to the protogalaxies. For instance, Dekel & Silk (1986) have argued that protogalaxies formed from high ν fluctuations would have higher velocity dispersions and escape velocities than low ν peaks. High ν peaks are more able to retain gas that might be blown out of low ν peaks by e.g. explosive processes (supernovae); they argue that bright galaxies *must* originate from high density peaks ($2\sigma_o \div 3\sigma_o$) in the initial fluctuation field, while typical peaks ($\sim 1\sigma_o$) either cannot produce a luminous galaxy at all, or they make very faint dwarf galaxies with very low gas content. This would lead to a selective bias, in which bright galaxies are biased but dwarf galaxies do trace accurately the DM distribution. There is, as yet, no definitive observational evidence to confirm or reject the assumption that ξ_{gg} for bright galaxies is different than ξ_{gg} for dwarfs.

6.7 Bias in a 'Top-Down' Scenario (Neutrinos)

A bias mechanism is generated *automatically* in any top-down scenario where the perturbations below $\sim 30\,h^{-1}Mpc$ have all damped out, as in neutrino universe. Motions of the baryonic matter from proto-voids to proto-pancakes are followed by collapses into flattened structures ('pancakes') accompanied by streaming toward their intersections ('filaments') and knots where rich clusters form; there the gas collapses dissipatively into high density regions, within which cooling and galaxy formation start. Galaxies are thus limited to very specific 'biased' regions. However, if the efficiency of galaxy formation is similar in all the collapsed regions, this natural bias just makes the timing-scaling problems more severe; one has to invoke a mechanism that would suppress the formation of galaxies in the high density regions, or enhance their formation in the low density regions, but such a mechanism is not

a natural outcome of a dissipative pancake scenario.

Dekel (1983) proposed an alternative *non-dissipative* pancake scenario, which would arise from a *hybrid scenario*: if galaxies form independently of pancakes, e.g. from another component of density perturbations, the timing-scaling constraint becomes irrelevant: galaxies could have formed at $z \geq 3$ and large scale pancakes at $z \sim 1$. Therefore galaxies would not be limited to pancakes but rather be present everywhere, subject to the biasing mechanisms that are relevant in general bottom-up scenario. Such a hybrid scenario could consists of two types of DM, baryonic and/or non-baryonic, and of two types of initial fluctuations, adiabatic and isothermal (see e.g. Valdarnini & Bonometto 1985).

6.8 The Kaiser Biased Model

As we mentioned previously (see e.g. § 3.2), according to the observations, the rich clusters of galaxies are strongly correlated at distances where the correlation functions of the single galaxies have negligible amplitude, and the correlation length increases with the scale of the system. Kaiser (1984) suggested that the origin of such enhancement is primarily statistical and it is not due to an underlying substantial power spectrum on cluster scales. By assuming that the (rich) clusters of galaxies condense where the primordial (smoothed) Gaussian fluctuations exceed a suitable level $\nu\sigma_0$, then they exhibit a 2-point correlation amplified with respect to the mass correlation, and moreover this amplification increases when the scale is increased. We outline the mathematical details. We want now deduce the 2-point correlation of the up-crossing *regions* above the threshold $\nu\sigma_0(R)$ in the case in which δ_R is Gaussian distributed. In the simplest version of the Kaiser biasing scheme the galaxies trace the mass, therefore $\xi(r) = \xi_{gg}(r)$.

The 2-point correlations of the enhanced regions can be calculated as follows: by choosing at random a point, the probability $P_1^{(\nu)}$ that the Gaussian fluctuation δ_R exceeds

the sharp threshold $\nu\sigma_o(R)$ at that point is given by

$$P_1^{(\nu)} = \int_{\nu\sigma_o(R)}^{\infty} d\alpha\, p(\alpha) = \frac{1}{2}\,\mathrm{erfc}(\nu/\sqrt{2})\,, \tag{6.5}$$

where $p(\alpha)$ is showed in Eq.(A.1). $P_1^{(\nu)}$ is the fraction of space where $\delta_R > \nu\sigma_o(R)$. The probability $P_2^{(\nu)}(\mathbf{x}_2,\mathbf{x}_2)$ that in the points (in the neighborhood of the points) $\mathbf{x}_1$ and $\mathbf{x}_2$ is $\delta_R > \nu\sigma_o(R)$ is given by

$$P_2^{(\nu)}(\mathbf{x}_2,\mathbf{x}_2) = \int_{\nu\sigma_o(R)}^{\infty} d\alpha_1 \int_{\nu\sigma_o(R)}^{\infty} d\alpha_2\; p(\alpha_1,\alpha_2)\,, \tag{6.6}$$

where $p(\alpha_1,\alpha_2)$ is the bivariate Gaussian in Eq.(A.8).

Finally, the 2-point correlation function for the enhanced ($> \nu\sigma_o$) regions, $\xi_\nu^{(2)}$, is

$$1+\xi_\nu^{(2)}(r) = \frac{P_2^{(\nu)}(\mathbf{x}_2,\mathbf{x}_2)}{\left[P_1^{(\nu)}\right]^2}\,, \tag{6.7}$$

if $r \equiv |\mathbf{x}_1 - \mathbf{x}_2|$. The integral in (6.6) is difficult. The original approximation by Kaiser (1984) for large ν and small $\xi_\nu^{(2)}(r)$ (linear regime) was

$$\xi_\nu^{(2)}(r) \approx \frac{\nu^2}{\sigma_o(R)^2}\,\xi_R^{(2)}(r)\,. \tag{6.8}$$

A suitable choice of ν can therefore explain, as statistical enhancement, the amplification of the 2-point cluster correlation function and the trend of increasing r_c with richness by identifying richer clusters with higher levels. Other authors have analyzed the model in more detail. Politzer & Wise (1984) obtained the 2-point biased correlation in the form

$$1+\xi_\nu^{(2)}(r) \approx \mathrm{e}^{\nu^2\omega_R^{(2)}(r)}\,, \tag{6.9}$$

$\omega_R^{(2)}(r) \equiv \xi_R^{(2)}(r)/\sigma_o(R)$, which generalizes (6.8). They also computed N-point correlations in this approximation

$$1+\xi_\nu^{(N)} = \exp\left(\nu^2 \sum_{j>h}^{N} \omega_{R,jh}^{(2)}\right) = \prod_{j>h}^{N}\left(1+\xi_\nu^{(2)}(jh)\right)\,, \tag{6.10}$$

similar to the Kirkwood superposition. Politzer & Wise's result is only an approximation, obtained on the linear expansion of the exponent in the bivariate (multivariate) Gaussian

distribution. The exact result for sharp clipping was obtained by Jensen & Szalay (1986), using a series expansion for any ν

$$\xi_\nu^{(2)}(r) = \sum_{m=1}^{\infty} \frac{\omega_R(r)^m}{m!} A_m^2 \,, \tag{6.11}$$

$$A_m(\alpha) \equiv \frac{2\,\mathrm{e}^{-\alpha^2}\, H_{m-1}(\alpha)}{\sqrt{\pi}\,\sqrt{2}^{\,m}\,\mathrm{erfc}(\alpha)} \,, \tag{6.12}$$

where $\alpha = \nu/\sqrt{2}$, H_n is a Hermite polynomial of order n, *erfc* is the complementary error function; the leading term of the series corresponds to the Kaiser approximation.

All these results are obtained in the case of sharp threshold function, say $G(\delta) = \theta(\delta - \nu\sigma_0)$, where θ is the step function. Szalay (1988) considered the effects on the biased N-point correlations of a general nonlinear biasing function $G(\delta)$.

In the next section we consider a new "weighted" biasing scheme and analyze preliminary results (Catelan *et al.* 1993): as we shall see, generalizations of the previous expression can be obtained.

The calculation of ξ_ν we showed is physically meaningful when the two points with field values α_1 and α_2 lie in the disjoint regions of the field above the threshold, since only in such a case the two points correspond to different proto-objects, but no condition is given to ensure that $\mathbf{x}_1$ and $\mathbf{x}_2$ actually lie in different enhanced regions.

Coles (1986) showed that, unless ν is larger than ≈ 3, typical sizes of the regions are rather large, with a high probability of exceeding even $15 \div 20\, h^{-1} Mpc$. Some clusters are effectively counted more than once. This means that the simple calculation presented previously will seriously overestimate the two point cluster-cluster correlations at distances of this order (see Peacock & Heavens 1985; BBKS). For very high threshold ($\nu > 3$), the problem is not so acute, because the regions are then much smaller (see Coles 1986).

Another question is that all calculations based on the high-level region approximation predict that $\xi_{cc}(r) = 0$ whenever the underlying matter correlation function is zero (our 'weighted' biased scheme shows the same behaviour). Monte-Carlo simulations of 3D noise

by Otto, Politzer & Wise (1986a) reveal that true maxima do not possess this property. Unfortunately, their analytic expressions for the correlations of peaks are incorrect (Otto, Politzer & Wise 1986b) and they give no explanation of that. This point is particularly relevant to the CDM model, in which contex biasing is usually discussed; the CDM correlation function goes to zero at $r \sim 18\,h^{-1}Mpc$ if $\Omega = 1$ (Otto, Politzer & Wise 1986a), but the observed cluster-cluster 2-point correlation is non-zero at this distance.

In spite of the likely errors in the details of the statistical enhancements predicted by the simple Kaiser model, the qualitative explanation of such enhancements in terms of peaks of the density field above some level is extremely plausible. To avoid problems like those mentioned previously, what is required is a calculation of the 2-point correlation function of local maxima, not just regions above some level. The reason for studying true peaks rather than high regions is that peaks define a true spatial point process, with no disjointness problem of the sort discussed here.

Unfortunately, the statistical properties of maxima of 3D random fields are extremely difficult to compute rigorously. BBKS (1986) obtained asymptotic expressions for the correlation function of peaks of Gaussian random noise $\xi_{pk-pk}(r)$ as $r \rightarrow \infty$, but these expressions can only be accurate for monotonically decreasing covariance functions. Further progress with peaks of 3D fields, by handling fairly cumbersone relations, is given in Cline *et al.* (1987). The clustering of local maxima of random Gaussian fields is also analyzed in Couchman (1987a; 1987b), Coles (1989) and Lumsden, Heavens & Peacock (1989). For the reader interested in, technical details are reviewed in Chapter VII. Some generalizations of the statistical properties of maxima of D–dimensional non–Gaussian random fields are given by Catelan, Lucchin & Matarrese (1988a, b) [see Appendix C].

6.9 Weighted Bias and Galaxy Clustering

We consider a weighted biasing scheme for galaxy clustering. This differs from previous treatments in the fact that the biased density field coincides with the background mass–density whenever the latter exceeds a given threshold value. There is some physical motivation for this scheme and it is in better accord with intuitive ideas than models based on the Kaiser (1984) analysis of the clustering of rich clusters. We explain how different classes of object could be biased in different ways with respect to the underlying density distribution but still have $b = 1$. We also show that if one applies our scheme consistently a weak dependence of b upon density can be implied. This could also be the reason why the correlation function of galaxies in groups does not differ substantially from the correlation function of all galaxies (Jing & Zhang 1988; Maia & da Costa 1990; Ramella *et al.* 1990).

The assumption that bright galaxies are *biased* tracers of the mass distribution has featured strongly in theories of galaxy and structure formation in recent years. The simplest version of the Cold Dark Matter model (CDM) was found to be unable to explain the clustering properties of galaxies if the number density of galaxies and the density of gravitating material were simply proportional to each other (Davis *et al.* 1985). The observation by Kaiser (1984) that the strong clustering of rich clusters relative to galaxies could be a simple consequence of the fact that clusters form only in regions where the mass density is particularly large, led to the adoption of a simple phenomenological model for *biased* galaxy formation wherein galaxies themselves form only at high peaks of the density field. Because of the properties of Gaussian statistics – the simplest and best–motivated form for the distribution of primordial density fluctuations – high peaks have different statistical properties to 'typical' points (Peacock & Heavens 1985; Bardeen *et al.* 1986) so galaxies are biased tracers of the mass density field.

The Kaiser model offers a plausible phenomenological explanation for the clustering of clusters because clusters are defined to be high density regions in the matter distribution.

The applicability of this model to galaxies themselves is less clear, however, because in order for it to work one must suppress galaxy formation from peaks of lower density. Various authors (Rees 1985; Silk 1985; Dekel & Silk 1986; Dekel & Rees 1987) have offered some suggestions as to how a *local* (or *natural*) bias might arise. For example, the initial density of a collapsing proto–object might somehow affect the star formation rate so that low–density peaks form insufficient stars to produce an identifiable galaxy. Indeed, given the complexity of the galaxy formation process it would be surprising if there were not some kind of non–linear dependence of the space density of galaxies upon the density of the proto–galaxies from which they formed (Coles 1983). On the other hand, Peacock (1990) has found no evidence for such a local bias in the properties of elliptical galaxies. There is also no strong trend of clustering amplitude with galaxy luminosity (White *et al.* 1988; Hamilton 1988; Eder *et al.* 1989; Valls–Gabaud *et al.* 1989), which one would expect if the bias is controlled by star formation efficiency. Furthermore, the recent discovery by the COBE team of fluctuations in the sky temperature of the cosmic microwave background (Smoot et al. 1992) suggests that galaxy formation in the CDM model should be unbiased (or even anti–biased so that galaxies form preferentially in low–density regions). There is also the possibility that any bias is not even local: feedback from the first generation of objects may suppress or enhance galaxy formation on a large scale around them. Indeed such a non–local bias seems to be necessary to reconcile standard CDM with observations of very large scale galaxy clustering (Babul & White 1991; Bower *et al.* 1993).

So how can one square the observational evidence against biasing with the theoretical motivation for it? The answer may well lie in the naivety of the theoretical modelling. In this paper we shall look at the question of modelling locally–biased galaxy formation. We shall argue that the Kaiser model is probably not appropriate for galaxy clustering and suggest a simple alternative which is in better accord with intuition. In our scheme – the weighted biasing scheme – the biased density is proportional to the mass density but only where the mass density exceeds some threshold value.

The plan of this Section is as follows. After introducing the weighted biasing scheme,

we present the results for the two–point correlation of the biased density field (technical details are given in a final appendix). Finally we conclude with a general discussion.

– A weighted biasing scheme –

Here we construct a mathematical definition of our weighted biasing scheme. The underlying mass density fluctuation field will be denoted δ_R, where R is some smoothing scale used to define the mass scale of a proto–object:

$$\delta_R(\mathbf{x}) \equiv [\rho_R(\mathbf{x}) - \langle\rho\rangle]/\langle\rho\rangle \ . \tag{6.13}$$

The $\langle\ \rangle$ brackets denote averages over a probability distribution, and we shall assume throughout that these are equivalent to averages over a large volume of space i.e. that the field $\rho_R(\mathbf{x})$ is *ergodic* (Adler 1981).

In a local bias model, the *biased density field* (BDF) is a local function of $\rho_R(\mathbf{x})$. That is to say the probability of finding a galaxy at a point $\mathbf{x}$ is a function only of $\rho_R(\mathbf{x})$ or, equivalently, of $\delta_R(\mathbf{x})$: we take $dP(\mathbf{x}) = n_o f(\rho_R)\, dV/\langle f\rangle$ where n_o is the mean number density of galaxies. General constraints on this type of model are derived by Coles (1993). Because we shall be assuming the existence of some threshold ν, we define the BDF to be $f(\rho_R) = \rho_{\nu,R}(\mathbf{x})$. If $f(\rho_R) \propto \rho_R$ then galaxies trace the mass (in a statistical sense) and are therefore 'unbiased'. In the simplest model of biasing, suggested by Kaiser (1984), the BDF is defined as constant above a threshold and zero below it, i.e.

$$\rho_{\nu,R}(\mathbf{x}) \equiv \langle\rho\rangle\, \Theta(\delta_R(\mathbf{x}) - \nu\sigma_R) \ ; \tag{6.14}$$

the threshold is $\nu\sigma_R$ and σ_R is the *rms* value of δ_R. The function $\Theta(x)$ is the Heaviside step function. We shall henceforth refer to this model as the Kaiser model.

Notice that the Kaiser model possesses the property that for very low (i.e. negative) thresholds $\nu\sigma_R$ galaxy formation occurs with constant probability throughout space. This limit of the Kaiser model therefore produces an *unclustered* distribution of objects rather than an *unbiased* one. Similarly, there is a constant probability of galaxy formation above the threshold. This implies a one–to–one correspondence between high peaks and galaxies, which

may be reasonable if the threshold is very high (so that the galaxies are strongly biased) but a weak bias (which is what the observations imply) should merely modulate the spatial distribution of galaxies relative to the mass distribution. One also has the problem that merging and disruption of proto–objects in the non–linear regime is expected to destroy the correspondence between high peaks in the initial density field and subsequent bound structures (Coles et al. 1993). It is difficult therefore to justify the Kaiser model as a description of biased galaxy formation.

Our proposed weighted biasing scheme differs from the Kaiser model in that, above the threshold (which we take to be the same: $\nu\sigma_R$), the BDF coincides with the underlying density field:

$$\rho_{\nu,R}(\mathbf{x}) \equiv \rho_R(\mathbf{x})\,\Theta(\delta_R(\mathbf{x}) - \nu\sigma_R) \ . \tag{6.15}$$

In the limit of small $\nu\sigma_R$, galaxies trace the mass exactly and are therefore unbiased. For larger $\nu\sigma_R$ the weighted BDF traces the mass, but only in regions where the density exceeds some critical value. We do not therefore require a one–to–one correspondence between peaks and galaxies. Not only does this model agree better with our intuition in this limit, but it also agrees qualitatively with the results obtained from hydrodynamical simulations by Cen & Ostriker (1992). Indeed, there is good evidence for the existence of similar density–thresholding behaviour of star formation in the disks of spiral galaxies where the local gas density seems to provide the trigger (Guiderdoni 1987).

Note that $\rho_{\nu,R}(\mathbf{x})$ actually represents the true mass–density inside a smoothed sphere of filtering radius R centered on $\mathbf{x}$ for those mass fluctuations which exceed the threshold. We define the ratio

$$\mu_R(\nu) \equiv \frac{\langle \rho_{\nu,R} \rangle}{\langle \rho \rangle} \ , \tag{6.16}$$

which is the total mass fraction in *excursion regions* (i.e. those regions where the mass fluctuation δ_R exceeds the threshold $\nu\sigma_R$). Using the ergodic property, we can take the expectations to correspond to spatial averages over a large (formally infinite) volume V. It

is easy thus to see that

$$\mu_R(\nu) = \frac{\int_V d^3\mathbf{x}\,\rho_R(\mathbf{x})\,\Theta(\delta_R(\mathbf{x}) - \nu\sigma_R)}{\int_V d^3\mathbf{x}\,\rho_R(\mathbf{x})} = \frac{\int_{V_R(\nu)} d^3\mathbf{x}\,\rho_R(\mathbf{x})}{\int_V d^3\mathbf{x}\,\rho_R(\mathbf{x})} \equiv \frac{M_R(\nu)}{M_{TOT}}\,, \tag{6.17}$$

where $V_R(\nu)$ is the total volume of the excursion regions.

In the Kaiser and weighted bias models – and indeed in any local biasing scheme involving a threshold – one could define the total number of objects $N_{obj}(>\nu)$ as the total mass above the threshold $M(>\nu)$ divided by the mass of a single object M_{obj}. Thus

$$N_{obj}(>\nu) = \frac{M(>\nu)}{M_{obj}} \doteq \frac{M(>\nu)}{M_{TOT}}\left(\frac{M_{TOT}}{M_{obj}}\right)\,, \tag{6.18}$$

so that $N_{obj}(>\nu) = \mu_R(\nu)M_{TOT}/M_{obj}$. One is implicitly assuming that the objects form only out of the mass within the excursion set. If one allows for accretion, however, one could get a different expression. The quantity $\mu_R(\nu)$ is interesting in any case, however, because it illustrates one of the dangers of adopting the assumption of Gaussian statistics for the mass fluctuation field (Kaiser 1984; Peacock & Heavens 1985; Bardeen *et al.* 1986; Coles 1993). In such a case

$$\mu_R(\nu) = \frac{1}{2}\,\mathrm{erfc}\left(\frac{\nu}{\sqrt{2}}\right) + \frac{\sigma_R}{\sqrt{2\pi}}\,\mathrm{e}^{-\nu^2/2} \equiv [\Phi(\nu) + \nu\sigma_R]\,\frac{\mathrm{e}^{-\nu^2/2}}{\sqrt{2\pi}\,\nu}\,, \tag{6.19}$$

where $\mathrm{erfc}\,x \equiv (2/\sqrt{\pi})\int_x^\infty dy \mathrm{e}^{-y^2}$ is the complementary error function and the auxiliary function $\Phi(\nu)$ has a convenient asymptotic expansion:

$$\Phi(\nu) \equiv \sqrt{\frac{\pi}{2}}\,\nu\,\mathrm{e}^{\nu^2/2}\,\mathrm{erfc}\left(\frac{\nu}{\sqrt{2}}\right) \simeq 1 + \sum_{n=1}^{\infty}(-1)^n\,\frac{(2n-1)!!}{\nu^{2n}}\,. \tag{6.20}$$

We plot the function $\mu_R(\nu)$ for different values of σ_R in Figure 1 of Appendix E. As expected, the mass fraction $\mu_R(\nu)$ tends to unity as $\nu \to -\infty$, since in this case the BDF reduces to the mass density field. Note, however, that the maximum value $\mu_R(\nu_m) > 1$, is reached at $\nu_m = -1/\sigma_R$. The reason for this apparent paradox is that the underlying distribution permits the existence of regions with negative mass (i.e. $\rho_R < 0$). This point can be made more clear by writing eq (6.17) in terms of integrals over the probability distribution rather than spatial averages. The numerator in (6.17) becomes $\int_{\langle\rho_R\rangle(1+\nu\sigma_R)}^{\infty} d\rho_R\,\rho_R\,p(\rho_R)$, while the denominator can be split into two parts: $\int_{-\infty}^{\langle\rho_R\rangle(1+\nu\sigma_R)} d\rho_R\,\rho_R\,p(\rho_R) + \int_{\langle\rho_R\rangle(1+\nu\sigma_R)}^{\infty} d\rho_R\,\rho_R\,p(\rho_R)$. The integral

$\int_{-\infty}^{\langle\rho_R\rangle(1+\nu\sigma_R)} d\rho_R\, \rho_R\, p(\rho_R)$ in the denominator always contains a negative contribution coming from $\rho_R < 0$ events, which is indeed maximised (in absolute value) when $\nu = -1/\sigma_R$. The appropriate quantity in the Kaiser model (which is the volume fraction of the excursion regions) does not have any factors of ρ_R in the integrals and is therefore immune to this effect.

This illustrates an important problem with the modelling of galaxy clustering using Gaussian statistics: one must be very careful to ensure that unphysical events with $\rho_R < 0$ do not contribute to the statistics of the biased field. In the weighted biasing scheme, we can consistently apply our model with Gaussian statistics provided we restrict ourselves either to $\sigma_R \ll 1$, which reduces the probability of unphysical events, or to $\nu \gg 1/\sigma_R$, so that negative mass events have little effect on statistical properties such as $\mu_R(\nu)$. Different local biasing functions would lead to different constraints to be satisfied if the model is to be physically reasonable.

Alternatively, to get a fully self–consistent model we could use a distribution which only allows $\rho_R > 0$. We have therefore also computed $\mu_R(\nu)$ for an underlying *lognormal* distribution of density fluctuations (Coles & Jones 1991), which is a simple phenomenological model for the non–linear density field:

$$p(\delta_R) = \frac{(1+\delta_R)^{-1}}{\sqrt{2\pi\,\log(1+\sigma_R^2)}}\,\exp\left(-\frac{\log^2\left[(1+\delta_R)\sqrt{1+\sigma_R^2}\right]}{2\,\log(1+\sigma_R^2)}\right)\,. \tag{6.21}$$

Now we find

$$\mu_R(\nu) = \frac{1}{2}\,\mathrm{erfc}\left(\frac{\log\left[(1+\,\nu\sigma_R)/\sqrt{1+\sigma_R^2}\right]}{\sqrt{2\,\log(1+\sigma_R^2)}}\right)\,. \tag{6.22}$$

As expected, this takes its maximum value $\mu_R(\nu_m) = 1$ at $\nu_m = -1/\sigma_R$, corresponding to the unbiased case and there are no problems with μ_R exceeding unity. The behaviour of μ_R as a function of ν is illustrated also in Figure 1 of Appendix E.

– The two–point correlation function of the biased density field –

We shall now turn our attention to the BDF two–point correlation function, which is defined as

$$\xi_{\nu,R}(r) = \langle \delta_{\nu,R}(\mathbf{x}_1)\,\delta_{\nu,R}(\mathbf{x}_2)\rangle\,, \tag{6.23}$$

where $r \equiv |\mathbf{x}_1 - \mathbf{x}_2|$ and $\delta_{\nu,R}$ is the BDF fluctuation:

$$\delta_{\nu,R}(\mathbf{x}) = \mu_R(\nu)^{-1} \left[1 + \delta_R(\mathbf{x})\right] \Theta(\delta_R(\mathbf{x}) - \nu\sigma_R) - 1. \tag{6.24}$$

One thus obtains

$$\mu_R^2(\nu) \left[1 + \xi_{\nu,R}(r)\right] = \left\langle \left[1 + \delta_1 + \delta_2 + \delta_1\delta_2\right] \Theta(\delta_1 - \nu\sigma_R)\, \Theta(\delta_2 - \nu\sigma_R) \right\rangle , \tag{6.25}$$

where $\delta_i = \delta_R(\mathbf{x}_i)$. The expression (13) can be written

$$\mu_R^2(\nu) \left[1 + \xi_{\nu,R}(r)\right] = \int_{\nu\sigma_R}^{\infty} \int_{\nu\sigma_R}^{\infty} d\delta_1 d\delta_2 \left[1 + \delta_1 + \delta_2 + \delta_1\delta_2\right] p\left(\delta_1, \delta_2; \xi_R\right) . \tag{6.26}$$

For a Gaussian field, $p\left(\delta_1, \delta_2\,; \xi_R\right)$ is a bivariate Gaussian distribution with covariance ξ_R (and variance σ_R^2). One can further express the integral (6.26) in terms of integrals over derivatives of a bivariate Gaussian distribution. The details are given in appendix at the end of the Section. For this phenomenological discussion it is sufficient to discuss the *linear* biasing factor:

$$\xi_{\nu,R}(r) \simeq b_R^2(\nu)\, \xi_R(r), \tag{6.27}$$

obtained by Taylor expanding (6.26) up to first order in $\omega_R(r) = \xi_R(r)/\sigma_R^2$. The result is

$$b_R(\nu) = \frac{\sigma_R \Phi(\nu) + \nu(1 + \nu\sigma_R)}{\sigma_R \Phi(\nu) + \nu\sigma_R^2}. \tag{6.28}$$

The behaviour of this function is displayed in Figure 2 of the Appendix E. Of course, this parameter only describes the bias on large scales when ξ_R is small. In general the bias $(\xi_{\nu,R}(r)/\xi_R(r))^{1/2}$ will be a non–increasing function of r for any local bias model (Coles 1993). Galaxy clustering on scales where ξ is not small is surely dominated by non–linear dynamical evolution which we have no hope of modelling in a simple way, so we shall not place any emphasis on the behaviour for large ω_R. The behaviour of the function $b_R(\nu)$ in the weighted biasing scheme contrasts with the Kaiser (1984) expression,

$$b'_R(\nu) = \frac{\nu}{\sigma_R \Phi(\nu)}. \tag{6.29}$$

Note that our biasing factor reduces to unity in the unbiased Gaussian case, $b_R(-\infty) = 1$, unlike the Kaiser expression; like the Kaiser model it gives $b_R(\nu) \simeq \nu/\sigma_R$ in the high–ν limit.

Notice, however, that there is another way to obtain $b = 1$ in this version of the weighted biasing scheme, by choosing $\nu = \sigma_R - 1/\sigma_R$. For any σ_R, it therefore seems that there are two values of ν which can lead to an 'unbiased' model. However, the minimum of b_R corresponds exactly to the regime where $\mu_R > 1$ so one might suspect it to be related to the presence of negative mass events. To demonstrate this, we have also computed the linear bias factor for the lognormal distribution:

$$b_{LN}(\nu) = 1 + \frac{\tilde{\nu}}{\tilde{\sigma}_R \, \Phi(\tilde{\nu})}, \tag{6.30}$$

where

$$\tilde{\nu} = \frac{\log\left[(1+\nu\sigma_R)/\sqrt{1+\sigma_R^2}\right]}{\sqrt{2\log(1+\sigma_R^2)}}, \tag{6.31}$$

and

$$\tilde{\sigma}_R = \sqrt{\log(1+\sigma_R^2)}. \tag{6.32}$$

The behaviour of this function is also shown in Figure E2. Notice that one reproduces the Gaussian results in the limit $\sigma_R^2 \to 0$, but the bias is a much flatter function of ν at large σ_R than for the Gaussian case and is monotonically increasing. This shows that it is indeed the case that negative mass events distort the calculations for an underlying Gaussian field. To use our phenomenological model in situations where σ_R is not vanishingly small, we must therefore incorporate an underlying distribution in which $\rho_R > 0$ everywhere, such as the lognormal (6.21). Intruigingly, we find that in the Kaiser model for lognormal fluctuations we have simply:

$$b'_{LN}(\tilde{\nu}) = b_{LN}(\tilde{\nu}) - 1. \tag{6.33}$$

This again shows that $b \to 0$ in the Kaiser model in the limit of small threshold.

To conclude, our weighted bias model provides a simple phenomenological description of biased galaxy formation, in which galaxies trace the mass where the local density exceeds some threshold value. It is of course a simplistic model, but is reasonably plausible and probably an improvement upon the Kaiser model in that its behaviour in the limit of small threshold is to give an unbiased distribution rather than an unclustered one.

The first important point to emerge from this study is that the statement that $b = 1$ is not equivalent to the statement that galaxies trace the mass. The $b = 1$ version of the Kaiser has a very different relationship of galaxies to underlying mass than does the $b = 1$ weighted bias model. In the latter model, galaxies do trace the mass (in a well–defined statistical sense). In the former they do not. In other local bias models the relationship is different still. The evidence from COBE that $b \simeq 1$ in a CDM model does not therefore mean that a local bias of some form is excluded. Moreover, different populations of objects could have very different biasing functions but still have the same value of b. Perhaps this is the reason why spirals and ellipticals, though known to have different relative abundances in regions of different density (Dressler 1980), seem to have similar levels of bias.

Even if one supposes that galaxy formation is unbiased, our model finds a possible application in the behaviour of *groups* of galaxies. Ramella et al. (1990) have found, perhaps surprisingly, that the correlation function of galaxies in groups is similar to that of all galaxies (see also Jing & Zhang 1988; Maia & da Costa 1990). If one takes groups to be defined as regions where the local density exceeds some threshold, then our weighted biasing prescription should apply to the correlation function of galaxies within the groups, assuming galaxies trace the mass there. Our model therefore provides a plausible explanation for why the two correlation functions are similar.

Our weighted bias model cannot produce an anti–bias. In order to do this one has to have a biasing function which is a decreasing function of ρ; models that achieve this are given by Coles (1993). (The Kaiser model produces an anti–bias by virtue of the unnatural assumption that, in the limit of small thresholds, objects are seeded everywhere with constant probability.) Obviously, in view of the argument of the previous paragraph, there is no contradiction *in principle* with, for example, spirals being suppressed in high–density regions and still having $b = 1$.

We have also demonstrated explicitly that one must be very careful in using arguments based on Gaussian statistics to describe clustering in the regime where $\sigma_R \simeq 1$, even in a purely phenomenological way. Even the Kaiser model, which is not directly distorted by

events with $\rho_R < 0$ for reasons previously explained, involves a logical inconsistency in this regime. Any bias in galaxy clustering is expected to be imposed in the non–linear regime and the appropriate statistical distribution must reflect that fact. If the bias is imposed at very late times, when the distribution is highly skewed, then one can get a bias which depends very slowly on threshold. This could well be the explanation for why there seems to be little difference in bias for objects of widely–varying (presumed) initial density.

6.10 Appendix 1: Derivation of the Weighted Correlation Functions

In this Appendix we derive an explicit form for the BDF two–point peak correlation function $\xi_{\nu,R}(\mathbf{x}_1, \mathbf{x}_2)$, as defined by the relation

$$\mu_R^2(\nu)\,[1 + \xi_{\nu,R}(\mathbf{x}_1, \mathbf{x}_2)] =$$

$$\langle [1 + \delta(\mathbf{x}_1) + \delta(\mathbf{x}_2) + \delta(\mathbf{x}_1)\delta(\mathbf{x}_2)]\,\Theta(\delta(\mathbf{x}_1) - \nu\sigma_R)\,\Theta(\delta(\mathbf{x}_2) - \nu\sigma_R)\rangle\ , \qquad (6.34)$$

for an underlying Gaussian mass density field. In this case one can define $\alpha \equiv \delta_1/\sigma_R$, $\beta \equiv \delta_2/\sigma_R$; we then need $p(\alpha, \beta; \omega_R)$, which is a bivariate Gaussian:

$$p(\alpha, \beta; \omega_R) = \frac{1}{2\pi\sqrt{1 - \omega_R^2}} \exp\left[-\frac{\alpha^2 + \beta^2 - 2\,\omega_R\,\alpha\,\beta}{2\,(1 - \omega_R^2)}\right]\ . \qquad (6.35)$$

To perform the derivation, we decided to apply functional methods (see Appendix B) since they considerably reduce the calculations. The bivariate Gaussian pdf (6.35) may be derived from the Gaussian functional (Feynman & Hibbs 1965)

$$P[\delta] = Z[0]^{-1} \exp\left\{-\frac{1}{2}\int d\mathrm{x}\,d\mathrm{y}\,\delta(\mathrm{x})\,K(\mathrm{x},\mathrm{y})\,\delta(\mathrm{y})\right\}\ , \qquad (6.36)$$

with $\int [d\delta] P[\delta] = 1$. The kernel K is defined by the relations $K = \xi^{-1}$ and

$$\int d\mathrm{y}\,K(\mathrm{x},\mathrm{y})\,K^{-1}(\mathrm{y},\mathrm{z}) = \delta(\mathrm{x} - \mathrm{z})\ ,$$

as in the usual field theory (see e.g. Negele & Orland 1988; Ramond 1989), and therefore $P(k) = 1/\tilde{K}(k)$, with $\tilde{K}$ the Fourier transform of K. The constant of proportionality $Z[0]$

is obtained from the partition function $Z[J]$

$$Z[J] = \int [d\delta]\, P[\delta]\ \exp \int d\mathrm{x}\, J(\mathrm{x})\, \delta(\mathrm{x})\,, \tag{6.37}$$

where the "external source" J is an arbitrary funtion. With the specific choice $J(\mathrm{x}) \equiv i \sum_{h=1}^{2} \phi_h\, W_R(|\mathrm{x}_h - \mathrm{x}|)$, W_R being the smoothing filter, the 2–point peak correlation function may be written as

$$\mu_R^2(\nu)\,[1 + \xi_{\nu,R}] = (2\pi)^{-2} \int_{\nu\sigma_R}^{\infty} d\delta_1\, d\delta_2 \int_{-\infty}^{\infty} d\phi_1\, d\phi_2\, \mathrm{e}^{-i(\phi_1\delta_1 + \phi_2\delta_2)}\, \mathcal{D}_\phi\, Z[J]\,, \tag{6.38}$$

where $\mathcal{D}_\phi$ is the differential operator

$$\mathcal{D}_\phi \equiv 1 - i\frac{\partial}{\partial\phi_1} - i\frac{\partial}{\partial\phi_2} - \frac{\partial}{\partial\phi_1}\frac{\partial}{\partial\phi_2}\,. \tag{6.39}$$

To apply the operator $\mathcal{D}_\phi$ we express the partition function in terms of the background statistics; from Eqs.(6.36) and (6.37) we get

$$\ln Z[J] = -\frac{1}{2}\,(\sigma_R^2\,\phi_1^2 + \sigma_R^2\,\phi_2^2 + 2\,\xi\,\phi_1\,\phi_2)\,, \tag{6.40}$$

and

$$\mu_R^2(\nu)\,[1 + \xi_{\nu,R}] = (2\pi)^{-2} \int_{\nu\sigma_R}^{\infty} d\delta_1\, d\delta_2 \int_{-\infty}^{\infty} d\phi_1\, d\phi_2\, \mathrm{e}^{-i(\phi,\delta)}\, \mathcal{D}_\phi\, \mathrm{e}^{\frac{1}{2}(\phi, M\phi)}\,, \tag{6.41}$$

where $(\phi,\delta) \equiv \phi_1\delta_1 + \phi_2\delta_2$, $\xi \equiv \xi_R^{(2)}(\mathrm{x}_1, \mathrm{x}_2)$, $\mathrm{x}_1 \neq \mathrm{x}_2$, and M is the 2×2 covariance matrix of the Gaussian field δ_R

$$M = \begin{pmatrix} \sigma_R^2 & \xi \\ \xi & \sigma_R^2 \end{pmatrix}\,. \tag{6.42}$$

It is thus straightforward (although tedious!) to show that

$$\mu_R^2(\nu)\big[1 + \xi_{\nu,R}(r)\big] =$$

$$\int_{\nu}^{\infty} d\alpha\, d\beta \left[(1 + \sigma_R^2\,\omega_R) - 2\sigma_R(1 + \omega_R)\,\frac{\partial}{\partial\alpha} + 2\sigma_R^2\,\omega_R\,\frac{\partial^2}{\partial\alpha^2} + \sigma_R^2(1 + \omega_R^2)\,\frac{\partial^2}{\partial\alpha\,\partial\beta}\right] p(\alpha,\beta;\omega_R)\,. \tag{6.43}$$

Some of the integrals in Eq.(6.43) can be performed exactly; in particular, we use the basic integral relation

$$\int_{\nu}^{\infty} d\alpha\, \mathrm{e}^{-\frac{\alpha^2}{4\beta} - \gamma\alpha} = \sqrt{\pi\beta}\, \mathrm{e}^{\beta\gamma^2}\, \mathrm{erfc}\left[\gamma\sqrt{\beta} + \frac{\nu}{2\sqrt{\beta}}\right]\,.$$

Then we get the expression

$$\mu_R^2(\nu)\Big[1+\xi_{\nu,R}(r)\Big] = \frac{1+\sigma_R^2\omega_R}{2\sqrt{2\pi}}\int_\nu^\infty d\alpha\, \mathrm{e}^{-\alpha^2/2}\,\mathrm{erfc}\left(\frac{\nu-\alpha\,\omega_R}{\sqrt{2(1-\omega_R^2)}}\right) +$$

$$+\Big[1+\omega_R(1+\nu\sigma_R)\Big]\frac{\sigma_R\,\mathrm{e}^{-\nu^2/2}}{\sqrt{2\pi}}\,\mathrm{erfc}\left(\frac{\nu}{\sqrt{2}}\sqrt{\frac{1-\omega_R}{1+\omega_R}}\right) + \frac{\sigma_R^2\sqrt{1-\omega_R^2}}{2\pi}\,\mathrm{e}^{-\nu^2/(1+\omega_R)}\,. \qquad (6.44)$$

The expression for the standard bias (Kaiser 1984) is easily recovered from the latter equation, by taking the $\sigma_R \to 0$ limit at fixed ν and ω_R:

$$1+\xi_{\nu,R}(r) = \frac{\sqrt{2/\pi}}{[\mathrm{erfc}(\nu/\sqrt{2})]^2}\int_\nu^\infty d\alpha\,\mathrm{e}^{-\alpha^2/2}\,\mathrm{erfc}\left(\frac{\nu-\alpha\,\omega_R}{\sqrt{2(1-\omega_R^2)}}\right). \qquad (6.45)$$

The result (6.44) leads to an exact expression for the BDF variance in the limit of zero lag, $\omega_R \to 1$:

$$\sigma_{\nu,R}^2 = \frac{(1+\sigma_R^2)\Phi(\nu)+\nu\sigma_R(2+\nu\sigma_R)}{[\Phi(\nu)+\nu\sigma_R]^2\,(\mathrm{e}^{\nu^2/2}\sqrt{2\pi}\,\nu)} - 1\,, \qquad (6.46)$$

which in the limit $\nu \to -\infty$ reduces to the background mass variance, σ_R^2 (again, unlike the Kaiser model).

The linear weighted biasing factor (6.28), as explained in the text, can be obtained in the limit of small correlations by Taylor expanding (6.44) up to first order in ω_R. This involves approximations such as

$$\exp\left(-\frac{\nu^2}{(1+\omega_R)}\right) \simeq (1+\nu^2\omega_R)\,\mathrm{e}^{-\nu^2}\,, \qquad (6.47)$$

and

$$\mathrm{erfc}\left(\frac{\nu}{\sqrt{2}}\sqrt{\frac{1-\omega_R}{1+\omega_R}}\right) \simeq \mathrm{erfc}\left(\frac{\nu}{\sqrt{2}}\right) + \sqrt{\frac{2}{\pi}}\,\nu\,\omega_R\,\mathrm{e}^{-\nu^2/2}\,. \qquad (6.48)$$

We thus obtain equation (6.28).

High threshold ($\nu \gg 1$) relations can be obtained both for $\mu_R(\nu)$ and for the BDF correlation function, provided that $\omega_R \neq 1$. The first integral on the r.h.s. of Eq.(6.26) can be approximated, using Mehler's formula (see e.g. the appendix B in Chapter VII), by the asymptotic expression

$$\frac{1}{2\sqrt{2\pi}}\int_\nu^\infty d\alpha\,\mathrm{e}^{-\alpha^2/2}\,\mathrm{erfc}\left(\frac{\nu-\alpha\,\omega_R}{\sqrt{2(1-\omega_R^2)}}\right) \approx \frac{\mathrm{e}^{-\nu^2}}{2\pi\nu^2}\,\mathrm{e}^{\nu^2\omega_R}\,, \qquad (6.49)$$

while in the second term erfc $x \approx (\pi x^2)^{-1/2} \mathrm{e}^{-x^2}$, for $x \to \infty$. One therefore obtains $\mu_R(\nu) \approx (2\pi\nu^2)^{-1/2}(1+\nu\sigma_R)\,\mathrm{e}^{-\nu^2/2}$, and

$$1+\xi_{\nu,R} \approx \frac{(1+\sigma_R^2\omega_R)\,\mathrm{e}^{\nu^2\omega_R}}{(1+\nu\sigma_R)^2} + \frac{(2+\nu\sigma_R)\nu\sigma_R}{(1+\nu\sigma_R)^2}\sqrt{\frac{(1+\omega_R)^3}{1-\omega_R}}\;\mathrm{e}^{\nu^2\omega_R/(1+\omega_R)}\,. \tag{6.50}$$

In the limit $\sigma_R \to 0$ (actually for $\sigma_R \ll 1/\nu$) at fixed ν and ω_R we recover the Politzer & Wise (1984) relation

$$1+\xi_{\nu,R} \approx \exp(\nu^2\omega_R)\,. \tag{6.51}$$

On the contrary, for $\sigma_R \gg 1$, we get

$$1+\xi_{\nu,R} \approx \sqrt{\frac{(1+\omega_R)^3}{1-\omega_R}}\;\exp[\nu^2\omega_R/(1+\omega_R)]\,, \tag{6.52}$$

which is clearly not affected by the negative mass events of the Gaussian statistics. This also reduces to Eq.(6.51) at large distances ($\omega_R \ll 1$).

CHAPTER VII

Peaks of Random Fields *

This chapter is a review of recent functional methods used in the analysis of large–scale matter distribution in the Universe. Path–integral techniques recently applied in the context both in the Gaussian and non–Gaussian underlying matter distribution are discussed. This chapter is essentially divided in two parts. In the first part we review how to calculate, in the framework of the Kaiser biased model of galaxy clustering (Kaiser 1984), exact formulae for the probability that mass density – at a randomly given point – lies above a certain threshold and for the N–point correlation functions among the points above the same threshold, in the most general case of non–Gaussian underlying matter distribution (Matarrese, Lucchin & Bonometto 1986). The strong theoretical reasons for analyzing generic non–Gaussian density fields are reviewed in Section II.4. Even though the final expressions are rather difficult to handle directly, it is shown that in the high–threshold limit ($\nu \gg 1$; see below), which is the limit of physical interest, fairly simple expressions for the N–point excursion correlation functions may be obtained. These relations generalyze the results obtained by Politzer & Wise (1984) and Grinstein & Wise (1986) for underlying Gaussian density distributions. We restrict the analysis to the excursion regions above a fixed threshold, since the statistical description is much more simple. Rigorously, in the biased theory the observed objects coincide with density local maxima (peaks) exceeding some threshold. We consider this more complicated case in the second part of the chapter. The complications arise because the field quantities that must be specified at a point $\mathbf{r}_{pk}$ for it to be the site of a peak of the (smoothed) density field δ_R are the gradient $\nabla\delta_R$ which must vanish, and the second

derivative tensor $\nabla\nabla\delta_R$ which must be negative definite. Peak theory applied to cosmological models has been first developed by Doroshkevich (1970) and Doroshkevich and Shandarin (1978a, b) for models with a natural filter such as adiabatic hot dark matter models in which large structures form first (and galaxies form out of a highly nonlinear fragmentation process), and for hierarchical models such as the cold dark matter model by Peacock and Heavens (1985) and Bardeen et al. (1986). Following Bardeen *et al.* . 1986, we review how to derive fundamental statistics such as the mean number peak density and the genus of the density countours in the case of underlying Gaussian density fields. We shall demonstrate that in the very high threshold limit the density profiles are *simply connected* and in a one–to–one correspondence with the local maxima of the background Gaussian density field. A generalization of these Gaussian results to the non–Gaussian case may be found in Appendix C of the thesis (Catelan, Lucchin & Matarrese 1988a, b).

The next sections are mostly devoted to working out exact formulae and to discuss technical aspects. To avoid an excess of mathematical contorsions in the text, some technical appendices may be found at the end of this chapter.

7.1 Path-Integral Approach to Galaxy Clustering

The purpose of this section is to derive the analytical expressions for the N–point correlation functions for the regions above a threshold ν and in the case of an arbitrary distribution of the matter in the Universe. At first we will consider Gaussian density fluctuations, then non–Gaussian density fields. We state at once that the Gaussian results are a particular case of the more general non–Gaussian results. In spite of this, we believe there is an opportunity to treat in some detail both cases for reasons of clarity. Many general definitions and concepts, introduced in the first case, are valid in the second case too, and they will no be exposed again. All calculations are made at constant cosmic time t.

7.1.1 Gaussian Random Fields

Let us now consider the Gaussian random isotropic homogeneous field $\delta(\mathbf{x}) \equiv [\rho(\mathbf{x}) - \langle\rho\rangle]/\langle\rho\rangle$, with mean zero and variance $\sigma = (\langle\delta^2\rangle)^{1/2}$. Such field is completely described by the probability distribution $P[\delta]$. For a Gaussian scalar random field it has the form (Feynman & Hibbs 1965; Ramond 1989; see Appendix B)

$$P[\delta] = Z[0]^{-1} \exp\left\{-\frac{1}{2}\int d\mathbf{x}\, d\mathbf{y}\, \delta(\mathbf{x})\, K(\mathbf{x},\mathbf{y})\, \delta(\mathbf{y})\right\} ; \tag{7.1}$$

the normalization factor is given by the functional integral

$$Z[0] = \int [d\delta] \exp\left\{-\frac{1}{2}\int d\mathbf{x}\, d\mathbf{y}\, \delta(\mathbf{x})\, K(\mathbf{x},\mathbf{y})\, \delta(\mathbf{y})\right\} , \tag{7.2}$$

in such a way that $P[\delta]$ is normalized to unit:

$$\int [d\delta]\, P[\delta] = 1 . \tag{7.3}$$

K is defined by the relations $K = \xi^{-1}$ and $\int d\mathbf{y}\, K(\mathbf{x},\mathbf{y})\, K^{-1}(\mathbf{y},\mathbf{z}) = \delta(\mathbf{x}-\mathbf{z})$, as in the usual field theory (see e.g. Negele & Orland 1988; Ramond 1989), and therefore $P(k) = 1/\tilde{K}(k)$, with $\tilde{K}$ the Fourier transform of K. The mathematical theory of Gaussian random fields is given in books by Adler (1981) and Vanmarcke (1983). Many properties are also analyzed in beautiful classical works e.g. Chandrasekhar (1943) and Rice (1954).

The scalar field $\delta(\mathbf{x})$ is in an equivalent way described by the moments of the probability distribution

$$\langle\delta(\mathbf{x}_1)\ldots\delta(\mathbf{x}_N)\rangle \equiv \int [d\delta]\delta(\mathbf{x}_1)\ldots\delta(\mathbf{x}_N)P[\delta] , \tag{7.4}$$

provided that the r.h.s. integral does exist. The second order moment,

$$\langle\delta(\mathbf{x}_1)\delta(\mathbf{x}_2)\rangle = \xi^{(2)}(\mathbf{x}_1 - \mathbf{x}_2) = \xi^{(2)}(\mathbf{x}_1,\mathbf{x}_2) = \xi^{(2)}(r_{12}) , \tag{7.5}$$

(we have indicated all symbols that we will use in equivalent way) is the 2–point correlation function of the field $\delta(\mathbf{x})$. For a Gaussian distribution all N–point connected correlation functions in Eq.(7.4) are zero if $N > 2$ (see Appendix B).

We want now deduce the N–point correlations of the up–crossing regions above the threshold $\nu\sigma(R)$ for a Gaussian distribution of $\delta_R(\mathbf{x})$.

As stated, according to the observations the rich clusters of galaxies are strongly correlated at distances where the correlation functions of the single galaxies have negligible amplitude. Moreover the coherence length increases with the scale and the richness of the system. Kaiser (1984) suggested that the origin of such enhancement is essentially statistical. By assuming that the rich clusters of galaxies condense where the primordial Gaussian fluctuations exceed a suitable level, the N–point correlation function of the rich clusters can be expressed in terms of the 2–point correlation function $\xi_R^{(2)}$ of the smoothed field δ_R (Kaiser 1984; Politzer & Wise 1984; Jensen & Szalay 1986): the 2–point correlation for the rich clusters is amplified with respect to the mass correlation, and moreover this amplification increases when the scale is increased.

The demand that the (smoothed) mass fluctuation exceeds a given threshold is a constraint on its distribution, but it involves no one derivative of the fluctuation field itself. Actually, if the fluctuation field is above the threshold in a certain point, it is above the same threshold in a neighborhood of the point and, in general, what is done is to associate the rich clusters only with the local maxima (i.e. *peaks*; remember that the local maxima in the mass field are the local minima of the gravitational potential) of the smoothed mass fluctuations exceeding the threshold. Such a more general case is debated in Bardeen *et al.* (1986), Couchman (1987) and, using other techniques, in Cline *et al.* (1987). In the next section we limit ourselves to the simpler case, relating the rich clusters simply to the upcrossing regions.

– N–Point Correlation Functions of the Up–Crossing Regions –

Let us consider the probability $\mathcal{P}_N^{(t)}(\mathbf{x}_1,\ldots,\mathbf{x}_N)$ that in the points (in the neighborhood of the points) $\mathbf{x}_1,\ldots,\mathbf{x}_N$ is $\delta_R(\mathbf{x}) > \nu\sigma_0(R) \equiv t$ (Politzer & Wise 1984)

$$\mathcal{P}_N^{(t)}(\mathbf{x}_1,\ldots,\mathbf{x}_N) = \int_t^\infty d\alpha_1 \cdots \int_t^\infty d\alpha_N \int [d\delta] \prod_{h=1}^{N} \delta_D(\delta_R(\mathbf{x}_h) - \alpha_h)\, P[\delta]\,. \qquad (7.6)$$

To perform the functional integration in Eq.(7.6), we use the integral representation of the Dirac δ function $\delta_D(x) = (2\pi)^{-1} \int_{-\infty}^{\infty} d\phi \, \exp(i\phi x)$ and the definition of the partition function (e.g. Ramond 1989; see Appendix B)

$$Z[J] \equiv \int [d\delta] \left[\exp \int d\mathrm{y} J(\mathrm{x}) \delta(\mathrm{y}) \right] P[\delta] \, , \tag{7.7}$$

where the external source J is an arbitrary function. Note that $Z[0] = 1$, corresponding to the probability normalization (7.3). With the specific choice (see Matarrese, Lucchin & Bonometto 1986)

$$J_1(\mathrm{y}) \equiv i \sum_{h=1}^{N} \phi_h \, W_R(|\mathrm{x}_h - \mathrm{y}|) \, , \tag{7.8}$$

we can write the joint probability as

$$\mathcal{P}_N^{(t)} = (2\pi)^{-N} \int_t^{\infty} d\alpha_1 \cdots \int_t^{\infty} d\alpha_N \int_{-\infty}^{\infty} d\phi_1 \cdots \int_{-\infty}^{\infty} d\phi_N \, \mathrm{e}^{-i \sum_{h=1}^{N} \phi_h \alpha_h} \, Z[J_1] \, . \tag{7.9}$$

By indicating the quadratic and the linear forms (possibly generalized to spaces of functions) by (g, Af) and (g, f) respectively, one has

$$Z[J] \equiv \int [d\delta] \exp \left\{ -\frac{1}{2} (\delta, K\delta) + (J, \delta) \right\} \, , \tag{7.10}$$

with $P[\delta]$ given by Eq.(7.1). The change of variables $\delta(\mathrm{x}) \equiv \delta'(\mathrm{x}) + K^{-1} J(\mathrm{x})$ reduces the argument of the exponential in (7.10) to the form

$$-\frac{1}{2}(\delta, K\delta) + (J, \delta) = -\frac{1}{2}(\delta', K\delta') + \frac{1}{2}(J, K^{-1}J) \, . \tag{7.11}$$

Since the measure in the $\delta(\mathrm{x})$–space invariant, i.e. $[d\delta(\mathrm{x})] = [d\delta'(\mathrm{x})]$, one has

$$Z[J] = \exp \frac{1}{2}(J, K^{-1}J) \, . \tag{7.12}$$

Observing that $(J, K^{-1}J) = -(\phi, M\phi)$, where $\phi \equiv (\phi_1, \ldots, \phi_N)$ and M is the $N \times N$ correlation matrix of real elements $M_{hj} \equiv \xi_R^{(2)}(\mathrm{x}_j - \mathrm{x}_h)$, $j, h = 1, \ldots, N$, the probability $\mathcal{P}_N^{(t)}$ reduces to

$$\mathcal{P}_N^{(t)} = (2\pi)^{-N} \int_t^{\infty} d\alpha_1 \cdots \int_t^{\infty} d\alpha_N \int_{-\infty}^{\infty} d\phi_1 \cdots \int_{-\infty}^{\infty} d\phi_N \, \mathrm{e}^{-\frac{1}{2}(\phi, M\phi) - i(\phi, \alpha)} \, , \tag{7.13}$$

with $\alpha \equiv (\alpha_1, \ldots, \alpha_N)$. Owing to the transformation $\phi \equiv \varphi - iM^{-1}\alpha$, one has

$$-\frac{1}{2}(\phi, M\phi) - i(\phi, \alpha) = -\frac{1}{2}(\varphi, M\varphi) - \frac{1}{2}(\alpha,\, M^{-1}\alpha)\,. \tag{7.14}$$

Being the measure invariant, i.e. $\prod_{h=1}^{N} d\phi_h = \prod_{h=1}^{N} d\varphi_h$, one finally obtains

$$\mathcal{P}_N^{(t)}(\mathrm{x}_1, \ldots, \mathrm{x}_N) = \int_t^\infty d\alpha_1 \cdots \int_t^\infty d\alpha_N \, \frac{\mathrm{e}^{-\frac{1}{2}(\alpha, M^{-1}\alpha)}}{(2\pi)^{N/2}\,(\mathrm{det}M)^{1/2}}\,. \tag{7.15}$$

Clearly, from this relation, we see that the N–point joint density probability defined in Eq.(7.6) that in the points $\mathrm{x}_1, \ldots, \mathrm{x}_N$ the fluctuations have values in the range $[\alpha_i, \alpha_1 + d\alpha_i]$, $i = 1, \ldots, N$, respectively, is a multi-variate Gaussian

$$P_N(\alpha_1, \ldots, \alpha_N) = [(2\pi)^N \mathrm{det}M]^{-1/2} \exp\left\{-\frac{1}{2}\sum_{j=1}^{N}\sum_{h=1}^{N} \alpha_j M_{jh}^{-1} \alpha_h\right\}\,. \tag{7.16}$$

It is convenient to employ normalized variables $\delta_R(\mathrm{x})/\sigma_0(R)$. The $N \times N$ correlation matrix M for the normalized field has elements $\omega_{R,\,jh}^{(2)} \equiv \xi_R^{(2)}(\mathrm{x}_j - \mathrm{x}_h)/\sigma_0(R)^2$. In such a case, the expression for $\mathcal{P}_N^{(\nu)}$ is given by the fundamental relation

$$\mathcal{P}_N^{(\nu)} = \sum_{m=0}^{\infty}\left[\prod_{j=1}^{N}\prod_{h=1}^{N} \tilde{\omega}_{jh}^{m_{jh}}\right]\left[\prod_{h=1}^{N} \mathrm{e}^{-\nu^2/2}\,\frac{H_{m_h-1}(\nu/\sqrt{2})}{\sqrt{\pi}\sqrt{2}^{\,m_h}}\right]\,, \tag{7.17}$$

as deduced from Eq.(A.121), provided that $H_{-1}(\nu/\sqrt{2}) \equiv (\sqrt{\pi}/2)\exp(\nu^2/2)\,\mathrm{erfc}(\nu/\sqrt{2})$, where erfc(x) is the complementary error function. In Eq.(7.17) $H_m(x)$ are the Hermite polynomials; the set $\{m_{jh}\}$ is formed by all non–negative integers satisfying $\sum_{j,h=1}^{N} m_{jh} = m$; the non–negative integers $m_h \equiv \sum_{j=1}^{N}(m_{jh} + m_{hj})$ are such that $\sum_{h=1}^{N} m_h = 2m$; the $m = 0$ term in Eq.(7.17) is defined to be 1; terms reading 0^0 are also defined to be 1; $\tilde{\omega}_{jh} \equiv \frac{1}{2}(1 - \delta_{jh})\,\omega_{R,\,jh}^{(2)}$ for simplicity.

The analytical result in Eq.(7.17) is important, because it expresses the N–point joint probability of the regions above the threshold ν as a series; in the asymptotic limit $\nu \gg 1$ only few leading terms are significant. Moreover, the knowledge of $\mathcal{P}_N^{(\nu)}$ allow analytical computations of the N–point correlation functions for the up–crossing regions, which constitute the physical observables.

The complete N–point correlation functions of the regions where $\delta_R > \nu\sigma_0(R)$ are defined in a natural way by

$$1 + \xi_\nu^{(N)}(\mathbf{x}_1, \ldots, \mathbf{x}_N) = \frac{\mathcal{P}_N^{(t)}(\mathbf{x}_1, \ldots, \mathbf{x}_N)}{\left[\mathcal{P}_1^{(\nu)}\right]^N} , \tag{7.18}$$

where $\mathcal{P}_1^{(\nu)} = \frac{1}{2}\,\mathrm{erfc}(\nu/\sqrt{2})$ does not depend on the position. The quantity $\mathcal{P}_1^{(\nu)}$ is the probability that the fluctuation δ_R exceeds the threshold $\nu\sigma_0(R)$, ie. the fraction of space where $\delta_R > \nu\sigma_0(R)$. It is immediately obtained from Eq.(7.17) and from the definition (7.18)

$$1 + \xi_\nu^{(N)}(\mathbf{x}_1, \ldots, \mathbf{x}_N) = \sum_{m=0}^{\infty} \left[\prod_{j=1}^{N} \prod_{h=1}^{N} \tilde{\omega}_{jh}^{m_{jh}} \right] \left[\prod_{h=1}^{N} \mathrm{e}^{-\nu^2/2} \frac{H_{m_h - 1}(\nu/\sqrt{2})}{\sqrt{\pi}\sqrt{2}^{\,m_h}\,\mathrm{erfc}(\nu/\sqrt{2})} \right] , \tag{7.19}$$

which is what we are looking for. This result has been obtained for the first time by Jensen & Szalay (1986). The knowledge of the N–point correlation functions for any order N permits us, by inverting Eq.(7.18), to obtain the probability distribution of the (above threshold) mass fluctuations in a fixed volume.

One thinks, however, that the case of physical interest corresponds to a value relatively high of the biasing level (actually $\nu \approx 2 \div 3$), high enough to allow one to consider the limit $\nu \gg 1$ everywhere (see Davis et al. 1985; Dekel & Silk 1986). In this limit the approximation $H_m(\nu/\sqrt{2}) \approx (\sqrt{2}\nu)^n$ and $\mathrm{erfc}(\nu/\sqrt{2}) \approx (2/\sqrt{2\pi})\nu^{-1}\exp(-\nu^2/2)[1 + o(\nu^{-2})]$ can be used (see e.g. Bateman 1953), and this leads to the following results.

The correlation $\xi_\nu^{(N)}$ reads

$$\xi_\nu^{(N)}(\mathbf{x}_1, \ldots, \mathbf{x}_N) \approx -1 + \exp \sum_{j>h=1}^{N} \left[\frac{\nu}{\sigma_0(R)} \right]^2 \xi_R^{(2)}(\mathbf{x}_j - \mathbf{x}_h) . \tag{7.20}$$

This result was obtained, with slightly different techniques, by Politzer and Wise (1984). We stress the fact that the Eq.(7.20) holds until $\nu \gg 1$ and moreover $\xi_R^{(2)}(\mathbf{x}_j - \mathbf{x}_h) \ll \sigma_0(R)^2$ [high threshold and linear regime (large scales)]. However, the N–point correlation function of the rich cluster of galaxies, $\xi_\nu^{(N)}$, is not necessarily small with respect to unity: this is a more general result than the Kaiser's result (see Kaiser 1984 and Section VI.8).

The 2–point correlation of the biased regions is, from Eq.(7.20),

$$\xi_\nu^{(2)}(\mathbf{x}_1 - \mathbf{x}_2) \approx -1 + \exp \left[\left(\frac{\nu}{\sigma_0(R)} \right)^2 \xi_R^{(2)}(\mathbf{x}_1 - \mathbf{x}_2) \right] , \tag{7.21}$$

which is compatible with the Kaiser's result whenever $\xi_\nu^{(2)} \ll 1$, namely

$$\xi_\nu^{(2)}(\mathbf{x}_1 - \mathbf{x}_2) \approx \left(\frac{\nu}{\sigma_0(R)}\right)^2 \xi_R^{(2)}(\mathbf{x}_1 - \mathbf{x}_2) \,. \tag{7.22}$$

Incidentally, if the galaxies trace the mass, then the 2–point galaxy correlation function satisfies the relation

$$\xi_g^{(2)}(\mathbf{x}_1 - \mathbf{x}_2) \approx \xi_R^{(2)}(\mathbf{x}_1 - \mathbf{x}_2) \,, \tag{7.23}$$

and the N–point correlation functions of the up–crossing regions can be expressed in terms of the 2–point galaxy correlation.

Taking advantage of Eqs.(7.20) and (7.21), we can write the N–point correlations of the biased regions in terms of the 2–point correlation ones

$$1 + \xi_\nu^{(N)}(\mathbf{x}_1, \ldots, \mathbf{x}_N) = \prod_{j>h=1}^{N} \left[1 + \xi_\nu^{(2)}(\mathbf{x}_j - \mathbf{x}_h)\right] \,, \tag{7.24}$$

This result does not depend on the fact that galaxies be or not good tracers of the mass distribution, and it holds even where the 2–point correlation of the biased regions is large with respect to unity: the 2–point correlation is therefore the fundamental quantity in the statistical analysis of the large–scale matter distribution.

In particular the 3–point complete correlation function of the up–crossing regions is given by the Kirkwood superposition relation (see e.g. Reichl 1980; Politzer & Wise 1984)

$$1 + \xi_\nu^{(3)}(1,2,3) = \left[1 + \xi_\nu^{(2)}(1,2)\right] \left[1 + \xi_\nu^{(2)}(2,3)\right] \left[1 + \xi_\nu^{(2)}(1,3)\right] \,. \tag{7.25}$$

According to this relation, one expects that the probability of finding e.g. three galaxies in a given configuration is equal to the probability that each pair will be found there independent of the third particle. Note that the Kirkwood relation originates the hierarchical form with the extra term ξ^3.

7.1.2 Non–Gaussian Random Fields

We extend now the previous calculations to the case in which the primordial density fluctuations are non–Gaussian distributed (Matarrese, Lucchin & Bonometto 1986). Since the

background distribution is not specified, the results are *model independent*, the only hypotheses we need being the homogeneity and isotropy of the underlying random field.

– N–Point Correlation Functions of the Up–Crossing Regions –

According to the Eq.(7.13), the joint probability $\mathcal{P}_N^{(\nu)}$ of the regions above the ν–threshold is given by the Fourier transform of the partition function $Z[J_1]$

$$\mathcal{P}_N^{(\nu)}(\mathrm{x}_1,\ldots,\mathrm{x}_N) = (2\pi)^{-N} \int_{\nu\,\sigma_0(R)}^{\infty} (d\alpha) \int_{-\infty}^{\infty} (d\phi)\, \mathrm{e}^{-i(\phi,\,\alpha)}\, Z[J_1]\,. \tag{7.26}$$

The quantity J_1 is the external formal current defined in Eq.(7.8). Contained in $Z[J]$, $P[\delta]$ is the probability distribution in the $\{\delta(\mathrm{x})\}$–space, which is completely specified once the set of connected correlations $\xi^{(n)}$ of the field δ is known. These appear as the coefficients of the functional Taylor expansion in powers of J of $\ln Z[J]$

$$\langle \delta(\mathrm{x}_1)\cdots\delta(\mathrm{x}_N)\rangle_c = \left.\frac{\delta^N \ln Z[J]}{\delta J(\mathrm{x}_1)\cdots\delta J(\mathrm{x}_N)}\right|_{J=0}\,. \tag{7.27}$$

Therefore, $\ln Z[J]$ is the generating functional of the connected correlations $\xi^{(N)}(\mathrm{x}_1,\ldots,\mathrm{x}_N)$, whatever the probability distribution is (a more detailed discussion may be found in Appendix B).

The N–point connected correlations of the smoothed homogeneous isotropic non–Gaussian random field $\delta_R(\mathrm{x})$ are given by

$$\xi_R^{(N)}(\mathrm{x}_1,\ldots,\mathrm{x}_N) = \int \left\{ \prod_{h=1}^{N} d\mathrm{y}_h\, W_R(|\mathrm{x}_h - \mathrm{y}_h|) \right\} \xi_\nu^{(N)}(\mathrm{x}_1,\ldots,\mathrm{x}_N)\,. \tag{7.28}$$

The partition function $Z[J_1]$ can be expressed in terms of the connected correlations of $\delta_R(\mathrm{x})$

$$Z[J_1] = \exp \sum_{n=2}^{\infty} \frac{1}{n!} \int d\mathrm{y}_1 \cdots \int d\mathrm{y}_n\, \xi^{(n)}(\mathrm{y}_1,\ldots,\mathrm{y}_n)\, J_1(\mathrm{y}_1)\cdots J_1(\mathrm{y}_n) =$$

$$= \exp \sum_{n=2}^{\infty} \frac{i^n}{n!} \sum_{[h_n]=1}^{N} \phi_{h_1}\cdots\phi_{h_n}\, \xi_R^{(n)}(\mathrm{x}_{h_1},\ldots,\mathrm{x}_{h_n})\,, \tag{7.29}$$

where $\sum_{[h_n]=1} \equiv \sum_{h_n=1}\cdots\sum_{h_n=1}$. The probability $\mathcal{P}_\nu^{(n)}$ becomes

$$\mathcal{P}_N^{(\nu)} = (2\pi)^{-N} \int_{\nu\,\sigma_0(R)}^{\infty} (d\alpha) \int_{-\infty}^{\infty} (d\phi)\; \mathrm{e}^{-i(\phi,\alpha)+\sum_{n=2}^{\infty}\frac{i^n}{n!}\sum_{[h_n]=1}^{N}\phi_{h_1}\cdots\phi_{h_n}\,\xi_{R,[h_n]}^{(n)}}\,, \tag{7.30}$$

with $\xi^{(N)}_{R,[h_n]} \equiv \xi^{(n)}_R(\mathbf{x}_{h_1},\ldots,\mathbf{x}_{h_n})$ and $\sigma_R \equiv \sigma_0(R)$ for simplicity. Furthermore, if we define the following quantities

$$\begin{aligned} \omega^{(2)}_{R,[h_2]} &\equiv \xi^{(2)}_{R,[h_2]}\,\sigma_R^{-2} \qquad \text{if } h_1 \neq h_2 \,, \\ \omega^{(2)}_{R,[h_2]} &\equiv 0 \qquad\qquad \text{if } h_1 = h_2 \,, \\ \omega^{(n)}_{R,[h_n]} &\equiv \xi^{(n)}_{R,[h_n]}\,\sigma_R^{-n} \qquad \text{if } n > 2 \,, \end{aligned} \tag{7.31}$$

we can write $\mathcal{P}^{(\nu)}_N$ as follows

$$\mathcal{P}^{(\nu)}_N = (2\pi)^{-N/2} \int_\nu^\infty (d\alpha)\, \mathrm{e}^{\sum_{n=2}^\infty \frac{(-1)^n}{n!} \sum_{[h_n]=1}^N \omega^{(n)}_{R,[h_n]} \prod_{j=1}^N \frac{\partial}{\partial\alpha_j}}\, \mathrm{e}^{-\frac{1}{2}(\alpha,\alpha)} \,, \tag{7.32}$$

making use of the *integration–by–parts relation* for path–integrals (see e.g. Ramond 1989). To apply the differential operator in the exponential in Eq.(7.32) we take advantage of the *multinomial expansion theorem*, which reads

$$\left(\sum_{[h_n]=1}^N a_{[h_n]} \right)^m = m! \sum_{\{m_{[h_n]}\}} \prod_{[h_n]=1}^N \frac{a_{[h_n]}^{m_{[h_n]}}}{m_{[h_n]}!} \,, \tag{7.33}$$

where $\sum_{[h_n]=1}^N m_{[h_n]} = m$ (multinomial constraint), and of the *cluster expansion theorem* (see e.g. Huang 1963; Reichl 1980; Ma 1985)

$$\exp \sum_{n=1}^N u_n = \sum_{M=0}^\infty \sum_{[m_M]} \prod_{n=1}^M \frac{u_n^{m_n}}{m_n!} \,, \tag{7.34}$$

with $[m_M] \equiv m_1,\ldots,m_M$ and $\sum_{n=1}^M n\, m_n = M$ (cluster constraint). In our case, by considering $u_1 \equiv 0$ and, for $n \geq 2$, $u_n \equiv [(-1)^n/n!] \sum_{[h_n]=1}^N \omega^{(n)}_{R,[h_n]} \prod_{j=1}^N \frac{\partial}{\partial\alpha_j}$, with the convention $0^0 \equiv 1$, from Eqs.(7.32), (7.33) and (7.34) we get

$$\prod_{n=1}^M \frac{u_n^{m_n}}{m_n!} = \left\{ \prod_{n=1}^M \sum_{\{m_{n,[h_n]}\}} \prod_{[h_n]=1}^N \frac{\left[(-1)^n\, \omega^{(n)}_{R,[h_n]}/n!\right]^{m_{n,[h_n]}}}{m_{n,[h_n]}!} \right\} \prod_{h=1}^N \left(\frac{\partial}{\partial\alpha_h} \right)^{m_h} . \tag{7.35}$$

In the Eq.(7.35), the set $\left\{m_{n,[h_n]}\right\}$ is formed by all non–negative integers satisfying the relation $\sum_{[h_n]=1}^N m_{n,[h_n]} = m_n$; the non–negative integers $m_h \equiv \sum_{n=1}^M m_{n,h}$ [where $m_{n,h_1} \equiv \sum_{[h_n/h_1]=1}^N (m_{n,h_1,\ldots,h_n} + \cdots + m_{n,h_n,\ldots,h_1})$ with $[h_n/h_1] \equiv h_2, h_3, \ldots, h_n$ and the role of h_1 could be played by any h_j] are such that $M = \sum_{h=1}^N m_h$. Finally

$$\mathcal{P}^{(\nu)}_N = \sum_{M=0}^\infty \sum_{[m_M]} \left\{ \prod_{n=1}^M \prod_{[h_n]=1}^N \frac{\left[(-1)^n\, \omega^{(n)}_{R,[h_n]}/n!\right]^{m_{n,[h_n]}}}{m_{n,[h_n]}!} \right\} \prod_{h=1}^N a_{m_h}(\nu/\sqrt{2}) \,, \tag{7.36}$$

with

$$a_{m_h}(z) \equiv \begin{cases} \mathrm{e}^{-\nu^2/2} H_{m_h-1}(z)/(\sqrt{\pi}\sqrt{2}^{\,m_h}), & m_h \geq 1 \\ \frac{1}{2}\,\mathrm{erfc}(z), & m_h = 0\,. \end{cases} \tag{7.37}$$

In particular, the relation (7.36) in the case $N = 1$ reduces to the probability that the density exceeds the threshold ν in an arbitrary point of the Universe

$$\mathcal{P}_1^{(\nu)} = \sum_{M=0}^{\infty} \sum_{[m_M]} \left\{ \prod_{n=1}^{M} \frac{\left[\omega_R^{(n)}/n!\right]^{m_n}}{m_n!} \right\} a_M(\nu/\sqrt{2})\,. \tag{7.38}$$

Here the quantities $\omega_R^{(n)}$ are obtained from (7.31) with $\mathbf{x}_1 = \cdots = \mathbf{x}_n$.

Starting from these results, by means of the general definition (7.18), the N–point complete correlation functions of the up–crossing regions where $\epsilon_R > \nu\sigma_0(R)$ can be calculated to arbitrary accuracy, whatever the background density distribution is. These results are the generalization of those obtained in the previous subsection, which can be recovered in the case that the background distribution is Gaussian; in such a case only the (connected) correlations with $n = 2$ survive. Potential applications include more complicated cases, such as cross–correlation of different objects selected by different biasing levels (ν_1, ν_2) and/or different filtering scales (R_1, R_2) (see e.g. Matarrese, Lucchin & Bonometto 1986).

– Asymptotical Limits –

We study now the high threshold limit. In the limit $\nu \gg 1$, the function $a_m(\nu/\sqrt{2})$ can be approximated by

$$a_m(\nu/\sqrt{2}) \approx (2\pi)^{-1/2} \nu^{m-1} \mathrm{e}^{-\nu^2/2}\,, \qquad m \geq 2\,. \tag{7.39}$$

Let us consider at first the probability $\mathcal{P}_1^{(\nu)}$ that the density fluctuations exceeds the high threshold $\nu \gg 1$; from the Eq.(7.38),

$$\mathcal{P}_1^{(\nu)} = (2\pi\nu^2)^{-1/2} \nu^{m-1} \mathrm{e}^{-\nu^2/2} \sum_{M=0}^{\infty} \sum_{[m_M]} \prod_{n=1}^{M} \frac{\left[\nu^n\, \omega_R^{(n)}/n!\right]^{m_n}}{m_n!}\,, \tag{7.40}$$

i.e.

$$\mathcal{P}_1^{(\nu)} = (2\pi\nu^2)^{-1/2} \nu^{m-1} \mathrm{e}^{-\nu^2/2} \exp \sum_{n=3}^{\infty} \frac{\nu^n}{n!}\, \omega_R^{(n)}\,. \tag{7.41}$$

In the same manner it can be immediately demonstrated that

$$\mathcal{P}_N^{(\nu)} = \left[(2\pi\nu^2)^{-1/2}\nu^{m-1}\mathrm{e}^{-\nu^2/2}\right]^N \exp\sum_{n=2}^{\infty}\sum_{[h_n]=1}^{N}\frac{\nu^n}{n!}\,\omega_{R,[h_n]}^{(n)}\,. \tag{7.42}$$

Finally, from Eqs.(7.41) and (7.42), the complete N–point correlation functions for the high threshold regions are

$$1+\xi_\nu^{(N)} \approx \exp\sum_{n=2}^{\infty}\frac{\nu^n}{n!}\left\{\sum_{[h_n]=1}^{N}\omega_{R,[h_n]}^{(n)} - N\,\omega_R^{(n)}\right\}\,. \tag{7.43}$$

This relation indicates that all the N loop–terms are canceled out.

If $n=2$ identically (Gaussian case), then

$$1+\xi_\nu^{(N)} \approx \exp\frac{\nu^2}{2!}\sum_{[h_2]=1}^{N}\omega_{R,[h_2]}^{(2)}\,, \tag{7.44}$$

which coincides with the Politzer and Wise's result.

Reconsidering the Eq.(7.43), when at large distances the n–point correlations of the background density are small with respect to σ_R^n, a further approximation is possible; namely

$$\xi_\nu^{(N)} \approx \sum_{n=2}^{\infty}\frac{\nu^n}{n!}\left\{\sum_{[h_n]=1}^{N}\omega_{R,[h_n]}^{(n)} - N\,\omega_R^{(n)}\right\}\,. \tag{7.45}$$

If $n=2$, corresponding to a Gaussian matter distribution

$$\xi_\nu^{(N)} \approx \frac{\nu^2}{2!}\sum_{[h_2]=1}^{N}\omega_{R,[h_2]}^{(2)}\,, \tag{7.46}$$

as obtained from Eq.(7.44), which coincides with the Kaiser's result if $N=2$. The Eq.(7.42) indicates that

$$\mathcal{P}_N^{(\nu)} = \left[(2\pi\nu^2)^{-1/2}\nu^{m-1}\mathrm{e}^{-\nu^2/2}\right]^N Z\left[\frac{\nu}{\sigma_R}\sum_{h=1}^{N}W_R(|\mathrm{x}_h-\mathrm{x}|)\right]\,. \tag{7.47}$$

Grinstein and Wise (1986) have obtained a similar relation in the high threshold limit where, however, two unprecised constants T and S appear. Instead, in Eq.(7.47), T and C are completely determined: we have respectively $T=\nu/\sigma_R$ and $C=\left[(2\pi\nu^2)^{-1/2}\nu^{m-1}\mathrm{e}^{-\nu^2/2}\right]^N$ (see Grinstein & Wise 1986).

– Hierarchical Formulae –

Starting from the Eq.(7.43) it is possible, in principle, to obtain generalized hierarchical laws among different correlation functions of the rich clusters. As an interesting and usually discussed example, we give an expression of the 3–point connected correlation of the rich clusters $\xi^{(3)}_{\nu,c}$ in terms of the 2–point correlation ones, $\xi^{(2)}(i,j)$, where $i,j = 1,2,3$; the index R, assumed the same for each $\xi^{(2)}_\nu$ and $\xi^{(3)}_\nu$, will not be indicated.

As already shown, in the limit $\nu \gg 1$, it results that

$$1 + \xi^{(3)}_\nu(1,2,3) \approx \exp \sum_{n=2}^{\infty} \frac{\nu^n}{n!} \left\{ \sum_{[h_n]=1}^{3} \omega^{(n)}_{R,[h_n]} - 3\,\omega^{(n)}_R \right\} , \tag{7.48}$$

$$1 + \xi^{(2)}_\nu(i,j) \approx \exp \sum_{n=2}^{\infty} \frac{\nu^n}{n!} \left\{ \sum_{[h_n]=(ij)} \omega^{(n)}_{R,[h_n]} - 2\,\omega^{(n)}_R \right\} , \tag{7.49}$$

where the symbol (ij) means that in the sum any index h_n takes *only* the values i and j. The sum in Eq.(7.48) can be written as

$$\sum_{[h_n]=1}^{3} \omega^{(n)}_{R,[h_n]} - 3\,\omega^{(n)}_R = \sum_{j=0}^{n} \sum_{h=0}^{n-j} \binom{n}{j} \binom{n-j}{h} \omega^{(n)}_{R,[j,h,n-j-h]} , \tag{7.50}$$

where, corresponding to $\omega^{(n)}_{R,[j,h,n-j-h]}(\mathbf{x}_1,\mathbf{x}_2,\mathbf{x}_3)$,

$$\xi^{(n)}_{R,[j,h,n-j-h]}(\mathbf{x}_1,\mathbf{x}_2,\mathbf{x}_3) \equiv$$

$$\int \Big[\prod_{a=1}^{j} d\mathbf{y}_a\, W_R(|\mathbf{x}_1-\mathbf{y}_a|)\Big] \Big[\prod_{b=j+1}^{h} d\mathbf{y}_b\, W_R(|\mathbf{x}_2-\mathbf{y}_b|)\Big] \Big[\prod_{c=h+j+1}^{n} d\mathbf{y}_c\, W_R(|\mathbf{x}_3-\mathbf{y}_c|)\Big] \xi^{(n)}_\nu(\mathbf{x}_1,\ldots,\mathbf{x}_n). \tag{7.51}$$

The combinatorial factor in Eq.(7.51) records the number of objects $\omega^{(n)}_{R,[h_n]}$ equivalent, by a permutation of the arguments, to the same object $\omega_{R,[j,h,n-j-h]}$. From Eq.(7.50) we obtain

$$\begin{aligned} \sum_{[h_n]=1}^{3} \omega^{(n)}_{R,[h_n]} - 3\,\omega^{(n)}_R \;&=\; \sum_{h=1}^{n-1} \binom{n}{h} \left[\omega_{R,[h,n-h,0]} + \omega_{R,[h,0,n-h]} + \omega_{R,[0,h,n-h]} \right] + \\ &+ \sum_{j=1}^{n-2} \sum_{h=1}^{n-j-1} \binom{n}{j} \binom{n-j}{h} \omega^{(n)}_{R,[j,h,n-j-h]} = \end{aligned}$$

$$= \left[\sum_{[h_n]=(12)} \omega^{(n)}_{R,[h_n]} - 2\,\omega^{(n)}_R \right] + \left[\sum_{[h_n]=(13)} \omega^{(n)}_{R,[h_n]} - 2\,\omega^{(n)}_R \right] + \left[\sum_{[h_n]=(23)} \omega^{(n)}_{R,[h_n]} - 2\,\omega^{(n)}_R \right] +$$

$$\sum_{j=1}^{n-2}\sum_{h=1}^{n-j-1}\left(\begin{array}{c} n \\ j \end{array}\right)\left(\begin{array}{c} n-j \\ h \end{array}\right)\omega^{(n)}_{R,[j,h,n-j-h]}\,. \tag{7.52}$$

Defining the quantity

$$F(1,2,3)\equiv \exp\sum_{n=3}^{\infty}\left(\frac{\nu}{\sigma_R}\right)^n\sum_{j=1}^{n-2}\sum_{h=1}^{n-j-1}\left(\begin{array}{c} n \\ j \end{array}\right)\left(\begin{array}{c} n-j \\ h \end{array}\right)\frac{\xi^{(n)}_{R,[j,h,n-j-h]}}{j!\,h!\,(n-j-h)!}\,, \tag{7.53}$$

from Eqs.(7.48)–(7.53) one obtains

$$1+\xi^{(3)}_{\nu}(1,2,3)\;\approx\; F(1,2,3)\left[1+\xi^{(2)}_{\nu}(1,2)\right]\left[1+\xi^{(2)}_{\nu}(1,3)\right]\left[1+\xi^{(2)}_{\nu}(2,3)\right]\,, \tag{7.54}$$

i.e. the expression for the connected 3–point correlation of the rich clusters is given by

$$\xi^{(3)}_{\nu}(1,2,3)\approx F(1,2,3)\left[\xi^{(2)}_{\nu}(1,2)\,\xi^{(2)}_{\nu}(2,3)+\xi^{(2)}_{\nu}(1,2)\,\xi^{(2)}_{\nu}(1,3)+\xi^{(2)}_{\nu}(1,3)\,\xi^{(2)}_{\nu}(2,3)+\right.$$

$$\left.+\xi^{(2)}_{\nu}(1,2)\,\xi^{(2)}_{\nu}(1,2)\,\xi^{(2)}_{\nu}(1,2)\right]+\left[F(1,2,3)-1\right]\left[1+\xi^{(2)}_{\nu}(1,2)+\xi^{(2)}_{\nu}(2,3)+\xi^{(2)}_{\nu}(1,3)\right]\,. \tag{7.55}$$

It can be easily understood that each deviation of $F(1,2,3)$ from unity indicates that the mass fluctuations, which determine F, are characterized by a non–Gaussian distribution. For $F=1$, the Eq.(7.55) reduces to the Kirkwood superposition relation.

7.2 Mathematical Overview of the Peaks Technique

In this section, the rich clusters of galaxies are explicitely related to the local maxima (*peaks*) above a threshold of the Gaussian fluctuation field $\delta_R(\mathrm{x})$. In the previous sections, more simply, the cluster of galaxies have been identified with the excursion regions above the fixed threshold of the stochastic process $\delta_R(\mathrm{x})$. Such regions are in general 'topologically' complex, since they contain more than one maximum, consequently minima and saddle points in the isodensity surfaces too. The excursion regions thus contain many substructures. What one instead expects is that a (rich) cluster of galaxies is not in general topologically complex, since it corresponds to a virialized system of galaxies: the correspondence cluster

$\leftrightarrow$ above–threshold region is not *a priori* correct. However, we have to anticipate that, in the limit $\nu \gg 1$, which is the limit of physical interest, it is reasonable to think that an up–crossing region will contain only a unique local maximum; this will be demonstrated in a next section.

7.2.1 Local Maxima of the Gaussian Density Field

– Mean Number Density of Peaks above the Threshold ν –

Let consider the homogeneous and isotropic Gaussian density field $\delta_R(\mathbf{x})$. The peak number density of the continuos field $\delta_R(\mathbf{x})$ may be expressed by mean a sum of Dirac–functions:

$$n_{pk}(\mathbf{x}) = \sum_m \delta_D^{(3)}(\mathbf{x} - \mathbf{x}_m) \,, \tag{7.56}$$

the sum being over the positions $\mathbf{x}_m$ in the space where $\delta_R(\mathbf{x}_m)$ is a local *maximum* value. The Taylor expansion around $\mathbf{x}_m$ of the gradient $\nabla\delta_R(\mathbf{x})$ to the first order is

$$\partial_j \delta_R(\mathbf{x}) = \sum_{j=1}^{3} \omega_{ij}(\mathbf{x}_m)\,(\mathbf{x} - \mathbf{x}_m)_j \,, \qquad i = 1,2,3 \,, \tag{7.57}$$

where $\mathcal{W} = (\omega_{ij})_{i,j=1,2,3}$ is the matrix of the values of the field $\partial_i\partial_j\delta_R(\mathbf{x})$ at the point $\mathbf{x}_m$. Since the matrix $\mathcal{W}$ is not singular in $\mathbf{x}_m$, one has, from Eq.(7.57), $\mathbf{x}-\mathbf{x}_m = \mathcal{W}^{-1}(\mathbf{x}_m)\nabla\delta_R(\mathbf{x})$, then $\delta_D^{(3)}(\mathbf{x} - \mathbf{x}_m) = |\det \mathcal{W}(\mathbf{x}_m)|\, \delta_D^{(3)}(\nabla\delta_R(\mathbf{x}))$ and finally

$$\sum_m \delta_D^{(3)}(\mathbf{x} - \mathbf{x}_m) = |\det \mathcal{W}(\mathbf{x})|\, \delta_D^{(3)}(\nabla\delta_R(\mathbf{x})) \,. \tag{7.58}$$

This condition holds for each maximum, but the function $\delta_D^{(3)}$ counts all the (stationary) points that are zeros of $\nabla\delta_R(\mathbf{x})$: more than $\nabla\delta_R(\mathbf{x})$ vanishes, the local maxima are characterized by the constraint that the symmetric 3×3 matrix $\mathcal{W}$ has negative eigenvalues. Therefore, the number density of the local maxima corresponding to values of δ_R above the global threshold $t = \nu\sigma_0(R)$ is given by (see e.g. Cline *et al.* 1987):

$$n_{pk}^{(t)}(\mathbf{x}) = \int_t^\infty d\alpha \int_{\mathcal{D}} d\omega |\det \mathcal{W}|\, \delta_D(\delta_R(\mathbf{x}) - \alpha)\, \delta_D^{(3)}(\nabla\delta_R(\mathbf{x}))\, \delta_D^{(6)}(\nabla\nabla\delta_R(\mathbf{x}) - \omega) \,. \tag{7.59}$$

The region of integration $\mathcal{D}$ extends over all values of $\mathcal{W}_{ij}$ negative definite, and it is a complicated 6-dim submanifold; explicitely, the integration domain is

$$d\omega \equiv d\omega_{11}\, d\omega_{22}\, d\omega_{33}\, d\omega_{12}\, d\omega_{13}\, d\omega_{23}\ . \tag{7.60}$$

In principle, we could compute an infinite hierarchy of peak correlation functions by mean of Eq.(7.59). In practice, only the average over the ensemble of the Eq.(7.59) may be worked out in a relatively simple way:

$$n_{pk}^{(t)} \equiv \langle n_{pk}^{(t)}(\mathbf{x}) \rangle = \int [d\delta]\, n_{pk}^{(t)}(\mathbf{x})\, P[\delta]\ . \tag{7.61}$$

The functional $P[\delta]$ is the Gaussian probability distribution normalized to unity [see Eq.(7.1)]. The isotropy and homogeneity of the density field guarantees that $\langle n_{pk}^{(t)}(\mathbf{x}) \rangle$ doesn't depend on the spatial position $\mathbf{x}$. In particular, the Eq.(7.61) is a special case of the more general relation

$$\mathcal{P}_N^{(t)}(\mathbf{x}_1, \ldots, \mathbf{x}_N) = \langle \prod_{h=1}^{N} n_{pk}^{(t)}(\mathbf{x}_h) \rangle = \int [d\delta] \prod_{h=1}^{N} n_{pk}^{(t)}(\mathbf{x}_h)\, P[\delta]\ , \tag{7.62}$$

where $\mathcal{P}_N^{(t)}(\mathbf{x}_1, \ldots, \mathbf{x}_N)$ is now the probability of finding N *peaks* of the field $\delta_R(\mathbf{x})$ at the locations $\mathbf{x}_1, \ldots, \mathbf{x}_N$ and above the (same) threshold $\nu\sigma_0(R)$. Eq.(7.62) is a direct generalization of Eq.(7.6). One gets that

$$\mathcal{P}_1^{(t)} = n_{pk}^{(t)}\ , \tag{7.63}$$

and the mean number density of the above threshold peaks is equal to the probability of finding one peak above the threshold in an arbitrary point of the space. The final expression of $\mathcal{P}_1^{(t)}$ reduces to

$$n_{pk}^{(t)} = \mathcal{P}_1^{(t)} = \int_t^{\infty} d\alpha \int_{\mathcal{D}} d\omega\, |\det \mathcal{W}| \frac{\mathrm{e}^{-\frac{1}{2}(\mathbf{s}, \Lambda^{-1}(10)\mathbf{s})}}{\sqrt{(2\pi)^{10} \det \Lambda(10)}}\ . \tag{7.64}$$

The quantity $\mathbf{s}$ is the 'threshold vector' and $\Lambda(10) \equiv (\Lambda_{ab})$ is the 10×10 covariance matrix of the fields δ_R, $\nabla\delta_R$ and $\nabla\nabla\delta_R$ at the arbitrary point $\mathbf{x}$; it is not difficult to show that

$$\Lambda(10) = \begin{pmatrix}
\sigma_0^2 & 0 & 0 & 0 & -\sigma_1^2/3 & -\sigma_1^2/3 & -\sigma_1^2/3 & 0 & 0 & 0 \\
0 & \sigma_1^2/3 & 0 & 0 & 0 & 0 & 0 & 0 & 0 & 0 \\
0 & 0 & \sigma_1^2/3 & 0 & 0 & 0 & 0 & 0 & 0 & 0 \\
0 & 0 & 0 & \sigma_1^2/3 & 0 & 0 & 0 & 0 & 0 & 0 \\
-\sigma_1^2/3 & 0 & 0 & 0 & 3\sigma_2^2/15 & \sigma_2^2/15 & \sigma_2^2/15 & 0 & 0 & 0 \\
-\sigma_1^2/3 & 0 & 0 & 0 & 3\sigma_2^2/15 & \sigma_2^2/15 & \sigma_2^2/15 & 0 & 0 & 0 \\
-\sigma_1^2/3 & 0 & 0 & 0 & 3\sigma_2^2/15 & \sigma_2^2/15 & \sigma_2^2/15 & 0 & 0 & 0 \\
0 & 0 & 0 & 0 & 0 & 0 & 0 & \sigma_2^2/15 & 0 & 0 \\
0 & 0 & 0 & 0 & 0 & 0 & 0 & 0 & \sigma_2^2/15 & 0 \\
0 & 0 & 0 & 0 & 0 & 0 & 0 & 0 & 0 & \sigma_2^2/15
\end{pmatrix} . \tag{7.65}$$

The quantities σ_0, σ_1 and σ_2 are elements of a set of spectral parameters weighted by powers of k^2

$$\sigma_\ell^2(R) \equiv \int_0^\infty \frac{k^2 dk}{2\pi^2} P_R(k)\, k^{2\ell} , \tag{7.66}$$

and $P_R(k)$ is the filtered power spectrum. The reader interested in the formalism, may find in Cline *et al.* (1987) a relation analogous to Eq.(7.64) for the joint probability with N arbitrary.

– Interpolating Formula for the Differential Peak Density –

In accordance with the Eq.(7.64), the joint probability distribution of the values of the fields δ_R, $\nabla\delta_R$ and $\nabla\nabla\delta_R$ at the generic point $\mathbf{x}$ is

$$f(\tilde{\alpha},\beta,\omega)d\alpha\, d\beta\, d\omega = \frac{\mathrm{e}^{-\frac{1}{2}(\mathbf{F}_{10},\Lambda^{-1}(10)\mathbf{F}_{10})}}{\sqrt{(2\pi)^{10}\det\Lambda(10)}} d\alpha\, d\beta\, d\omega . \tag{7.67}$$

i.e. $f(\tilde{\alpha},\beta,\omega)\, d\alpha\, d\beta\, d\omega$ is the joint probability that δ_R, $\nabla\delta_R$ and $\nabla\nabla\delta_R$ assume values in the ranges $[\alpha, \alpha + d\alpha]$, $[\beta, \beta + d\beta]$ and $[\omega, \omega + d\omega]$ respectively and in an arbitrarly chosen point of the Universe; $\mathbf{F}_{10}$ is the vector in the 10–dimensional space

$$\mathbf{F}_{10} \equiv (\tilde{\alpha},\, \beta_1,\, \beta_2,\, \beta_3,\, \omega_{11},\, \omega_{22},\, \omega_{33},\, \omega_{12},\, \omega_{13},\, \omega_{23}) . \tag{7.68}$$

It helps to take now full advantage of the isotropy of the random field to handle the covariance matrix. Changing variables from $\tilde{\alpha}$, ω_{11}, ω_{22} and ω_{33} to

$$\begin{aligned} \alpha &\equiv \tilde{\alpha}/\sigma_0 \\ x &\equiv -(\omega_{11}+\omega_{22}+\omega_{33})/\sigma_2 \\ y &\equiv -(\omega_{11}-\omega_{33})/2\sigma_2 \\ z &\equiv -(\omega_{11}-2\omega_{22}+\omega_{33})/2\sigma_2 \ , \end{aligned} \tag{7.69}$$

reduces $\Lambda(10)$ to a quasi–diagonal form in which

$$\langle \alpha^2 \rangle = 1 \ ; \qquad \langle x^2 \rangle = 1 \ ; \qquad \langle y^2 \rangle = \frac{1}{15} \ ; \qquad \langle z^2 \rangle = \frac{1}{5} \ , \tag{7.70}$$

the only non–zero cross–correlation being

$$\gamma \equiv \langle x\nu \rangle = \sigma_1^2/\sigma_0\,\sigma_2 \ , \tag{7.71}$$

which is an important spectral parameter: as we'll show, it is only via γ that the peak height distribution depends on the *shape* of the power spectrum. The condition that $\mathcal{W}$ has to be negative definite is simplified by the choice of coordinate axes along the principal axes of the tensor ω_{ij}, adding the constraints

$$-\omega_{11} = \lambda_1 \geq -\omega_{22} = \lambda_2 \geq -\omega_{33} = \lambda_3 > 0 \ . \tag{7.72}$$

The integral in Eq.(7.67) then reduces to an integral over x, y, z and the Euler angles specyfying the orientation of the principal axes. The ranges of x, y and z are determined by the condition (7.72). Finally, the joint probability (7.67) may be reduced to the differential peak density in the range $[\alpha, \alpha + d\alpha]$

$$f(\alpha)\,d\alpha = \frac{\mathrm{e}^{-\alpha^2/2}}{(2\pi)^2\,R_*^3}\,G(\gamma, \gamma\alpha)\,d\alpha \tag{7.73}$$

where R_* is a further spectral parameter defined by

$$R_* \equiv \sqrt{3}\,\sigma_1(R)/\sigma_2(R) \ . \tag{7.74}$$

The function $G(\gamma, x_*)$, where $x_* \equiv \gamma\alpha$ is interpolated by the equation (BBKS)

$$G(\gamma, x_*) = \frac{x_*^3 - 3\,\gamma^2 x_* [B(\gamma) x_*^2 + C_1(\gamma)]\,\mathrm{e}^{-A(\gamma)x_*^2}}{1 + C_2(\gamma)\,\mathrm{e}^{C_3(\gamma)x_*}}\,, \tag{7.75}$$

where the coefficients $A(\gamma)$, $B(\gamma)$, $C_i(\gamma)$, $i = 1, 2, 3$ are given by the relations

$$A(\gamma) = \frac{5}{2(9 - 5\gamma^2)}\,, \tag{7.76}$$

$$B(\gamma) = \frac{432}{\sqrt{10\pi}(9 - 5\gamma^2)^{5/2}}\,, \tag{7.77}$$

$$C_1(\gamma) = 1.84 + 1.13\,(1 - \gamma^2)^{5.72}\,, \tag{7.78}$$

$$C_2(\gamma) = 8.91 + 1.27\,\mathrm{e}^{6.51\gamma^2}\,, \tag{7.79}$$

$$C_3(\gamma) = 2.58\,\mathrm{e}^{1.05\gamma^2}\,. \tag{7.80}$$

The interpolating formula (7.75) is accurate more than 1% in the range $0.3 < \gamma < 0.7$ and $-1 < x_* < \infty$, and the accuracy increases until 0.1% for $x_* > 1$. To obtain the number of peaks (rich clusters) above the threshold ν, $n_{pk}^{(\nu)}$, it is necessary to integrate (7.73). Again, this integral must be tackled with numerical techniques, even if one employes the interpolating formula (7.75).

– Spectral Parameters –

The equations for the peak densities involve the parameters γ and R_*, which are related to the different moments of the smoothed spectrum $P_R(k) = P(k)\,\widetilde{W}_R^2(k)$

$$\gamma \equiv \frac{\sigma_1^2(R)}{\sigma_0(R)\,\sigma_2(R)} = \frac{\langle k^2 \rangle}{\sqrt{\langle k^4 \rangle}}\,, \tag{7.81}$$

$$R_* \equiv \sqrt{3}\,\frac{\sigma_1(R)}{\sigma_2(R)} = \sqrt{3}\,\sqrt{\frac{\langle k^2 \rangle}{\langle k^4 \rangle}}\,, \tag{7.82}$$

since $\langle k^2 \rangle = \sigma_1^2/\sigma_0^2$ and $\langle k^4 \rangle = \sigma_2^2/\sigma_0^2$. We stress the fact that the differential density of the peaks depends on the spectrum only through γ and, over that, through the multiplicative volume parameter R_*^3 [see Eq.(7.74)]. The value of γ indicates the range where $k^3 P_R(k)$

[remember that $k^3 P_R(k)/2\pi^2$ is the contribution to $\sigma_0(R)$ for logarithmic interval of k] is large, since

$$\sqrt{\frac{\langle (k^2 - \langle k^2 \rangle)^2 \rangle}{\langle k^2 \rangle^2}} = \sqrt{\frac{1}{\gamma^2} - 1} \tag{7.83}$$

measures the relative spectral width (see Vanmarcke 1983). If the spectrum is a delta function, then $\gamma = 1$; on the contrary, if $k^3 P_R(k)$ is constant over a wide range of k, then $\gamma \ll 1$.

– Cumulative and Differential Peak Density –

To illustrate the results, the differential number density of the peaks (7.73) in the range $[\alpha, \alpha + d\alpha]$ is plotted in Fig.VII-1, for different values of γ. Typically, there exists a sharp peak for local maxima with height nearly equal to the variance, $\alpha \approx 1$. Note that for small γ ($\gamma \approx 0.3$; flat spectrum), the peak is at $\alpha \approx 0$, indicating that many maxima exist above the variance; the contribution comes from all the components of the spectrum. For large γ ($\gamma \approx 0.9$; peaked spectrum) the concentrate contribution of the spectrum creates relatively high maxima ($\alpha \approx 2$). In any case, for α higher than $\alpha \approx 2$, the differential density decreases rapidly.

The cumulative number density of the peaks higher than the ν–threshold is [see Eq.(7.59)]

$$n_{pk}^{(\nu)} \equiv \int_\nu^\infty d\alpha \, f(\alpha) \, , \tag{7.84}$$

which is plotted in Fig.VII-2 for different values of γ. The asymptotic cumulative peak number density (number of peaks per unit volume of arbitrary height) is an useful quantity which can be analytically evaluated (e.g. Bardeen *et al.* 1986; Couchman 1987)

$$n_{pk}^{(-\infty)} = \frac{29 - 6\sqrt{6}}{5^{3/2}\, 2\, (2\pi)^2 R_*^3} = 0.016\, R_*^{-3} \, . \tag{7.85}$$

Finally, we want to study the asymptotical expression of the peak number density above the high threshold ($\nu \gg 1$). In the limit $x_* \gg 1$, the function $G(\gamma, x_*)$ becomes

$$G(\gamma, \gamma\alpha \gg 1) \approx \gamma^3 \, (\alpha^3 - 3\alpha) \, , \tag{7.86}$$

and the differential density (7.73) reduces to

$$f(\alpha)d\alpha \approx \frac{(\langle k^2\rangle/3)^{3/2}}{(2\pi)^2}(\alpha^3 - 3\alpha)\,\mathrm{e}^{-\alpha^2/2}d\alpha\,, \tag{7.87}$$

since $R_*^{-3} = (\langle k^2\rangle/3)^{3/2}\gamma^{-3}$; from Eqs.(7.84) and (7.87)

$$n_{pk}^{(\nu\gg 1)} = \frac{(\langle k^2\rangle/3)^{3/2}}{(2\pi)^2}(\nu^2 - 1)\,\mathrm{e}^{-\nu^2/2}\,. \tag{7.88}$$

This fundamental result has been obtained in the high threshold limit by many authors employing different techniques (Doroshkevich 1970; Adler 1981; Vanmarcke 1983; Couchman 1987). In the next section, we shall draw the asymptotical peak number density in an analytical way, after analyzing the topology of the isodensity surfaces above threshold of the Gaussian field δ.

– Topology of the Gaussian Density Profile –

In this subsection we briefly analyze the topology of the isodensity contours (level–surfaces of constant density) in the neighborhood of the peaks of the Gaussian field $\delta_R(\mathbf{x})$. We shall demonstrate that in the very high threshold limit the density profiles are *simply connected* and in a one–to–one correspondence with the local maxima of the Gaussian field $\delta_R(\mathbf{x})$. Furthermore, this analysis leads in a natural manner to the definition of the *Euler–Poincaré characteristic*, which is an interesting topological measure.

In the three–dimensional space, the condition $\delta_R(\mathbf{x}) = \nu\sigma_0(R)$ defines a set of two–dimensional surfaces of constant density, whose "topological" properties can be described in terms of the critical points of the contours themselves, relatively to any set of cartesian axes. Indeed such topological properties are independent from the choice of the axes if the fluctuation density field is homogeneous and isotropic i.e. whose properties are invariant with respect to the space translations and rotations [1]. Therefore we can assume that one

[1]The use of the words "topology" and "topological" is however here mathematically improper: rigorously, a topology is a collection of *open sets*, without any *metric* defined.

direction is specified. Locally, the bidimensional surfaces can be defined by the function $x_3(x_1, x_2)$, where the x_3 coordinate has been isolated as dipendent variable.

In some region S we define the number m_k being the number of points $\mathbf{x}_k \in S$ such that $\delta_R(\mathbf{x}_k) = \nu\sigma_0(R)$, $\partial_1\delta_R(\mathbf{x}_k) = \partial_2\delta_R(\mathbf{x}_k) = 0$, $\partial_3\delta_R(\mathbf{x}_k) > 0$ and the symmetric matrix

$$\begin{pmatrix} \partial_1^2\delta_R(\mathbf{x}_k) & \partial_1\partial_2\delta_R(\mathbf{x}_k) \\ \partial_1\partial_2\delta_R(\mathbf{x}_k) & \partial_2^2\delta_R(\mathbf{x}_k) \end{pmatrix} , \tag{7.89}$$

has k negative eigenvalues. In such a way in $\mathbf{x}_k$ the density along the $\hat{3}$–direction increases if x_3 increases and, in addition, in the planes parallel to the plane (x_1, x_2) and tangent in $\mathbf{x}_k$ to the density profile $\delta = \nu\sigma_0(R)$, the function $\delta_R(x_1, x_2)$ has a minimum if $k = 0$, a saddle point if $k = 1$, a maximum if $k = 2$. As discussed by Adler (1981), the Euler characteristic χ of the scalar field δ_R is defined as

$$\chi \equiv m_0 - m_1 + m_2 \, . \tag{7.90}$$

One can show that, for instance (see Adler 1981)

$$\begin{aligned} \chi &= 1 \, , \quad \text{if the contour is simply connected} \, , \\ \chi &= 0 \, , \quad \text{if the contour is twice connected} \, . \end{aligned} \tag{7.91}$$

The advantage of this measure of the complexity of the isodensity contour surface is that the mean value of χ can be easily calculated. Let be indeed $f(\delta_R, \beta, \omega_{11}, \omega_{22}, \omega_{12})$ the joint differential probability of the fields $\delta_R, \beta \equiv \nabla\delta_R, \omega \equiv (\partial_i\partial_j\delta_R)_{i,j=1,2}$ and $\mathbf{a}$ the vector

$$\mathbf{a} = \begin{pmatrix} \delta_R - \nu\sigma_0 \\ \beta_1 \\ \beta_2 \end{pmatrix} . \tag{7.92}$$

Taylor expanding $\mathbf{a}$ around the point $\mathbf{x}_k$ one gets

$$\mathbf{a}(\mathbf{x}) \approx \sum_j \partial_j \mathbf{a}(\mathbf{x}_k)\,(\mathbf{x} - \mathbf{x}_k)_j \, . \tag{7.93}$$

The statistics of the point–like process $n_{pk}(\mathbf{x}) = \sum_k \delta_D^{(3)}(\mathbf{x}-\mathbf{x}_k)$ can be evaluated by applying the methods of the previous section; from Eqs.(7.56) and (7.93) the mean density of the k–points is (see e.g. Doroshkevich 1970; Adler 1981)

$$\langle\, \delta_D(\delta - \nu\sigma_0)\, \delta_D(\beta_1)\, \delta_D(\beta_2)\, \theta(\beta_3)\, |\beta_3|\, |\omega_{11}\omega_{12} - \omega_{12}^2|\,\rangle =$$

$$\int_{(\beta_3>0)} \int_{(\omega_{ij}eigvls<0)} d^3\omega_{ij}\, |\beta_3 \det \omega_{ij}|\, f(\nu\sigma_0,\, 0,\, 0,\, \beta_3,\, \omega_{11},\, \omega_{22},\, \omega_{12})\,. \tag{7.94}$$

Then it follows that the mean value of χ per unit volume is

$$\langle m_0 - m_1 + m_2 \rangle = \int_0^\infty d\beta_3\, \beta_3 \int_{space} d^3\omega_{ij}\, \det w_{ij}\, f\,. \tag{7.95}$$

The probability distribution function is a Gaussian with mean zero

$$f(\delta_R,\, \beta,\, \omega_{11},\, \omega_{22},\, \omega_{12}) = \frac{\mathrm{e}^{-\frac{1}{2}(\mathbf{F}_7,\, \Lambda^{-1}(7)\mathbf{F}_7)}}{\sqrt{(2\pi)^7 \det \Lambda(7)}}\,. \tag{7.96}$$

where $\mathbf{F}_7$ is a 7–dim vector

$$\mathbf{F} = (\delta_R,\, \beta,\, \omega_{11},\, \omega_{22},\, \omega_{12})\,, \tag{7.97}$$

and $\Lambda(7)$ is the 7×7 covariance matrix of the fields δ_R, β and ω_{ij} at the generic point $\mathbf{x}$ [see Eq.(7.65)]. The determinant is

$$\det \Lambda(7) = 8\, \sigma_0^2 \left(\frac{\sigma_1^2}{3}\right)^3 \left(\frac{\sigma_2^2}{15}\right)^3 \left(1 - \frac{5}{6}\gamma^2\right) \tag{7.98}$$

where $\gamma = \sigma_1^2(R)/\sigma_0(R)\,\sigma_2(R)$. The integral (7.95) corresponds to (see Bardeen *et al.* 1986; Couchman 1987; Hamilton, Gott III & Weinberg 1986)

$$\langle \chi \rangle = \frac{(\langle k^2 \rangle/3)^{3/2}}{(2\pi)^2}\, (\nu^2 - 1)\, \mathrm{e}^{-\nu^2/2}\,. \tag{7.99}$$

Following Couchman (1987), we introduce another useful measure of the complexity of the topology of the isodensity surfaces, the mean number of connexions defined by

$$p = \frac{\langle m_0 + m_1 + m_2 \rangle}{\langle m_0 + m_2 \rangle} \geq 1\,. \tag{7.100}$$

The definition of p corresponds in some way to the intuitive idea that the connexion–degree is related to the presence of the saddle points. If all the surfaces have the same topology, they should be p–times connected. From Eq.(7.94)

$$\langle m_0 + m_1 + m_2 \rangle = \int_0^\infty d\beta_3\, \beta_3 \int_{space} d^3\omega_{ij}\, |\det w_{ij}|\, f\,. \tag{7.101}$$

Following a calculation completely analogous to that ended in Eq.(7.99) (Bardeen *et al.* 1986; Couchman 1987)

$$\langle m_0 + m_1 + m_2 \rangle = \frac{(\langle k^2 \rangle/3)^{3/2}}{(2\pi)^2} \left(\nu^2 - 1 + \frac{4\sqrt{3}}{5\gamma^2\sqrt{1-5\gamma^2/9}} \, \mathrm{e}^{-\frac{5}{18}\frac{\gamma^2\nu^2}{1-5\gamma^2/9}} \right) \mathrm{e}^{-\nu^2/2} \, . \qquad (7.102)$$

Being

$$\langle m_0 + m_2 \rangle = \frac{(\langle k^2 \rangle/3)^{3/2}}{(2\pi)^2} \left[2\left(\nu^2 - 1\right) + A\mathrm{e}^{-B\nu^2} \right] \mathrm{e}^{-\nu^2/2} \, , \qquad (7.103)$$

where we have defined

$$A \equiv \frac{4\sqrt{3}}{5\gamma^2\sqrt{1-5\gamma^2/9}} \, ; \qquad B \equiv \frac{5\gamma^2}{18(1-5\gamma^2/9)} \, , \qquad (7.104)$$

one finally obtains

$$p = 1 + \frac{B\,\mathrm{e}^{-A\nu^2}}{2(\nu^2-1) + B\mathrm{e}^{-A\nu^2}} \, . \qquad (7.105)$$

In the asymptotic limit $\nu \gg 1$, $p \to 1$. This result demonstrates that the level surfaces $\delta_R = \nu\sigma_0(R)$ assume a simpler topological configuration as the threshold increases, and they become *simply connected* in the limit $\nu \to \infty$ (actually $\nu \gtrsim 3$).

The expression (7.99) for the mean Euler characteristic $\langle \chi \rangle$ can be compared with the asymptotic expression (7.88) for the number of peaks higher than a given threshold ν, $n_{pk}^{(\nu \gg 1)}$. We deduce that for high threshold values there exists a one–to–one correspondence among the peaks and the simply–connected excursion regions.

The parameter p is visualized in Fig.VII-3. The symmetry of the funtion $p(\nu)$ obviously records the specular nature of the maxima and minima (at least in the linear regime). The results we obtained imply that, on large scales, the fluctuation regions above $\approx 2\sigma_0$ level are essentially localized and they permit the identification of these regions as the peaks of the matter distribution on large scales, which are thought to be the spots where the cosmological bound systems form; any property which can be calculated for these overdense regions starting from the statistics of the linear perturbations (for instance the number of peaks of small size that they possibly contain), may give informations with concerning the final structure of the bound objects (like galaxies or clusters of galaxies) arising after the non linear collapse.

7.3 Appendix 1: The N–point probability distribution $\mathcal{P}_N^{(\nu)}$

The probability distribution of the normalized field $\delta_R(\mathbf{x})/\sigma_0(R)$ is

$$\mathcal{P}_N^{(\nu)}(\mathbf{x}_1,\ldots,\mathbf{x}_N) = (2\pi)^{-N}\int_\nu^\infty (d\alpha)\int_{-\infty}^\infty (d\phi)\,\exp\left[-\frac{1}{2}(\phi,M\phi)-i(\phi,\alpha)\right]\,, \qquad (7.106)$$

where $(d\alpha)\equiv\prod_{h=1}^N d\alpha_h$ and $(d\phi)\equiv\prod_{h=1}^N d\phi_h$; the correlation matrix M for the normalized field has elements $\omega_{R,jh}^{(2)}\equiv\xi_R^{(2)}(\mathbf{x}_j-\mathbf{x}_h)/\sigma_0(R)^2$ if $j\neq h$, $j,h=1,\ldots,N$, and $\omega_{R,hh}^{(2)}=1$, $h=1,\ldots,N$. Moreover, the correlation matrix M can be factorized in the form $M=I+\mathcal{M}$, where I is the identity matrix and $\mathcal{M}=\left((1-\delta_{jh})\,\omega_{R,jh}^{(2)}\right)_{j,h=1,\ldots,N}$. We can write:

$$\mathrm{e}^{-\frac{1}{2}(\phi,M\phi)}=\mathrm{e}^{-\frac{1}{2}(\phi,\phi)}\,\mathrm{e}^{D}=\mathrm{e}^{-\frac{1}{2}(\phi,\phi)}\sum_{m=0}^\infty\frac{D^m}{m!}\,, \qquad (7.107)$$

where $D\equiv-\frac{1}{2}(\phi,\mathcal{M}\phi)=-\frac{1}{2}\sum_{j,h=1}^N\phi_j\phi_h(1-\delta_{jh})\,\omega_{R,jh}^{(2)}$. Thus, from the relations (7.106) and (7.107), one gets

$$\mathcal{P}_N^{(\nu)}(\mathbf{x}_1,\ldots,\mathbf{x}_N) = (2\pi)^{-N}\int_\nu^\infty (d\alpha)\int_{-\infty}^\infty (d\phi)\left(\sum_{m=0}^\infty\frac{D^m}{m!}\right)\exp\left[-\frac{1}{2}(\phi,\phi)-i(\phi,\alpha)\right]\,. \qquad (7.108)$$

Since $i\,\frac{\partial}{\partial\alpha_j}\exp[-i(\phi,\alpha)]=\phi_j\exp[-i(\phi,\alpha)]$ it follows that $D\exp[-i(\phi,\alpha)]=\mathcal{D}\exp[-i(\phi,\alpha)]$, where $\mathcal{D}$ is the differential operator defined by

$$\mathcal{D}\equiv-\frac{1}{2}\sum_{j,h=1}^N(1-\delta_{jh})\,\omega_{R,jh}^{(2)}\,\frac{\partial}{\partial\alpha_j}\,\frac{\partial}{\partial\alpha_h}\,. \qquad (7.109)$$

This operator commutes with respect to the ϕ–variables and (7.108) reduces to

$$\mathcal{P}_N^{(\nu)}(\mathbf{x}_1,\ldots,\mathbf{x}_N) = (2\pi)^{-N/2}\int_\nu^\infty (d\alpha)\sum_{m=0}^\infty\frac{\mathcal{D}^m}{m!}\,\exp\left[-\frac{1}{2}(\alpha,\alpha)\right]\,. \qquad (7.110)$$

To apply the differential operator $\mathcal{D}^m$ we can take advantage of the *multinomial theorem* as expressed by

$$\left(\sum_{j,h=1}^N a_{jh}\right)^m = m!\sum_{\{m_{jh}\}}\prod_{j,h=1}^N\frac{a_{jh}^{m_{jh}}}{m_{jh}!}\,; \qquad (7.111)$$

the set $\{m_{jh}\}$ is formed by all non–negative integers satisfying the multinomial constraint $\sum_{j,h=1} m_{jh} = m$. In our case, by factorization of the operator $\mathcal{D}^m$,

$$\sum_{m=0}^{\infty} \frac{\mathcal{D}^m}{m!} = \sum_{m=0} \prod_{j,h=1}^{N} \left(\tilde{\omega}_{jh}^{m_{jh}}/m_{jh}!\right) \prod_{j,h=1}^{N} \left(\frac{\partial}{\partial\alpha_j}\right)^{m_{jh}} \left(\frac{\partial}{\partial\alpha_h}\right)^{m_{jh}} \tag{7.112}$$

$\tilde{\omega}_{jh} \equiv \frac{1}{2}(1-\delta_{jh})\,\omega_{R,jh}^{(2)}$ for semplicity. In (7.112) the sum with respect to $\{m_{jh}\}$ appears redundant, since the index m is defined. By the properties of the product and of the symmetric tensors,

$$\prod_{j,h=1}^{N} \left(\frac{\partial}{\partial\alpha_j}\right)^{m_{jh}} \left(\frac{\partial}{\partial\alpha_h}\right)^{m_{jh}} = \prod_{h=1}^{N} \left(\frac{\partial}{\partial\alpha_h}\right)^{m_h} , \tag{7.113}$$

where we have defined the new index $m_h \equiv \sum_{j,h=1}^{N}(m_{jh}+m_{hj})$ for which the remarkable property $\sum_{h=1}^{N} m_h = 2m$ holds; we can obtain, remembering that $\mathcal{D}^m$ acts on the function $\exp\left[-\frac{1}{2}(\alpha,\alpha)\right]$,

$$\prod_{h=1}^{N} \left(\frac{\partial}{\partial\alpha_h}\right)^{m_h} \exp\left[-\frac{1}{2}(\alpha,\alpha)\right] = \prod_{h=1}^{N} 2^{-m_h/2} \left(\frac{d}{du_h}\right)^{m_h} \exp(-u_h^2) , \tag{7.114}$$

where the new variable $u_h \equiv \alpha_h/\sqrt{2}$ has been introduced. The Hermite polynomials of order $n \geq 0$ satisfy the differential equation of order n (see e.g. Bateman 1953)

$$\frac{d^n}{du^n} \exp(-u^2) = (-1)^n\, H_n(u) \exp(-u^2) , \tag{7.115}$$

and therefore, from (7.114) and (7.115), we can write

$$\prod_{h=1}^{N} \left(\frac{\partial}{\partial\alpha_h}\right)^{m_h} \exp\left[-\frac{1}{2}(\alpha,\alpha)\right] = \prod_{h=1}^{N} \left(-\frac{1}{\sqrt{2}}\right)^{m_h} H_{m_h}(u_h) \exp(-u_h^2) . \tag{7.116}$$

Finally, the Politzer–Wise probability $\mathcal{P}_N^{(\nu)}$ in (7.110) becomes:

$$\mathcal{P}_N^{(\nu)} = (2\pi)^{-N/2} \sum_{m=0} \left(\frac{1}{2}\right)^m \left(\prod_{j,h=1}^{N} \tilde{\omega}_{jh}^{m_{jh}}/m_{jh}!\right) \left(\prod_{h=1}^{N} \int_{\nu}^{\infty} d\alpha_h\, H_{m_h}(\alpha_h/2) \exp(-\alpha_h^2/2)\right) . \tag{7.117}$$

By the relation (see Bateman 1953)

$$\int_0^u dy\, H_n(y)\, \mathrm{e}^{-y^2} = H_{n-1}(0) - \mathrm{e}^{-u^2}\, H_{n-1}(u) , \tag{7.118}$$

one can immediately obtain:

$$\int_{\nu}^{\infty} d\alpha_h \, H_{m_h}(\alpha_h/2) \, \exp(-\alpha_h^2/2) = \sqrt{2}\, \mathrm{e}^{\nu^2/2} \, H_{m_h-1}(\nu/\sqrt{2}) \; ; \tag{7.119}$$

in particular, this last relation holds if $m_h \geq 1$; if $m_h = 0$, we directly obtain

$$\int_{\nu}^{\infty} d\alpha_h \, \exp(-\alpha_h^2/2) = \sqrt{\frac{\pi}{2}} \, \mathrm{erfc}(\nu/\sqrt{2}) \; , \tag{7.120}$$

where $\mathrm{erfc}(x)$ is the complementary error function. Finally, Eq.(7.117) leads to the expression

$$\mathcal{P}_N^{(\nu)} = \sum_{m=0} \left(\prod_{j,h=1}^{N} \tilde{\omega}_{jh}^{m_{jh}} / m_{jh}! \right) \left(\prod_{h=1}^{N} \exp(-\nu^2/2) \, H_{m_h-1}(\nu/\sqrt{2}) / (\sqrt{\pi}\, \sqrt{2}^{\, m_h}) \right) \; , \tag{7.121}$$

provided that one formally defines $H_{-1}(\nu/\sqrt{2}) \equiv (\sqrt{\pi}/2) \exp(\nu^2/2) \, \mathrm{erfc}(\nu/\sqrt{2})$.

7.4 Appendix 2: Derivation of the Peak Correlation Function

We explicitely work out here the 2–point correlation of the excursion regions

$$1 + \xi_{\nu}^{(2)}(\mathbf{x}_1, \mathbf{x}_2) = \frac{\mathcal{P}_2^{(\nu)}(\mathbf{x}_1, \mathbf{x}_2)}{\left[\mathcal{P}_1^{(\nu)}\right]^2} \; . \tag{7.122}$$

For a Gaussian random field δ_R

$$\mathcal{P}_2^{(\nu)}(\mathbf{x}_1, \mathbf{x}_2) = \int_{\nu}^{\infty} d\alpha_1 \int_{\nu}^{\infty} d\alpha_2 \, \frac{\mathrm{e}^{-\frac{1}{2}(\alpha, M^{-1}\alpha)}}{[(2\pi)^2 \det M \,]^{1/2}} \; , \tag{7.123}$$

with

$$M = \begin{pmatrix} 1 & \omega \\ \omega & 1 \end{pmatrix} \; ; \qquad \omega \equiv \omega_R^{(2)}(\mathbf{x}_1, \mathbf{x}_2) \equiv \xi_R^{(2)}(\mathbf{x}_1, \mathbf{x}_2)/\sigma_0^2(R) \; , \qquad \mathbf{x}_1 \neq \mathbf{x}_2 \; . \tag{7.124}$$

The matrix M^{-1} is

$$M^{-1} = \frac{1}{1-\omega^2} \begin{pmatrix} 1 & -\omega \\ -\omega & 1 \end{pmatrix} \; , \tag{7.125}$$

from which

$$\mathcal{P}_2^{(\nu)}(\mathbf{x}_1, \mathbf{x}_2) = \left[2\pi\sqrt{1-\omega^2}\right]^{-1} \int_{\nu}^{\infty} \int_{\nu}^{\infty} d\alpha_1 \, d\alpha_2 \, \exp\left[-\frac{\alpha_1^2 + \alpha_2^2 - 2\,\omega\,\alpha_1\alpha_2}{2\,(1-\omega^2)} \right] \; , \tag{7.126}$$

and finally

$$1+\xi_{\nu}^{(2)}(\mathrm{x}_1,\mathrm{x}_2)=\left[\frac{1}{2}\,\mathrm{erfc}(\frac{\nu}{\sqrt{2}})\right]^{-2}\int_{\nu}^{\infty}\int_{\nu}^{\infty}d\alpha_1\,d\alpha_2\,\left[2\pi\sqrt{(1-\omega^2)}\right]^{-1}\exp\left[-\frac{\alpha_1^2+\alpha_2^2-2\omega\alpha_1\alpha_2}{2\,(1-\omega^2)}\right]. \tag{7.127}$$

Viceversa, by starting from the Gaussian bivariate distribution for normalized variables with mean zero

$$p(\alpha_1,\alpha_2;\,\omega)=\left[2\pi\sqrt{(1-\omega^2)}\right]^{-1}\exp\left[-\frac{\alpha_1^2+\alpha_2^2-2\,\omega\,\alpha_1\alpha_2}{2\,(1-\omega^2)}\right], \tag{7.128}$$

and by applying the classical Mehler's formula (see Bateman 1953):

$$\sum_{n=0}^{\infty}\frac{(z/2)^n}{n!}\,H_n(x)\,H_n(y)=(1-z^2)^{-1/2}\,\exp\left(-\frac{x^2z^2+y^2z^2-2xyz}{1-z^2}\right), \tag{7.129}$$

one has

$$p(\alpha_1,\alpha_2;\,\omega)=(2\pi)^{-1}\,\exp\Big[-\frac{1}{2}(\alpha_1^2+\alpha_2^2)\Big]\sum_{m=0}^{\infty}\frac{(\omega/2)^m}{m!}\,H_m(\alpha_1/\sqrt{2})\,H_m(\alpha_2/\sqrt{2})\,. \tag{7.130}$$

Thus, it is possible to obtain the result of Jensen and Szalay

$$\mathcal{P}_2^{(\nu)}(\mathrm{x}_1,\mathrm{x}_2)=\int_{\nu}^{\infty}\int_{\nu}^{\infty}d\alpha_1\,d\alpha_2\,p(\alpha_1,\alpha_2;\,\omega)=\sum_{m=0}^{\infty}\frac{\omega^m}{m!}\left[\frac{\exp(-\nu^2/2)\,H_{m-1}(\nu/\sqrt{2})}{\sqrt{\pi}\,\sqrt{2}^{\,m}\,\mathrm{erfc}(\nu/\sqrt{2})}\right]^2, \tag{7.131}$$

where formally $H_{-1}(x)\equiv(\sqrt{\pi}/2)\,\mathrm{e}^{x^2}\,\mathrm{erfc}(x)$. In the limit $\omega\ll 1$, considering only the leading term

$$\xi_{\nu}^{(2)}(\mathrm{x}_1,\mathrm{x}_2)\approx\left(\frac{\sqrt{2}\,\exp(-\nu^2/2)}{\sqrt{\pi}\,\mathrm{erfc}(\nu/\sqrt{2})}\right)^2\frac{\xi_R^{(2)}(\mathrm{x}_1,\mathrm{x}_2)}{\sigma_0^2(R)}\,. \tag{7.132}$$

Therefore, as far as the 2–point correlation for the above threshold regions are concerned, the results obtained with functional methods can be easily worked out with classical techniques. The linear regime approximation (7.132) has been firstly deduced by Kaiser (1984). See the relation (6.4).

Figure Captions

Figure VII-1. Differential number density of peaks between ν and $\nu + d\nu$ for various values of γ. Spectral parameters γ and R_* are defined by Eqs.(7.81) and (7.82) [from BBKS].

Figure VII-2. Cumulative number density $n_{pk}(\nu)$ of peaks with height in excess of $\nu\sigma_0$ [from BBKS].

Figure VII-3. The parameter p in Eq.(7.105), describing the average number of connections of the surfaces ν = constant, plotted for several filter scales against ν for the Cold dark Matter spectrum. The scales are 1, 10 and 100 kpc, 1, 10, and 100 Mpc; the curves become less sharply peaked for the smaller filter scales. It can be seen that for the larger scales the regions rapidly become simply connected for increasing $|\nu|$ [from Couchman 1987a].

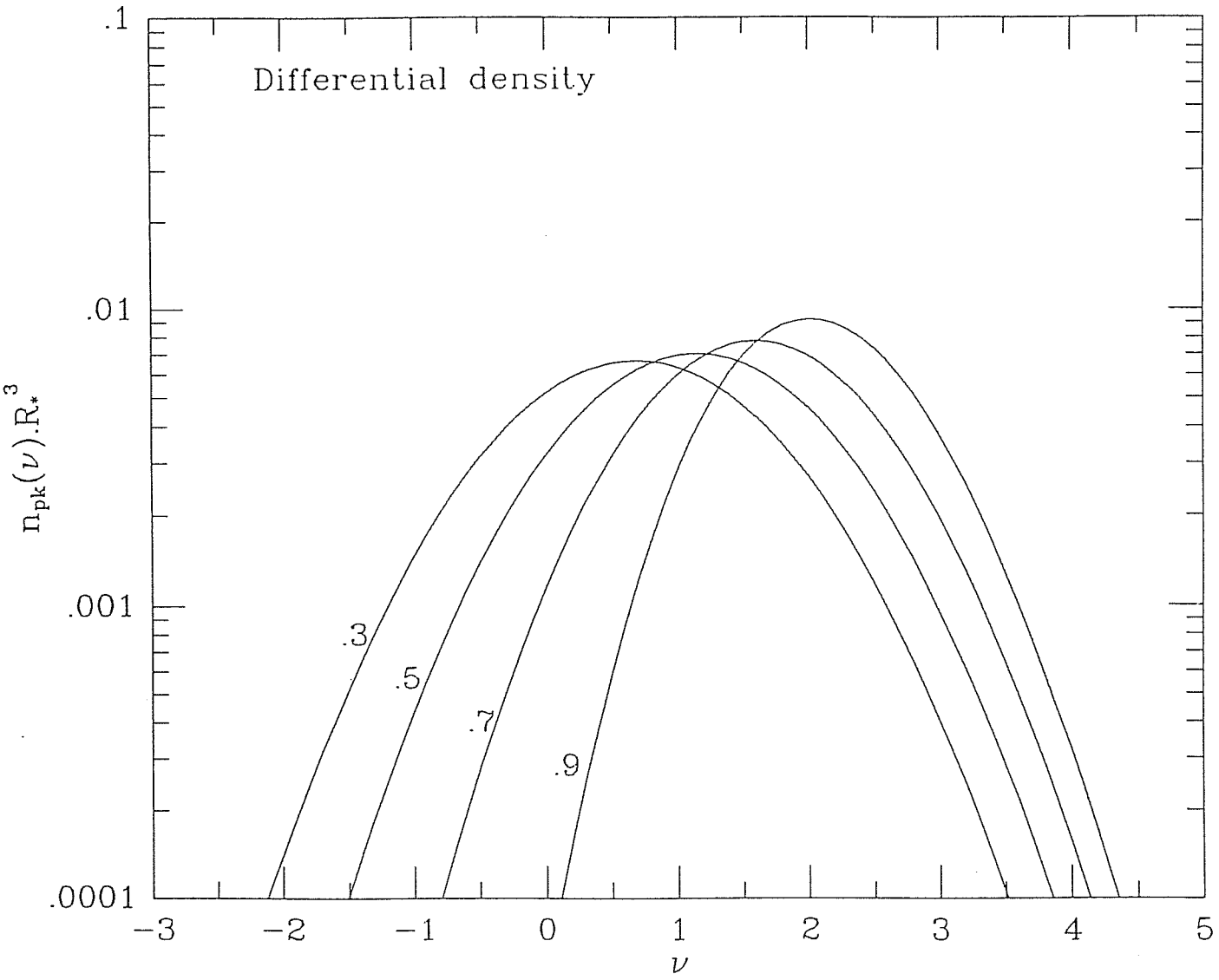
Differential density
.1
.01
.001
.0001
$n_{pk}(\nu).R_*^3$
.3
.5
.7
.9
−3
−2
−1
0
1
2
3
4
5
ν

Fig. VII-1

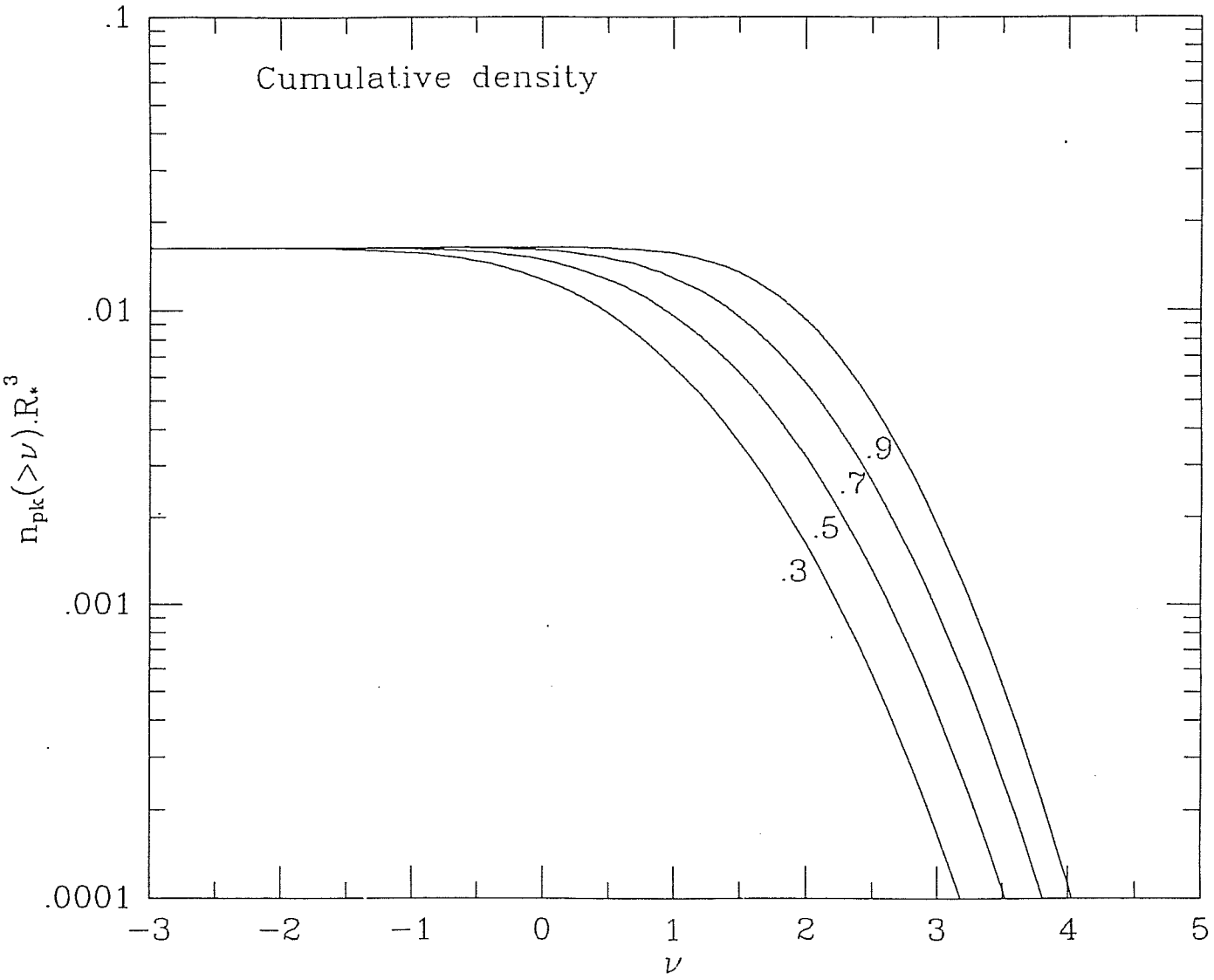

Fig. VII-2

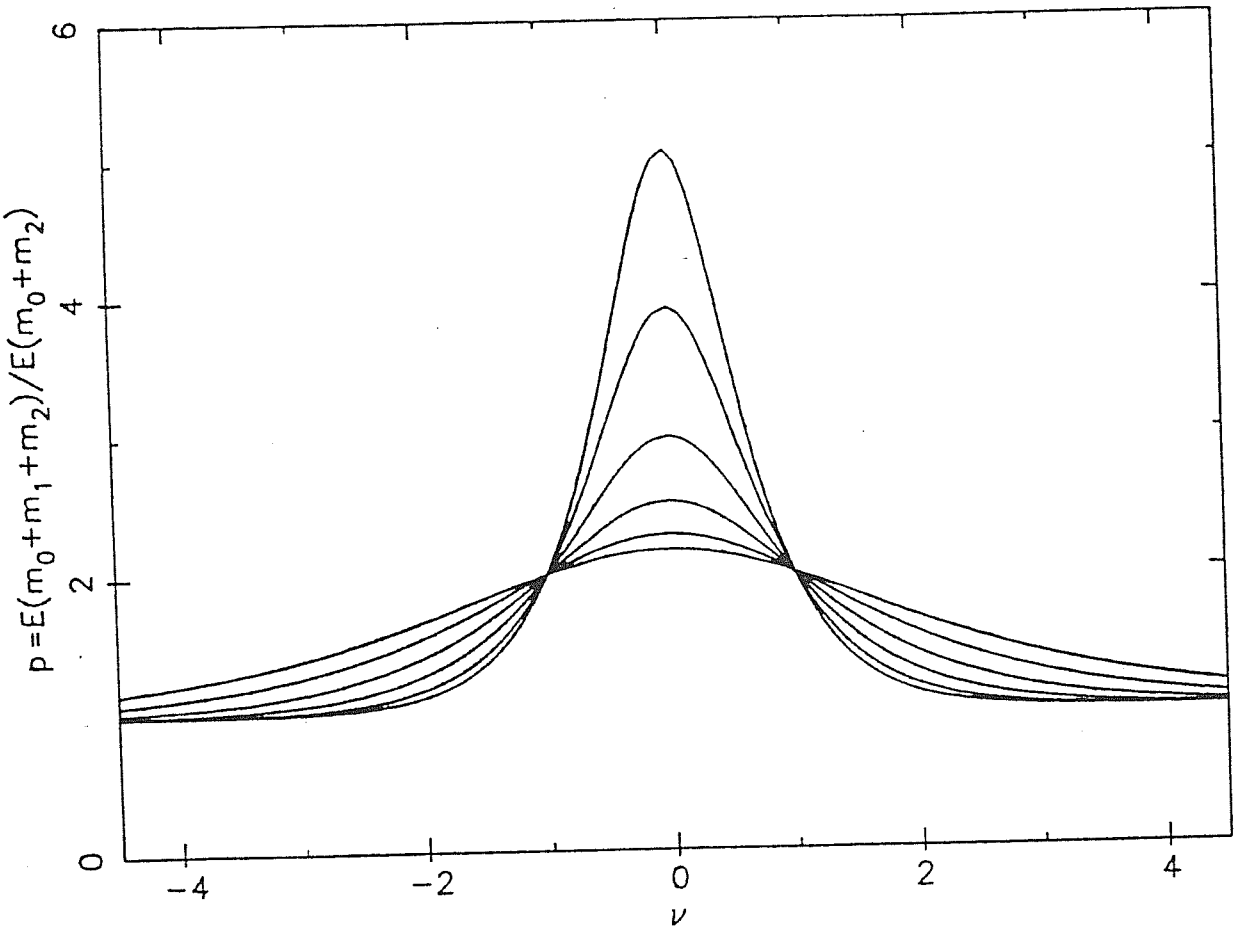

Fig. VII-3

CHAPTER VIII

Non Linear Gravitational Evolution

The linear growth laws discussed in Chapter IV hold until $\delta \approx 1$. When the perturbation amplitudes approach unity, non linear gravitational effects become important. For instance, by using a simple spherical top hat model, it is easy to show that collapse to a point of infinite density occurs at a time when (if $\Omega = 1$) the *linear* density contrast is $\delta \approx 1.68$ (see Peebles 1980). However, to follow the non–linear stage of the gravitational collapse is undoubtly very hard to do in an analytical way and the interest in such a type of analysis is drastically reduced. People are forced to resort to N–body techniques (Davis *et al.* 1985; Efstathiou *et al.* 1985; White *et al.* 1987a; 1987b, in the CDM framework), or various analytical approximations, as the *Zel'dovich approximation* (Zel'dovich 1970;), leading to another ones, the *adhesion approximation* (see e.g. Gurbatov, Saichev & Shandarin 1989; Shandarin & Zel'dovich 1989; Kofman, Pogosyan & Shandarin 1990) and, more able to follow the development of structures beyond the epoch of first caustic formation, the *frozen–flow approximation* (Matarrese *et al.* 1992); these approximations are useful for developing intuition, but they are not a substitute for exact or numerical non linear solutions.

A very interesting new general–relativistic algorithm to study the non–linear evolution of density perturbations of collisionless matter is given by Matarrese, Pantano & Saez (1993).

Recently the interest in the analytical treatment of non–linear gravity has grown and many efforts are devoted to understand the results.

The basic technique is the perturbative theory, the systematic development of the perturbative expansion being obtained by writing

$$\delta = \sum_n \delta^{(n)} , \tag{8.1}$$

where $\delta^{(n)} = 0(\delta^{(1)n})$, $\delta^{(1)}$ corresponding to the linear solution. Comparing terms of equal order in Eq.(4.11), one constructs the differential equation for the n–th term $\delta^{(n)}$, lower order solutions providing source terms for the higher orders.

The published literature on the perturbative approach is considerably growing.

The evolution of cosmological adiabatic perturbations in the so called weakly non–linear regime, when the second order contribution $\delta^{(2)}$ in (8.1) is not negligible, was analyzed by Juszkiewicz (1981): he showed that second order effects could induce tidal processes leading to the disruption of large scale inhomogeneities into smaller units; the articles of Vishniac (1983) and Juszkiewicz, Sonoda & Barrow (1984) treat in detail the consequences on the galaxy clustering pattern.

Fry (1984) calculates the evolution of cosmological density correlation functions to lowest non vanishing order in perturbative theory for an initially random Gaussian distribution; an extrapolation of the observed hierarchical form of the two–, three– and four–point correlation functions ξ, ζ and η (Groth & Peebles 1977; Fry & Peebles 1978; Sharp, Bonometto & Lucchin 1984) emerges quite generally. The form of the connected correlations induced by non–linearities in the time evolution of primordial Gaussian fluctuations is discussed also in Goroff *et al.* (1986). Fry (1986) stresses that the enhancement of clustering, proper of the biased scenario, is a general feature of non–linear processing of the galaxy distribution. The non–linear gravitational evolution is essential to predict a correct interpretation of large–scale deviations from the Hubble flow, as showed in Grinstein *et al.* (1987). The predictions of the Zel'dovich approximation, often used to mimic the effects of non–linear gravitational time evolution, are compared with those of the true non–linear regime in Grinstein & Wise (1987). More recently, Coles (1990) uses perturbative technique to explore the possibility of originating more power on large scales in the standard CDM cosmogony. Suto & Sasaki (1991) found that, even when fluctuations are in linear regime,

a non–linear correction might significantly affect the result for the corresponding velocity field predicted in the framework of linear theory. They show also that nonlinear effects either suppress or *enhance* the growth of perturbations on large scales, depending on the spectrum shape; the second order perturbations are analytically tractable for all power–law spectra (see also the very recent Makino, Sasaki & Suto 1992). Moutarde *et al.* (1991) in a rigorous Lagrangian perturbative theory (at the end of calculations physical observables are known in the rest frame of each fluid element), whose first order corresponds to the Zel'dovich approximation, found that density contrasts up to $\delta \sim 50$ could be appropriately described analytically. Bernardeau (1992b), using results of Bernardeau (1992a), derives an exact relationship between the density and the divergence of the velocity field.

The first direct observational suggestion that gravitational instability in the perturbative regime operates on large scales is in Baumgart & Fry (1991); the observed bispectrum obeys the hierarchical pattern, with a reduced three point amplitude that is consistent with gravitational instability in perturbative theory starting from Gaussian initial conditions. The trispectrum, marginally detected, is again consistent with the hierarchical pattern.

More emphasis was showed claiming the measurement of another second order effect: the distribution of IRAS galaxies out to $140\,h^{-1}Mpc$ is such that the inferred underlying distribution of density is found to be positive skewed, physically meaning that the superclusters (positive fluctuations) are smaller than the voids (negative fluctuations), but depart more from the mean density (Saunders *et al.* 1991). This result, with the detection of new superclusters and voids, "rule out the standard CDM model at least the 97% confidence limit" (previous reference, pag.37), already seriously challenged by the large–scale power detected in IRAS (Efstathiou *et al.* 1990) and APM (Maddox *et al.* 1990) catalogues.

8.1 Second and Third Order Perturbations

Second order perturbative theory has been discussed in a more general context (e.g. pressure included) by Hunter (1964) and Tomita (1967; 1971; 1972). Peebles (1980) indicates how to compute the growth of skewness (the third central moment) in second order approximation; positive skewness has been recently detected in IRAS data (Saunders *et al.* 1991) and analyzed by Park (1991); the importance of the sign of the skewness of the linear (non–Gaussian) density field as a predictor of the non–linear evolution has recently been emphasized by Moscardini *et al.* (1991), Matarrese *et al.* (1991) and Messina *et al.* (1992 and references therein) in the framework of CDM scenario (see also Weinberg & Cole 1992).

Gaussian fields have zero skewness, but the presence of a non–zero skewness in the e.g. IRAS data, does not necessarily imply non–Gaussian initial conditions: even if the initial probability distribution of the mass density contrast δ is Gaussian then symmetric, an asymmetry will inevitably develop later, as a second order effect, under the influence of gravity. Indeed, δ can grow indefinitely in regions where it was initially positive, whereas in the voids it can never decrease below -1.

We show here how gravity can induce skewness in an initially Gaussian distribution, computing and solving the second order solutions of the equations of motion of matter. Next, we calculate the skewness in density field, assumed Gaussian at early time (e.g. at recombination), also suggesting how to work out the skewness in the more general case in which δ is non–Gaussian at the beginning. We conclude discussing how the observations can be used to distinguish "conventional" models from an intrinsically non–Gaussian alternative. If someone is interested in the subject we advise Silk & Juszkiewicz (1991), Juszkiewicz & Bouchet (1991), Martel & Freudling (1991), Coles & Frenk (1991) and Bouchet *et al.* (1992).

Second–Order Equations: Solutions

In comoving coordinates, the equations of motion for the pressureless self–gravitating fluid

are the Eqs.(4.7), (4.8) and (4.9).

The perturbative series for δ and $\mathbf{v}$ may be written as

$$\delta = \delta^{(1)} + \delta^{(2)} + \cdots , \tag{8.2}$$

$$\mathbf{v} = \mathbf{v}^{(1)} + \mathbf{v}^{(2)} + \cdots , \tag{8.3}$$

where $\delta^{(n)}$ and $\mathbf{v}^{(n)}$ are of order n; $\delta^{(1)}$ and $\mathbf{v}^{(1)}$ are the linear solutions.

In particular, we consider only the growing mode $\delta^{(1)} \propto D$. The second order contribution $\delta^{(1)} + \delta^{(2)}$ is a solution of the differential equation (4.11), reducing to, once (4.12) is taken into account

$$\partial_\circ^2 \delta^{(2)} + 2\dot{a}a^{-1}\partial_\circ \delta^{(2)} - 4\pi G\rho_b \delta^{(2)} =$$

$$= 4\pi G\rho_b\, \delta^{(1)2} + a^{-2}\partial_\alpha \delta^{(1)}\, \partial_\alpha \phi^{(1)} + a^{-2}\partial_\alpha \partial_\beta\, v^{(1)\alpha} v^{(1)\beta} ; \tag{8.4}$$

$\delta^{(2)}$ is related to the second order peculiar potential $\phi^{(2)}$ by

$$\nabla^2 \phi^{(2)} = 4\pi G a^2 \rho_b\, \delta^{(2)} . \tag{8.5}$$

A common way to write (8.4) is

$$\partial_\circ^2 \delta^{(2)} + 2\dot{a}a^{-1}\partial_\circ \delta^{(2)} - 4\pi G\rho_b\, \delta^{(2)} = \left[4\pi G\rho_b + \left(\frac{\dot{D}}{D}\right)^2\right] \delta^{(1)2} +$$

$$\left[4\pi G\rho_b + 2\left(\frac{\dot{D}}{D}\right)^2\right] \partial_\alpha \delta^{(1)}\, \partial_\alpha \triangle^{(1)} + \left(\frac{\dot{D}}{D}\right)^2 \partial_\alpha \partial_\beta \triangle^{(1)}\, \partial_\alpha \partial_\beta \triangle^{(1)} , \tag{8.6}$$

where $D = D(t)$ is a solution of (4.14) and $\triangle^{(1)}$ is the linear gravitational potential defined in (4.26). We can see that each side of Eq.(8.6) is homogeneous in powers of t; we solve (8.6) in an Einstein–de Sitter universe: noting that $D^2 \propto \delta^{(2)} \equiv \delta_2(\mathbf{x})\, D(t)^2$,

$$\partial_\circ^2 D^2 + 2\dot{a}a^{-1}\partial_\circ D^2 - 4\pi G\rho_b\, D^2 = \frac{1}{2} f(\mathbf{x}, t) \left(\frac{\dot{D}}{D}\right)^2 , \tag{8.7}$$

where, since $4\pi G\rho_b = 2/3t^2$ and $\dot{D}/D = \dot{a}/a = 2/3t$,

$$\delta_2(\mathbf{x}) f(\mathbf{x}, t) \equiv 5\, \delta^{(1)2} + 7\, \partial_\alpha \delta^{(1)}\, \partial_\alpha \triangle^{(1)} + 2\, \partial_\alpha \partial_\beta \triangle^{(1)}\, \partial_\alpha \partial_\beta \triangle^{(1)}$$

ie. by (8.7),

$$\left[4\pi G\rho_b + 2\left(\frac{\dot{D}}{D}\right)^2\right] D^2 = \frac{1}{2}\left(\frac{\dot{D}}{D}\right)^2 f$$

or

$$f = 7D^2 \ .$$

Therefore the solution of (8.7) is given by (Peebles 1980, Eq.(18.8))

$$\delta^{(2)} = \frac{5}{7}\,\delta^{(1)2} + \partial_\alpha\delta^{(1)}\,\partial_\alpha\triangle^{(1)} + \frac{2}{7}\,\partial_\alpha\partial_\beta\triangle^{(1)}\,\partial_\alpha\partial_\beta\triangle^{(1)} \ . \tag{8.8}$$

It is not difficult to show that $\langle\delta^{(2)}\rangle = 0$, ie. mass is conserved.

We see from (8.8) that, to second order, the behaviour of δ is non local (and in fact it depends on spatial derivatives): the mass fluctuation at the position x depends on initial perturbations at other positions via $\triangle^{(1)}$ (Eq.(4.26)). Physically this means that, differently from the linear local case, when density fluctuation grows in amplitude, its spatial dependence, in comoving coordinates, changes. Thus the gravity field does change direction and particles are not accelerated in a fixed direction, as occurs in linear regime; the last term in right–hand side of Eq.(8.8) corresponds to the linear peculiar velocity shear contribution: indeed, if we write this, apart from a multiplicative factor, in the form $\sigma_{\alpha\beta} = (\frac{1}{3}\,\delta_{\alpha\beta}\nabla^2 - \partial_\alpha\partial_\beta)\,\phi^{(1)}$, we get $(\partial_\alpha\partial_\beta\triangle^{(1)})^2 = \sum_{\alpha,\beta=1}^{3}(\sigma_{\alpha\beta})^2$. Finally, if $\delta^{(1)}$ is Gaussian distributed, $\delta^{(2)}$ is no longer Gaussian distributed.

The second order velocity $\mathbf{v}^{(2)}$ is solution of the equations

$$\partial_\circ(a\,\mathbf{v}^{(2)}) = \left(\mathbf{v}^{(1)}\cdot\nabla\right)\mathbf{v}^{(1)} = a\,\mathbf{g}^{(2)} \ , \tag{8.9}$$

$$\partial_\circ\delta^{(2)} + a^{-1}\nabla\cdot\left(\mathbf{v}^{(2)} + \delta^{(1)}\,\mathbf{v}^{(1)}\right) = 0 \ , \tag{8.10}$$

where $\mathbf{g}^{(2)} \equiv -a^{-1}\nabla\phi^{(2)}$ is the second order peculiar acceleration. From (8.10)

$$\mathbf{v}^{(2)} = a\,\partial_\circ\left(\frac{\mathbf{g}^{(2)}}{4\pi G\rho_b\,a}\right) - \delta^{(1)}\mathbf{v}^{(1)} + \mathbf{F}_2 \ . \tag{8.11}$$

In the previous relation, the vector $\mathbf{F}_2$ is such that $\nabla\wedge\mathbf{v}^{(2)} = \mathbf{0}$. Substituting in (8.9) and taking the divergence,

$$\partial_\circ^2\delta^{(2)} + 2\dot{a}a^{-1}\partial_\circ\delta^{(2)} - 4\pi G\rho_b\,\delta^{(2)} =$$

$$= -a^{-1}\nabla\cdot\left[\left(\partial_o + \dot{a}\,a^{-1}\right)\delta^{(1)}\mathbf{v}^{(1)} - a^{-1}(\mathbf{v}^{(1)}\cdot\nabla)\,\mathbf{v}^{(1)}\right] , \qquad (8.12)$$

which is another form of (8.4).

Because $\delta^{(2)} \propto D^2$, we have $\mathbf{g}^{(2)} \propto \rho_b\, a\, D^2$; alternative forms of (8.11) are therefore

$$\begin{aligned}\mathbf{v}^{(2)} &= a\frac{\dot{D}}{D}\left[\frac{2\,\mathbf{g}^{(2)}}{4\pi G\rho_b\, a} + \delta^{(1)}\nabla\triangle^{(1)}\right] + \mathbf{F}_2 \\ &= a\frac{\dot{D}}{D}\left[\delta^{(1)}\nabla\triangle^{(1)} - 2\nabla\triangle^{(2)}\right] + \mathbf{F}_2 , \end{aligned} \qquad (8.13)$$

where $\triangle^{(2)} \equiv \phi^{(2)}/4\pi G\rho_b\, a^2$ is the second order gravitational potential. We stress the fact that $\mathbf{v}^{(2)}$ is *not* parallel to the second order acceleration $\mathbf{g}^{(2)}$: this is a consequence of the non locality. Finally, we remember that $\mathbf{v}^{(2)}$ is known only once $\delta^{(2)}$ is known.

The equation (8.6) can be solved exactly only if $\Omega = 1$, in which case all terms in right–hand side have the same time dependence, making the equation separable. For $\Omega \neq 1$ the equation (8.6) is not separable, and thus cannot be directly integrated.

Approximate expressions of $\delta^{(2)}$ in non–flat universes are given in Fry (1984) and in Martel & Freudling (1991), but the Eq.(8.6) is really solved, for a general Ω universe, only in Bouchet *et al.* (1992): using an elegant perturbative theory in Lagrangian representation, they find

$$\delta^{(2)} = \frac{1}{2}\left[1 - E(\Omega)/D^2\right]\delta^{(1)2} + \partial_\alpha\delta^{(1)}\partial_\alpha\triangle^{(1)} + \frac{1}{2}\left[1 + E(\Omega)/D^2\right]\partial_\alpha\partial_\beta\triangle^{(1)}\partial_\alpha\partial_\beta\triangle^{(1)} \qquad (8.14)$$

where $E(\Omega)$ is a very complicated function of Ω, but in the vicinity of $\Omega = 1$, actually in the range $0.05 \lesssim \Omega \lesssim 3$,

$$E(\Omega) = -\frac{3}{7}\,\Omega^{-2/63}\,D^2 + 0\left[(\Omega-1)^2\right] , \qquad (8.15)$$

from which (0.4% accuracy)

$$\delta^{(2)} = \frac{1}{2}\left[1 + \frac{3}{7}\Omega^{-2/63}\right]\delta^{(1)2} + \partial_\alpha\delta^{(1)}\partial_\alpha\triangle^{(1)} + \frac{1}{2}\left[1 - \frac{3}{7}\Omega^{-2/63}\right]\partial_\alpha\partial_\beta\triangle^{(1)}\partial_\alpha\partial_\beta\triangle^{(1)} . \qquad (8.16)$$

Therefore, the $\Omega \neq 1$ solutions scale with time almost exactly like D^2, since $\delta^{(1)} \propto \triangle^{(1)} \propto D(t)$, and $E(\Omega)$ is *extremely weakly* sensitive to Ω. This property has been also

noticed by Martel & Freudling (1991), who have integrated an approximate time evolution equation for $\delta^{(2)}$ with $\Omega = 0.2$.

- Fourier Transforms -

We compute now the Fourier transforms of $\delta^{(2)}$ and $\mathbf{v}^{(2)}$; although Peebles in his book (1980, §18) derives for an Einstein–de Sitter universe the induced–by–gravity skewness of an initially Gaussian density field directly in x–space, it is much simpler to do that in k–space.

We can obtain $\tilde{\delta}^{(2)}$ directly Fourier transforming the differential equation (8.6) (* indicates convolution)

$$\partial_\circ^2 \tilde{\delta}^{(2)} + 2\dot{a}a^{-1}\partial_\circ \tilde{\delta}^{(2)} - 4\pi G\rho_b\,\tilde{\delta}^{(2)} =$$

$$= \left[4\pi G\rho_b + \left(\frac{\dot{D}}{D}\right)^2\right]\tilde{\delta}^{(1)} * \tilde{\delta}^{(1)} + \left[4\pi G\rho_b + 2\left(\frac{\dot{D}}{D}\right)^2\right](k^\alpha \tilde{\delta}^{(1)}) * \left(\frac{k^\alpha}{k^2}\,\tilde{\delta}^{(1)}\right) +$$

$$+ \left(\frac{\dot{D}}{D}\right)^2 \left(\frac{k^\alpha k^\beta}{k^2}\,\tilde{\delta}^{(1)}\right) * \left(\frac{k^\alpha k^\beta}{k^2}\,\tilde{\delta}^{(1)}\right) . \qquad (8.17)$$

In the Einstein–de Sitter case, the left–hand side becomes $14\,\tilde{\delta}^{(2)}/9t^2$; therefore,

$$\tilde{\delta}^{(2)} = \frac{5}{7}\,\tilde{\delta}^{(1)} * \tilde{\delta}^{(1)} + (k^\alpha \tilde{\delta}^{(1)}) * \left(\frac{k^\alpha}{k^2}\,\tilde{\delta}^{(1)}\right) + \frac{2}{7}\left(\frac{k^\alpha k^\beta}{k^2}\,\tilde{\delta}^{(1)}\right) * \left(\frac{k^\alpha k^\beta}{k^2}\,\tilde{\delta}^{(1)}\right) , \qquad (8.18)$$

which is just the Fourier transform of (8.8).

Explicitly one gets

$$\tilde{\delta}^{(2)}(\mathrm{k},t) = \frac{1}{(2\pi)^3}\int d\mathrm{k}'\, J^{(2)}(\mathrm{k}',\mathrm{k}-\mathrm{k}')\,\tilde{\delta}^{(1)}(\mathrm{k}',t)\,\tilde{\delta}^{(1)}(\mathrm{k}-\mathrm{k}',t) , \qquad (8.19)$$

where we have defined the function

$$\begin{aligned} J^{(2)}(\mathrm{k},\mathrm{k}') &\equiv \frac{5}{7} + \frac{\mathrm{k}\cdot\mathrm{k}'}{k'^2} + \frac{2}{7}\left(\frac{\mathrm{k}\cdot\mathrm{k}'}{kk'}\right)^2 \\ &= \frac{17}{21} + \frac{k}{k'}\,P_1(\mu) + \frac{4}{21}\,P_2(\mu) , \end{aligned} \qquad (8.20)$$

$\mu \equiv \mathrm{k}\cdot\mathrm{k}'/kk'$, $P_1(\mu)$ and $P_2(\mu)$ being Legendre polynomials. Note that, because of mass conservation, $\langle\tilde{\delta}^{(2)}(\mathrm{k})\rangle = 0$.

For completeness, we give also the Fourier transform of $v^{(2)\alpha}$:

$$\tilde{v}^{(2)\alpha}(\mathbf{k},t) = i\,a\,\frac{\dot{D}}{D}\,\frac{k^\alpha}{k^2}\int d\mathbf{k}'\; K^{(2)}(\mathbf{k}',\mathbf{k}-\mathbf{k}')\,\tilde{\delta}^{(1)}(\mathbf{k}',t)\,\tilde{\delta}^{(1)}(\mathbf{k}-\mathbf{k}',t)\,, \tag{8.21}$$

where

$$\begin{aligned} K^{(2)}(\mathbf{k},\mathbf{k}') &\equiv 2\,J^{(2)}(\mathbf{k},\mathbf{k}') - \frac{(\mathbf{k}+\mathbf{k}')\cdot\mathbf{k}}{k^2} \\ &= \frac{13}{21} + \frac{k}{k'}\,P_1(\mu) + \frac{8}{21}\,P_2(\mu)\,. \end{aligned} \tag{8.22}$$

Note that $\langle \mathbf{v}^{(2)} \rangle = \mathbf{0}$. In an Einstein–de Sitter universe $\mathbf{v}^{(2)} \sim t$, slower than $\delta^{(2)} \sim t^{4/3}$. $\nabla \wedge \mathbf{v}^{(2)} = 0$. A more general expression of $\tilde{\delta}^{(2)}$, for a general Ω universe, is recovered if one takes the Fourier transform of (8.14).

Third–Order Equations: Solutions

The third–order contribution $\delta^{(3)}$ is solution of the equation

$$\begin{aligned} &\partial_\circ^2\delta^{(3)} + 2\dot{a}a^{-1}\partial_\circ\delta^{(3)} - 4\pi G\rho_b\,\delta^{(3)} = \\ &= 4\pi G\rho_b\,\left(2\delta^{(1)}\delta^{(2)}\right) + a^{-2}\left(\partial_\alpha\delta^{(1)}\partial_\alpha\phi^{(2)} + \partial_\alpha\delta^{(2)}\partial_\alpha\phi^{(1)}\right) + \\ &+ 2\,a^{-2}\partial_\alpha\partial_\beta\,v^{(1)\alpha}v^{(2)\beta} + a^{-2}\partial_\alpha\partial_\beta\,\delta^{(1)}\,v^{(1)\alpha}\,v^{(1)\beta}\,; \end{aligned} \tag{8.23}$$

however, from the third order on, the advantages of the Fourier transform for computation become more than obvious; we get, from the previous equation,

$$\begin{aligned} &\partial_\circ^2\tilde{\delta}^{(3)} + 2\dot{a}a^{-1}\partial_\circ\tilde{\delta}^{(3)} - 4\pi G\rho_b\,\tilde{\delta}^{(3)} = \\ &= 4\pi G\rho_b\left[2\,\tilde{\delta}^{(1)} * \tilde{\delta}^{(2)} + (k^\alpha\tilde{\delta}^{(1)}) * \left(\frac{k^\alpha}{k^2}\,\tilde{\delta}^{(2)}\right) + (k^\alpha\tilde{\delta}^{(2)}) * \left(\frac{k^\alpha}{k^2}\,\tilde{\delta}^{(1)}\right)\right] + \\ &+ a^{-2}(ik^\alpha)(ik^\beta)\left[2\,\tilde{v}^{(1)\alpha} * \tilde{v}^{(2)\beta} + \tilde{\delta}^{(1)} * \tilde{v}^{(1)\alpha} * \tilde{v}^{(1)\beta}\right]\,. \end{aligned} \tag{8.24}$$

In an Einstein–de Sitter Universe, because $\delta^{(3)} \propto D^2 \propto t^2$, we have $\partial_\circ^2\tilde{\delta}^{(3)} + 2\dot{a}a^{-1}\partial_\circ\tilde{\delta}^{(3)} - 4\pi G\rho_b\,\tilde{\delta}^{(3)} = 4\tilde{\delta}^{(3)}/t^2$; using the second order results it is not difficult to show that

$$\begin{aligned} &\tilde{\delta}^{(3)}(\mathbf{k},t) = \\ &= \int \frac{d\mathbf{k}_1\,d\mathbf{k}_2\,d\mathbf{k}_3}{(2\pi)^6}\,\delta_D(\mathbf{k}_1+\mathbf{k}_2+\mathbf{k}_3-\mathbf{k})\,J^{(3)}(\mathbf{k}_1,\mathbf{k}_2,\mathbf{k}_3)\,\tilde{\delta}^{(1)}(\mathbf{k}_1,t)\,\tilde{\delta}^{(1)}(\mathbf{k}_2,t)\,\tilde{\delta}^{(1)}(\mathbf{k}_3,t)\,, \end{aligned} \tag{8.25}$$

where

$$J^{(3)}(\mathbf{k}_1,\mathbf{k}_2,\mathbf{k}_3) \equiv J^{(2)}(\mathbf{k}_2,\mathbf{k}_3)\left[\frac{1}{3}+\frac{1}{3}\frac{\mathbf{k}_1\cdot(\mathbf{k}_2+\mathbf{k}_3)}{(\mathbf{k}_2+\mathbf{k}_3)^2}+\frac{4}{9}\frac{\mathbf{k}\cdot\mathbf{k}_1}{k_1^2}\frac{\mathbf{k}\cdot(\mathbf{k}_2+\mathbf{k}_3)}{(\mathbf{k}_2+\mathbf{k}_3)^2}\right]+$$

$$-\frac{2}{9}\frac{\mathbf{k}\cdot\mathbf{k}_1}{k_1^2}\frac{\mathbf{k}\cdot(\mathbf{k}_2+\mathbf{k}_3)}{(\mathbf{k}_2+\mathbf{k}_3)^2}\frac{(\mathbf{k}_2+\mathbf{k}_3)\cdot\mathbf{k}_3}{k_3^2}+\frac{1}{9}\frac{\mathbf{k}\cdot\mathbf{k}_2}{k_2^2}\frac{\mathbf{k}\cdot\mathbf{k}_3}{k_3^2}\,. \tag{8.26}$$

The third–order velocity $\mathbf{v}^{(3)}$ is solution of the equations

$$\partial_\circ\left(a\mathbf{v}^{(3)}\right)+\left(\mathbf{v}^{(1)}\cdot\nabla\right)\mathbf{v}^{(2)}+\left(\mathbf{v}^{(2)}\cdot\nabla\right)\mathbf{v}^{(1)}=a\,\mathbf{g}^{(3)}\,, \tag{8.27}$$

$$\partial_\circ\delta^{(3)}+a^{-1}\nabla\cdot\left(\mathbf{v}^{(3)}+\delta^{(3)}\mathbf{v}^{(2)}+\delta^{(2)}\mathbf{v}^{(1)}\right)=0\,. \tag{8.28}$$

The explicit expression of $\mathbf{v}^{(3)}$ is

$$\mathbf{v}^{(3)}=-\,a\frac{\dot{D}}{D}\left[3\,\nabla\triangle^{(3)}+\delta^{(1)\,2}\,\nabla\triangle^{(1)}-2\,\delta^{(1)}\,\nabla\triangle^{(2)}-\delta^{(2)}\,\nabla\delta^{(1)}\right]+\mathbf{F}_3\,, \tag{8.29}$$

where the additive term $\mathbf{F}_3$ ensures that $\nabla\wedge\mathbf{v}^{(3)}=\mathbf{0}$. The Fourier transform $\tilde{\mathbf{v}}^{(3)}$ looks like

$$\tilde{\mathbf{v}}^{(3)\alpha}(\mathbf{k},t)=i\,a\frac{\dot{D}}{D}\frac{k^\alpha}{k^2}\int\frac{d\mathbf{k}_1\,d\mathbf{k}_2\,d\mathbf{k}_3}{(2\pi)^6}$$

$$\delta_D(\mathbf{k}_1+\mathbf{k}_2+\mathbf{k}_3-\mathbf{k})\,K^{(3)}(\mathbf{k}_1,\mathbf{k}_2,\mathbf{k}_3)\,\tilde{\delta}^{(1)}(\mathbf{k}_1,t)\,\tilde{\delta}^{(1)}(\mathbf{k}_2,t)\,\tilde{\delta}^{(1)}(\mathbf{k}_3,t)\,, \tag{8.30}$$

and the kernel $K^{(3)}(1,2,3)$ id given by the relation

$$K^{(3)}(\mathbf{k}_1,\mathbf{k}_2,\mathbf{k}_3)\equiv 3\,J^{(3)}(\mathbf{k}_1,\mathbf{k}_2,\mathbf{k}_3)-\frac{\mathbf{k}\cdot\mathbf{k}_1}{k_1^2}\,J^{(2)}(\mathbf{k}_2,\mathbf{k}_3)-\frac{3}{2}\frac{\mathbf{k}\cdot(\mathbf{k}_1+\mathbf{k}_2)}{(\mathbf{k}_1+\mathbf{k}_2)^2}\,K^{(2)}(\mathbf{k}_1,\mathbf{k}_2)\,. \tag{8.31}$$

These solutions, although exact, are surely difficult to apply directly, because of the presence of non local terms. In Nusser *et al.* (1991), an approximate interpolation of the contributions up to third–order is given. In Catelan & Moscardini (1993a, b), the third–order results are used to compute the gravitationally–induced kurtosis (the fourth connected moment) of density and velocity fields.

8.2 An Application of the Non Linear Theory: Skewness as a Cosmological Probe

We have now all the ingredients for calculating the gravitationally induced skewness, starting from an initial Gaussian distributed random field $\delta^{(1)} = \delta_1 D$; the skewness at high redshifts, when the second order effects are negligible, is then

$$\langle \delta^{(1)3} \rangle = \zeta(0) = 0 \,, \tag{8.32}$$

where ζ is the three point correlation function. The lowest order non vanishing term is

$$\langle \delta^3 \rangle = 3 \langle \delta^{(1)2} \delta^{(2)} \rangle \,. \tag{8.33}$$

To evaluate this quantity, we have to multiply both sides of (8.8) by $\delta^{(1)2}$, than take averages. In k–space this is easily done; from (7.19) we derive the intermediate result

$$\left\langle \tilde{\delta}^{(1)}(\mathbf{k}_1)\, \tilde{\delta}^{(1)}(\mathbf{k}_2)\, \tilde{\delta}^{(2)}(\mathbf{k}_3) \right\rangle =$$

$$(2\pi)^3\, \delta_D(\mathbf{k}_1 + \mathbf{k}_2 + \mathbf{k}_3) \left[\frac{10}{7} + 2\, \frac{\mathbf{k}_1 \cdot \mathbf{k}_2}{k_2^2} + \frac{4}{7} \left(\frac{\mathbf{k}_1 \cdot \mathbf{k}_2}{k_1\, k_2} \right)^2 \right] P(k_1)\, P(k_2) \,, \tag{8.34}$$

where $P(k)$ is the primordial power spectrum, then

$$\langle \delta^3 \rangle_G = \frac{6}{(2\pi)^6} \int d\mathbf{k}\, d\mathbf{k}'\, J^{(2)}(\mathbf{k}, \mathbf{k}')\, P(k)\, P(k') \,. \tag{8.35}$$

Because of the addition theorem for spherical harmonics

$$\sum_m Y_l^m(\hat{k})\, Y_l^{-m}(\hat{k}) = \frac{2l+1}{4\pi}\, P_l(\mu) \,, \tag{8.36}$$

the integral in (8.35) is trivial; we get (Peebles 1980, Eq.(18.8))

$$\langle \delta^3 \rangle_G = \frac{34}{7}\, \xi(0)^2 \equiv S_3 \langle \delta^2 \rangle^2 \,, \tag{8.37}$$

where ξ is the two–point correlation. The expression for S_3 in k–space with $\Omega = 1$ was first derived by Fry (1984). Goroff *et al.* (1986) first properly included the filters W_R in their calculations and pointed out that S_3 may vary with scale when the slope of $P(k)$

changes. Expression (8.37) takes a different form in the case in which the primordial density distribution is non–Gaussian, as we shall see.

The generalization of (8.37) for $\Omega \neq 1$ is given by Bouchet *et al.* (1992): the parameter S_3 depends extremely weakly on Ω

$$S_3 = \frac{34}{7} + \frac{6}{7}(\Omega^{-2/63} - 1)\,, \tag{8.38}$$

or, in other words, S_3 is a very slowly varying function of time. This property improves the prospects of using observational estimates of $\langle \delta^3 \rangle$ (Saunders *et al.* 1991) to distinguish gravitational instability models with Gaussian initial conditions from more so called exotic scenarios, as pointed out in Silk & Juszkiewicz (1991). The quadratic scaling law (8.37) obtained here from Gaussian initial conditions and small δ, with S_3 expected to be constant in the conventional picture, is favoured by the IRAS data (Saunders *et al.* 1991; Bouchet, Strauss & Davis 1991; Kaiser 1991) and the QDOT data (Park 1991; Coles & Frenk 1991).

Recently, Turok & Spergel (1991), in the framework of global texture models, and Scherrer & Bertschinger (1991), in general intrinsically non–Gaussian models, computed the probability distribution of mass fluctuations δ and explicitly estimate the deviations from a Gaussian distribution in terms of the skewness; what is found is that the skewness scales like

$$\langle \delta^3 \rangle = S_3' \langle \delta^2 \rangle^{3/2}\,, \tag{8.39}$$

so that, for having an eventual agreement with data, we need $S_3' \propto \langle \delta^2 \rangle^{-1/2}$; we see that the power of the test for non conventional models increases with decreasing variance or, in other words, the possibility to detect non–standard departures from Gaussian distribution improves with the size of the sample. The last generation of catalogues may actually allow to make that detection.

The smoothing operation, necessary to do theoretical predictions comparable to observational estimates, modifies the skewness; for a top hat filter, Juszkiewicz, Bouchet &

Colombi (1991) found that, in an Einstein–de Sitter universe, there exists a dependence on the spectral index (see also Fry 1984)

$$S_3 = \frac{34}{7} - (3+n)\,, \qquad -3 \leq n < 1\,. \tag{8.40}$$

IRAS data (Kaiser 1991) and APM data (Hamilton *et al.* 1991) in the range $20 \div 100\,h^{-1}$ Mpc seem compatible with (8.40) if $n = -1$; if a Gaussian filter is used, S_3 changes from $34/7 = 4.9$, at $n = 3$, to 3.0 at $n = 1$. $34/7$ seems to be the saturation value of the skewness for the minimal small–scale power, $n = -3$. The skewness S_3 has been also estimated in recent N–body simulations (Bouchet & Hernquist 1991; Weinberg & Cole 1991), with results in agreement with those derived previously in the conventional scheme. We note that (8.40) contradicts a recent claim of Coles & Frenk (1991) which states that the expression for S_3 for the smoothed field "does not involve terms describing the initial spectrum". The problem is that they adopt as universal the value $S_3 \approx 3$, deduced by Goroff *et al.* (1986, fig.5) in the case $n = 1$ and Gaussian filter.

Skewness of a Primordial Non Gaussian Density Field

All the results previously presented have been obtained assuming that the primordial density distribution is Gaussian. An obvious generalization one may think to do is to extend the same techniques for computing the skewness $\langle \delta^3 \rangle$ starting from a *general* non–Gaussian primordial density field; in this case, we guess immediately, there is a contribution to the skewness from the lowest perturbative order: this is a 'primordial' contribution ie. already contained in the initial conditions. However, because of the difficulty of the calculations (at least for us!), is not so easy at all to compute the contribution to the skewness from the second order terms, which are the terms which take into account the non linear gravitational evolution.

We indicate here a manner for trying to compute the induced–by–gravity skewness starting from a primordial non–Gaussian random field. We do this, extending the previous

formalism, by working in k–space. However, it has been suggested (Fry, private communication) that the same calculation can be probably more easily concluded if one chooses to work in x–space.

All we need are the previous results up to the second perturbative order,

$$\begin{aligned} \langle \delta^3 \rangle_{nG} &= \langle \delta^{(1)3} \rangle + 3 \langle \delta^{(1)2} \delta^{(2)} \rangle \\ &= \zeta(0) + 3 \langle \delta^{(1)2} \delta^{(2)} \rangle \, . \end{aligned} \tag{8.41}$$

As in the Gaussian case, we compute the perturbative contribution in k–space, but now there is the connected contribution from the four point correlation

$$\left\langle \tilde{\delta}^{(1)}(\mathrm{k}_1)\tilde{\delta}^{(1)}(\mathrm{k}_2)\tilde{\delta}^{(2)}(\mathrm{k}_3) \right\rangle = \frac{1}{(2\pi)^3} \int d\mathrm{k}_a \, d\mathrm{k}_b \, \delta_D(\mathrm{k}_a + \mathrm{k}_b - \mathrm{k}_3) \, J^{(2)}(\mathrm{k}_a, \mathrm{k}_b) \times$$

$$\times \left[\left\langle \tilde{\delta}^{(1)}(\mathrm{k}_1)\tilde{\delta}^{(1)}(\mathrm{k}_2)\tilde{\delta}^{(1)}(\mathrm{k}_a)\tilde{\delta}^{(1)}(\mathrm{k}_b) \right\rangle_c + 2! \left\langle \tilde{\delta}^{(1)}(\mathrm{k}_1)\tilde{\delta}^{(1)}(\mathrm{k}_a) \right\rangle \left\langle \tilde{\delta}^{(1)}(\mathrm{k}_2)\tilde{\delta}^{(1)}(\mathrm{k}_b) \right\rangle \right] \, . \tag{8.42}$$

Instead of Eq.(8.35), one finds

$$3 \langle \delta^{(1)^2} \delta^{(2)} \rangle_{nG} = \frac{1}{(2\pi)^6} \int d\mathrm{k} \, d\mathrm{k}'$$

$$\left[6 \, J^{(2)}(\mathrm{k}, \mathrm{k}') \, P(k) \, P(k') + \frac{1}{(2\pi)^3} \int d\mathrm{k}'' \, J^{(2)}(\mathrm{k}'', \mathrm{k} - \mathrm{k}' - \mathrm{k}'') \, T(k, k', k'') \right] \, , \tag{8.43}$$

where $T(k, k', k'')$ is the primordial trispectrum.

Finally, the skewness for a general initially non–Gaussian random field is

$$\langle \delta^3 \rangle_{nG} - \zeta(0) = \frac{17}{7} \, \xi(0)^2 + \frac{17}{21} \langle \delta^{(1)4} \rangle + I \, , \tag{8.44}$$

where we have defined the quantity I as

$$I \equiv \frac{1}{(2\pi)^9} \int d\mathrm{k} \, d\mathrm{k}' \, d\mathrm{k}'' \left[\frac{k''}{\Sigma} \, P_1(\mu) + \frac{4}{21} \, P_2(\mu) \right] T(k, k', k'') \tag{8.45}$$

and $\mathbf{\Sigma} \equiv \mathrm{k} + \mathrm{k}' + \mathrm{k}''$, $\Sigma \equiv |\mathbf{\Sigma}|$, μ the cosine between the vectors k'' and $\mathbf{\Sigma}$.

From Eq.(8.44), we see that the skewness induced by gravity is different from the Gaussian case, this implying a deeper discussion about its cosmological significance.

Apart of integration in I, dependence on the Ω value (but we suppose that also in this case it is negligible) and on filtering the underlying field δ has yet to be discussed (Catelan & Moscardini, 1993, in preparation).

8.3 Kurtosis of Cosmological Density Field

In this section, we discuss the non–linear growth of the excess kurtosis parameter of the smoothed density fluctuation field δ, namely

$$S_4 \equiv [\langle \delta^4 \rangle - 3\langle \delta^2 \rangle^2]/\langle \delta^2 \rangle^3 \,, \tag{8.46}$$

in an Einstein–de Sitter universe. We assume Gaussian primordial density fluctuations with scale–free power spectrum $P(k) \propto k^n$ and analyze the dependence of S_4 on primordial spectral index n, after smoothing with a Gaussian filter. We apply up to third–order perturbative calculations. As already known for the skewness ratio S_3, the kurtosis parameter is a *decreasing function* of n, both in exact perturbative theory and in the Zel'dovich approximation. The parameter S_4 provides a powerful statistics to test different cosmological scenarios.

The study of the statistical distribution of the matter in the universe may be a way to address fundamental issues such as the origin and the formation of structures on large scales.

The simplest and most usually accepted hypothesis, supported by the inflationary model, is that the very early distribution is Gaussian. In such a case, the connected N–point correlations (and the N–th order connected moments) with $N > 2$ are zero. However, even if the primordial fluctuations δ are Gaussian, the non–linear time evolution will ensure that the mass density fluctuations become highly non–Gaussian (Peebles 1980; Fry 1984). It is important to understand the nature of the higher moments of the mass density induced by gravity in order to distinguish their effects from those of possible *primordial* non–Gaussian fluctuations: late–time phase transitions, cosmic string models and global textures are indeed models whose statistics may not be described by a Gaussian distribution (see e.g. Vilenkin 1985; Turok 1989; Scherrer & Bertschinger 1991). Moreover, variations of the inflationary model which lead to non–Gaussian primordial fluctuations have been recently discussed (see e.g. Salopek 1992).

A powerful method to distinguish if the non–Gaussian nature of the matter distribution is intrinsic, is to analyze the growth of higher moments, like the skewness or the kurtosis (third and fourth connected moments, respectively) of the density fluctuation field. Peebles (1980) first showed that gravity induces, for an unsmoothed initial Gaussian density field, a skewness ratio $S_3 \equiv \langle\delta^3\rangle/\langle\delta^2\rangle^2 = 34/7$, for any primordial power spectrum. Juszkiewicz, Bouchet, & Colombi (1993) find that the filtering operation actually introduces a dependence of S_3 on the primordial spectral index n; in particular for scale–free spectra, $S_3 = 34/7 - (n+3)$ for a top–hat window function, and a decreasing trend with n is recovered also for a Gaussian filter. Coles *et al.* (1993) investigate, using N–body simulations, the growth of the skewness ratio to test the hypothesis of Gaussian primordial density fluctuations against possible alternatives. Analytical expressions for S_3 arising from non–linear evolution in perturbation theory have been worked out for arbitrary non–Gaussian models by Fry & Scherrer (1993) and Catelan & Moscardini (1993). Finally, higher order moments are known to depend extremely weakly on the density parameter Ω (see Martel & Freudling 1991; Bouchet *et al.* 1992; Bernardeau 1992).

Here we analyse the dependence of the induced–by–gravity excess kurtosis of the density field, smoothed with a Gaussian filter, namely the parameter $S_4 \equiv [\langle\delta^4\rangle - 3\langle\delta^2\rangle^2]/\langle\delta^2\rangle^3$, on an initial (scale–free) power spectrum $P(k)$. To do this, we take advantage of the exact perturbative technique (Fry 1984; Goroff *et al.* 1986) and the Zel'dovich approximation (see Grinstein & Wise 1987). The kurtosis describes features such as sharpness or stretchiness of the mass distribution and the extent of its rare–event tail. Moreover, it is possibly related to the *initial* sign of the skewness – as predicted in some non–Gaussian models (see e.g. Luo & Schramm 1993) – which is important for the final galaxy clustering pattern (Moscardini *et al.* 1991; Messina *et al.* 1992; Weinberg & Cole 1992).

Since δ is initially Gaussian distributed, the lowest order non zero connected part of η_{1234} is of order 6 in $\delta^{(1)}$,

$$\eta \;=\; \left\langle \delta^{(1)}(\mathbf{x}_1)\,\delta^{(1)}(\mathbf{x}_2)\,\delta^{(2)}(\mathbf{x}_3)\,\delta^{(2)}(\mathbf{x}_4)\right\rangle + \text{c.p.}\,(6\text{ terms}) +$$

$$+ \quad \left\langle \delta^{(1)}(\mathbf{x}_1)\,\delta^{(1)}(\mathbf{x}_2)\,\delta^{(1)}(\mathbf{x}_3)\,\delta^{(3)}(\mathbf{x}_4)\right\rangle + \text{c.p.}\,(4\ \text{terms})\ . \tag{8.47}$$

In particular, the lowest order nonvanishing connected contribution to S_4 is (see Appendix 1)

$$\langle \delta^{(1)\,2}\rangle^3\ S_4\ =\ 6\,\langle\,\delta^{(1)\,2}\,\delta^{(2)\,2}\,\rangle_c\ +\ 4\,\langle\,\delta^{(1)\,3}\,\delta^{(3)}\,\rangle_c\ . \tag{8.48}$$

The subscript 'c' indicates the connected part of the higher–order moments. Note that there are two corrections (each one $\sim \delta_1^6$) to the density kurtosis, for which we need up to the *third*–order perturbative approximation. Therefore, in a sense, we disagree with the conclusions of Luo & Schramm (1993), who assert that the kurtosis of an evolved Gaussian distribution remains zero to second–order perturbative theory, in that they neglect the first non–zero contribution δ_1^6 correctly identified here [see the first connected term in the right hand side of Eq.(8.48) and the calculations leading to their Eq.(3.13)].

It is really much simpler to work in k–space; we have

$$\left\langle \tilde\delta^{(1)}(\mathbf{k}_1)\,\tilde\delta^{(1)}(\mathbf{k}_2)\,\tilde\delta^{(2)}(\mathbf{k}_3)\,\tilde\delta^{(2)}(\mathbf{k}_4)\right\rangle = (2\pi)^3\,\delta_D(\mathbf{k}_1+\mathbf{k}_2+\mathbf{k}_3+\mathbf{k}_4)\times 4\,P(k_1)\,P(k_2)\times$$

$$\Big[J^{(2)}(-\mathbf{k}_1,\mathbf{k}_1{+}\mathbf{k}_3)J^{(2)}(\mathbf{k}_2,\mathbf{k}_1{+}\mathbf{k}_3)P(|\mathbf{k}_1{+}\mathbf{k}_3|){+}J^{(2)}(\mathbf{k}_2{+}\mathbf{k}_3,-\mathbf{k}_2)J^{(2)}(\mathbf{k}_2{+}\mathbf{k}_3,\mathbf{k}_1)P(|\mathbf{k}_2{+}\mathbf{k}_3|)\Big]. \tag{8.49}$$

We need now of the piece $\langle \delta^{(1)3}\,\delta^{(3)}\rangle$; it is

$$\left\langle \tilde\delta^{(1)}(\mathbf{k}_1)\,\tilde\delta^{(1)}(\mathbf{k}_2)\,\tilde\delta^{(1)}(\mathbf{k}_3)\,\tilde\delta^{(3)}(\mathbf{k}_4)\right\rangle =$$

$$= (2\pi)^3\,\delta_D(\mathbf{k}_1+\mathbf{k}_2+\mathbf{k}_3+\mathbf{k}_4)\,3!\,P(k_1)\,P(k_2)\,P(k_3)\,J^{(3)}(\mathbf{k}_1,\mathbf{k}_2,\mathbf{k}_3)\ . \tag{8.50}$$

From Eqs.(8.48), (8.49) and (8.50), after tedious but straightforward algebra, one finally gets the integral expression of the kurtosis ratio,

$$S_4 = \frac{24}{\sigma^6}\int \frac{d\mathbf{k}_1\,d\mathbf{k}_2\,d\mathbf{k}_3}{(2\pi)^9}\ P(k_1)\,P(k_2)\,\Big[P(k_3)\,J^{(3)}(\mathbf{k}_1,\mathbf{k}_2,\mathbf{k}_3)\ +$$

$$+2\,J^{(2)}(-\mathbf{k}_2,\mathbf{k}_2+\mathbf{k}_3)\,J^{(2)}(\mathbf{k}_1,\mathbf{k}_2+\mathbf{k}_3)\,P(|\mathbf{k}_2+\mathbf{k}_3|)\Big]\ . \tag{8.51}$$

The expression in the Zel'dovich approximation is obtained by substituting the kernels $J^{(n)}$ with the corresponding $J^{(n)}_{ZA}$ in the previous relation, as discussed in Section VIII.5.

The angular integrations in Eq.(8.51) may be analytically performed. One obtains $S_4 = 60,712/1,323 \approx 45.9$ in the perturbative case (Fry 1984; Bernardeau 1992) and $S_4 = 88/3 \approx 29.3$ in the Zel'dovich approximation (Catelan & Moscardini 1993). These unsmoothed–case results are independent of the primordial spectral index, as is the skewness ratio S_3.

The kurtosis of the smoothed density field δ_R in the perturbative case is

$$S_4(R) = \frac{24}{\sigma_R^6} \int \frac{d\mathbf{k}_1\, d\mathbf{k}_2\, d\mathbf{k}_3}{(2\pi)^9}\, \widetilde{W}_R(k_1)\, \widetilde{W}_R(k_2)\, \widetilde{W}_R(k_3)\, \widetilde{W}_R(|\mathbf{k}_1+\mathbf{k}_2+\mathbf{k}_3|) \times$$

$$P(k_1)\, P(k_2)\, \left[P(k_3)\, J^{(3)}(\mathbf{k}_1,\mathbf{k}_2,\mathbf{k}_3) + 2\, J^{(2)}(-\mathbf{k}_2,\mathbf{k}_2+\mathbf{k}_3)\, J^{(2)}(\mathbf{k}_1,\mathbf{k}_2+\mathbf{k}_3)\, P(|\mathbf{k}_2+\mathbf{k}_3|)\right] ; \tag{8.52}$$

again the substitution $J^{(n)} \rightarrow J_{ZA}^{(n)}$ leads to the corresponding expression in the Zel'dovich approximation (see Section VIII.5). Note that $P(k)$ completely describes the process of growth of mass fluctuations from Gaussian initial perturbations.

To treat integral expression like this seems not easy at all, except for some naive configurations (see Fry 1984). Goroff *et al.* (1986) treat similar expressions in a CDM framework ($P(k) = k$) using standard Monte Carlo techniques, for Gaussian-filtered density fields: if the normalization of the primordial power spectrum is chosen so that $\langle \delta_R^2 \rangle$ is greater than $1/3$ at a distance $Rh^2 = 5\, Mpc$, then the connected part of $\langle \delta_R^4 \rangle$ dominates over the disconnected part indicating that for such normalizations the probability distribution for δ_R is still highly non–Gaussian at this distance (see their Fig.6).

We calculate the previous integrals, by an Adaptive Multidimensional Monte Carlo Integration subroutine, for scale–free power spectra $P(k) \propto k^n$ with n in the range $-3 \leq n \leq 1$. Due to the assumed primordial scale–invariance, S_4 only depends on the primordial spectral index n, and not on the scale R. In Figure F1, we plot the kurtosis ratio S_4 of the Gaussian–smoothed density field versus the spectral index n, for both the perturbative and Zel'dovich approximations. The main conclusions are drawn in Section VIII.6.

8.4 Kurtosis of Large-Scale Velocity Field

In this section we discuss the non–linear growth of the kurtosis of the smoothed peculiar velocity field (along an arbitrary direction $\widehat{\alpha}$), namely the parameter

$$S_{4,v} \equiv \frac{\langle v_\alpha^4 \rangle - 3 \langle v_\alpha^2 \rangle^2}{\langle v_\alpha^2 \rangle^2 \langle \delta^2 \rangle} , \tag{8.53}$$

in an Einstein–de Sitter universe. We assume Gaussian primordial density fluctuations δ with scale–free power spectrum $P(k) \propto k^n$ and analyze the dependence of $S_{4,v}$ on primordial spectral index n, after smoothing with a Gaussian filter. The velocity kurtosis is a *decreasing function* of n in exact perturbative theory but it is constant and consistent with zero in the Zel'dovich approximation. The parameter $S_{4,v}$ provides a powerful statistics to test different cosmological scenarios.

In the past decade astronomers and cosmologists devoted a great effort to measure the large–scale deviations from the Hubble flow and to interpret the cosmological inferences. The appearance of redshift–independent distance estimators (Aaronson *et al.* 1986; Dressler *et al.* 1987a; 1987b; Lynden–Bell *et al.* 1988; Faber & Burstein 1988) and all–sky catalogs of galaxy redshifts (e.g. Strauss *et al.* 1990; Saunders *et al.* 1991) allowed to estimate the (radial) peculiar motions of galaxies. The body of streaming motions data is currently used to constrain theories of large–scale structure formation (Vittorio, Juszkiewicz & Davis 1986; Villumsen & Strauss 1987; Kaiser & Lahav 1988; Bertschinger & Juskiewicz 1988; Juszkiewicz, Vittorio & Wise 1990). Undertaking detailed maps of the peculiar velocity field allows e.g. to make dynamical estimates of the density parameter Ω_o, to test the primordial power spectrum $P(k)$, and to measure directly the underlying total (luminous plus dark) mass distribution, once the gravitational instability picture is assumed (for a review see Gunn 1989; Lahav 1990; Bertschinger 1990). Conversely, POTENT people (Bertschinger & Dekel 1989; Dekel, Bertshinger & Faber 1990; Bertschinger *et al.* 1990; Nusser *et al.* 1991) extract the (smoothed) three–dimensional velocity, mass density and gravitational potential

fields from samples of galaxy distances and redshifts.

The *statistical* properties of the large–scale motions may be described in terms of the peculiar velocity correlation tensor (Górski 1988; Groth, Juszkievicz & Ostriker 1989; Górski *et al.* 1989; Kashlinsky 1992; Landy & Szalay 1992) and/or the central moments of the velocity probability distribution function (pdf) $p(\mathbf{v})$. Assuming that the very early density pdf is Gaussian, it results that, during the linear regime, $p(\mathbf{v})$ is a Gaussian too, with mean $\langle \mathbf{v} \rangle = 0$ and variance $\sigma_{\mathbf{v}}^2 = (H_o^2 \Omega_o^{1.2}/2\pi^2) \int_0^\infty dk\, P(k)$, H_o being the Hubble constant. Even if the primordial density field is Gaussian distributed, the non–linear time evolution will ensure that the mass density fluctuations δ become highly non–Gaussian (Peebles 1980; Fry 1984; Goroff *et al.* 1986; Juszkiewicz, Bouchet & Colombi 1993; Catelan & Moscardini 1993), this implying a modification of the original Gaussian pdf $p(\mathbf{v})$. However, due to the isotropy of the cosmological velocity field, it is expected that *all* the *odd* central moments of $p(\mathbf{v})$ remain zero during the growth of the density fluctuations. A particular case is the third central moment, the velocity skewness, which is discussed e.g. in Ruamsuwan and Fry (1992). Thus, any gravitationally induced departure from the Gaussian distribution may be sought only in the fourth central moment of $p(\mathbf{v})$, the velocity kurtosis, as well in higher order *even* central moments (Grinstein *et al.* 1987; Kofman *et al.* 1993). These have been also analyzed in the framework of global texture model (Turok 1989) by Scherrer (1992).

In this section, we study the non–Gaussian content of the velocity pdf in terms of the velocity kurtosis as induced by the gravitational growth of the initially Gaussian density fluctuations. The velocity kurtosis describes important features such as sharpness or stretchiness of the velocity pdf and the extent of its rare–event tail. In particular, we explore the dependence of the kurtosis of the peculiar velocity along a direction $\widehat{\alpha}$, namely the parameter $S_{4,v} \equiv [\langle v_\alpha^4 \rangle - 3 \langle v_\alpha^2 \rangle^2]/\langle v_\alpha^2 \rangle^2 \langle \delta^2 \rangle$, on an initial (scale–free) power spectrum $P(k) \propto k^n$, after smoothing with a Gaussian filter. To do this, we take advantage of the exact perturbative technique (Fry 1984; Goroff *et al.* 1986) and the Zel'dovich approximation (see Grinstein & Wise 1987).

Let us compute the gravitationally induced kurtosis $S_{4,v}$ of an initial Gaussian velocity field in a flat universe. We restrict the calculation along one chosen direction $\widehat{\alpha}$. The lowest order non–zero connected contribution to η_v is given by

$$\begin{aligned} k_4(v_\alpha) &= \left\langle v_\alpha^{(1)}(\mathbf{x}_1)\, v_\alpha^{(1)}(\mathbf{x}_2)\, v_\alpha^{(2)}(\mathbf{x}_3)\, v_\alpha^{(2)}(\mathbf{x}_4)\right\rangle + \text{c.p.}\,(6\ \text{terms}) + \\ &+ \left\langle v_\alpha^{(1)}(\mathbf{x}_1)\, v_\alpha^{(1)}(\mathbf{x}_2)\, v_\alpha^{(1)}(\mathbf{x}_3)\, v_\alpha^{(3)}(\mathbf{x}_4)\right\rangle + \text{c.p.}\,(4\ \text{terms})\,, \end{aligned} \tag{8.54}$$

because, due to isotropy, all odd moments are zero. From this, it is straightforward to obtain that the kurtosis ratio $S_{4,v}$ has the form

$$\langle v_\alpha^{(1)\,2}\rangle^2\, \langle \delta^{(1)\,2}\rangle\; S_{4,v} \equiv 6\, \langle\, v_\alpha^{(1)\,2}\, v_\alpha^{(2)\,2}\,\rangle_c + 4\, \langle\, v_\alpha^{(1)\,3}\, v_\alpha^{(3)}\,\rangle_c\,. \tag{8.55}$$

It is really much simpler to work in k–space; we have

$$\left\langle \tilde{v}_\alpha^{(1)}(\mathbf{k}_1)\, \tilde{v}_\alpha^{(1)}(\mathbf{k}_2)\, \tilde{v}_\alpha^{(2)}(\mathbf{k}_3)\, \tilde{v}_\alpha^{(2)}(\mathbf{k}_4)\right\rangle =$$

$$= \left(i\, a\, \frac{\dot{D}}{D}\right)^4 \frac{k_1^\alpha\, k_2^\alpha\, k_3^\alpha\, k_4^\alpha}{k_1^2\, k_2^2\, k_3^2\, k_3^2}\, (2\pi)^3\, \delta_D(\sum_{h=1}^{4} \mathbf{k}_h)\, 4\, P(k_1)\, P(k_2) \times$$

$$\left[K^{(2)}(-\mathbf{k}_1, \mathbf{k}_1{+}\mathbf{k}_3) K^{(2)}(\mathbf{k}_2, \mathbf{k}_1{+}\mathbf{k}_3) P(|\mathbf{k}_1{+}\mathbf{k}_3|) + K^{(2)}(\mathbf{k}_2{+}\mathbf{k}_3, -\mathbf{k}_2) K^{(2)}(\mathbf{k}_2{+}\mathbf{k}_3, \mathbf{k}_1) P(|\mathbf{k}_2{+}\mathbf{k}_3|)\right]. \tag{8.56}$$

We need now for the piece $\langle v_\alpha^{(1)3}\, v_\alpha^{(3)}\rangle$; it is

$$\left\langle \tilde{v}_\alpha^{(1)}(\mathbf{k}_1)\, \tilde{v}_\alpha^{(1)}(\mathbf{k}_2)\, \tilde{v}_\alpha^{(1)}(\mathbf{k}_3)\, \tilde{v}_\alpha^{(3)}(\mathbf{k}_4)\right\rangle = \left(i\, a\, \frac{\dot{D}}{D}\right)^4 \frac{k_1^\alpha\, k_2^\alpha\, k_3^\alpha\, k_4^\alpha}{k_1^2\, k_2^2\, k_3^2\, k_3^2} \times$$

$$(2\pi)^3\, \delta_D(\sum_{h=1}^{4} \mathbf{k}_h)\, 3!\, P(k_1)\, P(k_2)\, P(k_3)\, J^{(3)}(\mathbf{k}_1, \mathbf{k}_2, \mathbf{k}_3)\,. \tag{8.57}$$

From Eqs.(8.54), (8.55) and (8.56), after tedious but straightforward algebra, one finally gets the integral expression of the kurtosis ratio,

$$S_{4,v} = \frac{24}{\sigma_v^4\, \sigma^2} \left(a\, \frac{\dot{D}}{D}\right)^4 \int \frac{d\mathbf{k}_1\, d\mathbf{k}_2\, d\mathbf{k}_3}{(2\pi)^9}\; \frac{k_1^\alpha\, k_2^\alpha\, k_3^\alpha\, (-k_1^\alpha - k_2^\alpha - k_3^\alpha)}{k_1^2\, k_2^2\, k_3^2\, |\mathbf{k}_1 + \mathbf{k}_2 + \mathbf{k}_3|^2} \times$$

$$P(k_1)\, P(k_2) \left[P(k_3)\, K^{(3)}(\mathbf{k}_1, \mathbf{k}_2, \mathbf{k}_3) + 2\, K^{(2)}(-\mathbf{k}_2, \mathbf{k}_2 + \mathbf{k}_3)\, K^{(2)}(\mathbf{k}_1, \mathbf{k}_2 + \mathbf{k}_3)\, P(|\mathbf{k}_2 + \mathbf{k}_3|)\right]. \tag{8.58}$$

The expression in the Zel'dovich approximation is obtained by substituting the kernels $K^{(n)}$ with the corresponding $K_{ZA}^{(n)}$ in the previous relation (see next section). These unsmoothed–case results are independent of the primordial spectral index.

The perturbative kurtosis of the smoothed velocity field $\mathbf{v}_R$ in the is

$$S_{4,v}(R) = \frac{24}{\sigma_v^4(R)\,\sigma^2(R)} \left(a\frac{\dot{D}}{D}\right)^4 \int \frac{d\mathbf{k}_1\,d\mathbf{k}_2\,d\mathbf{k}_3}{(2\pi)^9} \frac{k_1^\alpha\,k_2^\alpha\,k_3^\alpha\,(-k_1^\alpha-k_2^\alpha-k_3^\alpha)}{k_1^2\,k_2^2\,k_3^2\,|\mathbf{k}_1+\mathbf{k}_2+\mathbf{k}_3|^2} \times$$

$$\widetilde{W}_R(k_1)\,\widetilde{W}_R(k_2)\,\widetilde{W}_R(k_3)\,\widetilde{W}_R(|\mathbf{k}_1+\mathbf{k}_2+\mathbf{k}_3|)\times$$

$$P(k_1)\,P(k_2)\left[P(k_3)\,K^{(3)}(\mathbf{k}_1,\mathbf{k}_2,\mathbf{k}_3)+2\,K^{(2)}(-\mathbf{k}_2,\mathbf{k}_2+\mathbf{k}_3)\,K^{(2)}(\mathbf{k}_1,\mathbf{k}_2+\mathbf{k}_3)\,P(|\mathbf{k}_2+\mathbf{k}_3|)\right]\;; \tag{8.59}$$

again the substitution $K^{(n)} \to K_{ZA}^{(n)}$ leads to the corresponding expression in the Zel'dovich approximation. Note that $P(k)$ completely describes the process of growth of mass fluctuations from Gaussian initial perturbations.

We calculate the previous integrals, by an Adaptive Multidimensional Monte Carlo Integration subroutine, for scale–free power spectra $P(k) \propto k^n$ with n in the range $-1 \leq n \leq 1$. Due to the assumed scale–invariance, $S_{4,v}$ only depends on the primordial spectral index n, and not on the scale R. In Figure G1, we plot the kurtosis ratio $S_{4,v}$ of the Gaussian–smoothed velocity field versus the spectral index n, for both the perturbative and Zel'dovich approximations. The main conclusions are drawn in the last section of this chapter.

8.5 Higher Order Moments in Zel'dovich Approximation *

In the Zel'dovich approximation (Zel'dovich 1970) any mass point has the comoving coordinates (see Section IV.4)

$$\mathbf{x}(\mathbf{q},t) = \mathbf{q} + D(t)\,\mathbf{S}(\mathbf{q})\;, \tag{8.60}$$

where $\mathbf{q}$ is the initial comoving coordinate (Lagrangian coordinate) and $D(t)$ is a function of time describing the growing mode of linear perturbation; in an Einstein–de Sitter model,

$D(t) = t^{2/3}$. Writing the peculiar velocity as

$$\mathbf{v} = a(t)\frac{d\mathbf{x}}{dt} = a\dot{D}\frac{d\mathbf{x}}{dD} = \frac{2}{3}t^{1/3}\mathbf{S}\ , \tag{8.61}$$

we see that a "momentum" may be defined

$$\frac{\mathbf{p}}{m} = \mathbf{S}\ . \tag{8.62}$$

The Zel'dovich approximation provides an exact solution of the equations of motion for one–dimensional perturbations, and reduces to the linear approximation when δ and $\mathbf{v}$ are small. In general, the Zel'dovich approximation is not an exact solution of the equations of motion, in that in a finite time particles converge into singular regions of infinite density (caustics), and the map in Eq.(8.60) becomes multi–valued. The treatment of these formal singularities is the main problem to solve during the highly non–linear stage of structure formation. Smoothing on a suitable scale R partially solves this problem. Grinstein & Wise (1987) give an Eulerian representation of the Zel'dovich approximation by a diagrammatic perturbative approach similar to that of the previous section. We summarize it.

To derive an expression for the mass density fluctuation in Zel'dovich approximation, we introduce the phase–space density distribution (e.g. Reichl 1980; Ma 1985)

$$f(\mathbf{x},\mathbf{p},t)\,d\mathbf{x}\,d\mathbf{p} = \#\text{ of particles in the volume } d\mathbf{x}\,d\mathbf{p}\ , \tag{8.63}$$

Since the particle with the comoving coordinate $\mathbf{x}$ at time t originated at the comoving coordinate

$$\mathbf{q} = \mathbf{x} - t^{2/3}\frac{\mathbf{p}}{m}\ , \tag{8.64}$$

the appropriate phase–space distribution for particles that were evenly distributed initially is

$$f(\mathbf{x},\mathbf{p},t)\,d\mathbf{x}\,d\mathbf{p} = \frac{\rho_b}{m}\,\delta_D[\mathbf{p} - m\mathbf{S}(\mathbf{q})]\,d\mathbf{x}\,d\mathbf{p}\ , \tag{8.65}$$

where $\mathbf{q}$ is just defined in Eq.(8.64). Before orbit crossing, when the correspondence between $\mathbf{p}$ and $\mathbf{S}$ is one–to–one, we can expand the Dirac function ($m \equiv 1$)

$$\delta_D[\mathbf{p} - \mathbf{S}(\mathbf{q})] = \frac{1}{(2\pi)^3}\int d\mathbf{y}\,e^{i\mathbf{y}\cdot(\mathbf{p}-\mathbf{S}(\mathbf{q}))} = \frac{1}{(2\pi)^3}\int d\mathbf{y}\,e^{i\mathbf{y}\cdot\mathbf{p}}\sum_{n=0}^{\infty}\frac{(-i)^n}{n!}\left(\sum_{h=1}^{3}y_h S_h\right)^n$$

$$= \sum_{n=0}^{\infty} \frac{(-i)^n}{n!} \sum_{[h_n]=1}^{3} \prod_{j=1}^{n} S_{h_j} \int \frac{d\mathbf{y}}{(2\pi)^3} \prod_{k=1}^{n} y_{h_k} \, \mathrm{e}^{i\mathbf{y}\cdot\mathbf{p}} \,, \tag{8.66}$$

i.e.

$$\delta_D[\mathbf{p} - \mathbf{S}(\mathbf{q})] = \sum_{n=0}^{\infty} \frac{(-1)^n}{n!} \sum_{[h_n]=1}^{3} \prod_{j=1}^{n} S_{h_j} \frac{\partial}{\partial p_{h_j}} \delta_D(\mathbf{p}) \,, \tag{8.67}$$

where the commutator $\left[\mathbf{S}, \partial/\partial\mathbf{p}\right] \neq 0$. The mass density is obtained by f through

$$\rho(\mathbf{x}, t) = m \int d\mathbf{p}\, f(\mathbf{x}, \mathbf{p}, t) = \int d\mathbf{p}\, f(\mathbf{x}, \mathbf{p}, t) \,. \tag{8.68}$$

From Eqs.(8.65) and (8.67), and integrating by parts, we get

$$\frac{\rho(\mathbf{x}, t)}{\rho_b} = 1 + \delta(\mathbf{x}, t) = \sum_{n=0}^{\infty} \frac{(-1)^n}{n!} t^{2n/3} \sum_{[h_n]=1}^{3} \frac{\partial}{\partial x_{h_1}} \cdots \frac{\partial}{\partial x_{h_1}} \left[S_{h_1}(\mathbf{x}) \cdots S_{h_n}(\mathbf{x})\right] . \tag{8.69}$$

This is an Eulerian expression of the density fluctuation field evolved in Zel'dovich approximation. The first–order term is

$$\delta(\mathbf{x}, t) = -t^{2/3} \nabla \cdot \mathbf{S} + o(t^{4/3}) = t^{2/3} \delta_1(\mathbf{x}) + o(t^{4/3}) \,. \tag{8.70}$$

From linear theory, we see that, $\mathbf{S} = \mathbf{v}_1$, since $\delta_1(\mathbf{x}) = -\nabla \cdot \mathbf{v}_1$. Fourier–transforming the Eq.(8.69) shows that Zel'dovich approximation corresponds to assign to the functions $J^{(n)}$ the values

$$J^{(n)}_{ZA}(\mathbf{k}_1, \cdots, \mathbf{k}_n) = \frac{1}{n!} \frac{\mathbf{k}\cdot\mathbf{k}_1}{k_1^2} \cdots \frac{\mathbf{k}\cdot\mathbf{k}_n}{k_n^2} \,, \tag{8.71}$$

where $\mathbf{k} \equiv \sum_{h=1}^{n} \mathbf{k}_h$. As an exercise, we can demonstrate the previous relation in the case $n = 2$; we have (the symbol $\mathcal{F}$ indicates the Fourier transform operation)

$$\mathcal{F}\left(\sum_{h,j} \partial_h\, \partial_j\, v_1^h\, v_1^j\right) = \sum_{h,j} \mathcal{F}(\partial_h\, \partial_j\, v_1^h\, v_1^j) = \sum_{h,j} (ik_h)\,(ik_j)\,(\tilde{v}_1^h * \tilde{v}_1^j) =$$

$$= \sum_{h,j} (ik_h)\,(ik_j)\,(i\frac{k^h}{k^2}\,\tilde{\delta}_1 * i\frac{k^j}{k^2}\,\tilde{\delta}_1) = k_h\, k_j \int \frac{d\mathbf{k}_1\, d\mathbf{k}_2}{(2\pi)^3}\, \delta_D(\mathbf{k}_1 + \mathbf{k}_2 - \mathbf{k})\, \frac{k_1^h}{k_1^2}\, \tilde{\delta}_1(\mathbf{k}_1)\, \frac{k_2^j}{k_2^2}\, \tilde{\delta}_1(\mathbf{k}_2) =$$

$$= \int \frac{d\mathbf{k}_1\, d\mathbf{k}_2}{(2\pi)^3}\, \delta_D(\mathbf{k}_1 + \mathbf{k}_2 - \mathbf{k})\, \frac{\mathbf{k}\cdot\mathbf{k}_1}{k_1^2}\, \frac{\mathbf{k}\cdot\mathbf{k}_2}{k_2^2}\, \tilde{\delta}_1(\mathbf{k}_1)\, \tilde{\delta}_1(\mathbf{k}_2) \quad q.e.d. \,. \tag{8.72}$$

The full expression of the second–order density field therefore is

$$\delta^{(2)}(\mathbf{x}, t) = t^{4/3}\, \delta_2(\mathbf{x}) \,, \tag{8.73}$$

$$\tilde{\delta}_2(\mathbf{k}) = \frac{1}{2}\int \frac{d\mathbf{k}_1\, d\mathbf{k}_2}{(2\pi)^3}\, \delta_D(\mathbf{k}_1+\mathbf{k}_2-\mathbf{k})\, \frac{\mathbf{k}\cdot\mathbf{k}_1}{k_1^2}\, \frac{\mathbf{k}\cdot\mathbf{k}_2}{k_2^2}\, \tilde{\delta}_1(\mathbf{k}_1)\, \tilde{\delta}_1(\mathbf{k}_2)\,. \tag{8.74}$$

Also, from Eqs.(8.61) and (8.69), we can derive the expression of $\delta^{(2)}(\mathbf{x},t)$ in terms of first–order quantities; one gets

$$\delta^{(2)}(\mathbf{x},t) = \frac{1}{2}\,\delta^{(1)2} + \partial_\alpha\delta^{(1)}\,\partial_\alpha\triangle^{(1)} + \frac{1}{2}\,\partial_\alpha\partial_\beta\triangle^{(1)}\,\partial_\alpha\partial_\beta\triangle^{(1)}\,. \tag{8.75}$$

In a similar fashion, we can to explicit the previous calculations up to the third order in perturbative expansion. The expression of the third–order density field in Zel'dovich approximation is

$$\delta^{(3)}(\mathbf{x},t) = t^{\,2}\,\delta_3(\mathbf{x}) = D^3\delta_3(\mathbf{x})\,, \tag{8.76}$$

where

$$\tilde{\delta}_3(\mathbf{k}) = \int \frac{d\mathbf{k}_1\, d\mathbf{k}_2\, d\mathbf{k}_3}{(2\pi)^3}\, \delta_D(\sum_{h=1}^{3}\mathbf{k}_2-\mathbf{k})\, J^{(3)}_{ZA}(\mathbf{k}_1,\mathbf{k}_2,\mathbf{k}_3)\, \tilde{\delta}_1(\mathbf{k}_1)\, \tilde{\delta}_1(\mathbf{k}_2)\, \tilde{\delta}_1(\mathbf{k}_3)\,. \tag{8.77}$$

The third order kernel $J^{(3)}_{ZA}$ is explicitely given by

$$J^{(3)}_{ZA}(\mathbf{k}_1,\mathbf{k}_2,\mathbf{k}_3) = \frac{1}{3!}\,\frac{\mathbf{k}\cdot\mathbf{k}_1}{k_1^2}\,\frac{\mathbf{k}\cdot\mathbf{k}_2}{k_2^2}\,\frac{\mathbf{k}\cdot\mathbf{k}_3}{k_3^2}$$

$$= \frac{1}{3!}\left(1+\frac{k_2}{k_1}\mu_{12}+\frac{k_3}{k_1}\mu_{13}\right)\left(1+\frac{k_1}{k_2}\mu_{12}+\frac{k_3}{k_2}\mu_{23}\right)\left(1+\frac{k_2}{k_3}\mu_{23}+\frac{k_1}{k_3}\mu_{13}\right)\,, \tag{8.78}$$

where $\mathbf{k}=\mathbf{k}_1+\mathbf{k}_2+\mathbf{k}_3$ and $\mu_{jh}=\mathbf{k}_j\cdot\mathbf{k}_h/k_j\,k_h$. The expression of $\delta^{(3)}$ in $\mathbf{x}$–space may be derived directly from the perturbative expansion in Eq.(8.69); we get

$$\delta^{(3)}(\mathbf{x},t) = \frac{1}{6}\,\delta^{(1)3} + \delta^{(1)}\partial_\alpha\delta^{(1)}\,\partial_\alpha\triangle^{(1)} + \frac{1}{2}\delta^{(1)}\,\partial_\alpha\partial_\beta\triangle^{(1)}\,\partial_\alpha\partial_\beta\triangle^{(1)} + \partial_\alpha\delta^{(1)}\,\partial_\beta\triangle^{(1)}\,\partial_\alpha\partial_\beta\triangle^{(1)} +$$

$$\frac{1}{2}\partial_\alpha\partial_\beta\delta^{(1)}\,\partial_\alpha\triangle^{(1)}\,\partial_\beta\triangle^{(1)} + \frac{1}{3}\partial_\alpha\partial_\beta\triangle^{(1)}\,\partial_\beta\partial_\gamma\triangle^{(1)}\,\partial_\gamma\partial_\alpha\triangle^{(1)} + \partial_\alpha\triangle^{(1)}\,\partial_\beta\partial_\gamma\triangle^{(1)}\,\partial_\alpha\partial_\beta\partial_\gamma\triangle^{(1)}\,. \tag{8.79}$$

We have now all the ingredients to compute the higher order density moments in Zel'dovich approximation. Following the mathematical track suggested in the previous section, it results that the density skewness in Zel'dovich approximation may be written as

$$\langle\delta^3\rangle_{ZA} = \frac{6}{(2\pi)^6}\int d\mathbf{k}_1 d\mathbf{k}_2\, J^{(2)}_{ZA}(\mathbf{k}_1,\mathbf{k}_2)\, P(\mathbf{k}_1)\, P(\mathbf{k}_2)\,, \tag{8.80}$$

where the Zel'dovich kernel $J^{(2)}_{ZA}$ is explicitely given by

$$\begin{aligned} J^{(2)}_{ZA}(\mathbf{k}_1,\mathbf{k}_2) &= \frac{1}{2!}\,\frac{\mathbf{k}\cdot\mathbf{k}_1}{k_1^2}\,\frac{\mathbf{k}_1\cdot\mathbf{k}_2}{k_2^2} \\ &= \frac{1}{2}\left(1+2\,\frac{k_1}{k_2}\,\mu_{12}+\mu_{12}^2\right) \\ &= \frac{2}{3}+\frac{k_1}{k_2}\,P_1(\mu_{12})+P_2(\mu_{12})\,, \end{aligned} \tag{8.81}$$

being the functions $P_l(\mu)$ the Legendre polynomial of order l. The integral in Eq.(8.80) is trivial; applying the addition theorem for spherical harmonics

$$\sum_m Y_l^m(\hat{k})\,Y_l^{-m}(\hat{k}) = \frac{2l+1}{4\pi}\,P_l(\mu)\,, \tag{8.82}$$

we get

$$\langle\delta^3\rangle_{ZA} = 4\,\langle\delta^2\rangle^2\,, \tag{8.83}$$

or

$$S_3^{(ZA)} = 4\,, \tag{8.84}$$

instead of the exact perturbative result, 34/7 [cfr. Eq.(8.37)]. We see that the Zel'dovich approximation is successful in reproducing the correct sign of the skewness, but it significantly underestimates the magnitude.

The gravitationally induced skewness of the smoothed $\delta_R = \delta * W_R$ is

$$\langle\delta^3(R)\rangle_{ZA} = \frac{6}{(2\pi)^6}\int d\mathbf{k}_1 d\mathbf{k}_2\,\widetilde{W}_R(k_1)\,\widetilde{W}_R(k_2)\,\widetilde{W}_R(|\mathbf{k}_1+\mathbf{k}_1|)\,J^{(2)}_{ZA}(\mathbf{k}_1,\mathbf{k}_2)\,P(\mathbf{k}_1)\,P(\mathbf{k}_2)\,, \tag{8.85}$$

in this case the integration is not so trivial as in the previous case, due to the mixing of the vectors $\mathbf{k}_1$ and $\mathbf{k}_2$ in the argument of the window function.

As discussed in Juskiewicz, Bouchet and Colombi (1993), for the smoothed density field, Eq.(8.84) my be regarded only as an approximation, valid in the regime when the density *gradients* across the filtering scale R small. For a density field with a coherence length, $R_c \equiv \sigma/\sigma_1$, where $\sigma_1^2 = (2\pi^2)^{-1}\int dk k^4\,P(k)\,\widetilde{W}_R^2(k)$ is the variance of the density gradient field. In the limit $R \ll R_c$, the function $\widetilde{W}_R(k_1)\,\widetilde{W}_R(k_2)\,\widetilde{W}_R(|\mathbf{k}_1+\mathbf{k}_1|)$ may be Taylor expanded about the origin, $k_1 = k_2 = 0$, and then evaluate the integral. One obtains

(see e.g. Juskiewicz, Bouchet & Colombi 1993)

$$S_3(R) = 4 - 2(R/R_c)^2 + O(R/R_c)^4 \ . \tag{8.86}$$

The first term describes the local contribution, as in the unsmoothed Eq.(8.84); the second term is the tidal correction, which lowers S_3, and the decrease is stronger for fields with smaller coherence lenght. A similar trend holds for pure power–law spectra: S_3 is anticorrelated with the amount of power on small scale.

For power–law spectra, $P(k) \propto k^n$, the integration in (8.85) leads to

$$S_3(R) = 4 - (3+n) \qquad -3 \leq n \leq 1 \ , \tag{8.87}$$

for a top–hat filter: as in the exact perturbative case, the skewness parameter is strongly sensitive to the primordial spectral index, n.

Similar argumentation may be extended to the fourth-central moment, the density kurtosis (Catelan & Moscardini 1993). The kurtosis describes features such as sharpness or stretchiness of the mass distribution and the extent of its rare–event tail. Moreover, it is possibly related to the *initial* sign of the skewness – as predicted in some non–Gaussian models (see e.g. Luo & Schramm 1993) – which is important for the final galaxy clustering pattern (Moscardini *et al.* 1991; Messina *et al.* 1992; Weinberg & Cole 1992).

Following a diagrammatic expansion similar to that in previous section (see Appendix 1 too) one finally gets the integral expression of the kurtosis ratio in Zel'dovich approximation

$$S_4 = \frac{24}{\sigma^6} \int \frac{d\mathbf{k}_1\, d\mathbf{k}_2\, d\mathbf{k}_3}{(2\pi)^9}\ P(k_1)\, P(k_2)\, \Big[P(k_3)\, J^{(3)}_{ZA}(\mathbf{k}_1, \mathbf{k}_2, \mathbf{k}_3) \ + $$
$$+ 2\, J^{(2)}_{ZA}(-\mathbf{k}_2, \mathbf{k}_2 + \mathbf{k}_3)\, J^{(2)}_{ZA}(\mathbf{k}_1, \mathbf{k}_2 + \mathbf{k}_3)\, P(|\mathbf{k}_2 + \mathbf{k}_3|) \Big] \ . \tag{8.88}$$

The angular integrations in Eq.(8.88) may be analytically performed. One obtains $S_4 = 88/3 \approx 29.3$ (Catelan & Moscardini 1993). This unsmoothed–case result is independent of the primordial spectral index, as is the skewness ratio S_3.

The kurtosis of the smoothed density field δ_R in the Zel'dovich approximation is

$$S_4(R) = \frac{24}{\sigma_R^6} \int \frac{d\mathbf{k}_1\, d\mathbf{k}_2\, d\mathbf{k}_3}{(2\pi)^9}\ \widetilde{W}_R(k_1)\, \widetilde{W}_R(k_2)\, \widetilde{W}_R(k_3)\, \widetilde{W}_R(|\mathbf{k}_1 + \mathbf{k}_2 + \mathbf{k}_3|) \times$$

$$P(k_1)\,P(k_2)\,\left[P(k_3)\,J^{(3)}_{ZA}(\mathbf{k}_1,\mathbf{k}_2,\mathbf{k}_3)\,+\,2\,J^{(2)}_{ZA}(-\mathbf{k}_2,\mathbf{k}_2+\mathbf{k}_3)\,J^{(2)}_{ZA}(\mathbf{k}_1,\mathbf{k}_2+\mathbf{k}_3)\,P(|\mathbf{k}_2+\mathbf{k}_3|)\right]\,. \tag{8.89}$$

Note that $P(k)$ completely describes the process of growth of mass fluctuations from Gaussian initial perturbations.

We calculate the previous integrals, by an Adaptive Multidimensional Monte Carlo Integration subroutine, for scale–free power spectra $P(k) \propto k^n$ with n in the range $-3 \leq n \leq 1$. Due to the assumed primordial scale–invariance, S_4 only depends on the primordial spectral index n, and not on the scale R. In Figure F1, we plot the kurtosis ratio S_4 of the Gaussian–smoothed density field versus the spectral index n, for both the perturbative and Zel'dovich approximations. Similar argumentation hold for the velocity kurtosis $S_{4,v}$. The main conclusions are drawn in the next section.

8.6 Discussion and Conclusions

From the analysis of Figure F1, it clearly appears that S_4 *strongly* depends on the primordial spectral index n. In particular the kurtosis parameter is a *decreasing* function of n. This is also confirmed by Bernardeau (1993), who, applying the exact perturbative technique, finds a similar trend in the case of top–hat filtering. An anticorrelation with the amount of small–scale power has also been found for the skewness parameter S_3 (Fry 1984; Juszkiewicz, Bouchet, & Colombi 1993), and it seems therefore a general property of higher order moments of the smoothed matter distribution: larger values of n correspond indeed to higher power on small scales, where the filtering operation acts.

Furthermore, the Zel'dovich approximation underestimates the induced–by–gravity S_4 w.r.t. the rigorous perturbative one, as already noted by Grinstein & Wise 1987 (although in the framework of the "standard" cold dark matter model). This is hardly surprising, since the Zel'dovich approximation fails to fully describe the gravitational effects causing particle trajectories to depart from their original directions. It results that the Zel'dovich

approximation makes higher orders in the perturbative series for δ smaller on *large* scales than they actually are (see e.g. Wise 1988).

Finally, note that the values for the kurtosis measured at a point, $S_4 = 60,712/1,323$ for full gravitational instability and $S_4 = 88/3$ for the Zel'dovich approximation, tend to match the Gaussian windowed values for $n = -3$. The underlying reason is that for $n = -3$, which originates an infrared logarithmic divergence in any connected density correlation, all the power is transferred on (very) large scales, beyond any reasonable filtering scale.

We stress that, due to the importance of the smoothing procedure, but also to its arbitrariness, one must be cautious about making quantitative comparisons between our results and both observational and N–body data. A Gaussian filter is used for instance by Saunders *et al.* (1991), who however estimated only the skewness in the QDOT–*IRAS* catalog. The only observational estimates up–to–now of the kurtosis of the galaxy distribution are obtained by counts–in–cells, corresponding to a top–hat filtering (Gaztañaga 1992; Bouchet *et al.* 1993; Fry & Gaztañaga 1993); a similar method is applied by Lahav *et al.* (1993) and Lucchin *et al.* (1993) in N–body simulations with scale–free power spectra. Very recently, using N–body simulations with $n = -1$, Juszkiewicz *et al.* (1993) have found $S_4 = 20$ by a good eye–fit to their Gaussian smoothed results, which is in excellent agreement with our evaluation.

Our results can be used to constrain both the probability distribution and the power spectrum of primordial density fluctuations and thus help to select the most reliable mechanism for the generation of large–scale structures.

We also explored the mildly–nonlinear effects on the one–point pdf of an initially Gaussian velocity field in terms of the gravitationally induced fourth connected moment $S_{4,v}$. We applied both the rigorous perturbative theory and the Zel'dovich approximation. We anticipate here some preliminary results.

From the diagram in Figure G1, it clearly appears that, in the perturbative description, the gravity induces a non–Gaussian signature in the peculiar velocity field: in

particular, $S_{4,v}$ is positive and roughly constant for any value of the primordial spectral index n. The highly–nonlinear mass concentrations on any scale dominate the dynamics and induce very large values of $|v_\alpha|$ in their vicinity: the kurtosis of $p(\mathbf{v})$ appear to be positive, i.e. $p(v_\alpha)$ is more strongly peaked near $v_\alpha = 0$ but it has higher tails at large value of $|v_\alpha|$ than the Gaussian distribution.

In Figure G1, we also plot $S_{4,v}$ obtained according to the Zel'dovich prescription. It may be noted that, unlike the perturbative case, the velocity kurtosis is practically constant and consistent with zero for any value of n. This is hardly surprising, since the Zel'dovich approximation fails to fully describe the gravitational effects causing particle trajectories to depart from their original directions. Moreover, we confirm the results of Kofman *et al.* (1993), who show that the Eulerian Gaussian one–point pdf $p(\mathbf{v})$ is *time–invariant* as long as the Zel'dovich approximation holds. This is essentially due to the simple time scaling of the particle Eulerian position $\mathbf{x}(\mathbf{q}, t)$ in Eq.(19).

Further evaluations of $S_{4,v}$ for physical spectra (as CDM spectrum) are in progress.

Finally we want to stress that one has to be cautious about making quantitative comparisons between our results, directly related to the underlying mass (dark plus luminous) distribution, and both observational and N–body data. In particular, Grinstein *et al.* (1987) suggest that when point–like luminous objects, like galaxies, are used to sample the peculiar flow within a region of the sky, it is the volume average of $n(\mathbf{x})\mathbf{v}(\mathbf{x})$ which is actually measured instead of the volume average of $\mathbf{v}(\mathbf{x})$, $n(\mathbf{x})$ being the number density of luminous tracers. If the objects are biased tracers of the underlying mass distribution (Kaiser 1984), then nonlinear effects on small–scales may preclude any direct comparison of the observed velocity moments with ensemble expectations. A further analysis of this problem is in progress.

8.7 Appendix 1: Structure of the Six–point Correlation Function

We treat here explicitely the integrals in Eqs.(8.49) and (8.50). Essentially, in Eq.(8.49) we have to work out the six–point correlation function

$$\langle \tilde{\delta}^{(1)}(\mathbf{k}_1)\,\tilde{\delta}^{(1)}(\mathbf{k}_2)\,\tilde{\delta}^{(1)}(\mathbf{k}_a)\,\tilde{\delta}^{(1)}(\mathbf{k}_b)\,\tilde{\delta}^{(1)}(\mathbf{k}_c)\,\tilde{\delta}^{(1)}(\mathbf{k}_d)\rangle \equiv \langle 1\,2\,a\,b\,c\,d\rangle \ . \tag{8.90}$$

In the Gaussian case, this function corresponds to a sum of 15 terms; namely:

$$\begin{aligned}
&\langle 1\,2\,a\,b\,c\,d\rangle = \\
&\langle 1\,2\rangle\,\langle a\,b\rangle\,\langle c\,d\rangle \ + \ \langle 1\,2\rangle\,\langle a\,c\rangle\,\langle b\,d\rangle \ + \ \langle 1\,2\rangle\,\langle a\,d\rangle\,\langle b\,c\rangle \ + \\
&\langle 1\,a\rangle\,\langle 2\,c\rangle\,\langle b\,d\rangle \ + \ \langle 1\,a\rangle\,\langle 2\,b\rangle\,\langle c\,d\rangle \ + \ \langle 1\,a\rangle\,\langle 2\,d\rangle\,\langle b\,c\rangle \ + \\
&\langle 1\,b\rangle\,\langle 2\,a\rangle\,\langle c\,d\rangle \ + \ \langle 1\,b\rangle\,\langle 2\,d\rangle\,\langle a\,c\rangle \ + \ \langle 1\,b\rangle\,\langle 2\,c\rangle\,\langle a\,d\rangle \ + \\
&\langle 1\,c\rangle\,\langle 2\,a\rangle\,\langle b\,d\rangle \ + \ \langle 1\,c\rangle\,\langle 2\,b\rangle\,\langle a\,d\rangle \ + \ \langle 1\,c\rangle\,\langle 2\,d\rangle\,\langle a\,b\rangle \ + \\
&\langle 1\,d\rangle\,\langle 2\,a\rangle\,\langle b\,c\rangle \ + \ \langle 1\,d\rangle\,\langle 2\,a\rangle\,\langle b\,c\rangle \ + \ \langle 1\,d\rangle\,\langle 2\,b\rangle\,\langle a\,c\rangle \ .
\end{aligned} \tag{8.91}$$

Now, the self–contractions vanish (because $\langle \delta^{(2)}\rangle = 0$) i.e. the 5 terms containing $\langle a\,b\rangle$ or $\langle c\,d\rangle$ or both of them; the loop pieces are higher order corrections of $\xi_{12}\,\xi_{34}$ and not a contribution to η: they correspond to the two terms $\langle \tilde{\delta}^{(1)}(\mathbf{k}_1)\,\tilde{\delta}^{(1)}(\mathbf{k}_2)\rangle\,\langle \tilde{\delta}^{(1)}(\mathbf{k}_3)\,\tilde{\delta}^{(1)}(\mathbf{k}_4)\rangle$, that indeed are separable; for the remaining 8 terms, only 2 of them are independent, the others can be obtained by interchanging the dummy integration variables i.e.

$$\begin{aligned}
\langle 1\,a\rangle\,\langle 2\,c\rangle\,\langle b\,d\rangle \quad &\overset{(a\leftrightarrow b)}{\rightsquigarrow} \quad \langle 1\,b\rangle\,\langle 2\,c\rangle\,\langle a\,d\rangle \ , \\
&\overset{(c\leftrightarrow d)}{\rightsquigarrow} \quad \langle 1\,a\rangle\,\langle 2\,d\rangle\,\langle b\,c\rangle \ , \\
&\overset{(1\leftrightarrow 2)}{\rightsquigarrow} \quad \langle 1\,c\rangle\,\langle 2\,a\rangle\,\langle b\,c\rangle \ ,
\end{aligned} \tag{8.92}$$

and

$$\begin{aligned}
\langle 1\,d\rangle\,\langle 2\,b\rangle\,\langle a\,c\rangle \quad &\overset{(a\leftrightarrow b)}{\rightsquigarrow} \quad \langle 1\,d\rangle\,\langle 2\,a\rangle\,\langle b\,c\rangle \ , \\
&\overset{(c\leftrightarrow d)}{\rightsquigarrow} \quad \langle 1\,c\rangle\,\langle 2\,b\rangle\,\langle a\,d\rangle \ , \\
&\overset{(1\leftrightarrow 2)}{\rightsquigarrow} \quad \langle 1\,b\rangle\,\langle 2\,d\rangle\,\langle a\,c\rangle \ .
\end{aligned} \tag{8.93}$$

We can write (the integration in Eq.(8.49) is partially indicated here)

$$\int \langle 1\,2\,a\,b\,c\,d\rangle = 4 \int \left[\langle 1\,a\rangle \langle 2\,c\rangle \langle b\,d\rangle + \langle 1\,d\rangle \langle 2\,b\rangle \langle a\,c\rangle \right] . \tag{8.94}$$

The 6–point correlation function in Eq.(8.50) is instead

$$\langle \tilde{\delta}^{(1)}(\mathbf{k}_1)\, \tilde{\delta}^{(1)}(\mathbf{k}_2)\, \tilde{\delta}^{(1)}(\mathbf{k}_3)\, \tilde{\delta}^{(1)}(\mathbf{k}_a)\, \tilde{\delta}^{(1)}(\mathbf{k}_b)\, \tilde{\delta}^{(1)}(\mathbf{k}_c)\rangle \equiv \langle 1\,2\,3\,a\,b\,c\rangle . \tag{8.95}$$

In such a case, it results that

$$\begin{aligned} &\langle 1\,2\,3\,a\,b\,c\rangle = \\ &\langle 1\,2\rangle \langle 3\,a\rangle \langle b\,c\rangle + \langle 1\,2\rangle \langle 3\,b\rangle \langle a\,c\rangle + \langle 1\,2\rangle \langle 3\,c\rangle \langle a\,b\rangle + \\ &\langle 1\,3\rangle \langle 2\,a\rangle \langle b\,c\rangle + \langle 1\,3\rangle \langle 2\,b\rangle \langle a\,c\rangle + \langle 1\,3\rangle \langle 2\,c\rangle \langle a\,b\rangle + \\ &\langle 1\,a\rangle \langle 2\,3\rangle \langle b\,c\rangle + \langle 1\,a\rangle \langle 2\,b\rangle \langle 3\,c\rangle + \langle 1\,a\rangle \langle 2\,c\rangle \langle 3\,b\rangle + \\ &\langle 1\,b\rangle \langle 2\,3\rangle \langle a\,c\rangle + \langle 1\,b\rangle \langle 2\,a\rangle \langle 3\,c\rangle + \langle 1\,b\rangle \langle 2\,c\rangle \langle 3\,a\rangle + \\ &\langle 1\,c\rangle \langle 2\,3\rangle \langle a\,b\rangle + \langle 1\,c\rangle \langle 2\,a\rangle \langle 3\,b\rangle + \langle 1\,c\rangle \langle 2\,b\rangle \langle 3\,a\rangle . \end{aligned} \tag{8.96}$$

All the separable terms are not higher order contributions to η (9 terms); the remaining 6 terms are equivalent by interchange the integration variables; finally

$$\int \langle 1\,2\,3\,a\,b\,c\rangle = 3! \int \langle 1\,a\rangle \langle 2\,b\rangle \langle 3\,c\rangle . \tag{8.97}$$

CHAPTER IX

Non–linear Evolution of Collisionless Matter Perturbations: Further Approximations

A relevant cosmological problem is to understand the physical processes that occurred during the gravitational collapse of the matter which gave rise to the observed structure of the universe on large scales. A complementary issue is to reconstruct the initial conditions of the clustering process, e.g. the value of the cosmological parameters, the type of dark matter, the statistics of the primordial perturbations, starting from observational data such as the spatial distribution of galaxies or their peculiar velocities. Much work has recently focused in the latter direction, since more and more data on peculiar velocities of optical galaxies, as well as very large and complete galaxy redshift surveys have become available both in the optical and in the infrared.

A widely applied approximation when dealing with the dynamics of dark matter, either cold or hot, is to treat it as a system of particles having negligible non–gravitational interactions, a self–gravitating collisionless system. The dynamics of such a system is usually approached by different techniques, depending on the specific application. For instance, the evolution of small perturbations on a Friedmann–Robertson–Walker (FRW) background is followed by analytical methods. The non–linear evolution in cases where some symmetries are present can also sometimes be followed analytically: typical examples being the spherical top–hat model for the Newtonian case and the Tolman–Bondi solution in General Relativity (GR). There are also useful approximations valid in the mildly non–linear regime, such as the Zel'dovich approximation (Zel'dovich 1970; see section IV.4). Besides this classical approach,

a number of variants have been proposed, all trying to overcome the inability to follow the development of structures beyond caustic formation. A promising approach is *adhesion theory* (e.g. Shandarin & Zel'dovich 1989 and references therein), where artificial viscosity is introduced to mimic the gravitational sticking of particles around pancakes. An alternative method, called frozen–flow approximation, recently proposed by Matarrese *et al.* (1992), allows an extrapolation beyond the time when orbit–crossing would have occurred according to the Zel'dovich formulation. This is based on the idea of extrapolating the growing mode of the linear velocity field beyond its actual range of validity, while solving exactly the continuity equation. Other approximations have been explored, such as the second order Lagrangian perturbation expansion (Buchert 1989, 1992; Moutarde *et al.* 1991; Bouchet *et al.* 1992; Gramann 1993a, b; Lachièze–Rey, 1993a, b), and the algorithm proposed by Giavalisco *et al.* (1993). Different approximations apply in the highly non–linear regime, such as the hierarchical closure ansatz for the BBGKY equations (Peebles 1980; Ruamsuwan & Fry 1992) The most general problem of studying the fully non–linear dynamics of a collisionless system in Newtonian theory can only be followed by numerical techniques, such as N–body codes.

A General Relativistic (GR) approach to the non–linear evolution of scalar perturbations of a zero–pressure fluid has been proposed by Matarrese, Pantano and Saez (1993a, b), under the assumption of vanishing vorticity and negligible gravitational–wave interactions with the rest of the system. In more technical terms the latter condition amounts to disregarding the so–called magnetic part of the Weyl tensor, during the non–linear evolution of perturbations prior to shell–crossing. Exact GR solutions with vanishing vorticity and magnetic components have been studied by Barnes and Rowlingson (1989) in a general context. The main advantage of such a treatment is that the fluid flow can be entirely followed in terms of strictly *local* evolution equations. Recently, this kind of approach has attracted some attention because of the advantages of a purely local algorithm. In particular, Croudace *et al.* (1993) have shown the connection of the GR pancake solution found by Matarrese, Pantano and Saez (1993a) with the Szekeres line element (Szekeres 1975). Bertschinger and

Jain (1993) have reached relevant conclusions about the Lagrangian behaviour of fluid elements during collapse. The relation of the GR treatment with the traditional Newtonian theory is discussed in detail in Matarrese, Pantano and Saez (1993b).

In this last chapter, we review a particular implementation of the Zel'dovich approximation, namely the *adhesion approximation* where an artificial addition of a tiny amount of viscosity to the Euler equation – converting it into a three–dimensional generalization of the well known Burgers' equation – stops the matter particles at the pancakes. Furthermore, after reviewing the frozen–flow approximation, we anticipate the first few calculations leading to a new approximation scheme, named *Local–Flow approximation* – LFA – (Catelan *et al.* 1993a). In this approximation the peculiar velocity field $\mathbf{u}$ is considered up to the second–order contribution as given by the standard perturbative theory, expanding in series the gravitational potential ϕ and the velocity potential Φ. An advantage of this approach is that we can easily work out the higher order velocity contributions $\mathbf{v}^{(n)}$ in a manifestly irrotational form in Eulerian configuration space [all the previous irrotational expressions for $\mathbf{v}^{(n)}$ were obtained in Fourier space (see Goroff *et al.* 1986)]. The importance of having explicit irrotational expressions for the velocity field at any perturbative order lies on the fact that a collisionless gravitating fluid cannot generate vorticity (before orbit mixing) and that the conservation of circulation is applicable well beyond the linear regime. In LFA one still solves exactly the continuity equation, but the local flow is no longer stationary, since the local acceleration is taken into account. Considering a dynamical instead of a stationary flow is expected to partially solve the lack of merging processes of the first generation of pancakes which is the main difficulty of the FFA.

9.1 Beyond Zel'dovich Approximation: Adhesion Model

The Zel'dovich approximation breaks down after the first–generation of collapsing objects since it forces that particles sail through pancakes and clusters unperturbed. This failure is

particularly problematic for modelling hierarchical scenarios, in which the primordial density fluctuations have power on all scales and small structures collapse early (see Section IV.4). The adhesion model (hereafter ADM) aims to overcome the difficulties met by Zel'dovich approximation after caustic formation. The Zel'dovich approach is modified by adding an artificial viscosity term to the Euler equation $d\mathbf{u}/da = 0$ [see e.g. Eq.(4.45)], which is thus replaced by

$$\frac{d\mathbf{u}}{da} = \nu\nabla^2\mathbf{u} \; . \tag{9.1}$$

This viscosity term is introduced to mimic the actual sticking of particles around pancakes, caused by the action of gravity even in a collisionless medium. The parameter ν plays the role of a coefficient of *kinematical viscosity* which controls the thickness of pancakes.

The previous equation is the vector generalization of the well–known non–linear diffusion or *Burgers equation* of strong turbulence (e.g. Burgers 1974). One can still define a velocity potential through $\mathbf{u}_{ADM} = \nabla\Phi_{ADM}$, which can be determined through the Hopf–Cole substitution $\Phi_{ADM} = -2\nu \ln U$, where the scalar field U satisfies the linear diffusion or Fokker–Planck equation $\partial U/\partial a = \nu\nabla^2 U$, with the initial condition $U_0(\mathbf{x}) = \exp[-\Phi_0(\mathbf{x})/2\nu]$. The velocity potential reads

$$\Phi_{ADM}(\mathbf{x},a) = -2\nu \ln\left[\frac{1}{(4\pi\nu a)^{3/2}}\int d\mathbf{q}\, \exp\left(-\frac{1}{2\nu}S(\mathbf{x},\mathbf{q},a)\right)\right] \; , \tag{9.2}$$

where one defines the action $S(\mathbf{x},\mathbf{q},a) \equiv \Phi_0(\mathbf{q}) + (\mathbf{x}-\mathbf{q})^2/2a$, satisfying the Hamilton–Jacobi Eq.(4.76). The corresponding velocity field is

$$\mathbf{u}_{ADM}(\mathbf{x},a) = \frac{\int d\mathbf{q}\, \frac{\mathbf{x}-\mathbf{q}}{a}\, \exp[-S(\mathbf{x},\mathbf{q},a)/2\nu]}{\int d\mathbf{q}\, \exp[-S(\mathbf{x},\mathbf{q},a)/2\nu]} \; . \tag{9.3}$$

The Eulerian positions are then found by direct integration of the integral equation (e.g. Nusser & Dekel 1990; Weinberg & Gunn 1990a,b)

$$\mathbf{x}(\mathbf{q},a) = \mathbf{q} + \int_0^a da'\, \mathbf{u}_{ADM}[\mathbf{x}(\mathbf{q},a'),a'] \; , \tag{9.4}$$

while the density field can be obtained from Eq.(4.62).

The Burgers equation is usually considered in the limit of small (but non–vanishing) ν, which corresponds to the limit of large *Reynolds* numbers, $\mathcal{R}_0 = u_0\ell_0/\nu$, where u_0 and ℓ_0

are the characteristic amplitude and scale of the initial velocity field (e.g. Gurbatov, Saichev & Yakushkin 1983)[1].

In the small–ν case the solution takes a simplified form which can be obtained from Eq.(9.2) through a saddle–point approximation,

$$\Phi_{ADM}(\mathbf{x},a) \approx -2\nu \ln \left\{ \sum_{\alpha} \mathcal{J}(\mathbf{q}_\alpha)^{-1/2} \exp\left[-\frac{1}{2\nu} S(\mathbf{x},\mathbf{q}_\alpha,a) \right] \right\} , \tag{9.5}$$

where $\mathcal{J}(\mathbf{q}) = \|\mathbf{1} + a\mathbf{D}_0(\mathbf{q})\|$, $\mathbf{D}_0$ is the deformation tensor and $\mathbf{q}_\alpha$ are the Lagrangian points which minimize the action S at given $\mathbf{x}$ and a. The Zel'dovich approximation is recovered in the limit $\nu \to 0$.

This model has been recently considered by many authors to perform numerical simulations of the large–scale structure of the universe (Weinberg & Gunn 1990a,b) or to obtain some physical insight into the structure formation process in simplified situations such as one–dimensional models (Williams *et al.* 1991). The model also allows to obtain the *skeleton* of the large–scale matter distribution by a geometrical technique based on the insertion of osculating paraboloids into the hypersurface $\phi_0(\mathbf{q})$ (e.g. Kofman, Pogosyan & Shandarin 1990; Kofman *et al.* 1992; see the discussion in Section IV.4). The asymptotic properties of the solutions of Burgers equation (e.g. Kida 1979; Gurbatov & Saichev 1981) have been used to compute analytically physical quantities such as the velocity distribution and the mass function of knots (Gurbatov, Saichev & Shandarin 1989; Doroshkevich & Kotok 1990; Williams *et al.* 1991).

---

[1]The product $u_0\ell_0$ can be estimated either from the *rms* initial velocity potential smoothed on some scale R, $\langle \Phi_0^2(R) \rangle^{1/2}$, if this is convergent, or from the square root of the *structural function* of Φ_0 (e.g. Shandarin & Zel'dovich 1989)

$$D(r) = \langle [\Phi_0(\mathbf{x}) - \Phi_0(\mathbf{x}+\mathbf{r})]^2 \rangle = \frac{1}{\pi^2} \int_0^\infty dk\, k^2\, \mathcal{P}_\phi(k) W^2(kR)[1 - j_0(kr)] ,$$

evaluated at a suitable lag, e.g. $r \approx R$. In the previous equation $\mathcal{P}_\phi$ is the power–spectrum of the initial gravitational potential and $W(kR)$ a suitable low–pass filter function.

9.2 Newtonian Dynamics in Eulerian Form: the Frozen–Flow Approximation

The standard Newtonian equations for the evolution of collisionless matter in the universe can be rewritten in terms of suitably rescaled variables and in comoving coordinates. In particular, it is sometimes convenient to use as time variable the growth factor of linear perturbations, which in a flat, matter dominated model, coincides with the expansion factor $a(t) \equiv t^{2/3}$. The Euler equations read (see Section IV.2)

$$\frac{d\mathbf{u}}{da} + \frac{3}{2a}\mathbf{u} = -\frac{3}{2a}\nabla\phi \,, \tag{9.6}$$

where $\mathbf{u} \equiv d\mathbf{x}/da$ is a rescaled comoving peculiar velocity field and the symbol $\frac{d}{da}$ stands for the total (convective) derivative $\frac{d}{da} = \frac{\partial}{\partial a} + \mathbf{u}\cdot\nabla$. The continuity equation can be written in terms of the comoving matter density $\eta(\mathbf{x},t) \equiv \rho(\mathbf{x},t)/\rho_b$ (where $\rho_b(t)$ is the background mass density at t)

$$\frac{d\eta}{da} + \eta\nabla\cdot\mathbf{u} = 0 \,, \tag{9.7}$$

while the local gravitational potential ϕ is determined by local density inhomogeneities $\delta(\mathbf{x},t) \equiv \eta(\mathbf{x},t) - 1$ through Poisson's equation

$$\nabla^2\phi = \frac{\delta}{a} \,. \tag{9.8}$$

[It is understood that the potential ϕ is rescaled in such a manner that the constant A appearing in Section IV.2 is equal to unity here.] We restrict our analysis to irrotational flow.

The Zel'dovich approximation, in these variables, corresponds to the ansatz $\mathbf{u} = -\nabla\phi$, as suggested by linear theory (IV.4). In this case the Euler and continuity equations decouple from Poisson's one, and the system describes inertial motion of particles with initial velocity field impressed by local gravity, as implied by the growing mode of linear perturbation theory: $\mathbf{u}_{ZA}(\mathbf{x},a) = -\nabla_{\mathbf{q}}\phi_0(\mathbf{q})$, where $\mathbf{q}$ is the initial (Lagrangian) position and a is adopted as a time variable. It follows that particles move along straight trajectories

$$\mathbf{x}(\mathbf{q},a) = \mathbf{q} - a\nabla_{\mathbf{q}}\phi_0(\mathbf{q}) \,. \tag{9.9}$$

The frozen–flow approximation (FFA) can be defined as the solution of the linearized Euler equations, where in the r.h.s. the growing mode of the linear gravitational force is assumed, $\mathbf{u}_{FFA}(\mathbf{x}, a) = \mathbf{u}_0(\mathbf{x}) = -\nabla_{\mathbf{x}}\phi_0(\mathbf{x})$, plus a negligible decaying mode. In this approximation the peculiar velocity field $\mathbf{u}(\mathbf{x}, a)$ is *frozen* at each point to its initial value, that is

$$\frac{\partial \mathbf{u}}{\partial a} = 0 \,, \tag{9.10}$$

which is just the condition for steady flow. The above equation, together with the continuity equation, defines FFA. Particle trajectories in FFA are described by the integral equation

$$\mathbf{x}(\mathbf{q}, a) = \mathbf{q} - \int_0^a da' \, \nabla_{\mathbf{x}}\phi_0[\mathbf{x}(\mathbf{q}, a')] \,. \tag{9.11}$$

Particles update their velocity at each infinitesimal step to the local value of the linear velocity field, without any memory of their previous motion, i.e. without *inertia*. Streamlines are then frozen to their initial shape and multi–stream regions cannot form. A particle moving according to FFA has zero component of the velocity in a place where the same component of the initial gravitational force is zero, it will then slow down its motion in that direction while approaching that place. Unlike the Zel'dovich approximation, these particles move along curved paths: once they come close to a pancake configuration they curve their trajectories, moving almost parallel to it, and trying to reach the position of the next filament. Again they cannot cross it, so they modify their motion, while approaching it, to finally fall, for $a \to \infty$, into the knots corresponding to the minima of the initial gravitational potential. This type of dynamics implies an artificial thickening of particles around pancakes, filaments and knots, which mimics the gravitational clustering around these structures (though these configurations do not necessarily occur in the right Eulerian locations, nor they necessarily involve the right Lagrangian fluid elements). In assuming that the velocity potential is linearly related at any time to the local value of the initial gravitational potential, FFA disregards the non–linear effects caused by the back–reaction of the evolving mass density on the peculiar velocity field itself (via the non–linear evolution of the gravitational potential). This implies that a number of physical processes such as merging of pancakes, fragmentation and disruption of low–density bridges, are totally absent in the

FFA dynamics. Unlike the velocity field, the FFA density field is non–locally determined by the initial fluctuations, via the continuity equation; this is clearly shown by the following analytic expression

$$1 + \delta_{FFA}(\mathbf{x}, a) = \exp \int_0^a da' \, \delta[\mathbf{x}(\mathbf{q}, a'), a'] \, . \tag{9.12}$$

Brainerd, Scherrer & Villumsen (1993) have recently shown that a similar formula also applies if one uses a different approximation (called LEP: linear evolution of potential), consisting in "freezing" the gravitational rather than the velocity potential [see also the equivalent "frozen–potential" approach by Bagla & Padmanabhan (1993)]. This approach shows many features in common to FFA, although multi–stream regions do occur in this case.

Numerical implementation of FFA is straightforward (for a more technical discussion, see Matarrese *et al.* (1992)) and involves small computing time: roughly speaking, FFA consists of a multi–step Zel'dovich approximation, and very few steps are required to follow the entire evolution. Matarrese *et al.* (1992) applied FFA to follow the evolution of structures in the standard CDM model, and found that it gives a fairly accurate representation of the density pattern from a resolution scale of ~ 500 km s^{-1}, while the two–point correlation function fits quite well the true non–linear result on even smaller scales. Further connections of FFA and the Zel'dovich approximation can be found, based on the Hamilton–Jacobi approach to the non–linear dynamics of collisionless matter. These, as well as other features of Eulerian perturbation expansions, will be discussed elsewhere (Catelan *et al.* 1993b). Recently, Melott *et al.* (1993) have tested FFA vs. the "truncated" Zel'dovich approximation (e.g. Melott, Pellman & Shandarin 1993) and a full N–body code. They compare a number of statistics between results of the FFA, truncated Zel'dovich approximation and N–body simulations and find that FFA performs reasonably well in a statistical sense, e.g. in reproducing the counts–in–cell distribution, at small scales, but it does poorly in the cross–correlation with N–body, especially in models with high initial small–scale power.

9.3 Beyond FFA: Local–Flow Approximation

The frozen flow approximation is based on the hypothesis that the velocity potential is linearly related at any time to the local value of the initial gravitational potential. One can see this directly from Eq.(9.10) defining a velocity potential Φ_{FFA} such that $\mathbf{u}_{FFA} \equiv \nabla\Phi_{FFA}$; one gets

$$\frac{\partial\Phi_{FFA}}{\partial a} = 0 \,, \tag{9.13}$$

whose solution is

$$\Phi_{FFA}(\mathbf{x}, a) = \Phi_1(\mathbf{x}) \,. \tag{9.14}$$

[We shall neglect the subscript FFA. The subscript '1' comes from the perturbative notation adopted in Chapter VIII, and indicates *linear* quantities, here also labelled by the index '0'.] Therefore FFA forces one to disregard the non–linear effects caused by the back–reaction of the growing mass density fluctuations on the peculiar velocity field itself when the gravitational potential evolves. Such an evolution on the contrary leads to a number of physical processes such as merging of first–generation pancakes, fragmentation and possibly disruption of bridges and filaments, which the FFA cannot describe. This lack of merging process in FFA has been confirmed by numerical analyses and comparisons with the true non–linear dynamics displayed by the N–body simulations (Matarrese *et al.* 1992). A manner to partially circumvent the difficulties mentioned before is to add a tiny artificial viscosity in the manner of the adhesion model. Alternatively, one can try to improve the simple FFA by considering higher–order perturbative corrections of the gravitational potential Φ, namely, instead of Eq.(9.13) one considers the dynamical equation

$$\frac{\partial^2\Phi}{\partial a^2} = 0 \,. \tag{9.15}$$

This equation, together with the continuity equation, defines LFA. It is immediate to show that Eq.(9.15) is equivalent to considering also the second–order perturbative contribution, namely

$$\Phi = \Phi^{(1)} + \Phi^{(2)} \equiv \Phi_1(\mathbf{x}) + a\,\Phi_2(\mathbf{x}) \,, \tag{9.16}$$

or, alternatively,

$$\mathbf{u} = \mathbf{u}^{(1)} + \mathbf{u}^{(2)} \equiv \mathbf{u}_1(\mathbf{x}) + a\,\mathbf{u}_2(\mathbf{x})\,, \tag{9.17}$$

where $\mathbf{u}^{(n)} \equiv \nabla\Phi^{(n)}$ (we are adopting the same perturbative notation as in Chapter VIII). In particular $\mathbf{u}_2$ may be regarded as a *local acceleration*, not considered in the simple FFA (an explicit derivation of Φ_2 i.e. $\mathbf{u}_2$ in terms of linear potentials is given in the Appendix 1).

Again, fluid particles update without inertia their velocity at each infinitesimal step to the local value of the linear velocity field *plus* a contribution $\mathbf{u}^{(2)}$ due to the local acceleration. Particles trajectories in LFA are described by the integral equation [compare it with the FFA relation in Eq.(9.11)]

$$\mathbf{x}(\mathbf{q},a) = \mathbf{q} - \int_0^a da'\,\nabla_{\mathbf{x}}\Big\{\phi_0[\mathbf{x}(\mathbf{q},a')] - a'\Phi_2[\mathbf{x}(\mathbf{q},a')]\Big\}\,. \tag{9.18}$$

As a result, the streamlines are not *frozen* at each point to their initial shape, since the LFA flow is no longer a steady flow, possibly leading to merging processes among first pancakes. However, as in FFA, multi–stream regions cannot form, since again a particle which moves according to LFA has zero component of the velocity in a place where the same component of the gravitational force is zero, and it will slow down its motion while approaching the minima of the gravitational potential (peaks of density field; note that these minima are not stationary now). Therefore, in LFA are preserved the typical advantages of the FFA (no orbit–crossing, small computing time,...) whilst a number of non–linear physical processes such as merging of pancakes, fragmentations and disruptions of low–density bridges are expected because of the introduction at any point of the local gravitational force $a\nabla\Phi_2$.

The local acceleration $\mathbf{u}_2$ may be written in terms of the linear quantities as

$$\mathbf{u}_2(\mathbf{x}) = \nabla\left(\frac{3}{7}\,f_2(\mathbf{x}) - \frac{2}{7}\,\mathbf{u}_1^2(\mathbf{x})\right)\,, \tag{9.19}$$

where the spatial function $f_2(\mathbf{x})$ satisfies the differential equation

$$\nabla^2 f_2(\mathbf{x}) = a^{-1}\nabla\cdot\left(\delta^{(1)}\mathbf{u}^{(1)}\right)\,. \tag{9.20}$$

We stress that the second–order velocity $\mathbf{u}^{(2)}$ is irrotational i.e. $\nabla\wedge\mathbf{u}^{(2)} = \mathbf{0}$. These and other technical details are shown in the Appendix 1, while a complete analysis with numerical implementation of the LFA will be given in a forthcoming paper (Catelan *et al.* 1993a).

9.4 Appendix 1: LFA Acceleration

In this appendix, we derive the expressions of the second–order contributions ϕ_2 and Φ_2. As shown in Section IV.2 the fundamental equations for the cosmological potentials Φ and ϕ are given by

$$\begin{cases} \dfrac{\partial \Phi}{\partial a} + \dfrac{1}{2}(\nabla\Phi)^2 = -\dfrac{3}{2a}(\Phi + \phi)\,, \\ \\ \dfrac{\partial}{\partial a}(a\phi) + \Phi + f = 0\,, \end{cases} \tag{9.21}$$

where the function f satisfies the differential equation

$$\nabla^2 f = a\nabla\cdot\left[\nabla^2\phi\nabla\Phi\right] = a\left[\nabla^2\phi\nabla^2\Phi + \nabla\nabla^2\phi\cdot\nabla\Phi\right]\,. \tag{9.22}$$

As in Eq.(9.16), to find approximate perturbative solutions of these equations we expand ϕ and f according to the relations

$$\phi = \phi^{(1)} + \phi^{(2)} \equiv \phi_1 + a\,\phi_2\,, \tag{9.23}$$

$$f = f^{(2)} \equiv a f_2\,, \tag{9.24}$$

where $\phi_h = \phi_h(\mathrm{x})$; for instance we have $\delta^{(1)} = a\nabla^2\phi^{(1)}$, while $\delta_1 = \nabla\phi_1$, where $\delta^{(1)} = a\delta_1$. Note that f is by definition at least a second–order quantity. In terms of the perturbed quantities one has

$$\begin{cases} \dfrac{5}{2}\Phi_2 + \dfrac{1}{2}(\nabla\Phi)^2 + \dfrac{3}{2}\phi_2 = 0\,, \\ \\ 2\phi_2 + \Phi_2 + f_2 = 0\,, \\ \\ \nabla^2 f_2 = -\delta_1^2 - \nabla\delta_1\cdot\nabla\phi_1 = -\delta_1^2 + (\mathbf{u}_1\cdot\nabla)\,\delta_1\,. \end{cases} \tag{9.25}$$

From the first two equations it is possible to obtain the expressions for ϕ_2 and Φ_2:

$$\phi_2 = -\frac{5}{7} f_2 + \frac{1}{7} (\nabla\phi_1)^2 = -\frac{5}{7} f_2 + \frac{1}{7} \mathbf{u}^{(1)\,2} , \tag{9.26}$$

$$\Phi_2 = \frac{3}{7} f_2 - \frac{2}{7} (\nabla\phi_1)^2 = \frac{3}{7} f_2 - \frac{2}{7} \mathbf{u}^{(1)\,2} . \tag{9.27}$$

Furthermore, it is immediate to derive the expression of $\nabla\phi$ and the velocity $\mathbf{u}$ up to the second–order expansion

$$\nabla\phi = \nabla\phi^{(1)} - \frac{5}{7} \nabla f^{(2)} + \frac{2}{7} a (\mathbf{u}^{(1)} \cdot \nabla) \mathbf{u}^{(1)\,2} , \tag{9.28}$$

$$\mathbf{u} = -\nabla\phi^{(1)} + \frac{3}{7} \nabla f^{(2)} - \frac{4}{7} a (\mathbf{u}^{(1)} \cdot \nabla) \mathbf{u}^{(1)\,2} . \tag{9.29}$$

We stress that, unlike Eq.(8.13), the velocity $\mathbf{u}$ is manifestly irrotational, namely

$$\mathbf{u} = \nabla \left[\Phi^{(1)} + \frac{3}{7} f^{(2)} - \frac{2}{7} a \mathbf{u}^{(1)\,2} \right] . \tag{9.30}$$

The final expression for δ and $\nabla \cdot \mathbf{u}$ are

$$\delta = \delta^{(1)} + \nabla^2 \left[-\frac{5}{7} a f^{(2)} + \frac{1}{7} a^2 \mathbf{u}^{(1)\,2} \right] , \tag{9.31}$$

$$- a \nabla \cdot \mathbf{u} = \delta^{(1)} + \nabla^2 \left[-\frac{3}{7} a f^{(2)} + \frac{2}{7} a^2 \mathbf{u}^{(1)\,2} \right] . \tag{9.32}$$

It is straightforward to show that these relations coincide with the second order approximations for the density and velocity fields obtained in Chapter VIII. For example, from the first one, we find

$$\begin{aligned} \delta &= \delta^{(1)} - \frac{5}{7} a \nabla^2 f^{(2)} + \frac{1}{7} a^2 \nabla^2 \mathbf{u}^{(1)\,2} \\ &= \delta^{(1)} - \frac{5}{7} a \left(-a \delta_1^2 + (\mathbf{u}^{(1)} \cdot \nabla) \delta_1 \right) + \frac{2}{7} a^2 \nabla \cdot \left[(\mathbf{u}^{(1)} \cdot \nabla) \mathbf{u}^{(1)} \right] \\ &= \delta^{(1)} + \frac{5}{7} \delta^{(1)\,2} - \frac{5}{7} a (\mathbf{u}^{(1)} \cdot \nabla) \delta^{(1)} - \frac{2}{7} a (\mathbf{u}^{(1)} \cdot \nabla) \delta^{(1)} + \frac{2}{7} a^2 \sum_{\alpha\beta} \left(\partial_\beta u_\alpha \right)^2 , \end{aligned}$$

from which

$$\delta = \delta^{(1)} + \frac{5}{7} \delta^{(1)\,2} - a (\mathbf{u}^{(1)} \cdot \nabla) \delta^{(1)} + \frac{2}{7} a^2 \sum_{\alpha\beta} \left(\partial_\beta u_\alpha \right)^2 , \tag{9.33}$$

which can be compared with Eq.(8.8). In a similar fashion,

$$- a \nabla \cdot \mathbf{u} = \delta^{(1)} + \frac{3}{7} \delta^{(1)\,2} - a (\mathbf{u}^{(1)} \cdot \nabla) \delta^{(1)} + \frac{4}{7} a^2 \sum_{\alpha\beta} \left(\partial_\beta u_\alpha \right)^2 \tag{9.34}$$

already obtained in Section (VIII.1).

APPENDIX A

Gaussian Random Fields

Let consider the homogeneous isotropic Gaussian random field $\delta(\mathbf{x}) \equiv [\rho(\mathbf{x}) - \langle\rho\rangle]/\langle\rho\rangle$, with mean zero and variance $\sigma_o^2 = \langle\rho\rangle^{1/2}$. The *pdf* of δ with power spectrum $P(k)$ is

$$p(\delta)\, d\delta = (2\pi\sigma_o^2)^{-1/2} \exp(-\delta^2/2\sigma_o^2)\,, \tag{A.1}$$

where (§ 3.3)

$$\sigma_o^2 = \frac{1}{2\pi^2}\int_o^\infty dk\, k^2\, P(k) = \xi(0)\,, \tag{A.2}$$

$\xi(r)$ being the 2-point correlation function. All statistical properties of δ can be expressed in terms of the correlation function $\xi(r)$ and its derivatives or, alternatively, in terms of integrals over the power spectrum. For instance, one useful moment is

$$\sigma_1^2 = -3\,\xi''(0) = \frac{1}{2\pi^2}\int_0^\infty dk\, k^4\, P(k)\,, \tag{A.3}$$

which is the mean-square derivative of the field along a line. One may define a related coherence length

$$r_c \equiv \frac{\sigma_o}{\sigma_1} = \langle k^2\rangle^{-1/2}\,, \tag{A.4}$$

which measures the effective range of the correlations present in the field. Many of the power spectra of interest in cosmology lead to a zero coherence length (ie. an infinite mean-square derivative). This happens because such fields have structures on all scales and are therefore not differentiable. The usual approach is to smooth away structure on scales less than some scale of interest R (§ 3.3).

Behind many statistical calculations is the *joint probability distribution* of the values of the field $\delta(\mathbf{x})$ and/or of the derivatives of the field δ in N points $\mathbf{x}_1, \ldots, \mathbf{x}_N$, which is a *multivariate* gaussian *pdf*

$$P_N(\alpha_1, \ldots, \alpha_N) = \left[(2\pi)^N \det M\right]^{-1/2} \exp\left\{-\frac{1}{2}\sum_{jh} \alpha_j M^{-1}_{jh} \alpha_h\right\} . \qquad \text{(A.5)}$$

$M_{jh} \equiv \langle \alpha_j \alpha_h \rangle$ is the $N \times N$ *correlation matrix*. A simple example is the joint probability distribution that δ has a value $\alpha_1 = \delta(\mathbf{x}_1)$ and a value $\alpha_2 = \delta(\mathbf{x}_2) = \delta(\mathbf{x}_1 + \mathbf{r})$. To make things as simple as possible, we use normalized variables $\alpha'_i \equiv \alpha_i/\sigma_o$ and define a normalized correlation function (autocorrelation) $\omega(r) \equiv \xi(r)/\sigma_o^2$. The correlation matrix and its inverse are

$$M = \begin{pmatrix} 1 & \omega \\ \omega & 1 \end{pmatrix} , \qquad M^{-1} = \frac{1}{1-\omega^2}\begin{pmatrix} 1 & -\omega \\ -\omega & 1 \end{pmatrix} , \qquad \text{(A.6)}$$

therefore,

$$p(\alpha_1, \alpha_2; \omega) = \left(2\pi\sqrt{1-\omega^2}\right)^{-1} \exp[-(\alpha_1^2 - 2\,\omega\,\alpha_1\alpha_2 + \alpha_2^2)/2\,(1-\omega^2)] . \qquad \text{(A.7)}$$

For those interested in the path-integral approach, we remember that, for a Gaussian scalar random field (Feynman & Hibbs 1965)

$$P[\delta] \propto \exp\left\{-\frac{1}{2}\int d\mathbf{x}\, d\mathbf{y}\, \delta(\mathbf{x})\, K(\mathbf{x},\mathbf{y})\, \delta(\mathbf{y})\right\} , \qquad \text{(A.8)}$$

with $\int [d\delta] P[\delta] = 1$, from which it is possible to obtain all the previous relations. K is defined by the relations $K = \xi^{-1}$ and $\int d\mathbf{y}\, K(\mathbf{x},\mathbf{y})\, K^{-1}(\mathbf{y},\mathbf{z}) = \delta(\mathbf{x}-\mathbf{z})$, as in the usual field theory (see e.g. Negele & Orland 1988; Ramond 1989), and therefore $P(k) = 1/\widetilde{K}(k)$, with $\tilde{K}$ the Fourier transform of K. The mathematical theory of Gaussian random fields is given in books by Adler (1981) and Vanmarcke (1983). Many properties are also analyzed in beautiful classical works e.g. Chandrasekhar (1943) and Rice (1954).

APPENDIX B

Cumulant Expansion

A general way of specifying the distribution functional (let suppose that we are treating the *continuous* field case)

$$P[\delta(\mathbf{x})]\, d[\delta(\mathbf{x})]\,, \tag{B.1}$$

is by (all of) its *moments*

$$\langle \delta(\mathbf{x}_1) \cdots \delta(\mathbf{x}_N) \rangle \equiv \mu_N(\mathbf{x}_1, \ldots, \mathbf{x}_N)\,. \tag{B.2}$$

A way for generating automatically these moments is by functional differentiation (e.g.Monin & Yaglom 1971; Zaidi 1983; Fry 1985) of the *moment generating functional* $Z[J]$

$$Z[J] \equiv \left\langle \exp \int dx\, \delta(\mathbf{x})\, J(\mathbf{x}) \right\rangle = \int d[\delta(\mathbf{x})] \exp \int dx\, \delta(\mathbf{x})\, J(\mathbf{x})\, P[\delta(\mathbf{x})] \;: \tag{B.3}$$

$$\mu_N(\mathbf{x}_1, \ldots, \mathbf{x}_N) = \frac{\delta^N Z[J]}{\delta J(\mathbf{x}_1) \cdots \delta J(\mathbf{x}_N)} |_{J=0}\,. \tag{B.4}$$

From either the original definition (B.2) or this expression, it is apparent that μ_N is unchanged by interchange of any subset of its arguments.

It is next convenient to introduce the *generating function*

$$K[J] \equiv \ln Z[J] = \left\langle \exp \left(\int dx\, \delta(\mathbf{x})\, J(\mathbf{x}) \right) - 1 \right\rangle_c\,, \tag{B.5}$$

from which one can obtain systematically, by functional differentiation, the *connected or reduced moments*

$$k_N(\mathbf{x}_1, \cdots, \mathbf{x}_N) \equiv \frac{\delta^N K[J]}{\delta J(\mathbf{x}_1) \cdots \delta J(\mathbf{x}_N)} |_{J=0} = \langle \delta(\mathbf{x}_1) \cdots \delta(\mathbf{x}_N) \rangle_c\,. \tag{B.6}$$

The k_N are the reduced correlation functions of the distribution $P[\delta(\mathrm{x})]d[\delta(\mathrm{x})]$, also known as *semi-invariants* and/or *cumulants* in probability theory (Monin & Yaglom 1971; Kendall & Stuart 1977) and in statistical studies of liquids (Rice & Gray 1965), and related to the connected Green's function of Quantum Field Theory (Brandenberger 1985; Ramond 1989). In QFT, $Z[J]$ is also know as the *partition functional* or *vacuum-vacuum transition amplitude* in the presence of the external source $J(\mathrm{x})$.

By (B.6), one can state the *cumulant expansion theorem* writing

$$Z[J] = \exp \sum_{N=1}^{\infty} \frac{1}{N!} \left(\prod_{h=1}^{N} \int d\mathrm{x}_h \, J(\mathrm{x}_h) \right) \langle \delta(\mathrm{x}_1) \cdots \delta(\mathrm{x}_N) \rangle_c \, , \tag{B.7}$$

from which, we see, one may reconstruct the generating functional $\ln Z[J]$ from the N-point connected correlation functions $\xi^{(N)}(\mathrm{x}_1, \ldots, \mathrm{x}_N) \equiv \langle \delta(\mathrm{x}_1) \cdots \delta(\mathrm{x}_N) \rangle_c$. The probability distribution functional $P[\delta(\mathrm{x})]$ then follows from the (inverse) functional Fourier transform of the functional Z[iJ], often called, in this case, the *characteristic functional* of the distribution (see e.g. Fry 1985): therefore, in principle, *the hierarchy of N-point correlation functions completely specifies the statistics of the homogeneous and isotropic continuous random field* $\delta(\mathrm{x})$(however see Bochner's theorem, Reed & Simon 1980, theorem IX.9).

The cumulant expansion theorem is known in classical (e.g. Ma 1985) and quantum statistical mechanics (e.g. Negele & Orland 1988) as the *linked-cluster theorem.*

The reduced correlation functions k_N have the desirable property that $k_N(\delta + \delta') = k_N(\delta) + k_N(\delta')$ and $k_N(\alpha\delta) = \alpha^N k_N(\delta)$. More importantly, any contribution to μ_N which can be separated as $\langle \delta^M \rangle \langle \delta^{N-M} \rangle$ has been removed from k_N. Thus, $k_N \to 0$ as any subset of $\{\mathrm{x}_1, \ldots, \mathrm{x}_N\}$ is removed to infinite separation.

The first few μ_N and k_N are related by the relations (with $\mu_1 = \langle \delta \rangle = 0$)

$$\mu_2 = k_2 \, ,$$

$$\mu_3 = k_3 \, ,$$

$$\mu_4 = k_4 + 3\, k_2^2 \, ,$$

$$\mu_5 = k_5 + 10\, k_2\, k_3 \, ,$$

$$\mu_6 = k_6 + 15\,k_2\,k_4 + 10\,k_3^2 + 15\,k_2^3\ ,$$

$$\mu_7 = k_7 + 21\,k_2\,k_5 + 35\,k_3\,k_4 + 105\,k_2^2\,k_3\ , \tag{B.8}$$

etc., where, for brevity, labels on the unconnected parts are omitted; one has to take all distinct subgroupings of $\{\mathrm{x}_1, \ldots, \mathrm{x}_N\}$, for instance,

$$\mu_4(1,2,3,4) = k_4(1,2,3,4) + k_2(1,2)\,k_2(3,4) + k_2(1,3)\,k_2(2,4) + k_2(1,4)\,k_2(2,3). \tag{B.9}$$

The first few k_N in galaxy clustering are known as $k_2(\mathrm{x}_1, \mathrm{x}_2) = \xi(x_{12})$, the two point function; $k_3(\mathrm{x}_1, \mathrm{x}_2, \mathrm{x}_3) = \zeta_{123}$, the three point function; and $k_4(\mathrm{x}_1, \mathrm{x}_2, \mathrm{x}_3, \mathrm{x}_4) = \eta_{1234}$, the four point function.

Finally, if one assumes that the random field δ is Gaussian distributed, then *all reduced moments k_N of the distribution vanish for $N \geq 3$*; since we have subtracted out the mean also, this means that the distribution is completely specified by its two-point correlation function $\xi(x)$ (ie. by its Fourier transform, the power spectrum $P(k)$). Thus, the *Nth moment*, $\mu_N = \langle \delta^N \rangle$, is obtained by connecting all possible pairs of points: $\mu_N = 0$ if N is odd, or $\mu_N = (N-1)!!\,\xi^{N/2}$ if N is even.

The particular form of $Z[J]$ in the case of Gaussian field is (Feynman & Hibbs 1965)

$$Z[J] = \int [\delta(\mathrm{x})] \exp\left\{ -\frac{1}{2} \int\int d\mathrm{x}\, d\mathrm{y}\, \delta(\mathrm{x})\, K(\mathrm{x},\mathrm{y})\, \delta(\mathrm{y}) + \int d\mathrm{x}\, \delta(\mathrm{x})\, J(\mathrm{x}) \right\}\ . \tag{B.10}$$

Some cosmologists state that the word *non–Gaussian* means nothing, in the same sense that the word e.g. *non–dog* means nothing.

We disagree.

With the generic word *non-Gaussian* we characterize *any* probability distribution with some higher reduced moment different from zero, and this is not a null-statement; of course, this is not sufficient for picking out a specific probability distribution. On the other hand, there exists one exception, namely the distribution $p(x) = \delta_D(x - a)$, with only a mean and no nonvanishing higher irreducible moments.

APPENDIX C

Generalization of the Peak Formalism to Non–Gaussian Density Fields

Peak Number Density of Non–Gaussian Random Fields

Paolo CATELAN [1], Francesco LUCCHIN [2] & Sabino MATARRESE [3]

[1] *SISSA - International School for Advanced Studies,*
Strada Costiera 11, 34014 Trieste, Italy

[2] *Dipartimento di Astronomia, Universita' di Padova*
vicolo dell'Osservatorio 5, I–35122 Padova, Italy

[3] *Dipartimento di Fisica* Galileo Galilei, *Universita' di Padova*
via Marzolo 8, I–35131 Padova, Italy

– Physical Review Letters, 61, 267 (1988) –

– Physical Review Letters, 61, 2627 (1988) –

Peak Number Density of Non-Gaussian Random Fields

Paolo Catelan, Francesco Lucchin, and Sabino Matarrese
Department of Physics "Galileo Galilei," University of Padova, I-35131 Padova, Italy
(Received 28 March 1988)

Asymptotic expressions are derived for the mean up-crossing rate, size, and number density of excursions above a high level by a stationary, non-Gaussian, random field in D dimensions. These formulas are relevant in the analysis of the large-scale matter distribution in the Universe.

PACS numbers: 98.60.Km, 05.40.+j

Much work has been devoted in recent years to the study of the cosmological implications of the statistics of "peaks" of a mass-density fluctuation field $\epsilon(\mathbf{x})=\rho(\mathbf{x})/\langle\rho\rangle-1$. These peaks correspond to local maxima of the random field where the latter exceeds its rms fluctuation σ by some factor ν. For large values of ν a statistical correspondence between local maxima and excursions of $\epsilon(\mathbf{x})$ above the $\nu\sigma$ threshold is expected; in such a case it is possible to restrict the study to these level excursions whose statistical description is simpler.[1-4]

This analysis was mainly limited to Gaussian fluctuations, both because of their simplicity and because, from a cosmological point of view, they typically arise during an inflationary expansion in the early Universe (see, e.g., Brandenberger[5]). In this framework the research followed along three main directions: (i) the calculation of spatial correlation functions, density profiles, and number densities of cosmic structures in the biased-galaxy-formation picture where the proto-objects are assumed to arise around the high peaks of the primordial density field[6]; (ii) the obtaining of the mass multiplicity of galaxies, groups, and clusters which originate, in a hierarchical scenario, from the turning around of lumps whose density exceeds some critical level[7]; and (iii) the analysis of the statistics of hot and cold spots in the surface brightness of the cosmic background radiation.[8]

Non-Gaussian-distributed primordial perturbations are, however, sometimes assumed to give rise to peculiar features in the large-scale structure of the Universe[9,10]: It seems in fact hard to reconcile the random-phase hypothesis with the observation of huge voids, bubblelike structures, long filaments, and large-scale streaming velocities in the galaxy distribution (see, e.g., Dekel,[11] and references therein). On the other hand, one would certainly have to deal with non-Gaussian statistics if the processes leading to protogalaxies were triggered by nongravitational mechanisms, such as the formation of a cosmic-string network[12] or the percolation of primordial explosions.[13,14] Moreover, the late nonlinear effect of the gravitational instability would in any case modify the initial statistics of the density field.[15] Finally, recent analyses of the inflationary scenario have shown that the "random-phase paradigm" is by no means mandatory: One could, in fact, imagine realistic models of inflation where non-Gaussian, scale-invariant, either adiabatic[16] or isocurvature,[17] fluctuations originate.

The role of the non-Gaussian statistics has been recently considered to analyze the clustering of density peaks in the biased-galaxy-formation theory[10,18] and to obtain the mass function of groups and clusters in the hierarchical, bottom-up scenario.[19] The two-dimensional statistics of rare events in the brightness of the microwave sky has been worked out for some non-Gaussian probabilities.[20] There have been attempts to test the random-phase hypothesis against the topology of the large-scale matter distribution also.[21]

The purpose of this Letter is to derive a number of average quantities which are essential for a full statistical description of level excursions of non-Gaussian processes. The literature on the subject is rather limited and only refers to quite peculiar statistics, such as χ^2, log-normal, and Rayleigh distribution,[1,20] all somehow related to the normal distribution. Our main results consist in asymptotic expressions for the mean up-crossing rate above a high level [Eq. (9)], the mean size of excursion regions [Eqs. (10) and (11)], and their number density [Eq. (12)] in terms of the cumulant generating function and of the mean square derivative of the process. To work out these results we took advantage of the path-integral technique (see, e.g., Raymond[22]) for it allows a straightforward evaluation of quantities involving derivatives of the random field. Functional methods have been recently applied in this context in both the Gaussian[23] and non-Gaussian cases.[10] Following a method originally due to Rice,[3] we obtain the statistics of the field's level excursions along a line and then we generalize to the full D-dimensional context (according to the prescriptions given by Vanmarcke[2]).

Since the problem we are considering is of general interest, we extend the analysis to a generic homogeneous and isotropic ("stationary") random field $\epsilon(\mathbf{x})$ in D dimensions. This is assumed to have zero mean and probability distribution specified by the functional $\mathcal{P}[\epsilon(\mathbf{x})]$. As we aim to describe the field on scales larger than a certain size R (in our case the typical size of a given proto-object) we convolute it with a low-pass filter W_R: $\epsilon_R(\mathbf{x})=\int d^D y\, W_R(|\mathbf{x}-\mathbf{y}|)\epsilon(\mathbf{y})$; this procedure also provides an "ultraviolet" cutoff. The variance of the

smoothed field,

$$\sigma^2(R)\equiv\int[\mathcal{D}\epsilon(\mathbf{x})]\mathcal{P}[\epsilon(\mathbf{x})]\epsilon_R^2(\mathbf{x}),$$

is the $l=0$ case of the spectral moments

$$\sigma_{(l)}^2(R)=\frac{2^{1-D}}{\pi^{D/2}\Gamma(D/2)}\int_0^\infty dk\,k^{D+2l-1}P(k)W_R^2(k). \tag{1}$$

Here $P(k)$ is the power spectrum (the Fourier transform of the two-point function), while $W_R(k)$ is the window function in momentum space. The joint probability that at $\mathbf{x}$ the field attains a value in the range $[\alpha,\alpha+d\alpha]$ and its ith directional derivative $\partial_i\epsilon_R(\mathbf{x})\equiv\partial\epsilon_R(\mathbf{x})/\partial x_i$ a value in the range $[\beta_i,\beta_i+d\beta_i]$ reads

$$P_{\epsilon\partial\epsilon}(\alpha,\beta_i)d\alpha\,d\beta_i=\int[\mathcal{D}\epsilon(\mathbf{x})]\mathcal{P}[\epsilon(\mathbf{x})]\delta(\epsilon_R(\mathbf{x})-\alpha)\delta(\partial_i\epsilon_R(\mathbf{x})-\beta_i)d\alpha\,d\beta_i. \tag{2}$$

Because of homogeneity and isotropy, this quantity depends neither on place nor on direction. [We shall therefore drop the label (i).] Given $P_{\epsilon\partial\epsilon}$ we can evaluate the mean rate of crossing $f_\nu=\int_{-\infty}^{\infty}d\beta\,|\beta|P_{\epsilon\partial\epsilon}(\nu\sigma,\beta)$ of the $\nu\sigma$ level along a line by the random process (more precisely by the one-dimensional process obtained by keeping all but one of the field's coordinates fixed). Isotropy demands that $P_{\epsilon\partial\epsilon}$ only depends on even powers of $\partial\epsilon_R$: We have symmetry with respect to inversion of the slope $\beta\to-\beta$ and $f_\nu=2\int_0^\infty d\beta\,\beta P_{\epsilon\partial\epsilon}(\nu\sigma,\beta)$. The mean up- and down-crossing rates are simply $f_{>\nu}=f_{<\nu}=f_\nu/2$; thus

$$f_{>\nu}=\int_0^\infty d\beta\,\beta\int[\mathcal{D}\epsilon(\mathbf{x})]\mathcal{P}[\epsilon(\mathbf{x})]\delta(\epsilon_R(\mathbf{x})-\nu\sigma)\delta(\partial\epsilon_R(\mathbf{x})-\beta). \tag{3}$$

Let us denote the mean length of stay above and below the level by $l_{>\nu}$ and $l_{<\nu}$, respectively. According to the theory of recurrent events[2] the mean separation between two successive up-crossings is given by $l_{>\nu}+l_{<\nu}=1/f_{>\nu}$ and the fractional length above the threshold becomes $l_{>\nu}/(l_{>\nu}+l_{<\nu})=P_{>\nu}$. The complementary cumulative distribution function $P_{>\nu}=\int[\mathcal{D}\epsilon(\mathbf{x})]\mathcal{P}[\epsilon(\mathbf{x})]\theta(\epsilon_R(\mathbf{x})-\nu\sigma)$ yields the probability that the stochastic process exceeds the threshold in a randomly chosen point or the fraction of D-dimensional space where this condition holds. One then finds $l_{>\nu}=P_{>\nu}/f_{>\nu}$.

To perform the functional integration in (2) we use the integral representation of the δ function $\delta(t)=(1/2\pi)\times\int_{-\infty}^{\infty}d\lambda\exp(i\lambda t)$ and the definition of the partition function

$$Z[J]\equiv\int[\mathcal{D}\epsilon(\mathbf{y})]\mathcal{P}[\epsilon(\mathbf{y})]\exp\left[\int d^Dy\,J(\mathbf{y})\epsilon(\mathbf{y})\right],$$

where the "external source" J is an arbitrary function. Note that $Z[0]=1$, corresponding to the probability normalization. With the specific choice $\tilde{J}(\mathbf{y})\equiv i(\lambda+\mu\,\partial/\partial x_i)W_R(|\mathbf{x}-\mathbf{y}|)|_{\mathbf{x}=0}$ we can write the joint probability as

$$P_{\epsilon\partial\epsilon}(\alpha,\beta)=(2\pi)^{-2}\int_{-\infty}^{\infty}d\lambda\,d\mu\,e^{-i(\lambda\alpha+\mu\beta)}Z[\tilde{J}].$$

Recalling the expansion of $\ln Z$ in connected correlation functions $\xi_n(\mathbf{x}_1,\ldots,\mathbf{x}_n)$ we obtain

$$\ln Z[\tilde{J}]=\sum_{n=2}^{\infty}\frac{i^n}{n!}\sum_{j=0}^{[n/2]}\binom{n}{2j}\lambda^{n-2j}\mu^{2j}\xi_{n/2j}(R) \tag{4}$$

($[n/2]\equiv n/2$ if n is even or $(n-1)/2$ if n is odd), where

$$\xi_{n|0}(R)\equiv\xi_n(R)\equiv\int\left[\prod_{a=1}^{n}d^Dy_a\,W_R(|\mathbf{y}_a|)\right]\xi_n(\mathbf{y}_1,\ldots,\mathbf{y}_n), \tag{5}$$

are the cumulants of the smoothed field, and, for $j\geq1$,

$$\xi_{n|2j}(R)\equiv\int\left[\prod_{a=1}^{n-2j}d^Dy_a\,W_R(|\mathbf{y}_a|)\right]\left[\prod_{b=n-2j+1}^{n}d^Dy_b\,\partial_iW_R(|\mathbf{x}-\mathbf{y}_b|)|_{\mathbf{x}=0}\right]\xi_n(\mathbf{y}_1,\ldots,\mathbf{y}_n). \tag{6}$$

Note that isotropy implies $\xi_{2|2}(R)=\sigma_{(1)}(R)/D$. It is common to introduce the (normalized) mean square derivative $\langle k^2\rangle/D\equiv(\sigma_{(1)}/\sigma)^2/D$. Using the "integration by parts" relation of path integrals we get

$$f_{>\nu}=\frac{1}{2\pi}\left(\frac{\langle k^2\rangle}{D}\right)^{1/2}\int_0^\infty d\beta\,\beta\exp\left[\sum_{n=2}^{\infty}\frac{(-1)^n}{n!}\sum_{j=0}^{[n/2]}\binom{n}{2j}w_{n|2j}\left(\frac{\partial}{\partial\nu}\right)^{n-2j}\left(\frac{\partial}{\partial\beta}\right)^{2j}\right]\exp[-\tfrac{1}{2}(\nu^2+\beta^2)], \tag{7}$$

where $w_{2|2j}\equiv 0$ and $w_{n|2j}\equiv D^j\xi_{n|2j}/\sigma^{n-2j}\sigma_{(1)}^{2j}$ for $n>2$. From the cluster expansion (see, e.g., Ma[24]) and the multinomial theory we get

$$f_{>\nu}=\left(\frac{\langle k^2\rangle}{D}\right)^{1/2}\sum_{M=0}^{\infty}\sum_{\{m_M\}}\left\{\prod_{n=1}^{M}\prod_{j=0}^{[n/2]}\frac{1}{m_{n,j}!}\left[\binom{n}{2j}\frac{w_{n|2j}}{n!}\right]^{m_{n,j}}\right\}a_{M,\mu}(\nu/\sqrt{2}), \tag{8}$$

with

$$a_{M,\mu}=(2\pi)^{-1}2^{-M/2}e^{-\nu^2/2}H_{M-2\mu}(\nu/\sqrt{2})b_\mu,$$

$H_m(t)$ the Hermite polynomials, $b_0=1$, and $b_\mu=(-1)^\mu\times(2\mu)!/(2\mu-1)\mu!$ for $\mu\geq 1$. In Eq. (8) the set $\{m_M\}=m_1,\ldots,m_M$ is formed by all nonnegative integers satisfying $\sum_{n=1}^{M}nm_n=M$; the nonnegative integers $m_{n,j}$ are such that $\sum_{j=0}^{[n/2]}m_{n,j}=m_n$ and $\mu\equiv\sum_{n=1}^{M}\sum_{j=0}^{[n/2]}jm_{n,j}$. The $M=0$ term in the curly brackets of Eq. (8) is defined to be 1; terms reading 0^0 are also defined to be 1. For large values of ν we can use the approximation $H_m(t)\approx(2t)^m$. For each value of M in Eq. (8) the terms with $\mu\neq 0$ in the internal sum are suppressed by a factor $\nu^{-2\mu}$; thus, to leading order in ν, only the $\mu=0$ terms survive. We then get the expression

$$f_{>\nu}\approx\frac{1}{2\pi}\left(\frac{\langle k^2\rangle}{D}\right)^{1/2}\exp[-\nu^2+\mathcal{H}(\nu/\sigma)], \tag{9}$$

where $\mathcal{H}(\phi)=\sum_{n=2}^{\infty}\phi^n\xi_n(R)/n!$ is the cumulant generating function which is defined as $\ln Z[J_\phi]$, with $J_\phi(y)=\phi W_R(|y|)$. To obtain the mean excursion size we need an expression for $P_{>\nu}$. The calculation is similar and leads to (see, e.g., Ref. 19)

$$P_{>\nu}=\sum_{M=0}^{\infty}\sum_{\{m_M\}}\left[\prod_{n=1}^{M}\frac{(w_{n|0}/n!)^{m_n}}{m_n!}\right]a_M(\nu/\sqrt{2}),$$

with $a_0=\frac{1}{2}\operatorname{erfc}(\nu/\sqrt{2})$, erfc the complementary error function, and

$$a_M=\pi^{-1/2}2^{-M/2}e^{-\nu^2/2}H_{M-1}(\nu/\sqrt{2})$$

for $M\geq 1$. To leading order in ν one gets

$$a_M\approx(2\pi)^{-1/2}\nu^{M-1}\exp(-\nu^2/2)$$

and

$$P_{>\nu}\approx(2\pi\nu^2)^{-1/2}\exp[-\nu^2+\mathcal{H}(\nu/\sigma)].$$

Combining these results, we arrive at the expression

$$l_{>\nu}\approx(\langle k^2\rangle/2\pi D)^{-1/2}\nu^{-1}. \tag{10}$$

At high threshold the mean excursion size is independent of the functional form of the statistics.

It is conjectured[2] that the expected volume $V_{>\nu}$ of isolated domains of excursion above a high level ν can be obtained as the Dth power of the mean length $l_{>\nu}$, provided that the derivatives of the field along orthogonal directions are uncorrelated. This procedure is usually applied to Gaussian random fields, where the lack of correlation implies independence; in our case the derivatives are still uncorrelated because of isotropy but they can be nonindependent: For instance, a term like $\langle(\partial_i\epsilon\,\partial_j\epsilon)^2\rangle$ with $i\neq j$ is not *a priori* required to vanish. However, the very fact that expression (10) depends on derivatives through $\sigma_{(1)}$ shows that the details of the statistics are substantially ineffective at high threshold. One can then infer that $l_{>\nu}^{D}$ provides, in the general case, a fair estimate of $V_{>\nu}$, becoming exact as $\nu\rightarrow\infty$. We have

$$V_{>\nu}\approx(\langle k^2\rangle/2\pi D)^{-D/2}\nu^{-D}. \tag{11}$$

The mean number density of excursion regions $n_{>\nu}$ is finally obtained by the division of the probability of exceeding the level by the mean up-crossing volume:

$$n_{>\nu}\approx(2\pi)^{-1/2}\left(\frac{\langle k^2\rangle}{2\pi D}\right)^{D/2}\nu^{D-1}\exp[-\nu^2+\mathcal{H}(\nu/\sigma)]. \tag{12}$$

At high threshold each excursion region is expected to contain a single local maximum above $\nu\sigma$ but no minima nor saddle points; in this limit expression (12) also yields the number density of maxima and the density of the Euler characteristic of the $(D-1)$-dimensional surfaces $\delta(\epsilon_R(\mathbf{x})-\nu\sigma(R))$. Equation (12) complements the results on the N-point peak correlation functions of a non-Gaussian random field derived in Ref. 10. The asymptotic formulas for the normal distribution (see, e.g., Ref. 1) are recovered if $\mathcal{H}(\nu/\sigma)=\nu^2/2$ is replaced in Eqs. (9) and (12). All our expressions hold at high ν as asymptotic expressions and give an insight into the statistics of peaks in the most general, non-Gaussian case.

[1]R. J. Adler, *The Geometry of Random Fields* (Wiley, New York, 1981).

[2]E. H. Vanmarcke, *Random Fields, Analysis and Synthesis* (MIT Press, Cambridge, MA, 1983).

[3]S. O. Rice, Bell Syst. Tech. J. **23**, 282 (1944), and **24**, 41 (1945).

[4]M. S. Longuet-Higgins, Philos. Trans. Roy. Soc. London A **249**, 321 (1957); Yu. K. Belyaev and V. P. Nosko, Theory Probab. Its Appl. **14**, 296 (1969).

[5]R. H. Brandenberger, Rev. Mod. Phys. **57**, 1 (1985).

[6]A. G. Doroshkevich, Astrophysics **6**, 320 (1970); N. Kaiser, Astrophys. J. **284**, L9 (1984); H. D. Politzer and M. B. Wise, Astrophys. J. **285**, L1 (1984); J. A. Peacock and A. F. Heavens, Mon. Not. Roy. Astron. Soc. **217**, 805 (1985); J. M. Bardeen, J. R. Bond, N. Kaiser, and A. S. Szalay, Astrophys.

J. **304**, 15 (1986); L. G. Jensen and A. S. Szalay, Astrophys. J. **305**, L5 (1986); P. Coles, Mon. Not. Roy. Astron. Soc. **222**, 9p (1986); H. M. P. Couchman, Mon. Not. Roy. Astron. Soc. **225**, 777 (1987); E. Martínez-González and J. L. Sanz, Astrophys. J. **324**, 653 (1988).

[7]W. H. Press and P. Schechter, Astrophys. J. **187**, 125 (1974); R. Schaeffer and J. Silk, Astrophys. J. **292**, 319 (1985); Bardeen *et al.*, Ref. 6; J. L. Sanz and E. Martínez-González, Astrophys. J. (to be published).

[8]M. V. Sazhin, Mon. Not. Roy. Astron. Soc. **216**, 25 (1985); N. A. Zabotin and P. D. Nasel'skii, Astron. Zh. **62**, 1053 (1985) [Sov. Astron. **29**, 614 (1985)]; N. Vittorio and R. Juszkiewicz, Astrophys. J. **314**, L29 (1987); J. R. Bond and G. G. Efstathiou, Mon. Not. Roy. Astron. Soc. **226**, 655 (1987).

[9]P. J. E. Peebles, Astrophys. J. **274**, 1 (1983).

[10]B. Grinstein and M. B. Wise, Astrophys. J. **310**, 19 (1986); S. Matarrese, F. Lucchin, and S. A. Bonometto, Astrophys. J. **310**, L21 (1986).

[11]A. Dekel, in *Observational Cosmology*, edited by G. Burbidge and A. Hewitt (Reidel, Dordrecht, 1987).

[12]N. Turok, in *Nearly Normal Galaxies*, edited by S. Faber (Springer-Verlag, New York, 1986).

[13]S. Ikeuchi, Publ. Astron. Soc. Jpn. **33**, 211 (1981); J. R. Ostriker and L. L. Cowie, Astrophys. J. **243**, L127 (1981).

[14]T. Vicsek and A. S. Szalay, Phys. Rev. Lett. **58**, 2818 (1987).

[15]J. N. Fry, Astrophys. J. **279**, 499 (1984); M. H. Goroff, B. Grinstein, S.-J. Rey, and M. B. Wise, Astrophys. J. **311**, 6 (1986).

[16]A. Ortolan, F. Lucchin, and S. Matarrese, Phys. Rev. D **38**, 465 (1988).

[17]T. J. Allen, B. Grinstein, and M. B. Wise, Phys. Lett. B **197**, 66 (1987).

[18]J. N. Fry, Astrophys. J. **308**, L71 (1986); F. Lucchin, S. Matarrese, and N. Vittorio, Astrophys. J. (to be published).

[19]F. Lucchin and S. Matarrese, Astrophys. J. (to be published).

[20]P. Coles and J. D. Barrow, Mon. Not. Roy. Astron. Soc. **228**, 407 (1987).

[21]D. H. Weinberg, J. R. Gott, and A. L. Melott, Astrophys. J. **321**, 2 (1987).

[22]P. Ramond, *Field Theory, A Modern Primer* (Benjamin, Reading, 1981).

[23]Politzer and Wise, Ref. 6; S. Otto, H. D. Politzer, and M. B. Wise, Phys. Rev. Lett. **56**, 1878 (1986); J. M. Cline, H. D. Politzer, S.-Y. Rey, and M. B. Wise, Commun. Math. Phys. **112**, 217 (1987); E. Bertschinger, Astrophys. Lett. **323**, L103 (1987).

[24]S.-k. Ma, *Statistical Mechanics* (World Scientific, Singapore, 1985).

Comment on "Peak Number Density of Non-Gaussian Random Fields"

The paper of Catelan, Lucchin, and Matarrese[1] contains some interesting results which serve to extend the work we have done[2] on the statistical properties of non-Gaussian random fields. The authors give asymptotic expressions for the mean size of excursions of the field above some level whereas we obtained exact results for some specific distributions related at some level to the Gaussian.

One important comment must be made, however, concerning the statement the authors make after Eq. (10) that the behavior of the mean excursion size is *independent* of the functional form of the statistics in the limit $\nu \rightarrow \infty$. In Ref. 2, we obtained exact results for one particular random field (which we called Gumbel-1) where the mean excursion size clearly does not obey the relation (10). In fact, the mean excursion size drops exponentially as $\nu \rightarrow \infty$ for this random field. There is therefore (at least) one clear counterexample to the authors' assertion.

The question thus arises as to why Eq. (10) does not hold in this case. A careful look at the proof of (10) reveals that it is necessary to make a number of assumptions about the underlying statistics in order to derive the equation. In particular, it is necessary to assume that the mean square derivative of the process is finite. In the authors' notation this requires that $\int\int P_{\epsilon\partial\epsilon}(\alpha,\beta)\beta^2 d\alpha\, d\beta$ is finite. It is possible to construct many well-defined joint probability distributions for which this will not be true (including our example of the Gumbel-1 distribution). In fact for some distributions, such as the Cauchy distribution, no moments exist at all. It is clear therefore that the above-mentioned moment conditions play an important role in determining the limiting behavior of the mean excursion size. Whenever these conditions are obeyed, we expect that Eq. (10) and the results following it will hold, but it is important to point out that such conditions do place substantial limitations on the validity of these results.

P. Coles
Astronomy Centre
University of Sussex
Brighton BN1 9QH
United Kingdom

Received 1 August 1988
PACS numbers: 98.60.Km, 05.40.+j

[1]P. Catelan, F. Lucchin, and S. Matarrese, Phys. Rev. Lett. **61**, 267 (1988).
[2]P. Coles and J. D. Barrow, Mon. Not. Roy. Astron. Soc. **228**, 407 (1987).

Catelan, Lucchin, and Matarrese reply: In the Comment by Coles[1] the asymptotic behavior of the mean excursion size $l_{>\nu}$ of a non-Gaussian random field is considered. We agree that the validity of Eq. (10) in Ref. 2 requires a number of conditions which certain statistics may fail to satisfy. This is a general property of asymptotic expressions, such as those derived in Ref. 3 for the complementary cumulative distribution function $P_{>\nu}$ and the N-point correlation functions of excursion regions $\xi^{(N)}_{>\nu}$. This point has been discussed in Ref. 4 where it was shown that a necessary condition for the validity of the formula $P_{>\nu} \approx (2\pi\nu^2)^{-1/2}\exp[-\nu^2+\mathcal{H}(\nu/\sigma)]$ is that the cumulant generating function $\mathcal{H}$ is an entire function of its argument.

On the other hand, we believe that the independence of $l_{>\nu}$ of the functional form of the statistics in the high-ν limit [Eq. (10) in Ref. 2] plays an important role in the evaluation of the mean number density of peaks $n_{>\nu}$. This can be seen as follows. We apply directly the definition (see, e.g., Ref. 5)

$$n_{>\nu} = \int_{\mathcal{D}} d\omega (-1)^D \det\omega \int [\mathcal{D}\epsilon(\mathbf{x})]\mathcal{P}[\epsilon(\mathbf{x})]\theta(\epsilon_R(\mathbf{x})-\nu\sigma)\delta^{(D)}(\partial_i\epsilon_R(\mathbf{x}))\delta^{[D(D+1)/2]}(\partial_i\partial_j\epsilon_R(\mathbf{x})-\omega_{ij}), \quad (1)$$

where $d\omega = \prod_{i\le j} d\omega_{ij}$, with $i,j = 1,\ldots,D$ and the region of integration $\mathcal{D}$ is over all negative-definite symmetric matrices ω. A tedious but straightforward calculation yields

$$n_{>\nu} = \int_{\mathcal{D}} d\omega (-1)^D \det\omega \int_{\nu\sigma}^{\infty} da_1 \int_{-\infty}^{\infty} d^{\Delta}\varphi \exp\left(-i\sum_{l=1}^{\Delta}\varphi_l a_l\right) \exp\left(\sum_{n=2}^{\infty}\frac{i^n}{n!}\sum_{\{l_n\}=1}^{\Delta}\varphi_{l_1}\cdots\varphi_{l_n}\xi_{l_1\cdots l_n}\right), \quad (2)$$

where $a_l \equiv (a_1, 0, \omega_{ij})$, $l = 1,\ldots,\Delta$, with $\Delta = 1 + D + D(D+1)/2$, and

$$\xi_{l_1\cdots l_n} \equiv \int \left[\prod_{a=1}^{n} d^D x_a W_{l_a}(|\mathbf{x}_a|)\right] \xi_n(\mathbf{x}_1,\ldots,\mathbf{x}_n), \quad (3)$$

with $W_l \equiv (W_R, \partial_i W_R, \partial_i\partial_j W_R)$. A number of spatial properties of the distribution appear in Eq. (2) through the correlation functions $\xi_{l_1\cdots l_n}$. Our derivation of the asymptotic relation for $n_{>\nu}$ [Eq. (12) in Ref. 2] corresponds to neglecting many terms in Eq. (2), especially those where partial derivatives of ϵ_R along orthogonal directions appear, which can be shown to be subleading at high ν. It seems unlikely that the quantity $P_{>\nu}/l^D_{>\nu}$ could provide a reliable estimate of the mean number of density peaks[6,7] when this "reduction property" does not apply.

Paolo Catelan, Francesco Lucchin, and Sabino Matarrese
Dipartimento di Fisica "Galileo Galilei"
Universitá di Padova, via Marzolo 8
I-35131 Padova, Italy

Received 12 September 1988
PACS numbers: 98.60.Km, 05.40.+j

[1]P. Coles, preceding Comment [Phys. Rev. Lett. **61**, 2626 (1988)].
[2]P. Catelan, F. Lucchin, and S. Matarrese, Phys. Rev. Lett. **61**, 267 (1988).
[3]S. Matarrese, F. Lucchin, and S. A. Bonometto, Astrophys. J. **310**, L21 (1986); B. Grinstein and M. B. Wise, Astrophys. J. **310**, 19 (1986).
[4]F. Lucchin and S. Matarrese, Astrophys. J. **330**, 535 (1988).
[5]J. M. Cline, H. D. Politzer, S.-Y. Rey, and M. B. Wise, Commun. Math. Phys. **112**, 217 (1987).
[6]E. H. Vanmarcke, *Random Fields, Analysis and Synthesis* (MIT Press, Cambridge, MA, 1983).
[7]P. Coles and J. D. Barrow, Mon. Not. Roy. Astron. Soc. **228**, 407 (1987).

APPENDIX D

Evidence for Low Ω_o Universe

The QDOT and Cluster Dipoles: Evidence for a low Ω_o Universe?

Manolis PLIONIS [1], Peter COLES [2] & Paolo CATELAN [1]

[1] *SISSA - International School for Advanced Studies,*
Strada Costiera 11, 34014 Trieste, Italy

[2] *Astronomy Unit, School of Mathematical Sciences*
Queen Mary & Westfield College, Mile End Road
London E1 4NS, UK

– Mon. Not. R. Astron. Soc. 262, 465 (1993) –

Summary

We have reanalysed the QDOT survey in order to investigate the convergence properties of the estimated dipole and the consequent reliability of the derived value of $\Omega_o^{0.6}/b$. We find that there is no compelling evidence that the QDOT dipole has converged within the limits of reliable determination and completeness. Therefore the value of Ω_o derived by Rowan-Robinson *et al.* (1990) should be considered only as an upper limit. Furthermore, we find strong evidence that the shell between 140 and 160 h^{-1} Mpc does contribute significantly to the total dipole anisotropy and therefore to the motion of the Local Group with respect to the Cosmic Microwave Background. This shell contains the Shapley concentration, but we argue that this concentration itself cannot explain all the gravitational acceleration produced by it; there must exist a coherent anisotropy which includes this structure, but extends greatly beyond it. With the QDOT data alone, we cannot determine precisely the magnitude of any such anisotropy but any contribution to the Local Group motion from large scales would favour a value of $\Omega_o^{0.6}/b_{IRAS} \leq 0.6$, smaller than previous extimates based on IRAS galaxies; such a result would be consistent with the dipole measured from samples of rich clusters, which are much more complete at large depths.

Key Words: Galaxies: clustering – Infrared: Galaxies – large-scale Structure of the Universe.

D.1 Introduction

Assuming that gravitational instability is the cause of the observed peculiar motions, then the local deviations from a uniform Hubble flow provides a powerfull tool to study the *local* mass distribution and therefore to estimate the cosmological density parameter, Ω_o.

Using linear perturbation theory (Peebles 1980), the peculiar velocity can be related to the peculiar acceleration via $\underline{v} \propto f(\Omega_o)\underline{g}$. The local peculiar velocity ($\underline{v}$) has been determined, to great accuracy, from the dipole anisotropy of the Cosmic Microwave Background Radiation (CMB), which implies a Local Group (LG) motion of $\sim$ 600 km/sec towards $l \approx 270°$ and $b \approx 30°$ (Smoot *et al.* 1991 and references therein), while the peculiar acceleration is usually estimated from the dipole moment of the galaxy (or other mass tracer) distribution. To use linear theory one explicitly assumes that the motion of the LG is determined from large scales where non-linear effects can be ignored. It is also necessary to assume that the extragalactic objects, used to determine the peculiar acceleration, trace the underlying mass fluctuations. The latter assumption, however, can be directly tested from the data since the determined peculiar acceleration should be parallel to the peculiar velocity. Note, however, that if the extragalactic objects are *biased* tracers of the mass distribution (Kaiser 1984; Dekel & Rees 1987) then the picture becomes somewhat more complicated. If a simple phenomenonological model for the bias is adopted, in which $(\delta\rho/\rho)_g = b(\delta\rho/\rho)_m$, then the dipole moment test constrains a combination of b and Ω_o, namely $\Omega_o^{0.6}/b$ (see Section D.2 below). To deduce the value of Ω_o one therefore needs to know the value of b so the result is rather model-dependent even for this simple biasing scheme. In more complicated (i.e. more realistic) biasing schemes (e.g. Dekel & Rees 1987; Babul & White 1991; Bower *et al.* 1992) there might be no simple local relationship between galaxy numbers and mass density, making it even more difficult to relate galaxy velocities to density perturbations.

We should therefore state at the outset that the weakest link in the chain of reasoning that leads from velocity information to a value of Ω_0 lies in the choice of model for the bias.

Furthermore, it is very important to note that this test can be applied with success only if the galaxy (or other mass tracer) dipole has converged to its *final* value within the limits of the catalogue used. That is to say that the apparent convergence must not be dictated by insufficient sampling of depths from which contributions to the LG acceleration could be significant. Since most catalogues of extragalactic objects are either magnitude/flux or diameter limited there is a significant possibility of this happening. The alignment of the galaxy dipole with the CMB dipole direction and an apparent plateau of the cumulative dipole over some scales should not *a priori* be considered as evidence for the convergence of the acceleration to its final value because it could well be that:

- The structure producing the LG peculiar motion could be very extended and thus the alignment found within a small (inner) volume could just result from the fact that the galaxy catalogue traces only part of a coherent anisotropy which is larger than the sample can probe.

- Beyond an apparent plateau (which in most recent studies coincides with the characteristic depth of the sample !) there could be a further contribution to the dipole. In fact this actually seems to happen in the case of the cluster dipole; see Plionis & Valdarnini (1991) (hereafter PV91); Scaramella *et al.* (1991), hereafter SVZ. There is no *a priori* reason why the acceleration should grow continuously with depth up to its final value.

Up to now various populations of extragalactic objects have been used to estimate the peculiar acceleration induced on the LG: optical galaxies (Lahav 1987; Plionis 1988), IRAS galaxies (Yahil, Walker & Rowan-Robinson 1986; Meiksin & Davis 1986; Villumsen & Strauss 1987; Strauss and Davis 1988 and references therein; Rowan-Robinson *et al.* 1990, hereafter RR90), X-ray clusters (Lahav *et al.* 1989), X-ray AGNs (Miyaji and Boldt 1990) and Abell clusters (Plionis & Valdarnini 1991; Scaramella *et al.* 1991). Lahav *et al.* (1988)

and Lynden-Bell *et al.* (1989) found that the optical and IRAS dipole (using samples with characteristic depths of $\sim 60\ h^{-1}$ Mpc) are aligned with the CMB dipole and conclude that the source of the LG motion is within $\sim 40\ h^{-1}$ Mpc. However, RR90 using the deeper 0.6 Jy IRAS survey with a characteristic depth of $\sim 120\ h^{-1}$ Mpc, find that the dipole continues growing up to $\sim 100\ h^{-1}$ Mpc and flattens thereafter while it is also roughly aligned with the CMB dipole. Furthermore, PV91 and SVZ find that the dipole, as traced by Abell clusters, builds up in the same way as that of the optical galaxies (although it misses the local $< 25\ h^{-1}$ Mpc contributions) but has a further dipole contribution from depths $> 120 - 150\ h^{-1}$ Mpc, while it is aligned with the CMB dipole direction to within only $\sim 5° - 10°$. PV91 have shown that the cluster dipole, estimated in independent equal-volume shells of $\delta V \sim 4 \times 10^6\ h^{-3}$ Mpc^3 out to $160h^{-1}$ Mpc, is roughly aligned in each shell with the CMB dipole direction which provides evidence for a *coherent* anisotropy over a scale-length (diameter) of $\sim 300\ h^{-1}$ Mpc. To ignore the gravitational pull caused by such large correlated structure by assuming the dipole converges at a much smaller depth than $160h^{-1}$ Mpc, would lead to a large overestimate of the value of Ω_o.

Under the crucial assumption that the optical (ESO+UGC) and IRAS galaxy distributions contain the source of the LG motion then the amplitude of the optical and IRAS dipoles suggest that $\Omega_o \sim 1$ with $b_{op} \sim 2$ and $b_{IRAS} \sim 1.3$ (but bear in mind the comments above about the simplicity of the bias model adopted in these calculations). However, the value of Ω_o is sensitive to contributions to the dipole from depths beyond the scales sampled by the optical and IRAS catalogues and such contributions can significantly lower its value. In fact, the rich cluster samples, which probe much greater depths than those of galaxies, have led to a much smaller inferred value of $\Omega_o < 0.3$ if the bias factor for galaxies lies in its usual range of 1.6 to 2.5 (PV91; SVZ).

The question of convergence of the dipole has been addressed by other authors (Juszkiewicz, Vittorio & Wyse 1990; Lahav, Kaiser & Hoffman 1990; Strauss *et al.* 1992). These studies have, however, concentrated upon a model-dependent view of the problem; that is to say, given a particular model of clustering – such as CDM – at what depth can one

expect the dipole to converge? Or, put another way, how large a sample volume is required to contain the entire source of the Local Group motion in a CDM Universe? Although these are undoubtedly interesting questions to ask, it is in our view better to keep the analyses as data-oriented (rather than model-oriented) as possible. We would prefer to ask the question whether there is any evidence, given the data on galaxy clustering and minimal assumptions about models of structure, whether the dipole has converged within the depths probed by relevant galaxy and cluster samples. With this point of view in mind, we decided to reanalyse the IRAS galaxy dipole inferred from the QDOT survey, and compare the results obtained with the dipole inferred from the distribution of rich clusters. The main questions we shall ask are (i) Out to what depth is the sampling density of the QDOT survey sufficient to allow a reliable determination of the dipole? (ii) Is there any evidence for a significant contribution to the dipole from scales larger than $\sim 100h^{-1}$ Mpc that would make the QDOT analysis consistent with the results mentioned above obtained from samples of rich clusters?

The layout of the paper is as follows: in Section D.2 we review briefly the method we use for estimating dipoles and relating the result to Ω_o; in Section D.3 we give some details of the QDOT survey catalogue and apply our dipole method to it; in Section D.4 we discuss the results in the light of other observations; we state the main conclusions in Section D.5.

D.2 Dipole Calculations

The multipole components of the galaxy (or other extragalactic mass tracer) distribution are calculated by summing moments. The monopole and dipole moments are:

$$M = \frac{1}{4\pi}\sum_{i=1}^{n}\frac{1}{\phi(r_i)}\frac{1}{r_i^2} \;=\; \frac{1}{4\pi}H_\circ^2\mu \tag{D.1}$$

$$\underline{D} = \frac{3}{4\pi}\sum_{i=1}^{n}\frac{1}{\phi(r_i)}\frac{\underline{r}_i}{r_i^2} \;=\; \frac{3}{4\pi}H_\circ^2\underline{\gamma}\,, \tag{D.2}$$

where

$$\phi(r_i) = \int_{L_{min}(r_i)}^{L_{max}}\Phi(L)dL \tag{D.3}$$

is a selection function to take into account the fact that at different distances we sample different portions of the luminosity function. $L_{min}(r)$ is the luminosity of a source with the limiting flux-density at a comoving distance r, estimated by:

$$r = \frac{cD_L(z)}{H_\circ(1+z)}\,, \tag{D.4}$$

with $D_L(z)$ the luminosity distance, $D_L(z) = q_\circ^{-2}\left[q_\circ z + (q_\circ - 1)[(1+2q_\circ z)^{1/2} - 1]\right]$. Throughout this paper we use $q_\circ = 0.2$. Different values of $q_\circ$ affect the distances only by a small fraction. Note that although in our notation the monopole and dipole moments depend on the value of the Hubble parameter, their ratio does not. Furthermore, it has been shown (PV91), that the relative uncertainties in D/M are significantly smaller than in D, due to the fact that errors have a similar effect on the values of D and M and therefore cancel out in their ratio.

The relatively small size of flux, magnitude or diameter limited galaxy samples, especially at large distances, can introduce a net 'discretness' dipole and large shot noise errors. The shot-noise (discreteness) dipole can be estimated for a uniform population, sampled by N objects each having a weight w_i, by:

$$\langle\underline{\gamma}\cdot\underline{\gamma}\rangle^{\frac{1}{2}} = N^{\frac{1}{2}}\langle w^2\rangle^{\frac{1}{2}} \tag{D.5}$$

where $w_i = \phi(r_i)^{-1}\, r_i^{-2}$ and the corresponding shot noise dipole to monopole ratio is $\sigma_{D/M} \simeq 3\,\langle w^2\rangle^{\frac{1}{2}}/N^{\frac{1}{2}}\langle w\rangle$. Although this calculation gives an indication of the order-of-magnitude of

the dipole induced by shot-noise effects, it is not accurate for realistic data sets because of the non-uniform nature of the sampling. In order to compute the discreteness dipole and corresponding shot-noise errors in this paper, we use Monte Carlo simulations as described below.

D.2.2 An Illustrative Model

A reliable determination of the dipole from galaxy samples can be used to determine the cosmological density parameter, Ω_o. We have discussed many examples of this type of analysis in the Introduction, so we shall not go into much detail here. Here, however, we wish to pay particular attention to the question of convergence of the dipole and consequent uncertainty in the value of Ω_o. Many authors (e.g. Juszkiewicz *et al.* 1990; Lahav *et al.* 1990; Strauss *et al.* 1992) have discussed how one might expect the dipole to converge given a particular model for the density field, such as CDM. We will take an alternative approach in asking if there is any evidence in the observational data itself that the dipole has either converged or not converged. We stress again that any determination of Ω_o is only reliable if the total gravitational acceleration of the local group is completely accounted for by structures contained entirely within the sample volume and the value of Ω_o obtained depends upon the depth at which the cumulative dipole converges to its final value. To show explicitly how this happens we hall apply the formalism introduced in Section D.2.1 to a simple illustrative model.

The gravitational acceleration induced at a point (e.g. the Local Group) by the surrounding density inhomogeneity is

$$\underline{g} = G \int \frac{\rho(\underline{r})\underline{r}}{r^3} d\underline{r} = \frac{4\pi G}{3} \underline{D} \qquad \text{(D.6)}$$

where $\rho(\underline{r})$ is the continuous mass density and $\underline{D}$ is the dipole moment (D.2) of a set of mass tracers. Using linear perturbation theory (Peebles 1980), we can relate the peculiar velocity of the LG, due to the combined gravitational field of all mass tracers, with the dipole moment

and the value of Ω_o, as follows. We must first assume that the gravitational acceleration has converged to its final value within the limits of the sample and that acceleration and velocity are aligned. We now need to model the density distribution $\rho(\underline{r})$ in (D.6), taking into account the distribution of the mass tracers that are used. To do this, we first expand the mass density in spherical harmonics:

$$\rho(\underline{r}) = \rho_o + \underline{\delta}(\underline{r}) \cdot \underline{r} + \ldots ,$$

The dipole vector, $\underline{\delta}(\underline{r})$, is the only term that contributes to the acceleration so this is the term we need to model. For an arbitrary mass distribution, the manner in which the dipole amplitude builds up as a function of depth can be very complicated, but, for illustration, and without loss of generality, we assume that the dipole builds up in two steps (as indicated by the cluster dipole in PV91 and SVZ):

$$\underline{\delta}(\underline{r}) = \underline{\delta}_1(\underline{r})\Theta(R_1 - r) + \underline{\delta}_2(\underline{r})\Theta(R_2 - r)\Theta(r - R_1) , \qquad (D.7)$$

where $\Theta(x)$ is the Heaviside step function; $\underline{\delta}_1(\underline{r})$ is the dipole due to the distribution of mass-tracers in the sphere $[0, R_1]$; $\underline{\delta}_2(\underline{r})$ is the contribution to the dipole from the shell $[R_1, R_2]$. Assuming for simplicity that $|\underline{\delta}_1(\underline{r})| = \delta_1$ (constant) for $r \leq R_1$, $|\underline{\delta}_2(\underline{r})| = \delta_2$ (constant) for $R_1 < r \leq R_2$ and $|\underline{\delta}(\underline{r})| = 0$ for $r > R_2$ and picking a convenient coordinate system, we can express the density $\rho(\underline{r})$ as:

$$\rho(\underline{r}) = \begin{cases} \rho_o + \delta_1 \cos\theta & r \in [0, R_1] \\ \rho_o + \delta_2(\cos\theta\cos\chi + \sin\theta\sin\phi\sin\chi) & r \in [R_1, R_2] \\ \rho_o & r > R_2 \end{cases} , \qquad (D.8)$$

where θ, ϕ are the usual angular coordinates and χ is the angle between δ_1 and δ_2. θ is also the angle from the CMB dipole direction. The gravitational acceleration is then:

$$|\underline{g}| = \frac{4}{3}\pi G\Omega_o\rho_c \left[\left(R_1 \frac{\delta\rho_1}{\rho_o} \right)^2 + \left(\Delta R \frac{\delta\rho_2}{\rho_o} \right)^2 + 2 \left(R_1 \frac{\delta\rho_1}{\rho_o} \right) \left(\Delta R \frac{\delta\rho_2}{\rho_o} \right) \cos\chi \right]^{1/2} , \qquad (D.9)$$

where ρ_c ($\equiv 3H_o^2/8\pi G$) is the critical density and $\Delta R = R_2 - R_1$.

If the mass tracer distribution (indicated with suffix t) is modelled in the same way as in Eq. (D.8), we can express the monopole and dipole terms of the spherical harmonic expansion as:

$$M(\leq z_2) = \frac{1}{4\pi}\int_0^{R_2} \rho_t(\underline{r})\frac{1}{r^2}d\underline{r} = R_2\,\rho_{ot}\ , \tag{D.10}$$

$$\begin{aligned} |\underline{D}(\leq z_2)| &= \left|\frac{3}{4\pi}\left[\int_0^{R_1}\rho_t(\underline{r})\frac{\underline{r}}{r^3}d\underline{r} + \int_{R_1}^{R_2}\rho_t(\underline{r})\frac{\underline{r}}{r^3}d\underline{r}\right]\right| \\ &= \left[(R_1\delta\rho_{1t})^2 + (\Delta R\,\delta\rho_{2t})^2 + 2\,(R_1\delta\rho_{1t})(\Delta R\,\delta\rho_{2t})\cos\chi\right]^{1/2}. \end{aligned} \tag{D.11}$$

Using the standard "linear" picture of *biassing*, ie., $(\delta\rho/\rho)_t = b(\delta\rho/\rho)$ it is straightforward to show that

$$|\underline{g}| = \frac{4\pi G R_2 \Omega_o \rho_c}{3b}\frac{|\underline{D}(\leq z_2)|}{M(\leq z_2)} \tag{D.12}$$

and the resulting relation between v_p and the dipole moment (expressed as the ratio of dipole over monopole M, which is independent of H_o) is:

$$\underline{v}_p = d_{conv}\,\frac{\Omega_o^{0.6}}{3\,b}\frac{|\underline{D}|}{M}(\leq d_{conv})\ , \tag{D.13}$$

where $\underline{v}_p$ is the LG velocity with respect to the cosmic microwave background radiation rest frame, $d_{conv} = cz_2 \approx R_2 H_o$ is the depth at which the dipole converges to its final value and b is the bias factor that relates galaxy to mass overdensities and which is defined in the introduction. The $\Omega_0^{0.6}$ factor comes in when one uses the theory of linear gravitational instability to relate the peculiar velocity to the gravitational acceleration (Peebles 1980).

D.2.3 Comments

Although that we have worked out Eq. (D.13) on the basis of a two-step model this result is valid whatever model one assumes for the dipole growth, as would be expected from the fact that gravity is a conservative force. (For example, Villumsen & Strauss (1987), Lahav *et al.* (1988) and Miyaji & Boldt (1990), have all used an even simpler one-step model to derive the same result.) Equation (D.13) therefore holds for *any* continuous distribution

$\delta(\underline{r})$ since we can approximate $\delta(\underline{r})$ at each point by an infinitesimal step. Morover it is valid whether $\delta(\underline{r})$ increases smoothly until it reaches its final value or whether, for example, it increases in finite steps with large plateau between them. We have chosen the two-step model for illustration because it shows explicitly how such a mass distribution could produce a dipole that apparently converges at a depth less than R_2 (which is, by contruction the depth at which the dipole actually converges). If one had a data set which samples space poorly in between R_1 and R_2, one might interpret the plateau as evidence for convergence and thus overestimate the value of Ω_o.

We shall not be attempting to fit this simple model to the data; it serves only as a warning that one must be convinced that the dipole has converged before attempting to infer a value of Ω_o.

RR90 estimated the dipole from the QDOT sample and derived a value of Ω_o using a slightly different formulation from ours. We choose our formulation to highlight the point that the value of Ω_o inferred depends crucially on the value of d_{conv}.

D.3 Application to the QDOT Survey

The QDOT data set is a sparse-sampled (one in six) redshift survey of the IRAS galaxies with $S \geq 0.6$ Jy at 60-μm. The original IRAS catalogue and the area exclusion mask are described in RR90. Due to *cirrus* emission near the galactic plane we limit our analysis to the $|b| > 10^\circ$ (as in the original work of RR90). To get an idea of the depths traced by the QDOT sample we present in Figure D1 the space-density of QDOT galaxies evaluated in equal volume shells with $\delta V \simeq 1.2 \times 10^6\ h^{-3}$ Mpc^3. As expected from the fact that the IRAS galaxy sample is flux-limited, the galaxy space-density is a steeply decreasing function of distance. It is evident that at $\sim 100\ h^{-1}$ Mpc the QDOT galaxy space-density has dropped by a factor > 8 and therefore these depths are very sparsely sampled.

- FIGURE D1 -

We have estimated the galaxy weights (D.3) using the parametric form of the luminosity function derived by Saunders *et al.* (1990):

$$\Phi(L) \propto \left(\frac{L}{L_*(z)}\right)^{-\alpha} \exp\left[-\frac{1}{2\sigma^2}\log_{10}^2\left(1+\frac{L}{L_*(z)}\right)\right] \qquad \text{(D.14)}$$

with $\alpha = 1.09 \pm 0.12$, $\sigma = 0.724 \pm 0.031$ and $L_* = 10^{8.47\pm0.23}\ h^{-2}\ L_\odot$. We prefer to use this parametric form in order to test the stability of the resulting dipole to the details of the weighting scheme adopted (see below). No significant difference is found in the behaviour of the dipole if one uses the non parametric form given by Saunders *et al.* 1990, but this form does not allow one to model the uncertainties as easily.

The QDOT sample we use covers the regions with $|b| \geq 10^\circ$ ($\sim$ 82% of the sky), while there is still a $\sim$10% area not covered. In calculating the multipole components of the QDOT survey we must take into account the regions not surveyed. Our approach has been to use a composite method:

- The contribution to the dipole and to higher order moments of the excluded region $|b| \leq 10^\circ$ is estimated by expanding the observed surface density of IRAS galaxies using spherical harmonics ($l \leq 2$) and correcting the coefficients of the expansion for the masked region (*cf.* Yahil *et al.* 1986; Lahav 1987; Plionis 1988, 1989; PV91).

- Since the boundaries of the remaining $\sim$ 10% of unsurveyed sky are rather complicated we estimate its contribution to the dipole by assuming a uniform distribution of IRAS galaxies, having the average weight (as estimated from the rest of the sky).

Note that we have corrected the galaxy velocities to the LG rest frame and we have excluded all galaxies lying within 2 h^{-1} Mpc of the LG centroid as well as all galaxies with a luminosity $\leq 10^8\ h^{-2}\ L_\odot$ (in accordance with RR90).

Once the weights have been constructed and the correction for missing areas has been performed, one can determine the behaviour of the monopole as a function of radial depth. This is shown in Figure D1 (with an arbitrary vertical scaling). Note that, although

the density of galaxies is falling rapidly due to the selection of brighter and brighter galaxies, the monopole *increases* with depth. If the monopole had not carried on increasing in this way, one could have immediately concluded that sampling was too poor to make a reliable statement about the convergence of the dipole (PV91). On the other hand, a given monopole contribution could be made up of a large number of galaxies, each with the same weight, or just a few galaxies each with a much bigger weight. In the first case, the dipole properties would probably be well-defined but, in the second, there will be uncertainties because of small number statistics and also the fact that the weights require accurate knowledge of $\Phi(L)$. Thus, the continued growth of the monopole is a *necessary* condition for a 'good' dipole determination but not a *sufficient* one.

We now proceed to estimate the cumulative moments of the QDOT galaxy distribution in 20 distance bins each of width 10 h^{-1} Mpc. In the light of the above discussion, we must also estimate the shot-noise dipole produced just by virtue of the small number of galaxies sampled. We do this, using the same binning, by randomly redistributing the positions of the galaxies found in each bin. In this way we conserve the observed QDOT selection function; RR90 applied a similar method in their analysis but ours is much faster since we do not generate a random 3-d catalogue each time. We perform 50 such Monte-Carlo simulations and we then obtain the net QDOT dipole by subtracting the shot-noise dipole from the raw one. In Figure D2 we present the net QDOT dipole (filled circles), the raw dipole (dashed line) and the shot-noise dipole (open circles); errors are estimated from deviations around the mean simulation dipole. Although the uncertainties are quite large, the dipole certainly seems to have converged to its final value at $\sim$ 90 to 100 h^{-1} Mpc (in agreement with RR90): within this range the QDOT dipole points only $\sim 16^\circ$ away from the CMB dipole direction. The corresponding net amplitude ($|\underline{D}|/M\,(\leq 100\,\mathrm{Mpc}) \simeq 0.28$) implies $b_{IRAS}\,\Omega_o^{-0.6} \simeq 1.5$, a value which is about 20% larger than that derived in RR90. We are not quite sure why we get such a different answer but it can probably be attributed to the different way we choose to deal with regions of low galactic latitude ($|b| \leq 10^\circ$). We prefer to extrapolate the structural pattern of the surveyed to the unsurveyed sky, using

the spherical harmonic expansion to fill in the missing regions. RR90 replaced the missing regions with a uniform (Poisson) distribution of objects. We believe our method makes a more reasonable estimate of the contribution to the total dipole from the obscured region.

As we have discussed above, since the space density of QDOT galaxies is extremely low at large depths, distant galaxies are assigned an extremely large weight (Eq.(D.3)). The dipole contribution from these depths might therefore be extremely sensitive, to the details of the luminosity function.

- FIGURE D2 -

- FIGURE D3 -

D.4 Evidence for Contributions from Large Scales: Comparison with the Cluster Dipole

The dipole shown in Figure D2 certainly seems to have converged by around $100\,h^{-1}$ Mpc but how strong a statement can we make about whether there is any contribution to the dipole from distances $> 100\,h^{-1}$ Mpc when the sampling density and uncertainty in the luminosity function make the convergence of the amplitude of D/M difficult to determine?

To answer this question, we decided to look at the way in which the dipole changes as we increase the integration depth, not just in amplitude but also in *direction*. We find that when we integrate up to $\sim 90\ h^{-1}$ Mpc the dipole direction found by successively adding shells of radius $10\ h^{-1}$ Mpc is consistently aligned with the CMB dipole direction to an accuracy of $\sim 15°$. However, continuing the integration to larger volumes we find that the dipole direction deviates systematically from the CMB dipole direction by a random-walk only to be pulled back to the vicinity of the CMB dipole when we encompass the shell at

$150 \div 160\,h^{-1}$ Mpc where the Shapley concentration lies (Shapley 1930; Scaramella *et al.* 1989; Raychaudhury 1989). In Figure D4 we plot the QDOT dipole direction at each step of the volume integration. As we go to greater depths, the deviation from the vicinity from the MWB dipole direction as well as its consequent *realignment* is apparent.

- FIGURE D4 -

This is exactly the behaviour we would expect if the LG motion were influenced by structures at the these depths. In order to study the significance of the apparent influence to the dipole of the $150\,h^{-1} \div 160\,h^{-1}$ Mpc shell, we have determined the incremental dipole within equal volume shells of $\delta V \sim 3 \times 10^6\ h^{-3}$ Mpc^3. In other words, we measure the dipole contributed by each shell separately. In order to take into account the direction of each shell dipole, we define a signal to noise ratio (S/N) as follows:

$$\frac{S}{N} = \frac{|\underline{D}|/M \times \cos(\Delta\theta_{cmb})}{\sigma_{D/M}}, \tag{D.15}$$

where $\Delta\theta_{cmb}$ is the angle of deviation between the shell dipole and that of the CMB and $\sigma_{D/M}$ is the shell shot-noise dipole. In Figure D5 we plot S/N for each shell and it is evident that the only significant contributions to the total integrated dipole come, as expected, from the first bin ($\sim 4\,\sigma$) but also from the fourth bin ($\sim 1.5\,\sigma$) where the Shapley concentration lies. This finding is in agreement with the results of the cluster dipole (see PV91 and SVZ) which shows that up to 30% - 35% of the total dipole comes from depths $100 \leq r \leq 160\ h^{-1}$ Mpc. It is surprising that we can see anything given the uncertainties at such a distance but, even though we do find evidence of a signal, the QDOT survey samples depths beyond $\sim 100\ h^{-1}$ Mpc so sparsely (Figure D1) that we cannot determine the precise contribution of fluctuations at such depths to the LG acceleration using this data set.

- FIGURE D5 -

What we can do, however, is demonstrate the remarkable agreement between the incremental QDOT dipole and the corresponding results from the cluster dipole of PV91.

Table 1 shows the equal-volume shell limits, the number of clusters and IRAS galaxies respectively in the shell, the directions (in galactic co-ordinates) of the cluster and IRAS dipoles and the mis-match angle between these vectors and the CMB dipole vector. The agreement is remarkable for the $0 \div 99$ and $142.8 \div 157.3 h^{-1}$ Mpc bins particularly in the outer shell when one considers the huge drop in the number of IRAS galaxies out to this depth. One could argue that this contribution to the dipole is only aligned with the CMB vector by chance and it is really only a shot-noise effect. However, the probability of two random vectors aligning in this way is less than 3×10^{-4} while the joint random probability that both mass tracers (Abell clusters and IRAS galaxies) are aligned with the CMB dipole within the indicated angles, assuming that their respective distributions are independent of each other, is less than 10^{-7}. Although the two dipoles are aligned at around $150 h^{-1}$ Mpc, the difference is that the cluster dipole shows a clear increase in amplitude at this distance whereas the QDOT dipole does not. Without such a clear increase in amplitude our arguments are bound to be based upon circumstantial evidence. On the other hand the shot-noise errors we have estimated are certainly large enough to mask a 25 percent contribution to the QDOT dipole at this distance. It is not unreasonable therefore to interpret our results as evidence that the apparent convergence of the QDOT dipole is just due to poor sampling and that the real mass dipole converges at a much greater depth as indicated by the cluster dipole.

– TABLE 1 –

Some indications of the magnitude of the contribution from large scales to the LG motion can be seen in other work. Raychaudhury (1989; 1991) argues for a contribution $\leq 15\%$, while the cluster dipole analysis (PV91; SVZ) suggested a $\sim 35\%$ contribution. Note, however, that Raychaudhury's limits refer to the contribution to the dipole of one structure only, the Shapley concentration. PV91 estimated that the contribution of this structure is about 20% of the total dipole, which leaves about 15% to be due to other sources on scales $> 100\ h^{-1}$ Mpc. In effect what we find from the QDOT sample (Table 1), as well as in PV91, is that the dipole direction of the shell between 142.8 and 157.3 h^{-1} Mpc points towards

the CMB direction and not towards the direction of the Shapley concentration. This, in turn, implies that there is a correlated structure at this distance that consists not only of the Shapley concentration but also has considerable extent around the shell. This indicates that the $\sim 15\%$ contribution to v_p, derived by Raychaudhury, should be probably considered as a lower limit. In any case any contribution to the dipole from scales larger than the apparent convergence scale of $\sim 100\ h^{-1}$ Mpc implies a lower value of Ω_o than what we derived in section 4 (and from the RR90 value). For example, a contribution of 20% and 35% to the dipole results in $\Omega_o \sim 0.4$ and ~ 0.3 respectively (for $b_{IRAS} = 1$). A flat universe would require $b_{IRAS} \geq 1.8$. Additional constraints on b are obviously needed if we are to reach an unambiguous conclusion about the value of Ω_o. Some steps in this direction were made by Lahav, Nemiroff & Piran (1990) who calculated the correlation functions of galaxies selected by different criteria. The amplitude of the correlation function scales by b^2 in the linear bias model (Kaiser 1984). If different, for example, optical and infra-red selected galaxies possess different bias parameters b then they should therefore have different galaxy-galaxy correlation lengths (defined to be the separation, r_o, at which $\xi(r_o) = 1$). By comparing the auto- and cross-correlation functions of the ESO/UGC and IRAS samples of galaxies, Lahav *et al.* (1990) find that $b_{opt}/b_{IRAS} \simeq 1.7$. In order to reconcile this and the dipole result with $\Omega_o = 1$ we require $b_{opt} \simeq 3$; not impossible, but rather large for comfort. All this is predicated on the linear bias model being correct, which is by no means certain.

The picture that is emerging is therefore that there might well be a significant source of gravitational acceleration on a scale of $\sim 150\, h^{-1} Mpc$ which appears clearly in the cluster data but is masked by uncertainties induced by the sampling properties. The actual distribution on large scales might therefore be reasonably well modelled by the simple picture described in Section D.2.2. If this is true then it is an interesting corollary of Eq.(D.10) that, in the shell $[R_1, R_2]$ we have:

$$\left[\frac{\delta\rho}{\rho}\right]_2 \simeq \frac{\beta}{(R_2/R_1) - 1} \left[\frac{\delta\rho}{\rho}\right]_1$$

where β is the fractional contribution to the total dipole from that shell. This implies that the density fluctuation of QDOT galaxies in the shell $[100, 150]\ h^{-1}$ Mpc is $\sim 2\beta$ the density

fluctuation in the $[0,100]\ h^{-1}$ Mpc shell.

D.5 Conclusions

The main conclusion from this work is that there is no compelling evidence that the QDOT dipole has indeed converged to its final value within the sample volume. Consequently, the value of $\Omega_o^{0.6}/b$ quoted by RR90 should be interpreted only as an *upper limit.* Furthermore, even though the QDOT survey samples the galaxy distribution only very sparsely on scales $> 100\,h^{-1}$ Mpc, there is circumstantial evidence of a contribution from distances out to $\sim 160\,h^{-1}$ Mpc because there is a strong alignment of the incremental dipole at that distance with the MWB dipole vector. The most obvious source for this contribution is the Shapley concentration, which is known to contribute around 15 % of the optical dipole (Raychaudhury 1989). But if the Shapley concentration were the only source of the dipole anisotropy in the relevant distance bin, then the incremental vector in that bin should point in the direction of Shapley. It doesn't; it points in the CMB direction. There must therefore be some correlated structure in this distance bin that includes the Shapley concentration but also has significant extent around the shell. Although this structure is not visually prominent in the QDOT data set because of the low sampling density, we interpret the alignment as strong circumstantial evidence that there is significant structure in the galaxy distribution on scales $\sim 150\,h^{-1}$ Mpc; we cannot be more precise about the magnitude of its contribution to the dipole because the sampling is so poor.

We stress again that, in this respect, the QDOT data set possesses similar properties to the cluster catalogues analysed in PV91 and SVZ from which one infers a rather low value of $\Omega_o^{0.6}/b$. Bearing mind the large incompleteness of QDOT and the consequent insensitivity to structures beyond $\sim 100\,h^{-1}$ Mpc, it is impossible to derive anything other than an upper limit on $\Omega_o^{0.6}/b_{IRAS} < 0.6$ from this data set if there is such a contribution from this scale. Although the clusters (which are presumably much more biassed than IRAS galaxies)

suggest a value $\Omega_o^{0.6}/b_{clus} < 0.2$ (PV91) which is consistent with the IRAS dipole as long as we interpret the IRAS dipole as an upper limit rather than an exact determination. We should stress that the reason we get a higher value for the IRAS dipole than clusters might be nothing to do with a different bias for the two sets of objects; it could well be just because the cluster dipole contains the correct contribution from large scales whereas the IRAS data misses this. Thus, the QDOT and cluster data together suggest a low value of Ω_o, unless there is compelling evidence of gross systematic errors in the cluster catalogues and the QDOT dipole alignment at $160\,h^{-1}$ Mpc is a fluke.

We stress that this analysis is based on the assumption that any bias that exists can be modelled by the simple linear model mentioned in the introduction. If the appropriate value of b for IRAS galaxies is around unity, as has been suggested (RR90; Saunders *et al.* 1991) then our results are clearly incompatible with a flat $\Omega_o = 1$ Universe. The simplest interpretation would then be that we live in an open Universe with clusters moderately biassed, as expected on simple theoretical grounds (Kaiser 1984). IRAS galaxies may even be less clustered than the total mass distribution if $\Omega_o < 1$. An $\Omega_o = 1$ Universe is not excluded by these results, but the price to be paid is a much more complicated biassing scheme that would require much more detailed modelling.

Acknowledgments

Manolis Plionis and Paolo Catelan have been supported by the Ministero Italiano per la Ricerca Scientifica; Manolis Plionis further thanks SERC for support under the QMW visitors grant. Peter Coles acknowledges support from SERC under the QMW Theory Rolling Grant and thanks SISSA for their hospitality during a short visit when this work was begun. Paolo Catelan acknowledges Enzo Branchini for many stimulating discussions.

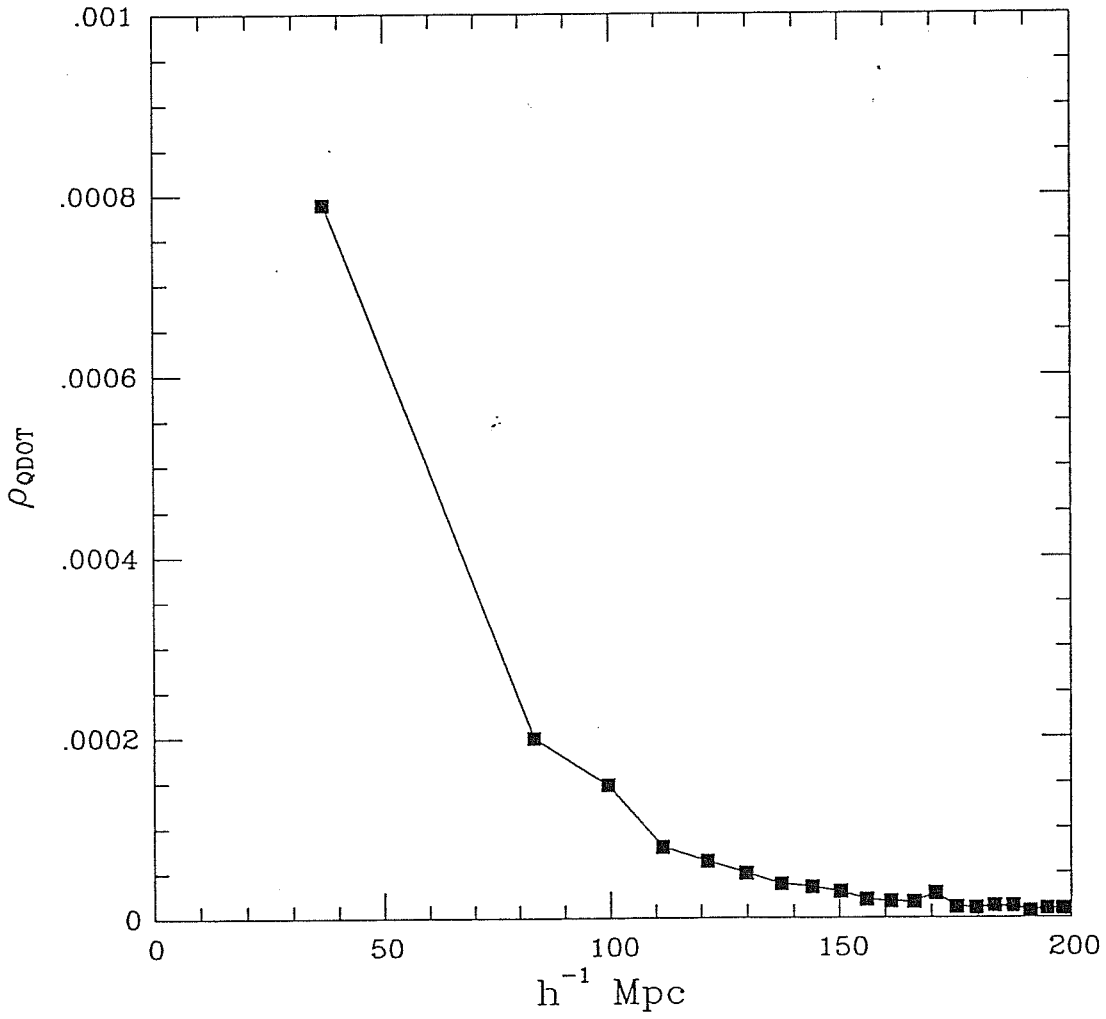

Fig. D1

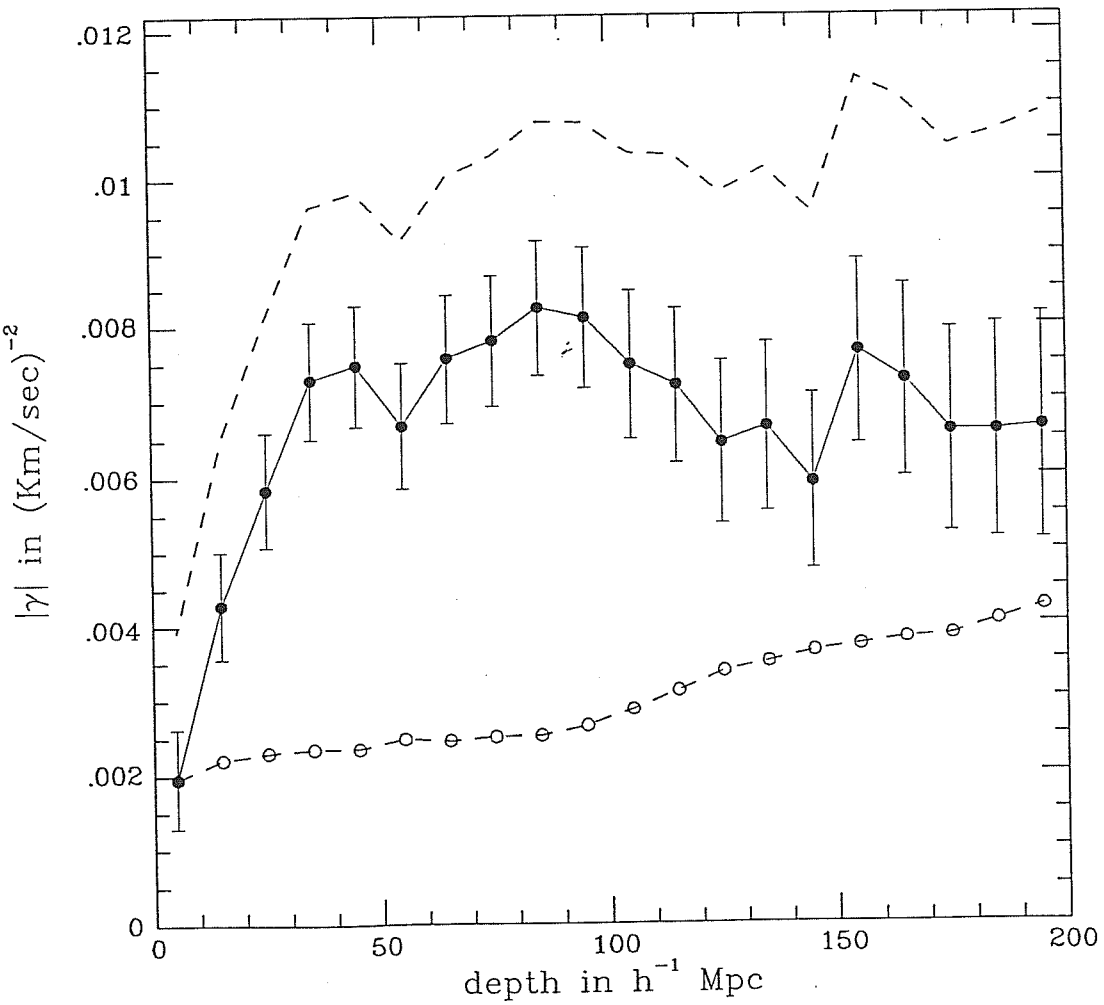
.012
.01
.008
.006
.004
.002
0
0
50
100
150
200
depth in h^{-1} Mpc
$|\gamma|$ in (Km/sec)$^{-2}$

Fig. D2

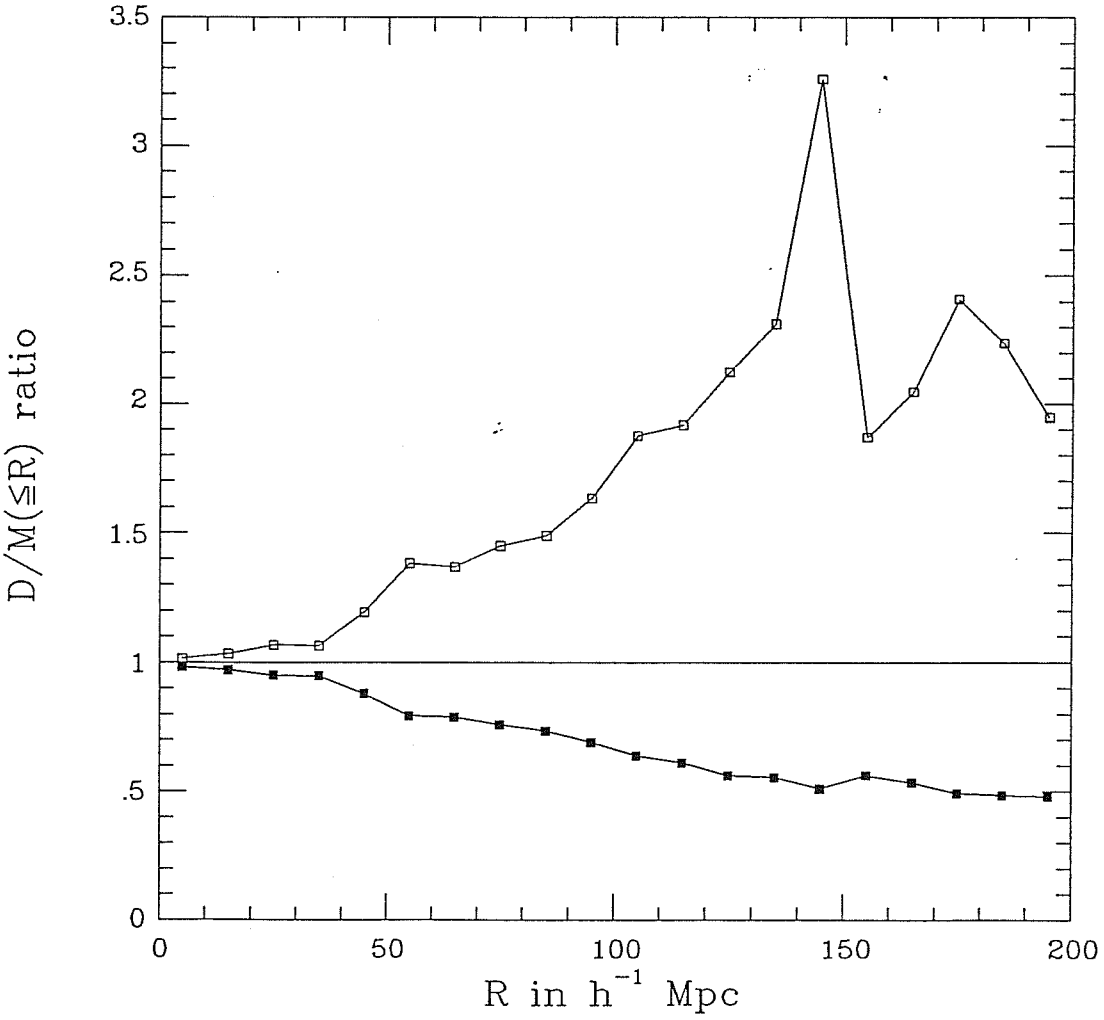

Fig. D3

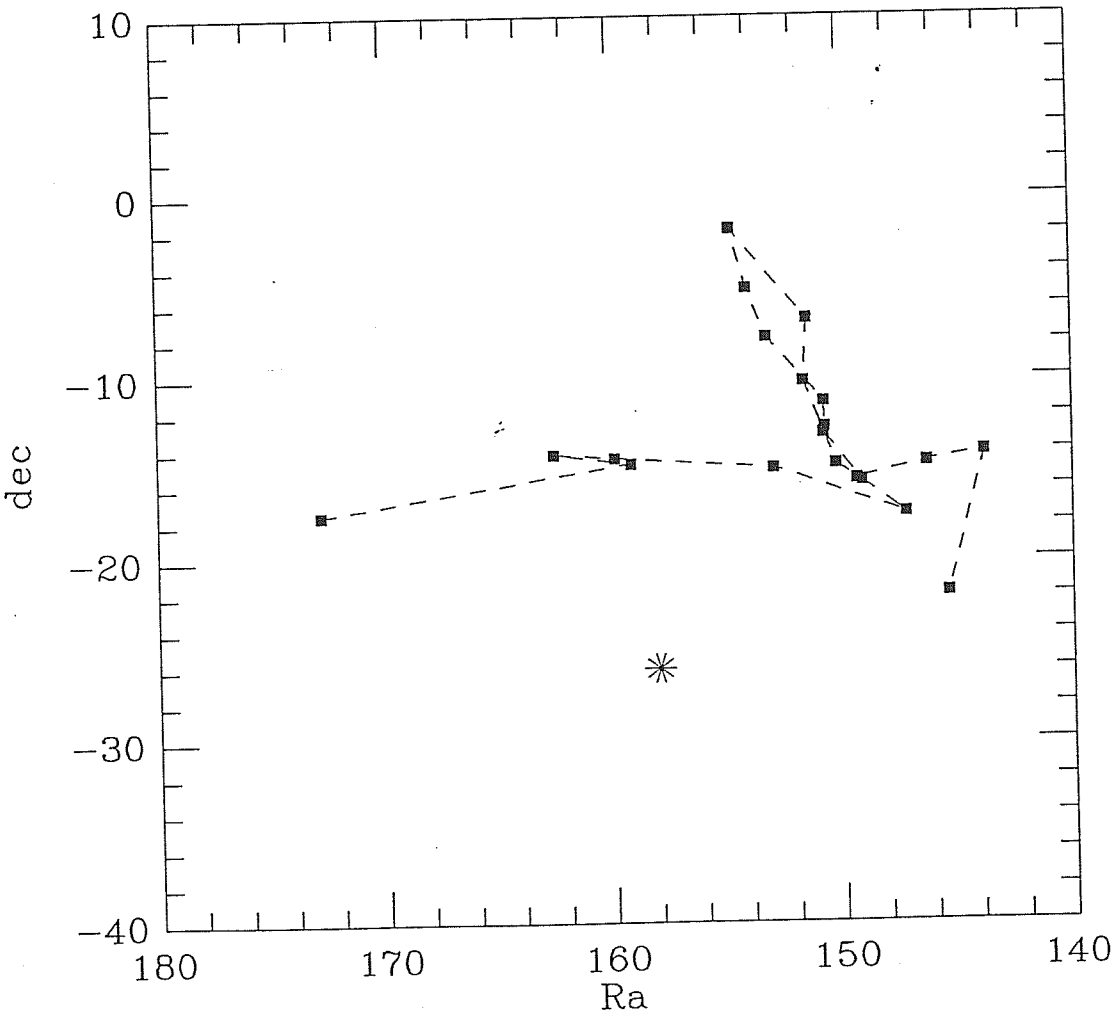

Fig. D4

EQUAL VOLUME SHELLS

$S/N = (D/M)_{shell} \times \cos(\delta\theta_{cmb}) \; / \; (\text{shot noise})_{shell}$

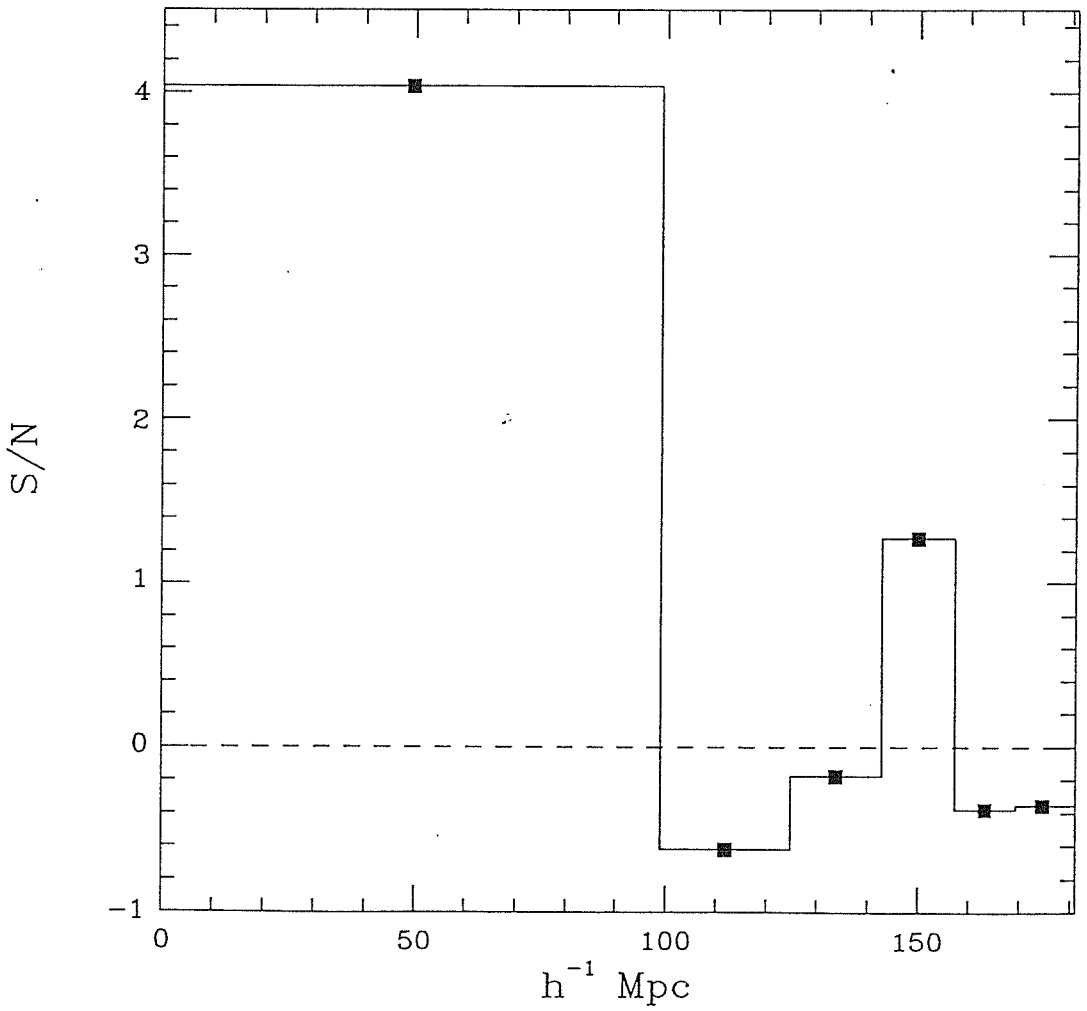

Fig 5

References of the Appendix D

Babul, A. & White, S.D.M., 1991. *Mon. Not. R. astr. Soc.*, **253**, 31P.

Bower, R.G., Coles, P., Frenk, C.S. & White, S.D.M., 1992. *Astrophys. J.*, in press.

Dekel, A. & Rees, M.J., 1987. *Nature*, **326**, 455.

Juszkiewicz, R., Vittorio, N. & Wyse, R.F.G., 1990. *Astrophys. J.*, **349**, 408.

Kaiser, N., 1984. *Astrophys. J.*, **326**, 19.

Kaiser, N. & Lahav, O., 1989. *Mon. Not. R. astr. Soc.*, **237**, 129.

Lahav, O., 1987. *Mon. Not. R. astr. Soc.*, **225**, 213.

Lahav, O., Edge, A.C., Fabian, A.C. & Putney, A., 1989. *Mon. Not. R. astr. Soc.*, **238**, 881.

Lahav, O., Kaiser, N. & Hoffman, Y., 1990. *Astrophys. J.*, **352**, 448.

Lahav, O., Nemiroff, R.J. & Piran, T., 1990. *Astrophys. J.*, **350**, 119.

Lahav, O., Rowan-Robinson, M. & Lynden-Bell, D., 1988. *Mon. Not. R. astr. Soc.*, **234**, 677.

Lynden-Bell, D., Lahav, O. & Burstein, D., 1989. *Mon. Not. R. astr. Soc.*, **241**, 325.

Meiksin, A. & Davis, M., 1986. *As. J.*, **91**, 191.

Miyaji, T. & Boldt, E., 1990. *Astrophys. J.*, **353**, L3.

Peebles, P.J.E., 1980. *The Large-Scale Structure of the Universe* Princeton University Press, Princeton.

Plionis, M., 1988. *Mon. Not. R. astr. Soc.*, **234**, 401.

Plionis, M., 1989. *Mon. Not. R. astr. Soc.*, **238**, 417.

Plionis, M. & Valdarnini, R., 1991. *Mon. Not. R. astr. Soc.* **249**, 46. (PV91)

Raychaudhury, S., 1989. *Nature*, **342**, 251.

Raychaudhury, S., 1991. In: NATO Advanced Study Institute *Clusters & Superclusters of Galaxies: Contributed Talks and Poster Papers*, eds Colless, M.M., Babul, A., Edge, A.C. , Johnstone, R.M. & Raychaudhury, S., pp. 3-4, Institute of Astronomy, Cambridge.

Rowan-Robinson, M., *et al.*, 1990. *Mon. Not. R. astr. Soc.* **247**, 1. (RR90)

Saunders, W., Rowan-Robinson, M., Lawrence, A., Efstathiou, G., Kaiser, N., Ellis, R.S., Frenk, C.S., 1990. *Mon. Not. R. astr Soc.*, **242**, 318.

Saunders, W. *et al.*, 1991. *Nature*, **349**, 32.

Scaramella, R., Baiesi-Pillastrini, G., Chincarini, G., Vettolani, G. & Zamorani, G., 1989. *Nature*, **338**, 562.

Scaramella, R., Vettolani, G. & Zamorani, G., 1991. *Astrophys. J. Lett.*, **376**, L1. (SVZ)

Shapley, H., 1930. *Harvard Obs. Bull.* **874**, 9.

Smoot, G.F., *et al.*, 1990. *Astrophys. J. Lett.* **371**, L1.

Strauss, M.A. & Davis, M., 1988. In *Proceedings of Vatican Study Week on Large-Scale Motions in Universe*, p. 219, eds Rubin, V.C. & Coyne, G., Princeton University Press, Princeton.

Strauss, M.A., Yahil, A., Davis, M., Huchra, J.P. & Fisher K., 1992. preprint.

Villumsen, J.V. & Strauss, M.A., 1987. *Astrophys. J.*, **322**, 37.

Yahil, A., Walker, D. & Rowan-Robinson, M., 1986. *Astrophys. J.*, **301**, L1.

Shell Limits	IRAS Galaxies				Rich Clusters			
(h^{-1} Mpc)	N	l°	b°	$\Delta\theta$	N	l°	b°	$\Delta\theta$
0.0-99.0	1181	251.9	34.7	15.8	50	247.1	24.5	18.9
99.0-124.8	225	120.2	23.8	120.5	40	325.6	11.3	56.2
124.8-142.8	118	338.7	-47.6	97.9	47	283.6	6.2	25.6
142.8-157.3	74	260.7	39.1	13.6	49	271.5	21.4	6.4
157.3-169.4	50	339.1	-75.5	111.5	36	69.1	5.7	142.5

Table 1. Incremental dipole in each of 5 equal-volume bins for both QDOT IRAS galaxies and Abell and ACO clusters (from PV91). The columns give (i) the radial distance limits of each bin; (ii)-(v) the number of QDOT galaxies in the bin, the dipole vector direction for that bin and the difference, $\Delta\theta$ between this vector and the CMB dipole vector; (vi)-(ix) give the number of clusters, dipole direction and CMB offset angle for the cluster data for comparison.

Figure Captions

Figure D1. The space density of QDOT galaxies in equal volume shells.

Figure D2. The QDOT dipole (filled circles) with its estimated errors given by equation (5), together with the raw dipole (dashed line) and the dipole simulated by reshuffling the galaxy positions (open circles).

Figure D3. The effect on D/M of varying the luminosity function parameters by 1σ. We plot the ratio of the D/M obtained with different luminosity function parameters to that obtained with the "standard" choice. The upper curve is that obtained if α, σ and L_* all lie at the bottom end of their allowed 1σ uncertainties and the lower curve shows what happens if these parameters take values at the top end of their uncertainty ranges.

Figure D4. The QDOT dipole (cumulative) direction at each step of the integration. The CMB dipole direction is marked with an asterisk.

Figure D5. The Signal-to-Noise ratio, S/N, for each equal volume shell as a function of distance (see text). The only significant contributions to the integrated dipole come from the nearby shell ($S/N \simeq 4$) and the shell between 140 - 160 h^{-1} Mpc ($S/N \simeq 1.5$).

APPENDIX E

Weighted Biasing Scheme

Weighted Bias and Galaxy Clustering

Paolo CATELAN [1], Peter COLES [2], Sabino MATARRESE [3]
& Lauro MOSCARDINI [4]

[1] *SISSA - International School for Advanced Studies,*
Strada Costiera 11, 34014 Trieste, Italy

[2] *Astronomy Unit, School of Mathematical Sciences*
Queen Mary & Westfield College, Mile End Road, London E1 4NS, UK

[3] *Dipartimento di Fisica* Galileo Galilei, *Università di Padova*
via Marzolo 8, I-35131 Padova, Italy

[4] *Dipartimento di Astronomia, Università di Padova*
vicolo dell'Osservatorio 5, I-35122 Padova, Italy

– *Mon. Not. R. Astron. Soc. (1993)*, submitted –

Summary

We consider a weighted biasing scheme for galaxy clustering. This differs from previous treatments in the fact that the biased density field coincides with the background mass–density whenever the latter exceeds a given threshold value. There is some physical motivation for this scheme and it is in better accord with intuitive ideas than models based on the Kaiser (1984) analysis of the clustering of rich clusters. We explain how different classes of object could be biased in different ways with respect to the underlying density distribution but still have $b = 1$. We also show that if one applies our scheme consistently a weak dependence of b upon density can be implied. This could also be the reason why the correlation function of galaxies in groups does not differ substantially from the correlation function of all galaxies.

Key Words: galaxies: clustering – galaxies: formation – large–scale structure of the Universe

E.1 Introduction

The assumption that bright galaxies are *biased* tracers of the mass distribution has featured strongly in theories of galaxy and structure formation in recent years. The simplest version of the Cold Dark Matter model (CDM) was found to be unable to explain the clustering properties of galaxies if the number density of galaxies and the density of gravitating material were simply proportional to each other (Davis *et al.* 1985). The observation by Kaiser (1984) that the strong clustering of rich clusters relative to galaxies could be a simple consequence of the fact that clusters form only in regions where the mass density is particularly large, led to the adoption of a simple phenomenological model for *biased* galaxy formation wherein galaxies themselves form only at high peaks of the density field. Because of the properties of Gaussian statistics – the simplest and best–motivated form for the distribution of primordial density fluctuations – high peaks have different statistical properties to 'typical' points (Peacock & Heavens 1985; Bardeen *et al.* 1986) so galaxies are biased tracers of the mass density field.

The Kaiser model offers a plausible phenomenological explanation for the clustering of clusters because clusters are defined to be high density regions in the matter distribution. The applicability of this model to galaxies themselves is less clear, however, because in order for it to work one must suppress galaxy formation from peaks of lower density. Various authors (Rees 1985; Silk 1985; Dekel & Silk 1986; Dekel & Rees 1987) have offered some suggestions as to how a *local* (or *natural*) bias might arise. For example, the initial density of a collapsing proto–object might somehow affect the star formation rate so that low–density peaks form insufficient stars to produce an identifiable galaxy. Indeed, given the complexity of the galaxy formation process it would be surprising if there were not some kind of non–linear dependence of the space density of galaxies upon the density of the proto–galaxies from

which they formed (Coles 1983). On the other hand, Peacock (1990) has found no evidence for such a local bias in the properties of elliptical galaxies. There is also no strong trend of clustering amplitude with galaxy luminosity (White *et al.* 1988; Hamilton 1988; Eder *et al.* 1989; Valls–Gabaud *et al.* 1989), which one would expect if the bias is controlled by star formation efficiency. Furthermore, the recent discovery by the COBE team of fluctuations in the sky temperature of the cosmic microwave background (Smoot et al. 1992) suggests that galaxy formation in the CDM model should be unbiased (or even anti–biased so that galaxies form preferentially in low–density regions). There is also the possibility that any bias is not even local: feedback from the first generation of objects may suppress or enhance galaxy formation on a large scale around them. Indeed such a non–local bias seems to be necessary to reconcile standard CDM with observations of very large scale galaxy clustering (Babul & White 1991; Bower *et al.* 1993).

So how can one square the observational evidence against biasing with the theoretical motivation for it? The answer may well lie in the naivety of the theoretical modelling. In this paper we shall look at the question of modelling locally–biased galaxy formation. We shall argue that the Kaiser model is probably not appropriate for galaxy clustering and suggest a simple alternative which is in better accord with intuition. In our scheme – the weighted biasing scheme – the biased density is proportional to the mass density but only where the mass density exceeds some threshold value.

The plan of the paper is as follows. In Section E.2 we introduce the weighted biasing scheme, while in Section E.3 we present the results for the two–point correlation of the biased density field (technical details are given in appendix 1). Section E.4 contains a general discussion.

E.2 A Weighted Biasing Scheme

Here we construct a mathematical definition of our weighted biasing scheme. The underlying mass density fluctuation field will be denoted δ_R, where R is some smoothing scale used to

define the mass scale of a proto–object:

$$\delta_R(\mathbf{x}) \equiv [\rho_R(\mathbf{x}) - \langle\rho\rangle]/\langle\rho\rangle \ . \tag{E.1}$$

The $\langle\ \rangle$ brackets denote averages over a probability distribution, and we shall assume throughout that these are equivalent to averages over a large volume of space i.e. that the field $\rho_R(\mathbf{x})$ is *ergodic* (Adler 1981).

In a local bias model, the *biased density field* (BDF) is a local function of $\rho_R(\mathbf{x})$. That is to say the probability of finding a galaxy at a point $\mathbf{x}$ is a function only of $\rho_R(\mathbf{x})$ or, equivalently, of $\delta_R(\mathbf{x})$: we take $dP(\mathbf{x}) = n_\circ f(\rho_R)\, dV/\langle f\rangle$ where $n_\circ$ is the mean number density of galaxies. General constraints on this type of model are derived by Coles (1993). Because we shall be assuming the existence of some threshold ν, we define the BDF to be $f(\rho_R) = \rho_{\nu,R}(\mathbf{x})$. If $f(\rho_R) \propto \rho_R$ then galaxies trace the mass (in a statistical sense) and are therefore 'unbiased'. In the simplest model of biasing, suggested by Kaiser (1984), the BDF is defined as constant above a threshold and zero below it, i.e.

$$\rho_{\nu,R}(\mathbf{x}) \equiv \langle\rho\rangle\, \Theta(\delta_R(\mathbf{x}) - \nu\sigma_R) \ ; \tag{E.2}$$

the threshold is $\nu\sigma_R$ and σ_R is the *rms* value of δ_R. The function $\Theta(x)$ is the Heaviside step function. We shall henceforth refer to this model as the Kaiser model.

Notice that the Kaiser model possesses the property that for very low (i.e. negative) thresholds $\nu\sigma_R$ galaxy formation occurs with constant probability throughout space. This limit of the Kaiser model therefore produces an *unclustered* distribution of objects rather than an *unbiased* one. Similarly, there is a constant probability of galaxy formation above the threshold. This implies a one–to–one correspondence between high peaks and galaxies, which may be reasonable if the threshold is very high (so that the galaxies are strongly biased) but a weak bias (which is what the observations imply) should merely modulate the spatial distribution of galaxies relative to the mass distribution. One also has the problem that merging and disruption of proto–objects in the non–linear regime is expected to destroy the correspondence between high peaks in the initial density field and subsequent bound struc-

tures (Coles et al. 1993). It is difficult therefore to justify the Kaiser model as a description of biased galaxy formation.

Our proposed weighted biasing scheme differs from the Kaiser model in that, above the threshold (which we take to be the same: $\nu\sigma_R$), the BDF coincides with the underlying density field:

$$\rho_{\nu,R}(\mathbf{x}) \equiv \rho_R(\mathbf{x})\,\Theta(\delta_R(\mathbf{x}) - \nu\sigma_R)\ . \tag{E.3}$$

In the limit of small $\nu\sigma_R$, galaxies trace the mass exactly and are therefore unbiased. For larger $\nu\sigma_R$ the weighted BDF traces the mass, but only in regions where the density exceeds some critical value. We do not therefore require a one–to–one correspondence between peaks and galaxies. Not only does this model agree better with our intuition in this limit, but it also agrees qualitatively with the results obtained from hydrodynamical simulations by Cen & Ostriker (1992). Indeed, there is good evidence for the existence of similar density–thresholding behaviour of star formation in the disks of spiral galaxies where the local gas density seems to provide the trigger (Guiderdoni 1987).

Note that $\rho_{\nu,R}(\mathbf{x})$ actually represents the true mass–density inside a smoothed sphere of filtering radius R centered on $\mathbf{x}$ for those mass fluctuations which exceed the threshold. We define the ratio

$$\mu_R(\nu) \equiv \frac{\langle\rho_{\nu,R}\rangle}{\langle\rho\rangle}\ , \tag{E.4}$$

which is the total mass fraction in *excursion regions* (i.e. those regions where the mass fluctuation δ_R exceeds the threshold $\nu\sigma_R$). Using the ergodic property, we can take the expectations to correspond to spatial averages over a large (formally infinite) volume V. It is easy thus to see that

$$\mu_R(\nu) = \frac{\int_V d^3\mathbf{x}\,\rho_R(\mathbf{x})\,\Theta(\delta_R(\mathbf{x}) - \nu\sigma_R)}{\int_V d^3\mathbf{x}\,\rho_R(\mathbf{x})} = \frac{\int_{V_R(\nu)} d^3\mathbf{x}\,\rho_R(\mathbf{x})}{\int_V d^3\mathbf{x}\,\rho_R(\mathbf{x})} \equiv \frac{M_R(\nu)}{M_{TOT}}\ , \tag{E.5}$$

where $V_R(\nu)$ is the total volume of the excursion regions.

In the Kaiser and weighted bias models – and indeed in any local biasing scheme involving a threshold – one could define the total number of objects $N_{obj}(>\nu)$ as the total mass above

the threshold $M(>\nu)$ divided by the mass of a single object M_{obj}. Thus

$$N_{obj}(>\nu) = \frac{M(>\nu)}{M_{obj}} = \frac{M(>\nu)}{M_{TOT}} \left(\frac{M_{TOT}}{M_{obj}}\right) , \tag{E.6}$$

so that $N_{obj}(>\nu) = \mu_R(\nu) M_{TOT}/M_{obj}$. One is implicitly assuming that the objects form only out of the mass within the excursion set. If one allows for accretion, however, one could get a different expression. The quantity $\mu_R(\nu)$ is interesting in any case, however, because it illustrates one of the dangers of adopting the assumption of Gaussian statistics for the mass fluctuation field (Kaiser 1984; Peacock & Heavens 1985; Bardeen *et al.* 1986; Coles 1993). In such a case

$$\mu_R(\nu) = \frac{1}{2}\,\mathrm{erfc}\left(\frac{\nu}{\sqrt{2}}\right) + \frac{\sigma_R}{\sqrt{2\pi}}\,\mathrm{e}^{-\nu^2/2} \equiv [\Phi(\nu) + \nu\sigma_R]\,\frac{\mathrm{e}^{-\nu^2/2}}{\sqrt{2\pi}\,\nu} , \tag{E.7}$$

where $\mathrm{erfc}\,x \equiv (2/\sqrt{\pi})\int_x^\infty dy \mathrm{e}^{-y^2}$ is the complementary error function and the auxiliary function $\Phi(\nu)$ has a convenient asymptotic expansion:

$$\Phi(\nu) \equiv \sqrt{\frac{\pi}{2}}\,\nu\,\mathrm{e}^{\nu^2/2}\,\mathrm{erfc}\left(\frac{\nu}{\sqrt{2}}\right) \simeq 1 + \sum_{n=1}^{\infty}(-1)^n\,\frac{(2n-1)!!}{\nu^{2n}} . \tag{E.8}$$

We plot the function $\mu_R(\nu)$ for different values of σ_R in Figure E1. As expected, the mass fraction $\mu_R(\nu)$ tends to unity as $\nu \to -\infty$, since in this case the BDF reduces to the mass density field. Note, however, that the maximum value $\mu_R(\nu_m) > 1$, is reached at $\nu_m = -1/\sigma_R$. The reason for this apparent paradox is that the underlying distribution permits the existence of regions with negative mass (i.e. $\rho_R < 0$). This point can be made more clear by writing eq (E.5) in terms of integrals over the probability distribution rather than spatial averages. The numerator in (E.5) becomes $\int_{\langle\rho_R\rangle(1+\nu\sigma_R)}^{\infty} d\rho_R\,\rho_R\,p(\rho_R)$, while the denominator can be split into two parts: $\int_{-\infty}^{\langle\rho_R\rangle(1+\nu\sigma_R)} d\rho_R\,\rho_R\,p(\rho_R) + \int_{\langle\rho_R\rangle(1+\nu\sigma_R)}^{\infty} d\rho_R\,\rho_R\,p(\rho_R)$. The integral $\int_{-\infty}^{\langle\rho_R\rangle(1+\nu\sigma_R)} d\rho_R\,\rho_R\,p(\rho_R)$ in the denominator always contains a negative contribution coming from $\rho_R < 0$ events, which is indeed maximised (in absolute value) when $\nu = -1/\sigma_R$. The appropriate quantity in the Kaiser model (which is the volume fraction of the excursion regions) does not have any factors of ρ_R in the integrals and is therefore immune to this effect.

- FIGURE E1 -

This illustrates an important problem with the modelling of galaxy clustering using Gaussian statistics: one must be very careful to ensure that unphysical events with $\rho_R < 0$ do not contribute to the statistics of the biased field. In the weighted biasing scheme, we can consistently apply our model with Gaussian statistics provided we restrict ourselves either to $\sigma_R \ll 1$, which reduces the probability of unphysical events, or to $\nu \gg 1/\sigma_R$, so that negative mass events have little effect on statistical properties such as $\mu_R(\nu)$. Different local biasing functions would lead to different constraints to be satisfied if the model is to be physically reasonable.

Alternatively, to get a fully self–consistent model we could use a distribution which only allows $\rho_R > 0$. We have therefore also computed $\mu_R(\nu)$ for an underlying *lognormal* distribution of density fluctuations (Coles & Jones 1991), which is a simple phenomenological model for the non–linear density field:

$$p(\delta_R) = \frac{(1+\delta_R)^{-1}}{\sqrt{2\pi \log(1+\sigma_R^2)}} \exp\left(-\frac{\log^2\left[(1+\delta_R)\sqrt{1+\sigma_R^2}\right]}{2\log(1+\sigma_R^2)}\right) . \tag{E.9}$$

Now we find

$$\mu_R(\nu) = \frac{1}{2}\,\mathrm{erfc}\left(\frac{\log\left[(1+\ \nu\sigma_R)/\sqrt{1+\sigma_R^2}\right]}{\sqrt{2\log(1+\sigma_R^2)}}\right) . \tag{E.10}$$

As expected, this takes its maximum value $\mu_R(\nu_m) = 1$ at $\nu_m = -1/\sigma_R$, corresponding to the unbiased case and there are no problems with μ_R exceeding unity. The behaviour of μ_R as a function of ν is illustrated also in Figure E1.

E.3 The Two–Point Correlation Function of the Biased Density field

We shall now turn our attention to the BDF two–point correlation function, which is defined as

$$\xi_{\nu,R}(r) = \langle \delta_{\nu,R}(\mathbf{x}_1)\, \delta_{\nu,R}(\mathbf{x}_2) \rangle , \tag{E.11}$$

where $r \equiv |\mathbf{x}_1 - \mathbf{x}_2|$ and $\delta_{\nu,R}$ is the BDF fluctuation:

$$\delta_{\nu,R}(\mathbf{x}) = \mu_R(\nu)^{-1}\,[1+\delta_R(\mathbf{x})]\;\Theta(\delta_R(\mathbf{x}) - \nu\sigma_R) - 1. \tag{E.12}$$

One thus obtains

$$\mu_R^2(\nu)\,[1+\xi_{\nu,R}(r)] = \langle [1+\delta_1+\delta_2+\delta_1\delta_2]\,\Theta(\delta_1-\nu\sigma_R)\,\Theta(\delta_2-\nu\sigma_R)\rangle\ , \tag{E.13}$$

where $\delta_i = \delta_R(\mathbf{x}_i)$. The expression (E.13) can be written

$$\mu_R^2(\nu)\,[1+\xi_{\nu,R}(r)] = \int_{\nu\sigma_R}^{\infty}\int_{\nu\sigma_R}^{\infty} d\delta_1 d\delta_2\,[1+\delta_1+\delta_2+\delta_1\delta_2]\,p\,(\delta_1,\delta_2;\xi_R)\ . \tag{E.14}$$

For a Gaussian field, $p\,(\delta_1,\delta_2\,;\xi_R)$ is a bivariate Gaussian distribution with covariance ξ_R (and variance σ_R^2). One can further express the integral (E.14) in terms of integrals over derivatives of a bivariate Gaussian distribution. The details are given in appendix 1. For this phenomenological discussion it is sufficient to discuss the *linear* biasing factor:

$$\xi_{\nu,R}(r) \simeq b_R^2(\nu)\,\xi_R(r), \tag{E.15}$$

obtained by Taylor expanding (E.14) up to first order in $\omega_R(r) = \xi_R(r)/\sigma_R^2$. The result is

$$b_R(\nu) = \frac{\sigma_R\Phi(\nu)+\nu(1+\nu\sigma_R)}{\sigma_R\Phi(\nu)+\nu\sigma_R^2}. \tag{E.16}$$

The behaviour of this function is displayed in Figure E2. Of course, this parameter only describes the bias on large scales when ξ_R is small. In general the bias $(\xi_{\nu,R}(r)/\xi_R(r))^{1/2}$ will be a non–increasing function of r for any local bias model (Coles 1993). Galaxy clustering on scales where ξ is not small is surely dominated by non–linear dynamical evolution which we have no hope of modelling in a simple way, so we shall not place any emphasis on the behaviour for large ω_R. The behaviour of the function $b_R(\nu)$ in the weighted biasing scheme contrasts with the Kaiser (1984) expression,

$$b'_R(\nu) = \frac{\nu}{\sigma_R\Phi(\nu)}. \tag{E.17}$$

Note that our biasing factor reduces to unity in the unbiased Gaussian case, $b_R(-\infty) = 1$, unlike the Kaiser expression; like the Kaiser model it gives $b_R(\nu) \simeq \nu/\sigma_R$ in the high–ν limit.

– FIGURE E2 –

Notice, however, that there is another way to obtain $b = 1$ in this version of the weighted biasing scheme, by choosing $\nu = \sigma_R - 1/\sigma_R$. For any σ_R, it therefore seems that there are two values of ν which can lead to an 'unbiased' model. However, the minimum of b_R corresponds exactly to the regime where $\mu_R > 1$ so one might suspect it to be related to the presence of negative mass events. To demonstrate this, we have also computed the linear bias factor for the lognormal distribution:

$$b_{LN}(\nu) = 1 + \frac{\tilde{\nu}}{\tilde{\sigma}_R \, \Phi(\tilde{\nu})}, \tag{E.18}$$

where

$$\tilde{\nu} = \frac{\log\left[(1 + \nu\sigma_R)/\sqrt{1 + \sigma_R^2}\right]}{\sqrt{2\log(1 + \sigma_R^2)}}, \tag{E.19}$$

and

$$\tilde{\sigma}_R = \sqrt{\log(1 + \sigma_R^2)}. \tag{E.20}$$

The behaviour of this function is also shown in Figure E2. Notice that one reproduces the Gaussian results in the limit $\sigma_R^2 \to 0$, but the bias is a much flatter function of ν at large σ_R than for the Gaussian case and is monotonically increasing. This shows that it is indeed the case that negative mass events distort the calculations for an underlying Gaussian field. To use our phenomenological model in situations where σ_R is not vanishingly small, we must therefore incorporate an underlying distribution in which $\rho_R > 0$ everywhere, such as the lognormal (E.9). Intruigingly, we find that in the Kaiser model for lognormal fluctuations we have simply:

$$b'_{LN}(\tilde{\nu}) = b_{LN}(\tilde{\nu}) - 1. \tag{E.21}$$

This again shows that $b \to 0$ in the Kaiser model in the limit of small threshold.

E.4 Discussion and Conclusions

Our weighted bias model provides a simple phenomenological description of biased galaxy formation, in which galaxies trace the mass where the local density exceeds some threshold

value. It is of course a simplistic model, but is reasonably plausible and probably an improvement upon the Kaiser model in that its behaviour in the limit of small threshold is to give an unbiased distribution rather than an unclustered one.

The first important point to emerge from this study is that the statement that $b = 1$ is not equivalent to the statement that galaxies trace the mass. The $b = 1$ version of the Kaiser has a very different relationship of galaxies to underlying mass than does the $b = 1$ weighted bias model. In the latter model, galaxies do trace the mass (in a well–defined statistical sense). In the former they do not. In other local bias models the relationship is different still. The evidence from COBE that $b \simeq 1$ in a CDM model does not therefore mean that a local bias of some form is excluded. Moreover, different populations of objects could have very different biasing functions but still have the same value of b. Perhaps this is the reason why spirals and ellipticals, though known to have different relative abundances in regions of different density (Dressler 1980), seem to have similar levels of bias.

Even if one supposes that galaxy formation is unbiased, our model finds a possible application in the behaviour of *groups* of galaxies. Ramella et al. (1990) have found, perhaps surprisingly, that the correlation function of galaxies in groups is similar to that of all galaxies (though see also Jing & Zhang 1988; Maia & da Costa 1990). If one takes groups to be defined as regions where the local density exceeds some threshold, then our weighted biasing prescription should apply to the correlation function of galaxies within the groups, assuming galaxies trace the mass there. Our model therefore provides a plausible explanation for why the two correlation functions are similar.

Our weighted bias model cannot produce an anti–bias. In order to do this one has to have a biasing function which is a decreasing function of ρ; models that achieve this are given by Coles (1993). (The Kaiser model produces an anti–bias by virtue of the unnatural assumption that, in the limit of small thresholds, objects are seeded everywhere with constant probability.) Obviously, in view of the argument of the previous paragraph, there is no contradiction *in principle* with, for example, spirals being suppressed in high–density regions and still having $b = 1$.

We have also demonstrated explicitly that one must be very careful in using arguments based on Gaussian statistics to describe clustering in the regime where $\sigma_R \simeq 1$, even in a purely phenomenological way. Even the Kaiser model, which is not directly distorted by events with $\rho_R < 0$ for reasons explained in Section E.2, involves a logical inconsistency in this regime. Any bias in galaxy clustering is expected to be imposed in the non–linear regime and the appropriate statistical distribution must reflect that fact. If the bias is imposed at very late times, when the distribution is highly skewed, then one can get a bias which depends very slowly on threshold. This could well be the explanation for why there seems to be little difference in bias for objects of widely–varying (presumed) initial density.

Acknowledgments

We all thank Francesco Lucchin for discussions; Paolo Catelan further thanks Manolis Plionis and Enzo Branchini. Peter Coles receives an SERC Advanced Fellowship; he is also grateful to the Dipartimento di Astronomia, Università di Padova for their hospitality during a visit when this paper was written and to the Consiglio Nazionale delle Ricerche for financial support. This work was partially supported by Italian MURST.

References of the Appendix E

Adler R.J., 1981, The Geometry of Random Fields, John Wiley & Sons, New York

Babul A., White S.D.M., 1991, MNRAS, 253, 1P

Bardeen J.M., Bond J.R., Kaiser N., Szalay A.S., 1986, ApJ, 304,15

Bower R.G., Coles P., Frenk C.S., White S.D.M., 1993, ApJ, 403, 405

Cen R.Y., Ostriker J.P., 1992, ApJ, 399, L113

Coles P., 1993, MNRAS, 262, 1065

Coles P., Jones B.J.T., 1991, MNRAS, 248, 1

Coles P., Melott A.L., Shandarin S.F., 1993, MNRAS, 260, 765

Davis M., Efstathiou G., Frenk C.S., White S.D.M., 1985, ApJ, 292, 371

Dekel A., Rees M.J., 1987, Nat, 330, 455

Dekel A., Silk J., 1986, ApJ, 303, 39

Dressler A., 1980, ApJ, 236, 351

Eder J.A., Schombert J.M., Dekel A., Oemler A., 1989, ApJ, 340, 29

Guiderdoni B., A& A, 1987, 172, 27

Hamilton A.J.S., 1988, ApJ, 331, L59

Jing Y., Zhang J., 1988, A& A, 190, L21

Kaiser N., 1984, ApJ, 284, L9

Maia M.A.G., da Costa L.N., 1990, ApJ, 349, 477

Peebles P.J.E., 1980, The Large–Scale Structure of the Universe, Princeton University Press, Princeton

Peacock J.A., 1990, MNRAS, 243, 517

Peacock J.A., Heavens A.F., 1985, MNRAS, 217, 805

Politzer H.D., Wise M.B., 1984, ApJ, 285, L1

Ramella M., Geller M.J., Huchra J.P., 1990, ApJ, 353, 51

Rees M.J., 1985, MNRAS, 213, 75P

Silk J., 1985, ApJ, 297, 1

Smoot G.F., et al., 1992, ApJ, 396, L1

Valls–Gabaud D., Alimi J.–M., Blanchard A., 1989, Nat, 341, 215

White S.D.M., Tully R.B., Davis M., 1988, ApJ, 333, L45

E.5 Appendix 1: Derivation of the Correlation Functions

In this Appendix we derive an explicit form for the BDF two–point correlation function $\xi_{\nu,R}(r)$, as defined in eq.(E.14) of the text, for an underlying Gaussian mass density field. In this case one can define $\alpha \equiv \delta_1/\sigma_R$, $\beta \equiv \delta_2/\sigma_R$; we then need $p(\alpha,\beta;\omega_R)$, which is a bivariate Gaussian:

$$p(\alpha,\beta;\omega_R) = \frac{1}{2\pi\sqrt{1-\omega_R^2}} \exp\left[-\frac{\alpha^2+\beta^2-2\,\omega_R\,\alpha\,\beta}{2\,(1-\omega_R^2)}\right]. \qquad \text{(E.22)}$$

It is straightforward thus to show that

$$I(\nu) \equiv \mu_R^2(\nu)\big[1+\xi_{\nu,R}(r)\big] = \int_\nu^\infty \int_\nu^\infty d\alpha\, d\beta \left[(1+\sigma_R^2\,\omega_R) - 2\,\sigma_R(1+\omega_R)\,\frac{\partial}{\partial\alpha} + 2\,\sigma_R^2\,\omega_R\,\frac{\partial^2}{\partial\alpha^2} + \sigma_R^2(1+\omega_R^2)\,\frac{\partial^2}{\partial\alpha\,\partial\beta}\right] p(\alpha,\beta;\omega_R). \qquad \text{(E.23)}$$

Some of the integrals in (E.23) can be performed exactly and we get the expression

$$I(\nu) = \big[1+\omega_R(1+\nu\sigma_R)\big]\frac{\sigma_R\,\mathrm{e}^{-\nu^2/2}}{\sqrt{2\pi}}\,\mathrm{erfc}\left(\frac{\nu}{\sqrt{2}}\sqrt{\frac{1-\omega_R}{1+\omega_R}}\right) + \frac{1+\sigma_R^2\,\omega_R}{2\sqrt{2\pi}}\int_\nu^\infty d\alpha\,\mathrm{e}^{-\alpha^2/2}\,\mathrm{erfc}\left(\frac{\nu-\alpha\,\omega_R}{\sqrt{2(1-\omega_R^2)}}\right) + \frac{\sigma_R^2\sqrt{1-\omega_R^2}}{2\pi}\,\mathrm{e}^{-\nu^2/(1+\omega_R)} \qquad \text{(E.24)}$$

The expression for the standard bias (Kaiser 1984) is easily recovered from the latter equation, by taking the $\sigma_R \to 0$ limit at fixed ν and ω_R:

$$1+\xi'_{\nu_R}(r) = \frac{\sqrt{2/\pi}}{[\mathrm{erfc}(\nu/\sqrt{2})]^2}\int_\nu^\infty d\alpha\,\mathrm{e}^{-\alpha^2/2}\,\mathrm{erfc}\left(\frac{\nu-\alpha\,\omega_R}{\sqrt{2(1-\omega_R^2)}}\right). \qquad \text{(E.25)}$$

The result (E.24) leads to an exact expression for the BDF variance in the limit of zero lag, $\omega_R \to 1$:

$$\sigma^2_{\nu,R} = \frac{(1+\sigma_R^2)\Phi(\nu)+\nu\sigma_R(2+\nu\sigma_R)}{[\Phi(\nu)+\nu\sigma_R]^2\,(\mathrm{e}^{\nu^2/2}\sqrt{2\pi}\,\nu)} - 1\,, \qquad \text{(E.26)}$$

which in the limit $\nu \to -\infty$ reduces to the background mass variance, σ_R^2 (again, unlike the Kaiser model).

The linear weighted biasing factor (E.16), as explained in the text, can be obtained in the limit of small correlations by Taylor expanding (E.24) up to first order in ω_R. This involves approximations such as

$$\exp\left(-\frac{\nu^2}{(1+\omega_R)}\right) \simeq (1+\nu^2\omega_R)\,\mathrm{e}^{-\nu^2}\ , \tag{E.27}$$

and

$$\mathrm{erfc}\left(\frac{\nu}{\sqrt{2}}\sqrt{\frac{1-\omega_R}{1+\omega_R}}\right) \simeq \mathrm{erfc}\left(\frac{\nu}{\sqrt{2}}\right) + \sqrt{\frac{2}{\pi}}\,\nu\,\omega_R\,\mathrm{e}^{-\nu^2/2}\ . \tag{E.28}$$

We thus obtain equation (E.16).

High threshold ($\nu \gg 1$) relations can be obtained both for $\mu_R(\nu)$ and for the BDF correlation function, provided that $\omega_R \neq 1$. The first integral on the r.h.s. of Eq.(E.25) can be approximated, using Mehler's formula (see Appendix VII.2), by the asymptotic expression

$$\frac{1}{2\sqrt{2\pi}}\int_\nu^\infty d\alpha\,\mathrm{e}^{-\alpha^2/2}\,\mathrm{erfc}\left(\frac{\nu-\alpha\,\omega_R}{\sqrt{2(1-\omega_R^2)}}\right) \approx \frac{\mathrm{e}^{-\nu^2}}{2\pi\nu^2}\,\mathrm{e}^{\nu^2\omega_R}\ , \tag{E.29}$$

while in the second term erfc $x \approx (\pi x^2)^{-1/2}\mathrm{e}^{-x^2}$, for $x \to \infty$. One therefore obtains $\mu_R(\nu) \approx (2\pi\nu^2)^{-1/2}(1+\nu\sigma_R)\,\mathrm{e}^{-\nu^2/2}$, and

$$1+\xi_{\nu,R} \approx \frac{(1+\sigma_R^2\omega_R)\,\mathrm{e}^{\nu^2\omega_R}}{(1+\nu\sigma_R)^2} + \frac{(2+\nu\sigma_R)\nu\sigma_R}{(1+\nu\sigma_R)^2}\sqrt{\frac{(1+\omega_R)^3}{1-\omega_R}}\,\mathrm{e}^{\nu^2\omega_R/(1+\omega_R)}\ . \tag{E.30}$$

In the limit $\sigma_R \to 0$ (actually for $\sigma_R \ll 1/\nu$) at fixed ν and ω_R we recover the Politzer & Wise (1984) relation

$$1+\xi_{\nu,R} \approx \exp(\nu^2\omega_R)\ . \tag{E.31}$$

On the contrary, for $\sigma_R \gg 1$, we get

$$1+\xi_{\nu,R} \approx \sqrt{\frac{(1+\omega_R)^3}{1-\omega_R}}\,\exp[\nu^2\omega_R/(1+\omega_R)]\ , \tag{E.32}$$

which is clearly not affected by the negative mass events of the Gaussian statistics. This also reduces to Eq.(E.31) at large distances ($\omega_R \ll 1$).

Figure Captions

Figure E1. Mass fraction μ_R as a function of ν for the weighted bias model assuming Gaussian (a) and lognormal (b) statistics for various values of σ_R.

Figure E2. Linear biasing factors as a function of ν in the weighted bias model (a) and Kaiser model (b) for underlying Gaussian statistics (c) and lognormal statistics (d). The lines refer to the same values of σ_R as those in Figure E1.

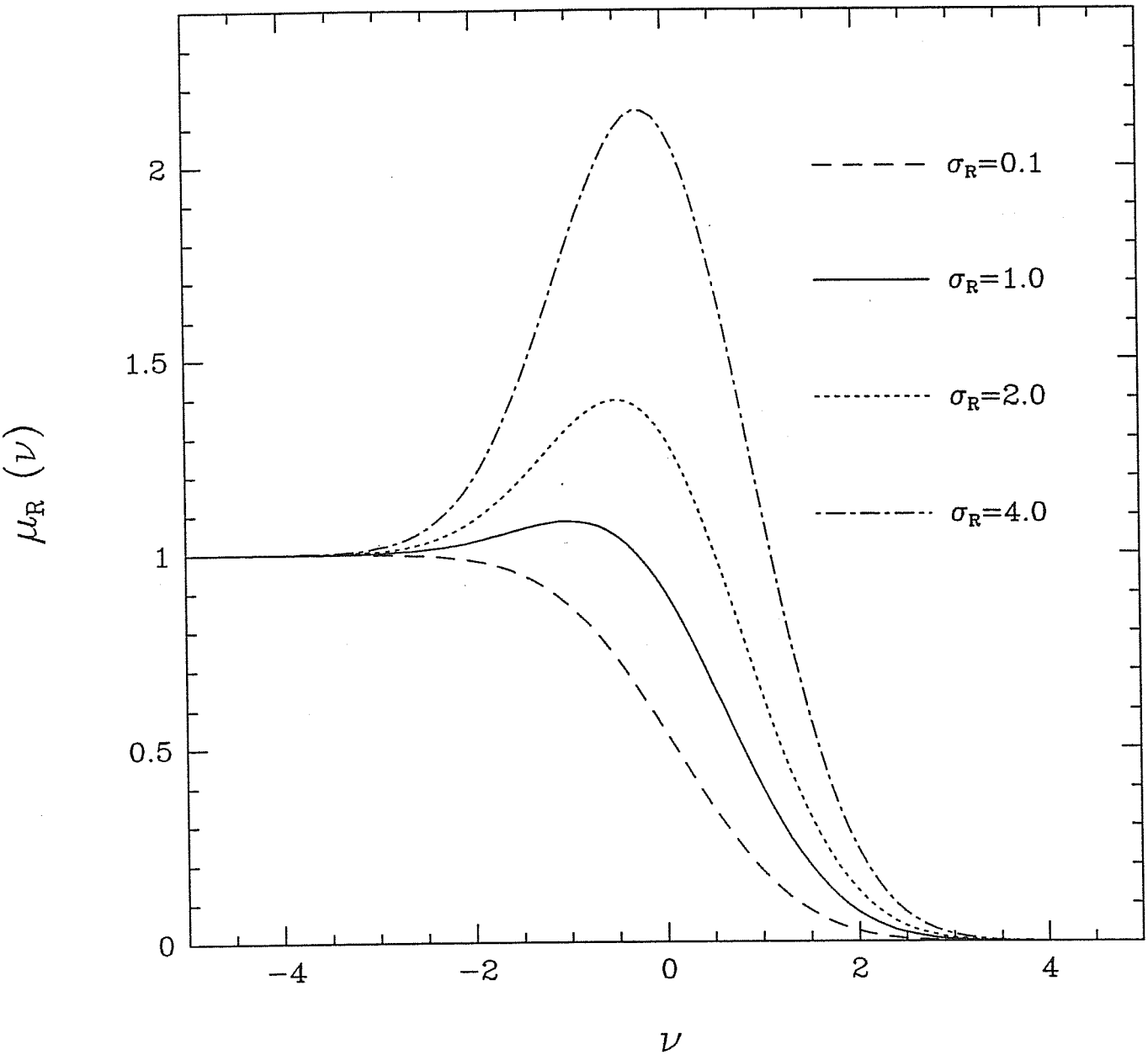
$\mu_R(\nu)$
2
1.5
1
0.5
0
−4
−2
0
2
4
ν
σ_R=0.1
σ_R=1.0
σ_R=2.0
σ_R=4.0

Fig. E1a

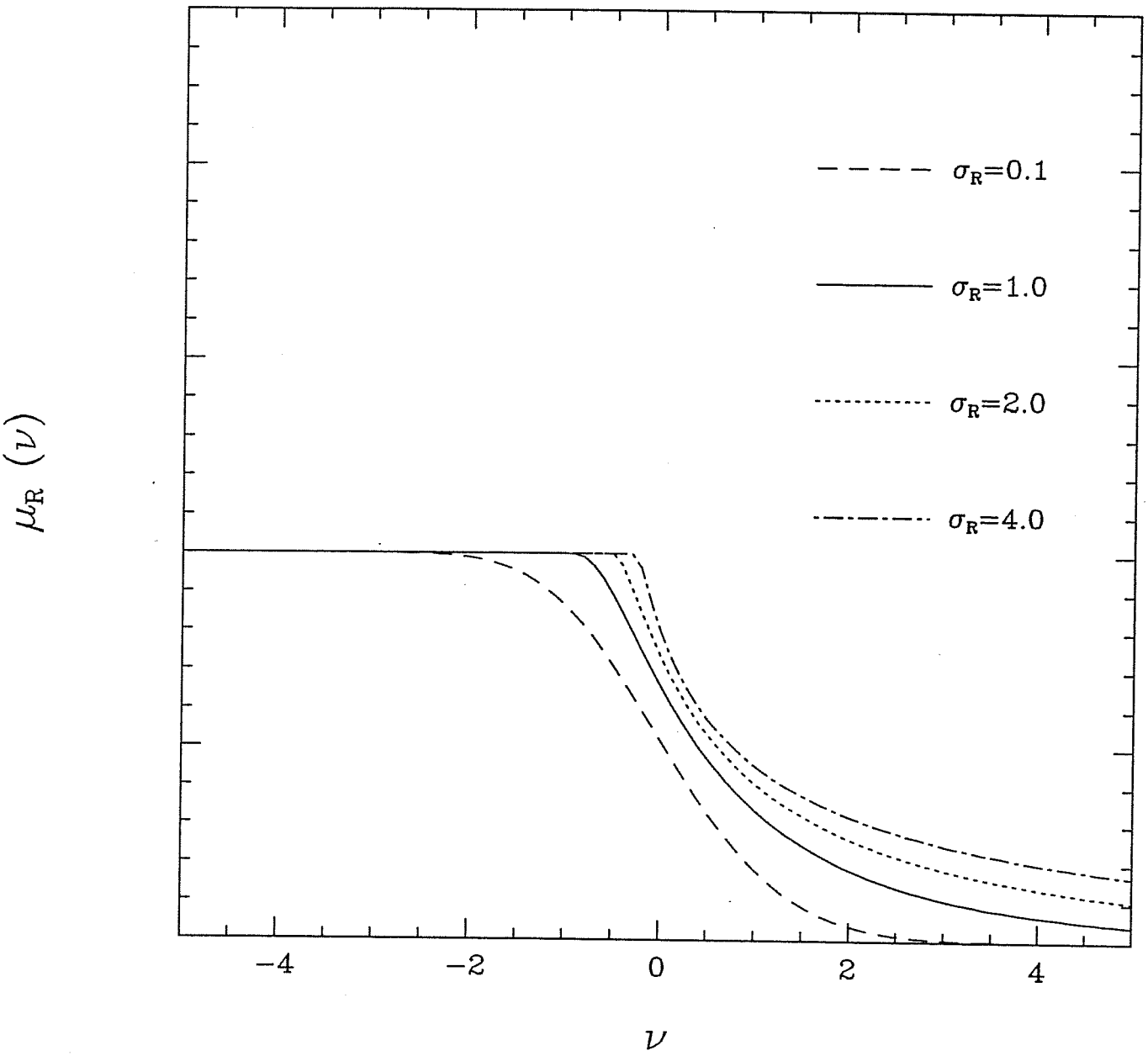

Fig. E1b

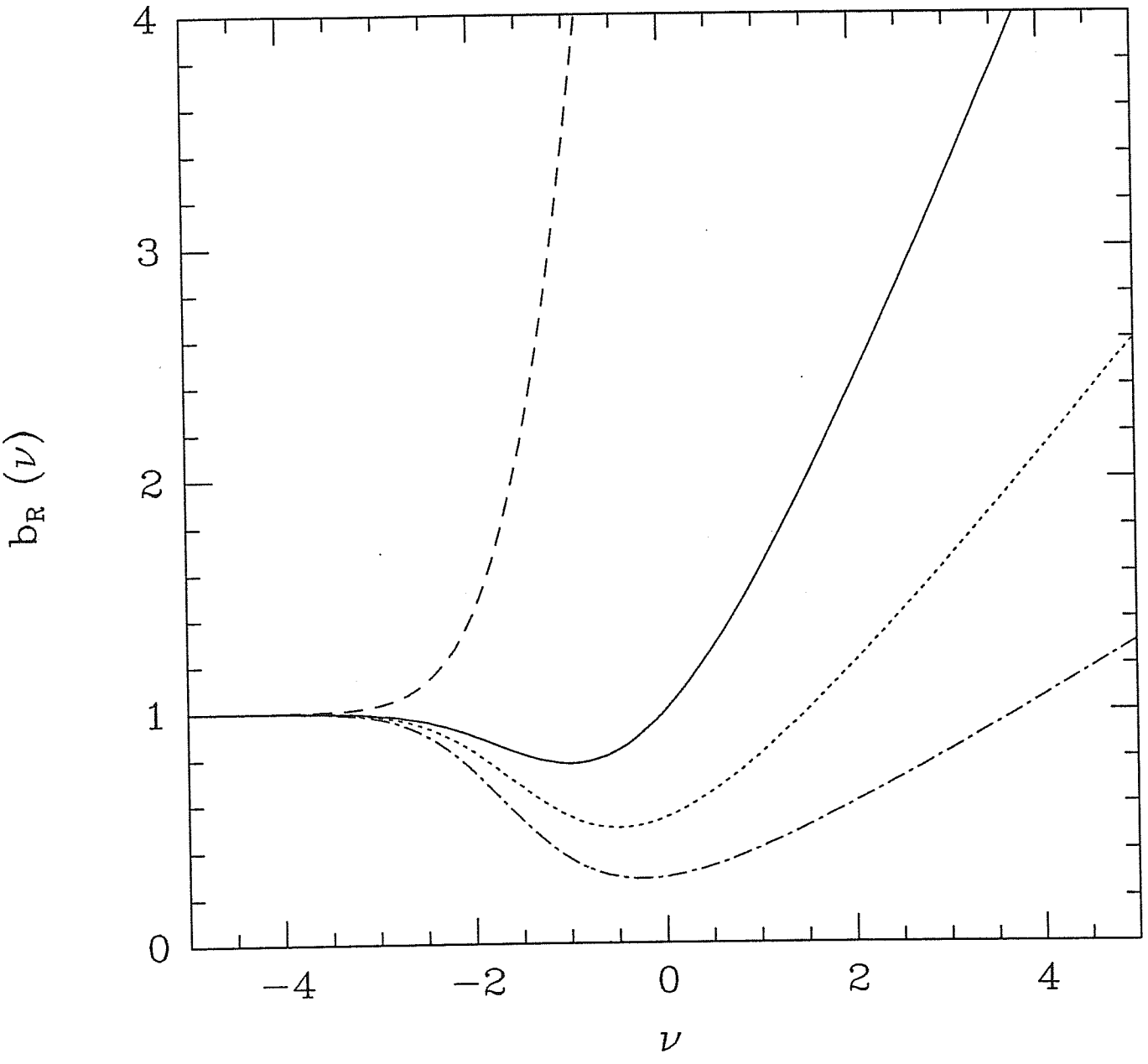

Fig. E2a

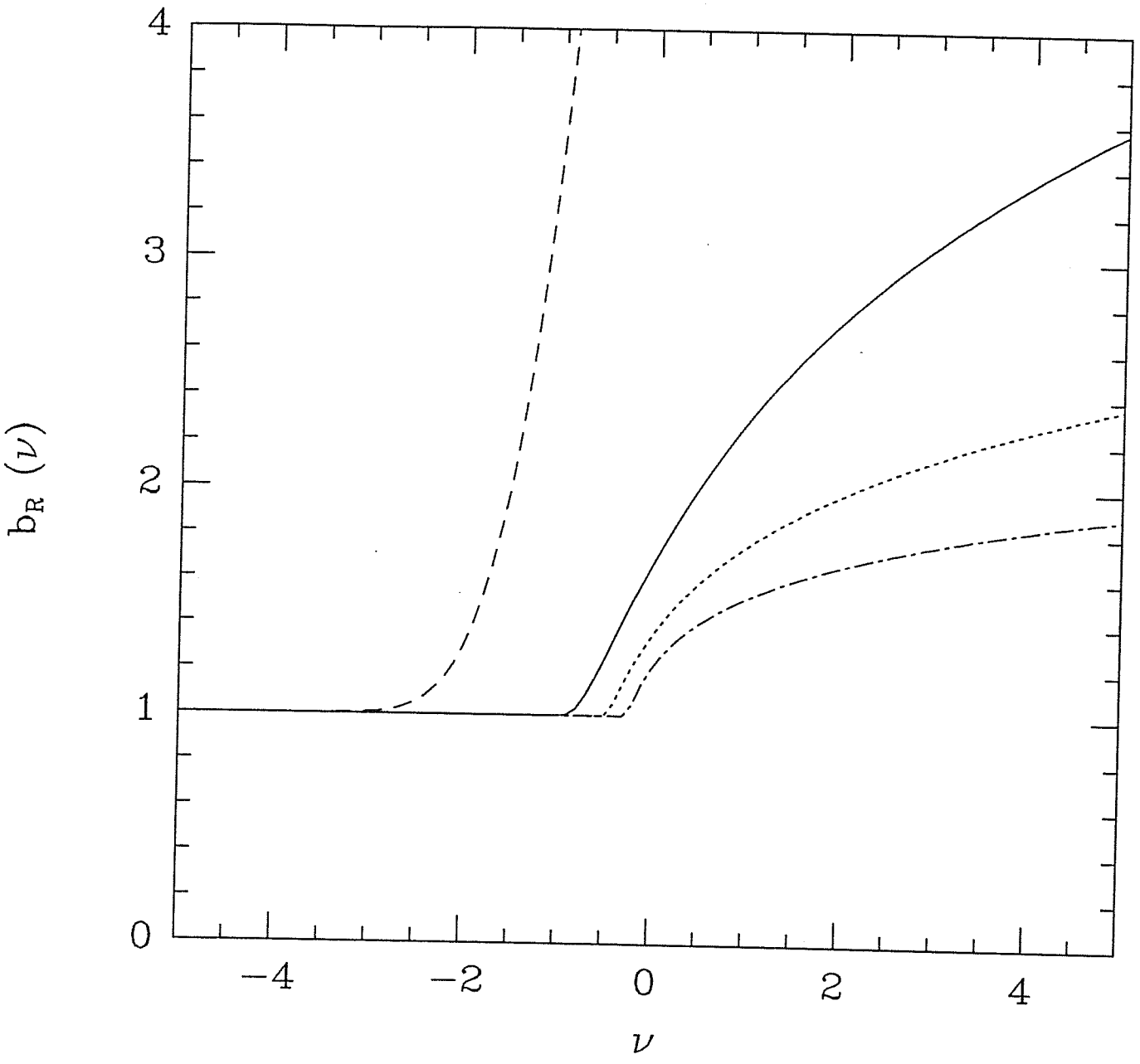

Fig. E2b

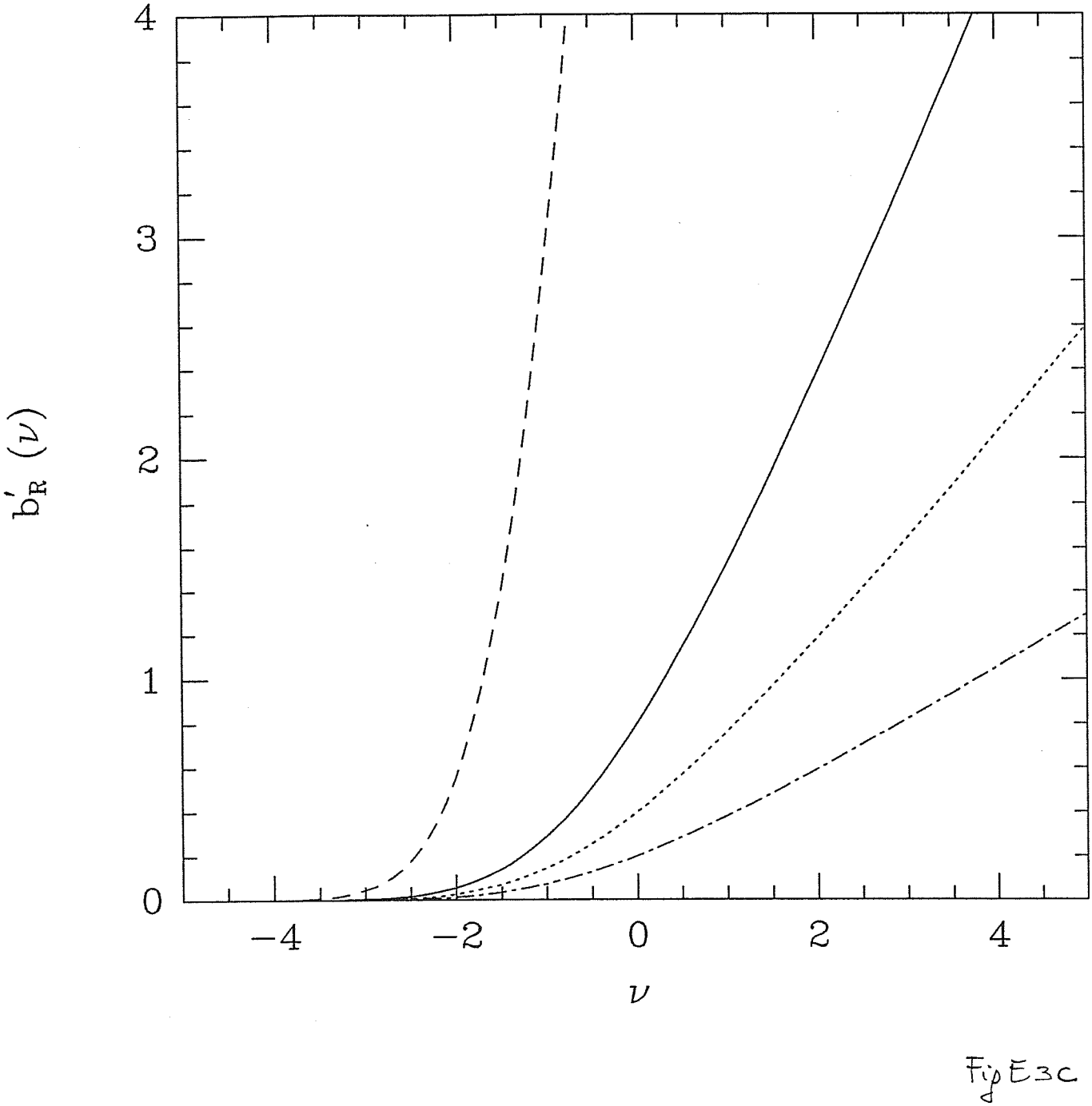

Fig E3c

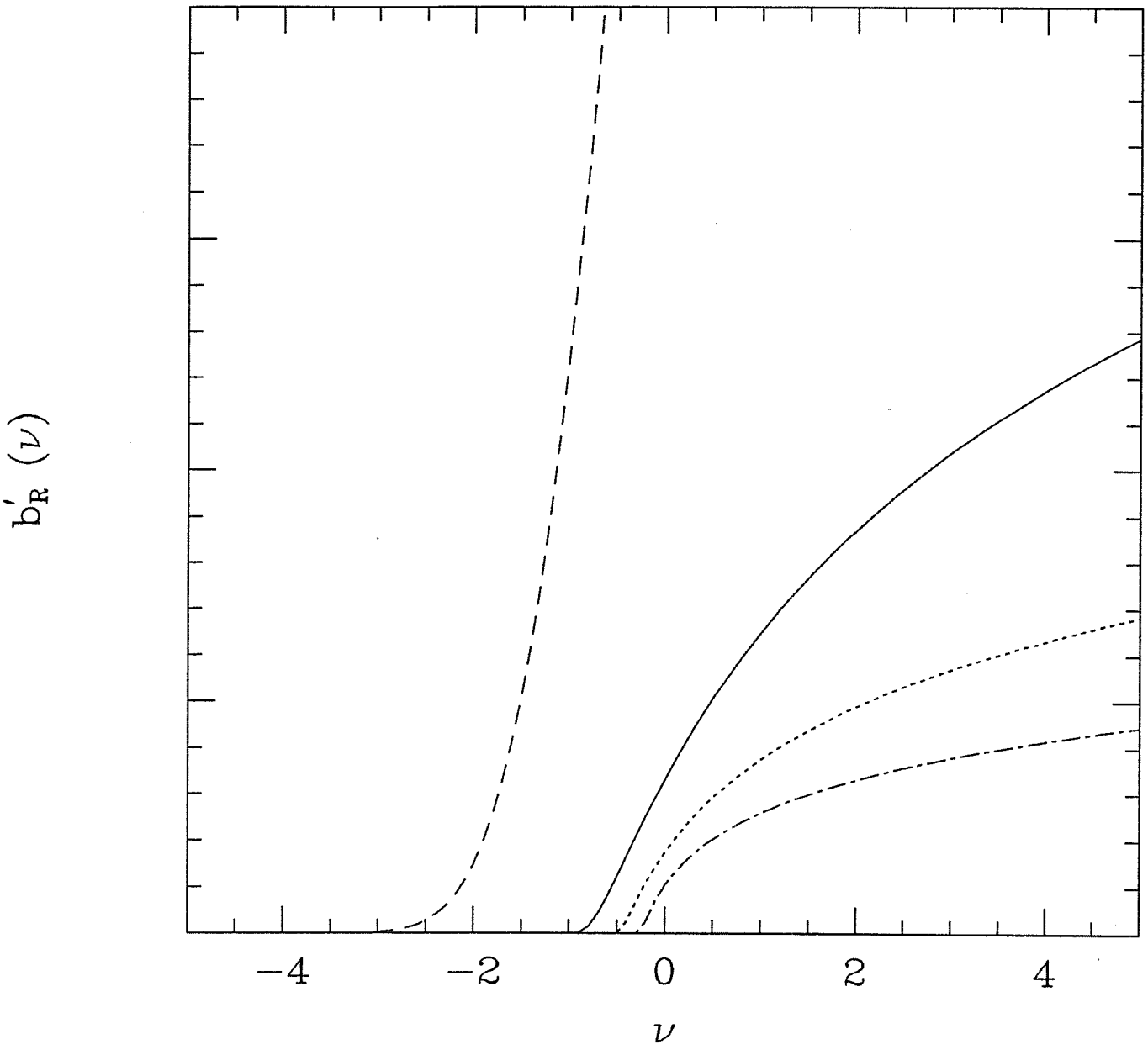

Fig E2d

APPENDIX F

Kurtosis of the Density Field

Kurtosis and Large–Scale Structure

Paolo CATELAN [1] & Lauro MOSCARDINI [4]

[1] *SISSA - International School for Advanced Studies,*
Strada Costiera 11, 34014 Trieste, Italy

[4] *Dipartimento di Astronomia, Università di Padova*
vicolo dell'Osservatorio 5, I–35122 Padova, Italy

– *Astrophysical Journal*, in press –

Summary

We discuss the non–linear growth of the excess kurtosis parameter of the smoothed density fluctuation field δ, $S_4 \equiv [\langle\delta^4\rangle - 3\langle\delta^2\rangle^2]/\langle\delta^2\rangle^3$ in an Einstein–de Sitter universe. We assume Gaussian primordial density fluctuations with scale–free power spectrum $P(k) \propto k^n$ and analyze the dependence of S_4 on primordial spectral index n, after smoothing with a Gaussian filter. As already known for the skewness ratio S_3, the kurtosis parameter is a *decreasing function* of n, both in exact perturbative theory and in the Zel'dovich approximation. The parameter S_4 provides a powerful statistics to test different cosmological scenarios.

Subject headings: Galaxies: clustering – large–scale structure of the Universe

F.1 Introduction

The study of the statistical distribution of the matter in the universe may be a way to address fundamental issues such as the origin and the formation of structures on large scales.
The simplest and most usually accepted hypothesis, supported by the inflationary model, is that the very early distribution is Gaussian. In such a case, the connected N–point correlations (and the N–th order connected moments) with $N > 2$ are zero. However, even if the primordial fluctuations δ are Gaussian, the non–linear time evolution will ensure that the mass density fluctuations become highly non–Gaussian (Peebles 1980; Fry 1984). It is important to understand the nature of the higher moments of the mass density induced by gravity in order to distinguish their effects from those of possible *primordial* non–Gaussian fluctuations: late–time phase transitions, cosmic string models and global textures are indeed models whose statistics may not be described by a Gaussian distribution (see e.g. Vilenkin 1985; Turok 1989; Scherrer & Bertschinger 1991). Moreover, variations of the inflationary model which lead to non–Gaussian primordial fluctuations have been recently discussed (see e.g. Salopek 1992).
A powerful method to distinguish if the non–Gaussian nature of the matter distribution is intrinsic, is to analyze the growth of higher moments, like the skewness or the kurtosis (third and fourth connected moments, respectively) of the density fluctuation field. Peebles (1980) first showed that gravity induces, for an unsmoothed initial Gaussian density field, a skewness ratio $S_3 \equiv \langle\delta^3\rangle/\langle\delta^2\rangle^2 = 34/7$, for any primordial power spectrum. Juszkiewicz, Bouchet, & Colombi (1993) find that the filtering operation actually introduces a dependence of S_3 on the primordial spectral index n; in particular for scale–free spectra, $S_3 = 34/7 - (n+3)$ for a top–hat window function, and a decreasing trend with n is recovered also for a Gaussian filter. Coles *et al.* (1993) investigate, using N–body simulations, the growth of the skewness ratio to

test the hypothesis of Gaussian primordial density fluctuations against possible alternatives. Analytical expressions for S_3 arising from non–linear evolution in perturbation theory have been worked out for arbitrary non–Gaussian models by Fry & Scherrer (1993) and Catelan & Moscardini (1993). Finally, higher order moments are known to depend extremely weakly on the density parameter Ω (see Martel & Freudling 1991; Bouchet *et al.* 1992; Bernardeau 1992).

Here we analyse the dependence of the induced–by–gravity excess kurtosis of the density field, smoothed with a Gaussian filter, namely the parameter $S_4 \equiv [\langle\delta^4\rangle - 3\langle\delta^2\rangle^2]/\langle\delta^2\rangle^3$, on an initial (scale–free) power spectrum $P(k)$. To do this, we take advantage of the exact perturbative technique (Fry 1984; Goroff *et al.* 1986) and the Zel'dovich approximation (see Grinstein & Wise 1987). The kurtosis describes features such as sharpness or stretchiness of the mass distribution and the extent of its rare–event tail. Moreover, it is possibly related to the *initial* sign of the skewness – as predicted in some non–Gaussian models (see e.g. Luo & Schramm 1993) – which is important for the final galaxy clustering pattern (Moscardini *et al.* 1991; Messina *et al.* 1992; Weinberg & Cole 1992).

The layout of this paper is as follows: in Section F2 we review the exact perturbative theory and the Zel'dovich approximation; in Section F3 we discuss the induced–by–gravity kurtosis parameter S_4 of an initial Gaussian density field and its dependence on the primordial spectral index; we state the main conclusions in Section F4.

F.2 Non–Linear Time Evolution

We assume that present–day structures in the universe formed by gravitational instability from Gaussian fluctuations δ in a pressureless fluid with matter density $\rho = \rho_b[1+\delta]$, where ρ_b is the background mean density. The density fluctuation field δ may be written as a Fourier integral, $\delta(\mathbf{x},t) = (2\pi)^{-3}\int d\mathbf{k}\,\tilde{\delta}(\mathbf{k},t)\,\mathrm{e}^{i\mathbf{k}\cdot\mathbf{x}}$, where $\mathbf{x}$ and $\mathbf{k}$ are the *comoving* Eulerian coordinate and wavevector respectively, t is the cosmic time. The power spectrum $P(k)$,

defined as the 2–point correlation function in Fourier space (at a given time), $\langle \tilde{\delta}(\mathbf{k}_1)\,\tilde{\delta}(\mathbf{k}_2)\rangle \equiv (2\pi)^3\,\delta_D(\mathbf{k}_1+\mathbf{k}_2)\,P(k_1)$, fully determines the statistics of the primordial Gaussian density field, whose variance is given by the relation $\sigma^2 = (1/2\pi^2)\int_0^\infty dk\,k^2\,P(k)$.

To bridge the gap between observational data and theory, it is *necessary* to filter the fluctuation field δ by means of a *window function* W_R, $\delta_R(\mathbf{x},t) \equiv \int dy\,\delta(\mathbf{y},t)\,W_R(|\mathbf{x}-\mathbf{y}|)$. In the following we will adopt a Gaussian window function, $W_R(x) = (2\pi R^2)^{-3/2}\,\exp(-x^2/2R^2)$. The mass variance on scale R, σ_R^2, is related to the primordial spectrum $P(k)$ by the integral expression $\sigma_R^2 = (1/2\pi^2)\int_0^\infty dk\,k^2\,P(k)\,[\widetilde{W}_R(k)]^2$, where $\widetilde{W}_R(k)$ is the Fourier transform of $W_R(x)$.

F.2.1 Equations of Motion: Perturbative Theory

The time evolution equations for the matter density fluctuation $\delta(\mathbf{x},t)$ and the peculiar velocity field $\mathbf{v}(\mathbf{x},t)$ are the Poisson equation, the Euler equation and the continuity equation, i.e.

$$\nabla^2\Phi = 4\pi\,G\,\rho_b\,a^2\,\delta\ , \tag{F.1}$$

$$\partial_\circ \mathbf{v} + \frac{1}{a}(\mathbf{v}\cdot\nabla)\,\mathbf{v} + \frac{\dot{a}}{a}\,\mathbf{v} = -\frac{1}{a}\,\nabla\Phi\ , \tag{F.2}$$

$$\partial_\circ\delta + \frac{1}{a}\,\nabla\cdot(1+\delta)\,\mathbf{v} = 0\ . \tag{F.3}$$

Here $\partial_\circ \equiv \partial/\partial t$ and spatial derivatives are with respect to $\mathbf{x}$. We analyze these equations assuming an Einstein–de Sitter universe with vanishing cosmological constant. In such a model, the scale factor a is proportional to $t^{2/3}$ during the matter dominated epoch, and the adiabatic expansion implies that $6\pi\,G\rho_b\,t^2 = 1$. The quantity Φ is the Newtonian gravitational potential. Combining the divergence of the Euler equation with the continuity equation, a second order differential equation for the density contrast δ may be introduced (Peebles 1980)

$$\partial_\circ^2\delta + 2\,\frac{\dot{a}}{a}\,\partial_\circ\delta - 4\pi\,G\rho_b\,\delta = 4\pi\,G\,\rho_b\,\delta^2 + \frac{1}{a^2}\left[\partial_\alpha\delta\,\partial_\alpha\Phi + \partial_\alpha\partial_\beta\,(1+\delta)v^\alpha v^\beta\right]\ . \tag{F.4}$$

The first term in the r.h.s. of Eq.(F.4) corresponds to the spherical collapse of an isolated proto–object, while the "geometrical" term in square brackets describes tidal and shear effects. The linear approximation, adequate when $\delta^2 \ll 1$, corresponds to dropping the r.h.s. of Eq.(F.4). The first order solution has the well–known self–similar form (considering only the growing mode)

$$\delta^{(1)}(\mathbf{x},t) = D(t)\,\delta_1(\mathbf{x})\,, \tag{F.5}$$

where $D(t) \propto a(t)$ is the time growth factor of the mass fluctuations. Higher order approximations of the solution of Eq.(F.4) may be recovered if one expands the mass density fluctuation field $\delta(\mathbf{x},t)$ about the background solution $\delta = 0$ (and $\mathbf{v} = \mathbf{0}$), namely $\delta = \sum_n \delta^{(n)}$ with $\delta^{(n)} = O(\delta_1^n)$, then solving the differential equation for any $\delta^{(n)}$ (Peebles 1980; Fry 1984). The perturbative expansion for δ is (e.g. Goroff *et al.* 1986)

$$\delta(\mathbf{x},t) = \sum_{n=1}^{\infty} [D(t)]^n\,\delta_n(\mathbf{x})\,. \tag{F.6}$$

The first term of the expansion corresponds to the linear approximation. Second and third order solutions have been discussed by Peebles (1980) and Fry (1984) respectively. We see that the scale factor $D(t)$ acts as a coupling constant in this perturbative approach, since $\delta^{(n)} \propto D^n$.

Here we review the exact perturbative technique to solve approximately the equations of motion of a pressureless gravitational fluid up to third order in the density fluctuation field. In particular, we will use the third order solution to compute the fourth order moment (namely the kurtosis parameter S_4). We use explicitly the same notation of Fry (1984).

(i) Second Order Density Solution

The second order contribution $\delta^{(2)}$ is related to the second order gravitational potential $\Phi^{(2)}$ by the Poisson equation $\nabla^2\Phi^{(2)} = 4\pi G a^2 \rho_b\,\delta^{(2)}$; it is solution of the differential equation

$$\partial_\circ^2\delta^{(2)} + 2\dot{a}a^{-1}\partial_\circ\delta^{(2)} - 4\pi G\rho_b\,\delta^{(2)} = \left[4\pi G\rho_b + \left(\frac{\dot{D}}{D}\right)^2\right]\delta^{(1)\,2} +$$

$$+ \left[4\pi G\rho_b + 2\left(\frac{\dot{D}}{D}\right)^2\right]\partial_\alpha\delta^{(1)}\,\partial_\alpha\triangle^{(1)} + \left(\frac{\dot{D}}{D}\right)^2\partial_\alpha\partial_\beta\triangle^{(1)}\,\partial_\alpha\partial_\beta\triangle^{(1)}\,, \tag{F.7}$$

where $\triangle^{(1)}$ is the rescaled linear gravitational potential defined by $\triangle^{(1)} \equiv \Phi^{(1)}/4\pi G\rho_b\, a^2$, for which $\nabla^2\triangle^{(1)} = \delta^{(1)}$. Each side of Eq.(F.7) is homogeneous in powers of t. For an Einstein–de Sitter universe, noting that $D^2 \propto \delta^{(2)} \equiv D^2(t)\,\delta_2(\mathbf{x})$, the solution of Eq.(F.7) is given by (Peebles 1980, §18; strictly, our definition of $\triangle^{(1)}$ differs from the Peebles' one by a factor -4π)

$$\delta^{(2)} = \frac{5}{7}\,\delta^{(1)2} + \partial_\alpha\delta^{(1)}\,\partial_\alpha\triangle^{(1)} + \frac{2}{7}\,\partial_\alpha\partial_\beta\triangle^{(1)}\,\partial_\alpha\partial_\beta\triangle^{(1)}\,. \tag{F.8}$$

Note that $\langle\delta^{(2)}\rangle = 0$, i.e. mass is conserved to second order. We see from Eq.(F.8) that the behaviour of δ at second order is non–local: the mass fluctuation at the position $\mathbf{x}$ depends on initial perturbations at other positions via $\triangle^{(1)}$. Physically this means that, unlike the linear local case, when density fluctuations grow in amplitude their spatial dependence, in comoving coordinates, changes. Thus, the gravitational field changes direction and particles are not accelerated in a fixed direction, as it occurs in linear regime. The last term in right–hand side of Eq.(F.8) corresponds to the velocity shear contribution.

We can obtain the Fourier transform $\tilde\delta^{(2)}$ directly from the differential equation (F.8). Explicitly (time dependence is understood),

$$\tilde\delta^{(2)}(\mathbf{k}) = \int \frac{d\mathbf{k}'}{(2\pi)^3}\; J^{(2)}(\mathbf{k}',\mathbf{k}-\mathbf{k}')\;\tilde\delta^{(1)}(\mathbf{k}')\,\tilde\delta^{(1)}(\mathbf{k}-\mathbf{k}')\,, \tag{F.9}$$

where we have defined the kernel

$$J^{(2)}(\mathbf{k},\mathbf{k}') \equiv \frac{5}{7} + \frac{\mathbf{k}\cdot\mathbf{k}'}{k'^2} + \frac{2}{7}\left(\frac{\mathbf{k}\cdot\mathbf{k}'}{k\,k'}\right)^2\,. \tag{F.10}$$

(ii) Third Order Density Solution

The third order approximation $\delta^{(3)}$ is solution of the differential equation

$$\partial_\circ^2\delta^{(3)} + 2\dot a a^{-1}\partial_\circ\delta^{(3)} - 4\pi G\rho_b\,\delta^{(3)} = 8\pi G\rho_b\,\delta^{(1)}\,\delta^{(2)} +$$

$$+\, a^{-2}\left(\partial_\alpha\delta^{(1)}\,\partial_\alpha\Phi^{(2)} + \partial_\alpha\delta^{(2)}\,\partial_\alpha\Phi^{(1)}\right) + a^{-2}\,\partial_\alpha\partial_\beta\left(2\,v^{(1)\alpha}v^{(2)\beta} + \delta^{(1)}\,v^{(1)\alpha}\,v^{(1)\beta}\right)\,. \tag{F.11}$$

In this case, working directly in Fourier space is much simpler. Since $\delta^{(3)} \propto D^3 \propto t^2$, we have $\partial_\circ^2\tilde\delta^{(3)} + 2\dot a a^{-1}\partial_\circ\tilde\delta^{(3)} - 4\pi G\rho_b\,\tilde\delta^{(3)} = 4\,\tilde\delta^{(3)}/t^2$; by using the second order results it is not

difficult to show that (Fry 1984)

$$\tilde{\delta}^{(3)}(\mathbf{k}) = \int \frac{d\mathbf{k}_1\, d\mathbf{k}_2\, d\mathbf{k}_3}{(2\pi)^6}\, \delta_D(\mathbf{k}_1+\mathbf{k}_2+\mathbf{k}_3-\mathbf{k})\, J^{(3)}(\mathbf{k}_1,\mathbf{k}_2,\mathbf{k}_3)\, \tilde{\delta}^{(1)}(\mathbf{k}_1)\, \tilde{\delta}^{(1)}(\mathbf{k}_2)\, \tilde{\delta}^{(1)}(\mathbf{k}_3)\ , \quad \text{(F.12)}$$

where the third order kernel is

$$J^{(3)}(\mathbf{k}_1,\mathbf{k}_2,\mathbf{k}_3) \equiv J^{(2)}(\mathbf{k}_2,\mathbf{k}_3) \left[\frac{1}{3} + \frac{1}{3}\,\frac{\mathbf{k}_1\cdot(\mathbf{k}_2+\mathbf{k}_3)}{(\mathbf{k}_2+\mathbf{k}_3)^2} + \frac{4}{9}\,\frac{\mathbf{k}\cdot\mathbf{k}_1}{k_1^2}\,\frac{\mathbf{k}\cdot(\mathbf{k}_2+\mathbf{k}_3)}{(\mathbf{k}_2+\mathbf{k}_3)^2}\right] +$$

$$- \frac{2}{9}\,\frac{\mathbf{k}\cdot\mathbf{k}_1}{k_1^2}\,\frac{\mathbf{k}\cdot(\mathbf{k}_2+\mathbf{k}_3)}{(\mathbf{k}_2+\mathbf{k}_3)^2}\,\frac{(\mathbf{k}_2+\mathbf{k}_3)\cdot\mathbf{k}_3}{k_3^2} + \frac{1}{9}\,\frac{\mathbf{k}\cdot\mathbf{k}_2}{k_2^2}\,\frac{\mathbf{k}\cdot\mathbf{k}_3}{k_3^2}\ . \quad \text{(F.13)}$$

It is clear from Eq.(F.11) that, in order to derive the solution $\delta^{(3)}$, we need to know explicitly the second order velocity $\mathbf{v}^{(2)}$. This is given by

$$\mathbf{v}^{(2)} = a\,\frac{\dot{D}}{D}\left[\delta^{(1)}\,\nabla\triangle^{(1)} - 2\,\nabla\triangle^{(2)}\right]\ , \quad \text{(F.14)}$$

where $\triangle^{(2)} \equiv \Phi^{(2)}/4\pi G\rho_b\, a^2$ is the rescaled second order gravitational potential. [In the solution (F.14) we neglect an additive term whose divergence is zero.] In an Einstein–de Sitter universe $\mathbf{v}^{(2)} \sim t$, slower than $\delta^{(2)} \sim t^{4/3}$. We stress the fact that $\mathbf{v}^{(2)}$ is *not* parallel to the second order acceleration $[\propto -\nabla\triangle^{(2)}]$: this is a consequence of non–locality. Finally, we note that $\mathbf{v}^{(2)}$ is known only once $\delta^{(2)}$ is known.

(iii) General Solution

As Goroff *et al.* (1986) have shown, the (Fourier transformed) n–th order mass fluctuation term may be represented in integral form as

$$\tilde{\delta}_n(\mathbf{k}) = \left\{\prod_{h=1}^{n}\int \frac{d\mathbf{k}_h}{(2\pi)^3}\,\tilde{\delta}_1(\mathbf{k}_h)\right\}\left[(2\pi)^3\delta_D(\sum_{j=1}^{n}\mathbf{k}_j - \mathbf{k})\right] J^{(n)}(\mathbf{k}_1,\ldots,\mathbf{k}_n)\ . \quad \text{(F.15)}$$

The presence of the Dirac delta function comes from momentum conservation in Fourier space. The kernels $J^{(n)}$ are symmetric homogeneous (with degree 0) functions of the wavevectors $\mathbf{k}_1,\ldots,\mathbf{k}_n$, describing the effects of non–linear collapse (tidal and shear forces). In general $J^{(n)}$ are very complicated for $n > 3$. [A discussion of the properties of the kernels $J^{(n)}$ is given in Wise (1988). Explicit recursion relations with their Feynman diagrammatic representation are given by Goroff *et al.* (1986) and Wise (1988).]

In the *Zel'dovich approximation* (Zel'dovich 1970) the motion of particles from the initial comoving (Lagrangian) positions $\mathbf{q}$ is approximated by straight paths. The Eulerian position at time t is then given by the uniform motion

$$\mathbf{x}[\mathbf{q},t] = \mathbf{q} + D(t)\,\mathbf{S}(\mathbf{q})\,, \tag{F.16}$$

where $D(t)$ is the growth factor of linear density perturbations and $\mathbf{S}(\mathbf{q})$ is the displacement vector related to the primordial velocity field. The Zel'dovich approximation provides an exact solution of the equations of motion for one–dimensional perturbations, and reduces to the linear approximation when δ and $\mathbf{v}$ are small. In general, the Zel'dovich approximation is not an exact solution of the equations of motion, in that in a finite time particles converge into singular regions of infinite density (caustics), and the map in Eq.(F.16) becomes multi–valued. The treatment of these formal singularities is the main problem to solve during the highly non–linear stage of structure formation. Smoothing on a suitable scale R partially solves this problem. Grinstein & Wise (1987) give an Eulerian representation of the Zel'dovich approximation by a diagrammatic perturbative approach similar to that of the previous section. They showed that the n–th order perturbative corrections $\delta_n(\mathbf{x})$, when the density fluctuation field δ is evolved according to the Zel'dovich approximation, are such that

$$\delta(\mathbf{x},t) = \sum_{n=1}^{\infty} \frac{(-1)^n}{n!}\,[D(t)]^n \sum_{[h_n]=1}^{3} \frac{\partial}{\partial x_{h_1}} \cdots \frac{\partial}{\partial x_{h_n}} \left[S_{h_1} \cdots S_{h_n} \right] . \tag{F.17}$$

Here $\sum_{[h_n]} \equiv \sum_{h_1} \cdots \sum_{h_n}$. Note that the first term recovers the linear approximation, in that $\mathbf{S} = \mathbf{v}_1$, where $\delta_1(\mathbf{x}) = -\nabla \cdot \mathbf{v}_1$. The perturbative expansion for δ of Eq.(F.17) simply corresponds to calculate different symmetric kernels $J_{ZA}^{(n)}$. These can be written in the following compact form

$$J_{ZA}^{(n)}(\mathbf{k}_1,\ldots,\mathbf{k}_n) = \frac{1}{n!} \prod_{h=1}^{n} \frac{\mathbf{k}\cdot\mathbf{k}_h}{k_h^2}\,, \tag{F.18}$$

where $\mathbf{k} \equiv \sum_{h=1}^{n} \mathbf{k}_h$. Note that, unlike the perturbative case, the kernels $J_{ZA}^{(n)}$ are manifestly symmetric by construction.

F.3 Kurtosis of the Density Field

In this section, we compute the induced–by–gravity kurtosis parameter S_4 of an initial Gaussian density field in a flat universe. The lowest order nonvanishing connected contribution to S_4 is

$$\langle \delta^{(1)\,2} \rangle^3 \, S_4 \, = \, 6 \, \langle \, \delta^{(1)\,2} \, \delta^{(2)\,2} \, \rangle_c \, + \, 4 \, \langle \, \delta^{(1)\,3} \, \delta^{(3)} \, \rangle_c \, . \tag{F.19}$$

Note that there are two corrections (each one $\sim \delta_1^6$) to the density kurtosis, for which we need up to the *third*–order perturbative approximation. Therefore, in a sense, we disagree with the conclusions of Luo & Schramm (1993), who assert that the kurtosis of an evolved Gaussian distribution remains zero to second–order perturbative theory, in that they neglect the first non–zero contribution δ_1^6 correctly identified here [see the first connected term in the right hand side of Eq.(F.19) and the calculations leading to their Eq.(3.13)].

From Eqs.(F.10) and (F.13), after tedious but straightforward algebra, one finally gets the integral expression of the kurtosis ratio,

$$S_4 = \frac{24}{\sigma^6} \int \frac{d\mathbf{k}_1 \, d\mathbf{k}_2 \, d\mathbf{k}_3}{(2\pi)^9} \; P(k_1) \, P(k_2) \, \Big[P(k_3) \, J^{(3)}(\mathbf{k}_1, \mathbf{k}_2, \mathbf{k}_3) \, + \\ + 2 \, J^{(2)}(-\mathbf{k}_2, \mathbf{k}_2 + \mathbf{k}_3) \, J^{(2)}(\mathbf{k}_1, \mathbf{k}_2 + \mathbf{k}_3) \, P(|\mathbf{k}_2 + \mathbf{k}_3|) \Big] \; . \tag{F.20}$$

The expression in the Zel'dovich approximation is obtained by substituting the kernels $J^{(n)}$ with the corresponding $J^{(n)}_{Z.A.}$ in the previous relation. The angular integrations in Eq.(F.20) may be analytically performed. One obtains $S_4 = 60,712/1,323 \approx 45.9$ in the perturbative case (Fry 1984; Bernardeau 1992) and $S_4 = 88/3 \approx 29.3$ in the Zel'dovich approximation. These unsmoothed–case results are independent of the primordial spectral index, as is the skewness ratio S_3.

The kurtosis of the smoothed density field δ_R in the exact perturbative case is

$$S_4(R) = \frac{24}{\sigma_R^6} \int \frac{d\mathbf{k}_1 \, d\mathbf{k}_2 \, d\mathbf{k}_3}{(2\pi)^9} \; \widetilde{W}_R(k_1) \, \widetilde{W}_R(k_2) \, \widetilde{W}_R(k_3) \, \widetilde{W}_R(|\mathbf{k}_1 + \mathbf{k}_2 + \mathbf{k}_3|) \times \\ P(k_1) \, P(k_2) \, \Big[P(k_3) \, J^{(3)}(\mathbf{k}_1, \mathbf{k}_2, \mathbf{k}_3) \, + \, 2 \, J^{(2)}(-\mathbf{k}_2, \mathbf{k}_2 + \mathbf{k}_3) \, J^{(2)}(\mathbf{k}_1, \mathbf{k}_2 + \mathbf{k}_3) \, P(|\mathbf{k}_2 + \mathbf{k}_3|) \Big] \; ; \tag{F.21}$$

again the substitution $J^{(n)} \rightarrow J_{ZA}^{(n)}$ leads to the corresponding expression in the Zel'dovich approximation. Note that $P(k)$ completely describes the process of growth of mass fluctuations from Gaussian initial perturbations.

We calculate the previous integrals, by an Adaptive Multidimensional Monte Carlo Integration subroutine, for scale–free power spectra $P(k) \propto k^n$ with n in the range $-3 \leq n \leq 1$. Due to the assumed primordial scale–invariance, S_4 only depends on the primordial spectral index n, and not on the scale R. In Figure F1, we plot the kurtosis ratio S_4 of the Gaussian–smoothed density field versus the spectral index n, for both the perturbative and Zel'dovich approximations. The main conclusions are drawn in the next section.

F.4 Discussion and Conclusions

From the analysis of Figure F1, it clearly appears that S_4 *strongly* depends on the primordial spectral index n. In particular the kurtosis parameter is a *decreasing* function of n. This is also confirmed by Bernardeau (1993), who, applying the exact perturbative technique, finds a similar trend in the case of top–hat filtering. An anticorrelation with the amount of small–scale power has also been found for the skewness parameter S_3 (Fry 1984; Juszkiewicz, Bouchet, & Colombi 1993), and it seems therefore a general property of higher order moments of the smoothed matter distribution: larger values of n correspond indeed to higher power on small scales, where the filtering operation acts.

Furthermore, the Zel'dovich approximation underestimates the induced–by–gravity S_4 w.r.t. the rigorous perturbative one, as already noted by Grinstein & Wise 1987 (although in the framework of the "standard" cold dark matter model). This is hardly surprising, since the Zel'dovich approximation fails to fully describe the gravitational effects causing particle trajectories to depart from their original directions. It results that the Zel'dovich approximation makes higher orders in the perturbative series for δ smaller on *large* scales than they actually are (see e.g. Wise 1988).

Finally, note that the values for the kurtosis measured at a point, $S_4 = 60,712/1,323$ for full gravitational instability and $S_4 = 88/3$ for the Zel'dovich approximation, tend to match the Gaussian windowed values for $n = -3$. The underlying reason is that for $n = -3$, which originates an infrared logarithmic divergence in any connected density correlation, all the power is transferred on (very) large scales, beyond any reasonable filtering scale.

We stress that, due to the importance of the smoothing procedure, but also to its arbitrariness, one must be cautious about making quantitative comparisons between our results and both observational and N–body data. A Gaussian filter is used for instance by Saunders *et al.* (1991), who however estimated only the skewness in the QDOT–*IRAS* catalog. The only observational estimates up–to–now of the kurtosis of the galaxy distribution are obtained by counts–in–cells, corresponding to a top–hat filtering (Gaztañaga 1992; Bouchet *et al.* 1993; Fry & Gaztañaga 1993); a similar method is applied by Lahav *et al.* (1993) and Lucchin *et al.* (1993) in N–body simulations with scale–free power spectra. Very recently, using N–body simulations with $n = -1$, Juszkiewicz *et al.* (1993) have found $S_4 = 20$ by a good eye–fit to their Gaussian smoothed results, which is in excellent agreement with our evaluation.

Our results can be used to constrain both the probability distribution and the power spectrum of primordial density fluctuations and thus help to select the most reliable mechanism for the generation of large–scale structures.

Acknowledgments

Sabino Matarrese is warmly thanked for addressing our attention to the cosmological density kurtosis, and for carefully reading the manuscript. PC acknowledges Robert J. Scherrer for his kind hospitality at the Ohio State University, Columbus, where part of this work begun. We thank the anonymous referee for his suggestions which improved the presentation of our results. This work has been supported by Italian MURST.

References of the Appendix F

Bernardeau, F. 1992, ApJ, 392, 1

Bernardeau, F. 1993, in preparation

Bouchet, F.R., Juszkiewicz, R., Colombi, S., & Pellat, R. 1992, ApJ, 394, L5

Bouchet, F.R., Strauss, M., Davis, M., Fisher, K.B., Yahil, A., & Huchra, J.P. 1993, ApJ, in press

Catelan, P., & Moscardini, L. 1993, in preparation

Coles, P., Moscardini, L., Lucchin, F., Matarrese, S., & Messina, A. 1993, MNRAS, 264, 749

Fry, J.N. 1984, ApJ, 279, 499

Fry, J.N., & Gaztañaga, E. 1993, preprint

Fry, J.N., & Scherrer, R.J. 1993, preprint

Gaztañaga, E. 1992, ApJ, 398, L17

Goroff, M.H., Grinstein, B., Rey, S.–J., & Wise, M.B. 1986, ApJ, 311, 6

Grinstein, B., & Wise, M.B. 1987, ApJ, 314, 448

Juszkiewicz, R., Bouchet, F.R., & Colombi, S. 1993, ApJ, 412, L9

Juszkiewicz, R., Weinberg, D.H., Amsterdamsky, P., Chodorowsky, M., & Bouchet, F.R. 1993, preprint

Lahav, O., Itoh, M., Inagaki, S., & Suto, Y. 1993, ApJ, 402, 387

Lucchin, F., Matarrese, S., Melott, A.L., & Moscardini, L. 1993, ApJ, in press

Luo, X.C., & Schramm, D.N. 1993, ApJ, 408, 33

Martel, H., & Freudling, W. 1991, ApJ, 371, 1

Messina, A., Lucchin, F., Matarrese, S., & Moscardini, L. 1992, Astroparticle Phys., 1, 99

Moscardini, L., Matarrese, S., Lucchin, F., & Messina, A. 1991, MNRAS, 248, 424

Peebles, P.J.E. 1980, The Large Scale Structure of the Universe (Princeton: Princeton Univ. Press)

Salopek, D.S. 1992, Phys. Rev., D45, 1135

Saunders, W., *et al.* 1991, Nature, 349, 32

Scherrer, R.J., & Bertschinger, E. 1991, ApJ, 381, 349

Turok, N. 1989, Phys. Rev. Lett., 63, 2625

Vilenkin, A. 1985, Phys. Rep., 121, 263

Weinberg, D.H., & Cole, S. 1992, MNRAS, 259, 652

Wise, M.B. 1988, in The Early Universe, ed. W.G. Unruh & G.W. Semenoff, Reidel Pub., p.215

Zel'dovich, Ya.B. 1970, A&A, 5, 160

Figure caption

Figure F1. The kurtosis ratio S_4 of the density field for power–law spectra $P(k) \propto k^n$ and Gaussian filter versus the primordial spectral index n, for both the perturbative (squares and solid line) and Zel'dovich approximations (triangles and dotted line). Note that the values at $n = -3$ correspond to the unsmoothed cases. Error bars refer to the associated uncertainty estimate from the Monte Carlo Integration.

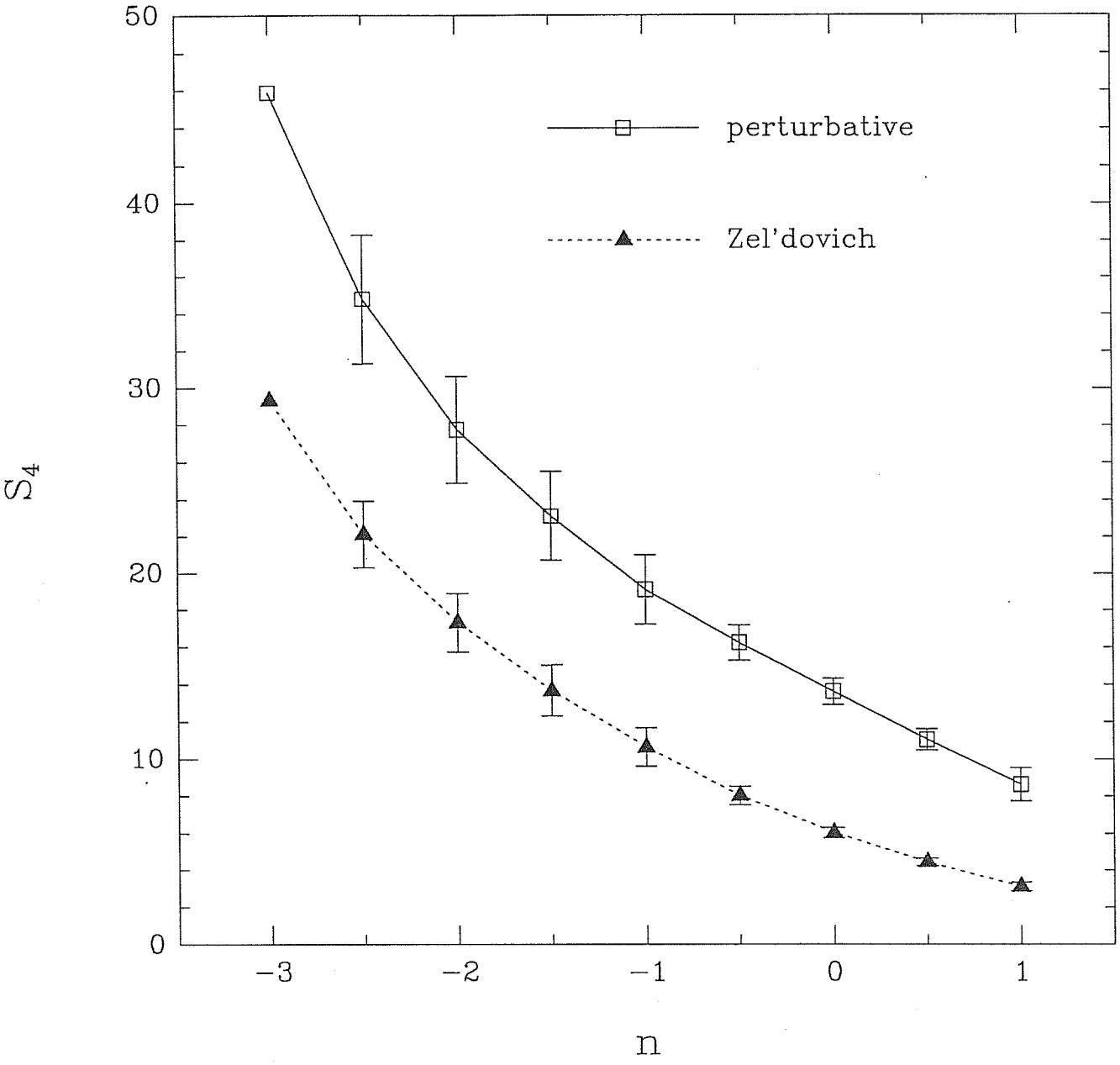

Fig. F1

APPENDIX G

Kurtosis of the Velocity Field

Kurtosis as a Non–Gaussian Signature of the Large–Scale Velocity Field

Paolo CATELAN [1] & Lauro MOSCARDINI [4]

[1] *SISSA - International School for Advanced Studies,*
Strada Costiera 11, 34014 Trieste, Italy

[4] *Dipartimento di Astronomia, Università di Padova*
vicolo dell'Osservatorio 5, I–35122 Padova, Italy

– *Astrophysical Journal Letters*, to be submitted –

Summary

We discuss the non–linear growth of the kurtosis $S_{4,v}$ of the smoothed peculiar velocity field (along an arbitrary direction $\widehat{\alpha}$), in an Einstein–de Sitter universe. We assume Gaussian primordial density fluctuations with scale–free power spectrum $P(k) \propto k^n$, with $-1 \leq n \leq 1$, and analyze the dependence of $S_{4,v}$ on primordial spectral index n, after smoothing with a Gaussian filter. The velocity kurtosis is positive and roughly constant for any value of n in exact perturbative theory but it is consistent with zero in the Zel'dovich approximation. The parameter $S_{4,v}$ provides a powerful statistics to test different cosmological models.

Subject headings: Galaxies: clustering – large–scale structure of the Universe

G.1 Introduction

In the past decade astronomers and cosmologists devoted a great effort to measure large–scale deviations from the Hubble flow and to interpret the cosmological inferences. Redshift–independent distance estimators and all–sky catalogs of galaxy redshifts allowed to estimate the (radial) peculiar motions of galaxies. Undertaking detailed maps of the peculiar velocity field allows for example to make dynamical estimates of the density parameter Ω_o, to test the primordial density fluctuation power spectrum $P(k)$, and to measure directly the underlying total (luminous plus dark) mass distribution, once the gravitational instability picture is assumed (for a review see e.g. Gunn 1989).

The *statistical* properties of the large–scale motions may be described in terms of the peculiar velocity correlation tensor (Górski *et al.* 1989; Groth, Juszkievicz, & Ostriker 1989; Tormen *et al.* 1993) and/or the central moments of the velocity probability distribution function (pdf) $p(\mathbf{v})$. Assuming that the very early density pdf is Gaussian, it results that, during the linear regime, $p(\mathbf{v})$ is a Gaussian too, with mean $\langle \mathbf{v} \rangle = \mathbf{0}$ and variance $\sigma_{\mathbf{v}}^2 = (H_o^2 \Omega_o^{1.2}/2\pi^2) \int_0^\infty dk\, P(k)$, H_o being the Hubble constant. Even if the primordial density field is Gaussian distributed, the non–linear time evolution will ensure that the mass density fluctuations δ become highly non–Gaussian (Peebles 1980; Fry 1984; Goroff *et al.* 1986; Juszkiewicz, Bouchet, & Colombi 1993; Catelan & Moscardini 1993), this implying a modification of the original Gaussian pdf $p(\mathbf{v})$. However, due to the isotropy of the cosmological velocity field, it is expected that *all* the *odd* moments of $p(\mathbf{v})$ remain zero during the growth of the density fluctuations. A particular case is the third central moment, the velocity skewness, discussed for example in Ruamsuwan & Fry (1992). Thus, any gravitationally induced departure from the Gaussian distribution may be sought only in the fourth central moment of $p(\mathbf{v})$, the velocity kurtosis, as well in higher order *even* central moments

(Grinstein *et al.* 1987; Kofman *et al.* 1993). These have been also analyzed in the framework of the global texture model by Scherrer (1992).

In this work, we study the non–Gaussian content of the velocity pdf in terms of the velocity kurtosis as induced by the gravitational growth of the initially Gaussian density fluctuations. The velocity kurtosis describes important features such as sharpness of the velocity pdf and the extent of its rare–event tail. In particular, we explore the dependence of the kurtosis of the peculiar velocity along a direction $\widehat{\alpha}$, namely the parameter $S_{4,v} \equiv [\langle v_\alpha^4 \rangle - 3\,\langle v_\alpha^2 \rangle^2]/[\langle v_\alpha^2 \rangle^2\,\langle \delta^2 \rangle]$, on an initial (scale–free) power spectrum $P(k) \propto k^n$, after smoothing with a Gaussian filter. To do this, we take advantage of the exact perturbative technique (Fry 1984; Goroff *et al.* 1986) and the Zel'dovich approximation (see Grinstein & Wise 1987).

The layout of this Letter is the following. In Section G.2 the exact perturbative theory and the (Eulerian version of the) Zel'dovich approximation are reviewed. In Section G.3 we discuss the gravitationally induced velocity kurtosis parameter $S_{4,v}$ of an initially Gaussian peculiar velocity field and explore its dependence on the primordial spectral index n. The main conclusions are drawn in Section G.4.

G.2 Non–Linear Time Evolution

We assume that present–day structures formed by gravitational instability from Gaussian fluctuations δ in a pressureless fluid with matter density $\rho = \rho_b[1+\delta]$, where ρ_b is the background mean density. The density fluctuation field δ may be written as a Fourier integral, $\delta(\mathrm{x},t) = (2\pi)^{-3} \int d\mathrm{k}\, \tilde{\delta}(\mathrm{k},t)\, \mathrm{e}^{i\mathrm{k}\cdot\mathrm{x}}$, where x and k are the *comoving* Eulerian coordinate and wavevector, t is the cosmic time. The power spectrum $P(k)$ fully determines the statistics of the primordial Gaussian density field, whose variance is $\sigma^2 = (1/2\pi^2) \int_0^\infty dk\, k^2\, P(k)$. We filter the field δ by means of a Gaussian window function $W_R(x) = (2\pi R^2)^{-3/2} \exp(-x^2/2R^2)$. The mass variance on scale R, σ_R^2, is related to $P(k)$ by $\sigma_R^2 = (1/2\pi^2) \int_0^\infty dk\, k^2\, P(k)\, [\widetilde{W}_R(k)]^2$,

where $\widetilde{W}_R(k)$ is the Fourier transform of $W_R(x)$.

G.2.1 Equations of Motion: Perturbative Theory

The time evolution equations for the matter density fluctuation $\delta(\mathbf{x},t)$ and the peculiar velocity field $\mathbf{v}(\mathbf{x},t)$ are the Euler equation and the continuity equation, i.e.

$$\partial_o \mathbf{v} + \frac{1}{a}(\mathbf{v}\cdot\nabla)\,\mathbf{v} + \frac{\dot{a}}{a}\mathbf{v} = \mathbf{g}\,, \tag{G.1}$$

$$\partial_o \delta + \frac{1}{a}\nabla\cdot(1+\delta)\,\mathbf{v} = 0\,. \tag{G.2}$$

Here $\partial_o \equiv \partial/\partial t$ and spatial derivatives are with respect to $\mathbf{x}$. The density contrast δ is related to the Newtonian gravitational potential $\triangle(\mathbf{x},t) \equiv -(4\pi)^{-1}\int d\mathbf{x}'\,\delta(\mathbf{x}',t)/|\mathbf{x}'-\mathbf{x}|$ via the Poisson equation, $\nabla^2\triangle = \delta$. In terms of $\triangle$ the peculiar gravitational acceleration is defined as $\mathbf{g} = -4\pi G\,\rho_b\,a\,\nabla\triangle$. We analyze these equations assuming an Einstein–de Sitter universe with no cosmological constant. In such a model, the scale factor a is proportional to $t^{2/3}$ during the matter dominated epoch, and the adiabatic expansion implies that $6\pi G\,\rho_b\,t^2 = 1$. The first–order density solution has the well–known self–similar form, namely, considering only the growing mode, $\delta^{(1)}(\mathbf{x},t) = D(t)\,\delta_1(\mathbf{x})$, where $D(t) \propto a(t)$ is the time growth factor of the mass fluctuations. In the linear regime, the peculiar velocity field is proportional to the gravitational acceleration

$$\mathbf{v} = -\,a\,\frac{\dot{D}}{D}\,\nabla\triangle\,. \tag{G.3}$$

This relation shows that the linear velocity field is irrotational; its growing mode corresponds to the growing mode of the density field and, for a flat universe, the classical law $\mathbf{v} = \mathbf{g}\,t \sim t^{1/3}$ is recovered. According to Eq.(G.3), the particles of the gravitating fluid move locally along the direction of the gravitational field.

It may be useful to give explicitly the Fourier transform of the Eq.(G.3), i.e., for the component along a fixed direction $\widehat{\alpha}$,

$$\tilde{v}_\alpha(\mathbf{k},t) = i\,a\,\frac{\dot{D}}{D}\,\frac{k^\alpha}{k^2}\,\tilde{\delta}(\mathbf{k},t)\,. \tag{G.4}$$

Higher order approximations of the density solution may be recovered if one expands the mass density fluctuation field $\delta(\mathbf{x},t)$ about the background solution $\delta = 0$, namely $\delta = \sum_n \delta^{(n)}$ with $\delta^{(n)} = O(\delta_1^n)$, then solving the differential equation for any $\delta^{(n)}$ (Peebles 1980; Fry 1984). The perturbative expansion for δ reads (e.g. Goroff *et al.* 1986): $\delta(\mathbf{x},t) = \sum_{n=1}^{\infty} [D(t)]^n \, \delta_n(\mathbf{x})$. The first term of the expansion corresponds to the linear approximation. We see that the scale factor $D(t)$ acts as a coupling constant, since $\delta^{(n)} \propto D^n$.

In a similar fashion, expanding $\mathbf{v}$ about the solution $\mathbf{v} = \mathbf{0}$, one obtains

$$\mathbf{v}(\mathbf{x},t) = \frac{2}{3}\frac{a}{t} \sum_{n=1}^{\infty} [D(t)]^n \, \mathbf{v}_n(\mathbf{x}) \, , \tag{G.5}$$

where $\mathbf{v}_n = O(\mathbf{v}_1^n)$ and $-\nabla \cdot \mathbf{v}_1 = \delta_1$. By the Kelvin circulation theorem, we assume that at any order $\nabla \wedge \mathbf{v}_n = \mathbf{0}$.

Here we review the exact perturbative technique to solve approximately the equations of motion (G.1) and (G.2) explicitly up to third order in the peculiar velocity field. In particular, we use the third–order solution to compute the fourth–order moment (namely the kurtosis $S_{4,v}$). We adopt the same notation of Fry (1984) and Catelan & Moscardini (1993).

(i) Second–Order Velocity Solution

The second–order peculiar velocity $\mathbf{v}^{(2)}$ is a solution of the equations

$$\partial_o \left(a \, \mathbf{v}^{(2)} \right) + \left(\mathbf{v}^{(1)} \cdot \nabla \right) \mathbf{v}^{(1)} = a \, \mathbf{g}^{(2)} \, , \tag{G.6}$$

$$\partial_o \, \delta^{(2)} + a^{-1} \, \nabla \cdot \left(\mathbf{v}^{(2)} + \delta^{(1)} \, \mathbf{v}^{(1)} \right) = 0 \, , \tag{G.7}$$

where the second–order peculiar acceleration is $\mathbf{g}^{(2)} = -4\pi G \, \rho_b \, a \, \nabla \triangle^{(2)}$ and $\nabla^2 \triangle^{(2)} \equiv \delta^{(2)}$. The second–order density contribution $\delta^{(2)}$ has been derived by Peebles (1980). Since $\delta^{(2)} \propto D^2$, it results that $\mathbf{g}^{(2)} \propto \rho_b \, a \, D^2$ and the second–order velocity solution reads

$$\mathbf{v}^{(2)} = -a \frac{\dot{D}}{D} \left[2 \, \nabla \triangle^{(2)} - \delta^{(1)} \, \nabla \triangle^{(1)} \right] + \mathbf{F}_2 \, , \tag{G.8}$$

where $\mathbf{F}_2$ is a vector such that $\nabla \wedge \mathbf{v}^{(2)} = \mathbf{0}$ (a thorough discussion of the higher–order rotational parts of the velocity $\mathbf{v}$ is given by Catelan *et al.* 1993). The Fourier transform

$\tilde{v}_\alpha^{(2)}$ may be directly obtained from the solution (8),

$$\tilde{v}_\alpha^{(2)}(\mathbf{k},t) = i\,a\,\frac{\dot{D}}{D}\,\frac{k^\alpha}{k^2}\int \frac{d\mathbf{k}'}{(2\pi)^3}\; K^{(2)}(\mathbf{k}',\mathbf{k}-\mathbf{k}')\;\tilde{\delta}^{(1)}(\mathbf{k}',t)\,\tilde{\delta}^{(1)}(\mathbf{k}-\mathbf{k}',t)\;, \qquad \text{(G.9)}$$

where we have defined the kernel

$$K^{(2)}(\mathbf{k}_1,\mathbf{k}_2) \equiv \frac{3}{7} + \frac{\mathbf{k}_1\cdot\mathbf{k}_2}{k_2^2} + \frac{4}{7}\left(\frac{\mathbf{k}_1\cdot\mathbf{k}_2}{k_1\,k_2}\right)^2 . \qquad \text{(G.10)}$$

It is straightforward to show that $\langle \mathbf{v}^{(2)} \rangle = \mathbf{0}$. In an Einstein–de Sitter universe $\mathbf{v}^{(2)} \sim t$, and it grows slower than $\delta^{(2)} \sim t^{4/3}$. We stress the fact that $\mathbf{v}^{(2)}$ is *not* parallel to the second–order acceleration [$\propto -\nabla\triangle^{(2)}$]: this is a consequence of non–locality. Thus, the gravitational field changes direction and particles are not accelerated in a fixed direction, as it occurs in linear regime. The density–velocity relation in the quasi–linear regime and the cosmological implications of non–locality have been recently explored by Nusser *et al.* (1991) and Gramann (1993a). The solution (G.9) is also derived by Gramann (1993b), who applies a second–order Lagrangian perturbative technique.

(ii) Third–Order Velocity Solution

The third–order approximation $\mathbf{v}^{(3)}$ is a solution of the differential equations

$$\partial_\circ\left(a\,\mathbf{v}^{(3)}\right) + \left(\mathbf{v}^{(1)}\cdot\nabla\right)\mathbf{v}^{(2)} + \left(\mathbf{v}^{(2)}\cdot\nabla\right)\mathbf{v}^{(1)} = a\,\mathbf{g}^{(3)}\;, \qquad \text{(G.11)}$$

$$\partial_\circ\,\delta^{(3)} + a^{-1}\,\nabla\cdot\left(\mathbf{v}^{(3)} + \delta^{(1)}\,\mathbf{v}^{(2)} + \delta^{(2)}\,\mathbf{v}^{(1)}\right) = 0\;. \qquad \text{(G.12)}$$

Here $\mathbf{g}^{(3)} = -4\pi G\,\rho_b\,a\,\nabla\triangle^{(3)}$ and $\nabla^2\triangle^{(3)} \equiv \delta^{(3)}$. The third–order density solution has been obtained by Fry (1984). Since $\mathbf{g}^{(3)} \propto \rho_b\,a\,D^3$, and using the results of the previous subsection, the velocity $\mathbf{v}^{(3)}$ may be written as

$$\mathbf{v}^{(3)} = -\,a\,\frac{\dot{D}}{D}\left[\,3\,\nabla\triangle^{(3)} + \delta^{(1)\,2}\,\nabla\triangle^{(1)} - 2\,\delta^{(1)}\,\nabla\triangle^{(2)} - \delta^{(2)}\,\nabla\delta^{(1)}\right] + \mathbf{F}_3\;. \qquad \text{(G.13)}$$

Again the additive term $\mathbf{F}_3$ is such that $\nabla\wedge\mathbf{v}^{(3)} = \mathbf{0}$. The Fourier transform of the previous expression is

$$\tilde{\mathbf{v}}^{(3)}(\mathbf{k},t) =$$

$$= i\,a\,\frac{\dot{D}}{D}\,\frac{\mathbf{k}}{k^2}\int \frac{d\mathbf{k}_1\,d\mathbf{k}_2\,d\mathbf{k}_3}{(2\pi)^6}\,\delta_D\Big(\sum_{h=1}^{3}\mathbf{k}_h-\mathbf{k}\Big)\;K^{(3)}(\mathbf{k}_1,\mathbf{k}_2,\mathbf{k}_3)\;\tilde{\delta}^{(1)}(\mathbf{k}_1,t)\,\tilde{\delta}^{(1)}(\mathbf{k}_2,t)\,\tilde{\delta}^{(1)}(\mathbf{k}_3,t)\,, \tag{G.14}$$

where the third–order kernel is

$$K^{(3)}(\mathbf{k}_1,\mathbf{k}_2,\mathbf{k}_3)=3\,J^{(3)}(\mathbf{k}_1,\mathbf{k}_2,\mathbf{k}_3)-\frac{\mathbf{k}\cdot\mathbf{k}_1}{k_1^2}\,J^{(2)}(\mathbf{k}_2,\mathbf{k}_3)-\frac{\mathbf{k}\cdot(\mathbf{k}_1+\mathbf{k}_2)}{(\mathbf{k}_1+\mathbf{k}_2)^2}\,K^{(2)}(\mathbf{k}_1,\mathbf{k}_2)\,, \tag{G.15}$$

and the functions $J^{(2)}$ and $J^{(3)}$, corresponding to the second– and third–order density solutions (see e.g. Fry 1984; Catelan & Moscardini 1993), read respectively

$$J^{(2)}(\mathbf{k}_1,\mathbf{k}_2)\equiv\frac{5}{7}+\frac{\mathbf{k}_1\cdot\mathbf{k}_2}{k_2^2}+\frac{2}{7}\left(\frac{\mathbf{k}_1\cdot\mathbf{k}_2}{k_1\,k_2}\right)^2\,, \tag{G.16}$$

$$J^{(3)}(\mathbf{k}_1,\mathbf{k}_2,\mathbf{k}_3)\equiv J^{(2)}(\mathbf{k}_2,\mathbf{k}_3)\left[\frac{1}{3}+\frac{1}{3}\,\frac{\mathbf{k}_1\cdot(\mathbf{k}_2+\mathbf{k}_3)}{(\mathbf{k}_2+\mathbf{k}_3)^2}+\frac{4}{9}\,\frac{\mathbf{k}\cdot\mathbf{k}_1}{k_1^2}\,\frac{\mathbf{k}\cdot(\mathbf{k}_2+\mathbf{k}_3)}{(\mathbf{k}_2+\mathbf{k}_3)^2}\right]+$$
$$-\frac{2}{9}\,\frac{\mathbf{k}\cdot\mathbf{k}_1}{k_1^2}\,\frac{\mathbf{k}\cdot(\mathbf{k}_2+\mathbf{k}_3)}{(\mathbf{k}_2+\mathbf{k}_3)^2}\,\frac{(\mathbf{k}_2+\mathbf{k}_3)\cdot\mathbf{k}_3}{k_3^2}+\frac{1}{9}\,\frac{\mathbf{k}\cdot\mathbf{k}_2}{k_2^2}\,\frac{\mathbf{k}\cdot\mathbf{k}_3}{k_3^2}\,. \tag{G.17}$$

It is not difficult to show that $\langle\mathbf{v}^{(3)}\rangle=\mathbf{0}$. In an Einstein–de Sitter universe, $\mathbf{v}^{(3)}\sim t^{5/3}$.

(iii) General Solution

As Goroff *et al.* (1986) have shown, the (Fourier transformed) n–th order velocity solution may be represented in integral form as

$$\tilde{\mathbf{v}}_n(\mathbf{k})=i\,\frac{\mathbf{k}}{k^2}\left\{\prod_{h=1}^{n}\int\frac{d\mathbf{k}_h}{(2\pi)^3}\,\tilde{\delta}_1(\mathbf{k}_h)\right\}\Big[(2\pi)^3\delta_D(\sum_{j=1}^{n}\mathbf{k}_j-\mathbf{k})\Big]\;K^{(n)}(\mathbf{k}_1,\ldots,\mathbf{k}_n)\,. \tag{G.18}$$

The presence of the Dirac delta function comes from momentum conservation in Fourier space. The kernels $K^{(n)}$ are homogeneous (with degree 0) functions of the wavevectors $\mathbf{k}_1,\ldots,\mathbf{k}_n$, describing the effects of non–linear collapse (tidal and shear forces). In general $K^{(n)}$ are very complicated for $n>3$. [A discussion of the properties of the kernels $K^{(n)}$ is given in Wise (1988). Explicit recursion relations with their Feynman diagrammatic representation are given by Goroff *et al.* (1986) and Wise (1988).]

G.2.2 Zel'dovich Approximation

In the *Zel'dovich approximation* (Zel'dovich 1970) the motion of particles from the initial comoving (Lagrangian) positions $\mathbf{q}$ is approximated by straight paths. The Eulerian position

at time t is then given by the uniform motion

$$\mathbf{x}(\mathbf{q},t) = \mathbf{q} + D(t)\,\mathbf{S}(\mathbf{q})\,, \tag{G.19}$$

where $D(t)$ is the growth factor of linear density perturbations and $\mathbf{S}(\mathbf{q})$ is the displacement vector related to the primordial velocity field. Grinstein & Wise (1987) give an Eulerian representation of the Zel'dovich approximation by a diagrammatic perturbative approach similar to that of the previous section. They showed that the n–th order perturbative corrections $\delta_n(\mathbf{x})$, when the density fluctuation field δ is evolved according to the Zel'dovich approximation, are such that

$$\delta(\mathbf{x},t) = \sum_{n=1}^{\infty} \frac{(-1)^n}{n!}\,[D(t)]^n \sum_{[h_n]=1}^{3} \frac{\partial}{\partial x_{h_1}} \cdots \frac{\partial}{\partial x_{h_n}} \left[S_{h_1} \cdots S_{h_n} \right] . \tag{G.20}$$

Here $\sum_{[h_n]} \equiv \sum_{h_1} \cdots \sum_{h_n}$. Note that the first term recovers the linear approximation, in that $\mathbf{S} = \mathbf{v}_1$, where $\delta_1(\mathbf{x}) = -\nabla \cdot \mathbf{v}_1$. This expansion for δ corresponds to different symmetric kernels $K_{ZA}^{(n)}$, which can be written in the following compact form

$$K_{ZA}^{(n)}(\mathbf{k}_1, \ldots, \mathbf{k}_n) = \frac{1}{n!} \prod_{h=1}^{n} \frac{\mathbf{k} \cdot \mathbf{k}_h}{k_h^2}\,, \tag{G.21}$$

where $\mathbf{k} \equiv \sum_{h=1}^{n} \mathbf{k}_h$. Note that, unlike the perturbative case, the kernels $K_{ZA}^{(n)}$ are symmetric by construction.

G.3 Kurtosis of the Velocity Field

In this section, we compute the gravitationally induced kurtosis $S_{4,v}$ of an initial Gaussian velocity field in a flat universe. We restrict the calculation to the velocity along one chosen direction $\widehat{\alpha}$. The lowest order non–zero reduced contribution to $S_{4,v}$ is

$$\langle v_\alpha^{(1)\,2} \rangle^2 \, \langle \delta^{(1)\,2} \rangle \; S_{4,v} \equiv 6 \, \langle \, v_\alpha^{(1)\,2} \, v_\alpha^{(2)\,2} \, \rangle_c + 4 \, \langle \, v_\alpha^{(1)\,3} \, v_\alpha^{(3)} \, \rangle_c \,, \tag{G.22}$$

where the subscript c indicates the connected part of the four–point velocity correlation. It is not difficult to verify that $S_{4,v}$ does not depend on the normalization of the power spectrum.

Furthermore it is constant in time. Due to these properties, observational estimates of $S_{4,v}$ allow one to detect *intrinsic* features of the evolved large–scale velocity field. From Eqs.(G.9), (G.14) and (G.22), after tedious but straightforward algebra, one finally gets the integral expression of the kurtosis ratio,

$$S_{4,v} = \frac{24}{\sigma_v^4\,\sigma^2}\left(a\,\frac{\dot{D}}{D}\right)^4 \int \frac{d\mathbf{k}_1\,d\mathbf{k}_2\,d\mathbf{k}_3}{(2\pi)^9}\;\frac{k_1^\alpha\;k_2^\alpha\;k_3^\alpha\;(-k_1^\alpha-k_2^\alpha-k_3^\alpha)}{k_1^2\;k_2^2\;k_3^2\,|\mathbf{k}_1+\mathbf{k}_2+\mathbf{k}_3|^2}\times$$

$$P(k_1)\,P(k_2)\left[P(k_3)\,K^{(3)}(\mathbf{k}_1,\mathbf{k}_2,\mathbf{k}_3)+2\,K^{(2)}(-\mathbf{k}_2,\mathbf{k}_2+\mathbf{k}_3)\,K^{(2)}(\mathbf{k}_1,\mathbf{k}_2+\mathbf{k}_3)\,P(|\mathbf{k}_2+\mathbf{k}_3|)\right]. \tag{G.23}$$

The analogous expression in the Zel'dovich approximation is obtained by replacing the kernels $K^{(n)}$ with the corresponding $K_{ZA}^{(n)}$. These unsmoothed–case results are independent of the primordial spectral index.

The perturbative kurtosis of the smoothed velocity field $\mathbf{v}_R$ is

$$S_{4,v}(R) = \frac{24}{\sigma_{v,R}^4\,\sigma_R^2}\left(a\,\frac{\dot{D}}{D}\right)^4 \int \frac{d\mathbf{k}_1\,d\mathbf{k}_2\,d\mathbf{k}_3}{(2\pi)^9}\;\frac{k_1^\alpha\;k_2^\alpha\;k_3^\alpha\;(-k_1^\alpha-k_2^\alpha-k_3^\alpha)}{k_1^2\;k_2^2\;k_3^2\,|\mathbf{k}_1+\mathbf{k}_2+\mathbf{k}_3|^2}\times$$

$$\widetilde{W}_R(k_1)\;\widetilde{W}_R(k_2)\;\widetilde{W}_R(k_3)\;\widetilde{W}_R(|\mathbf{k}_1+\mathbf{k}_2+\mathbf{k}_3|)\times$$

$$P(k_1)\,P(k_2)\left[P(k_3)\,K^{(3)}(\mathbf{k}_1,\mathbf{k}_2,\mathbf{k}_3)+2\,K^{(2)}(-\mathbf{k}_2,\mathbf{k}_2+\mathbf{k}_3)\,K^{(2)}(\mathbf{k}_1,\mathbf{k}_2+\mathbf{k}_3)\,P(|\mathbf{k}_2+\mathbf{k}_3|)\right]; \tag{G.24}$$

again the substitution $K^{(n)} \to K_{ZA}^{(n)}$ leads to the corresponding expression in the Zel'dovich approximation. Note that $P(k)$ completely describes the process of growth of the higher order velocity moments from Gaussian initial conditions.

We calculate the previous integrals, by an Adaptive Multidimensional Monte Carlo Integration subroutine, for scale–free power spectra $P(k) \propto k^n$ with n in the range $-1 \le n \le 1$. Due to the assumed scale–invariance, $S_{4,v}$ only depends on the primordial spectral index n, and not on the scale R. In Figure G1, we plot the kurtosis ratio $S_{4,v}$ of the Gaussian–smoothed velocity field versus the spectral index n, for both the perturbative and Zel'dovich approximations. The main conclusions are drawn in the next section.

G.4 Discussion and Conclusions

We explored the mildly–nonlinear effects on the one–point pdf of an initially Gaussian velocity field in terms of the gravitationally induced fourth connected moment $S_{4,v}$. We applied both the rigorous perturbative theory and the Zel'dovich approximation. We anticipate here some preliminary results.

From the diagram in Figure G1, it clearly appears that, in the perturbative description, the gravity induces a non–Gaussian signature in the peculiar velocity field: in particular, $S_{4,v}$ is positive and roughly constant for any value of the primordial spectral index n. The highly–nonlinear mass concentrations on any scale dominate the dynamics and induce very large values of $|v_\alpha|$ in their vicinity: the kurtosis of $p(\mathbf{v})$ appear to be positive, i.e. $p(v_\alpha)$ is more strongly peaked near $v_\alpha = 0$ but it has higher tails at large value of $|v_\alpha|$ than the Gaussian distribution.

In Figure G1, we also plot $S_{4,v}$ obtained according to the Zel'dovich prescription. It may be noted that, unlike the perturbative case, the velocity kurtosis is practically constant and consistent with zero for any value of n. This is hardly surprising, since the Zel'dovich approximation fails to fully describe the gravitational effects causing particle trajectories to depart from their original directions. Moreover, we confirm the results of Kofman *et al.* (1993), who show that the Eulerian Gaussian one–point pdf $p(\mathbf{v})$ is *time–invariant* as long as the Zel'dovich approximation holds. This is essentially due to the simple time scaling of the particle Eulerian position $\mathbf{x}(\mathbf{q}, t)$ in Eq.(19).

Further evaluations of $S_{4,v}$ for physical spectra (as CDM spectrum) are in progress.

Finally we want to stress that one has to be cautious about making quantitative comparisons between our results, directly related to the underlying mass (dark plus luminous) distribution, and both observational and N–body data. In particular, Grinstein *et al.* (1987) suggest that when point–like luminous objects, like galaxies, are used to sample the peculiar flow within a region of the sky, it is the volume average of $n(\mathbf{x})\mathbf{v}(\mathbf{x})$ which is actually measured instead of the volume average of $\mathbf{v}(\mathbf{x})$, $n(\mathbf{x})$ being the number density of luminous tracers.

If the objects are biased tracers of the underlying mass distribution (Kaiser 1984), then non-linear effects on small–scales may preclude any direct comparison of the observed velocity moments with ensemble expectations. A further analysis of this problem is in progress.

Acknowledgments

PC acknowledges Robert Scherrer for his kind hospitality at the Ohio State University, Columbus, where part of this work begun. We are grateful to Sabino Matarrese and Mark Wise for many fruitful discussions. This work has been supported by Italian MURST.

References of Appendix G

Catelan, P., Lucchin, F., Matarrese, S., & Moscardini, L. 1993, in preparation

Catelan, P., & Moscardini, L. 1993, ApJ, in press

Fry, J.N. 1984, ApJ, 279, 499

Goroff, M.H., Grinstein, B., Rey, S.–J., & Wise, M.B. 1986, ApJ, 311, 6

Gorski, K., Davis, M., Strauss, M.A., White, S.D.M., & Yahil, A. 1989, ApJ, 344, 1

Gramann, M. 1993a, ApJ, 405, 449

Gramann, M. 1993b, ApJ, 405, L47

Grinstein, B., Politzer, H.D., Rey, S.–J., & Wise, M.B. 1987, ApJ, 314, 431

Grinstein, B., & Wise, M.B. 1987, ApJ, 320, 448

Groth, E.J., Juszkiewicz, R., & Ostriker, J.P. 1989, ApJ, 346, 558

Gunn, J.E. 1989, in *The Extragalactic Distance Scale*, 4, A.S.P. Conference Series, eds Pritchet, C., & van den Bergh, Brigham Young University, Provo

Juszkiewicz, R., Bouchet, F.R., & Colombi, S. 1993, ApJ, 412, L9

Kaiser, N. 1984, ApJ, 284, L9

Kofman, L., Bertschinger, E., Gelb, J.M., Nusser, A., & Dekel, A. 1993, ApJ, submitted

Nusser, A., Dekel, A., Bertschinger, E., & Blumenthal, G.R. 1991, ApJ, 379, 6

Peebles, P.J.E. 1980, *The Large Scale Structure of the Universe* (Princeton: Princeton Univ. Press)

Ruamsuwan, L., & Fry, J.N. 1992, ApJ, 396, 416

Scherrer, R.J. 1992, ApJ, 390, 330

Tormen, G., Moscardini, L., Lucchin, F., & Matarrese, S. 1993, ApJ, 411, 16

Wise, M.B. 1988, in *The Early Universe*, eds W.G. Unruh & G.W. Semenoff, Reidel Publishing Company

Zel'dovich, Ya.B. 1970, A&A, 5, 160

Figure caption

Figure G1. The kurtosis ratio $S_{4,v}$ of the velocity field for power–law spectra $P(k) \propto k^n$ and Gaussian filter versus the primordial spectral index n, for both the perturbative (squares and solid line) and Zel'dovich approximations (triangles and dotted line). Error bars refer to the associated uncertainty estimate from the Monte Carlo Integration [preliminary results].

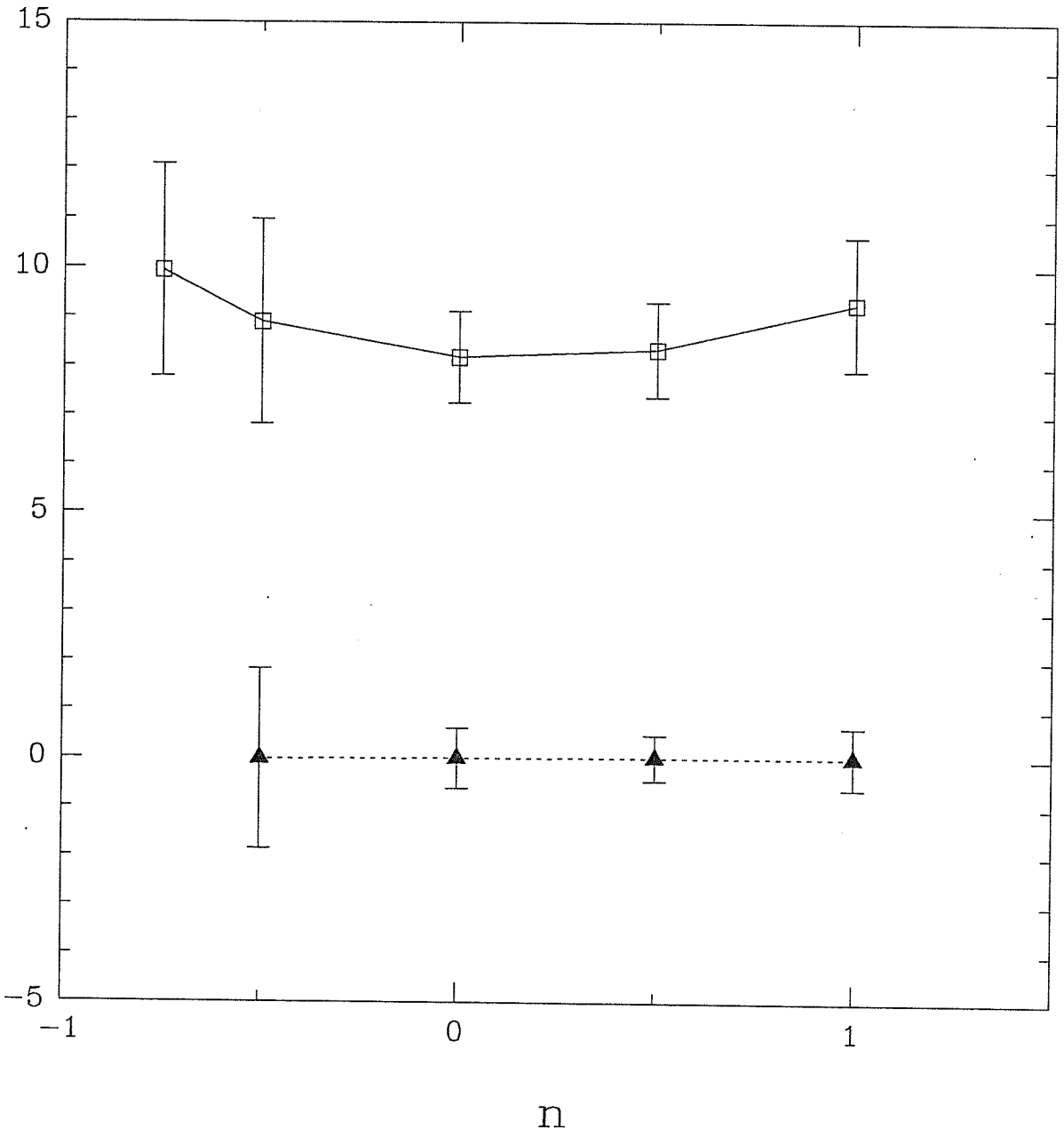

Fig. 61

APPENDIX H

Non–Gaussian Seeded Models *

Large–Scale Velocity Fields in Non–Gaussian Seeded Models[1]

Paolo CATELAN [1] **& Robert J. SCHERRER** [2]

[1] *SISSA - International School for Advanced Studies,*

Strada Costiera 11, 34014 Trieste, Italy

[2] *Department of Physics*

The Ohio State University, Columbus, OH 43210

[1]Contribution to the 9^{th} IAP Astrophysics Meeting on *COSMIC VELOCITY FIELDS*, July 11–17, 1993, Paris, France

Summary

The large–scale velocity distribution is analyzed in the framework of non–Gaussian seeded models. In particular, we calculate the skewness of the parallel component of the velocity difference distribution $p[v_{\|}(\mathbf{x}_1) - v_{\|}(\mathbf{x}_2)]$ for global textures in an $\Omega = 1$ Cold Dark Matter (CDM) model, demonstrating that the distribution of velocity differences is a good method for detecting intrinsic non–Gaussian behaviour.

H.1 Introduction

We analyze the large–scale velocity field in a special class of intrinsically non–Gaussian models, in which the initial inhomogeneities are stimulated by a primordial population of *seeds*, e.g. cosmic string loops (e.g. Vilenkin 1985) or global textures (Turok 1989), and the final linear matter fluctuations may not be described by a Gaussian distribution.

A method to detect the non–Gaussian behaviour of the matter distribution is to examine the large–scale peculiar velocity field, which is, in linear regime ie. large scales, directly related to the density field (Peebles 1980). The problem has been addressed by Scherrer (1992). Here we extend the previous analysis of Scherrer.

A common feature of the *seeded models* is that the linear density field $\delta(\mathbf{r})$ may be written as a convolution of a given density profile with a distribution of point–like seeds $n(m,\mathbf{x}) = \sum_h \delta_D(m-m_h)\,\delta_D(\mathbf{x}-\mathbf{x}_h)$,

$$\delta(\mathbf{r}) = \int dm\, d\mathbf{x}\; n(m,\mathbf{x})\, A(m,\mathbf{r}-\mathbf{x})\;. \tag{H.1}$$

where $\langle n(m,\mathbf{x})\rangle = n(m)$ is the mean number density of seeds characterized by the parameter m, and $\mathbf{x}$ are the (comoving) positions of the seeds. Usually m is the gravitational mass, but in general it is a label characterizing the accretion properties of the spatial distribution of the different seeds. For instance, Scherrer, Melott & Bertschinger (1989) characterized the cosmic strings by their formation redshift z; in the texture model, the seed label is the conformal time at which the textures unwind.

The function $A(m,\mathbf{r}-\mathbf{x})$ is the *accretion function* in $\mathbf{r}$ due to the presence of a seed with mass m in $\mathbf{x}$: it describes the accretion pattern density around each seed, and may be calculated once is given the amount and types of matter present, and the type of seeds (see Bertschinger & Watts 1988; Villumsen, Scherrer & Bertschinger 1991; van Dalen & Villumsen 1991; Scherrer & Bertschinger 1991)

The general statistical properties of the seeded density perturbation field $\delta(\mathbf{r})$ have been clarified by Scherrer & Bertschinger (1991). The density distribution results strongly non–Gaussian, and any (reduced) spatial density correlation function $\xi^{(N)}$ depends both on all seed correlation functions up to order N, say $\zeta^{(N)}$, and on the way matter is accreted by each seed.

In particular, we consider only models in which the seeds are *randomly* distributed, as in the seeded Hot Dark Matter (HDM) model of Villumsen, Scherrer & Bertschinger (1991) or in the texture model with CDM (Gooding *et al.* 1991). In such a case, the N–point matter density correlation $\xi^{(N)}$ reduces to (Scherrer & Bertschinger 1991)

$$\xi^{(N)}(\mathbf{r}_1, \ldots \mathbf{r}_N) = \int n(m)\, dm\, d\mathbf{x} \prod_{h=1}^{N} A(m, |\mathbf{r}_h - \mathbf{x}|)\,. \tag{H.2}$$

We see that, in the hypotheses, the seed mean number density $n(m)$ and the accretion function A *completely* determine the statistics of the seeded density field δ. In the previous relation, it is assumed that the accretion pattern is spherically symmetric ie. $A(m, \mathbf{r} - \mathbf{x}) = A(m, |\mathbf{r} - \mathbf{x}|)$, which is surely a good approximation in any model involving gravitational accretion around *static* seed masses, but it can be applied to the texture model, where the interaction is not purely gravitational.

The rms matter density σ and the power spectrum $P(k)$, the Fourier transform of the 2–point correlation $\xi^{(2)}$, are respectively given by

$$\sigma^2 = \int n(m)\, dm\, d\mathbf{x}\, [A(m, |\mathbf{x}|)]^2\,, \tag{H.3}$$

and

$$P(k) = \int dm\, n(m)\, \left|\tilde{A}(m, k)\right|^2\,, \tag{H.4}$$

where $\tilde{A}(m, k)$ is the Fourier–transformed accretion function. These results can be easily extended to give the statistics of the *smoothed* density field produced by seed masses. The new density field $\delta_R(\mathbf{r}) \equiv \delta * W_R$, where $(*)$ indicates the convolution operation, is identical to that which would be obtained with the same distribution of seeds and a new accretion function $A_R \equiv A * W_R$,

$$\delta_R(\mathbf{r}) = \int dm\, d\mathbf{x}\, n(m, \mathbf{x})\, A_R(m, |\mathbf{r} - \mathbf{x}|)\,; \tag{H.5}$$

the filtered accretion function is explicitely given by

$$A_R(m, |\mathbf{r}-\mathbf{x}|) \equiv \int d\mathbf{y}\, A(m, |\mathbf{y}-\mathbf{x}|)\, W_R(|\mathbf{r}-\mathbf{y}|)\,. \tag{H.6}$$

The window function W_R is more than a merely mathematical concept. For instance it can mimic the gravitational accretion around seed point–masses embedded in a CDM background (Scherrer & Bertschinger 1991).

In the next section we work out exact analytical expressions for the 1–point and 2–point velocity distributions, using the partition function for randomly distributed seed–objects. Our aim is to find possible indicators of the non–Gaussian behaviour of the matter distribution in the large–scale peculiar velocity field.

The formalism is completely general, and it can be applied to any model in which the matter is accreted around relic seeds, as primordial black holes (Carr & Rees 1984), or topological defects, such as solitons (Griest & Kolb 1989), cosmic strings (Vilenkin 1985; Holman *et al.* 1992), domain walls (Hill, Schramm & Fry 1989), and global textures (Turok 1989; Turok & Spergel 1990; Gooding, Spergel & Turok 1991; Park, Spergel & Turok 1991). It is likely that similar models will be proposed and explored in the next future. For instance, models in which relic seeds induce density perturbations in a Universe dominated by massive neutrinos have been recently explored (Scherrer, Melott & Bertschinger 1989; Villumsen, Scherrer & Bertschinger 1991; van Dalen & Villumsen 1991; Cen *et al.* 1991), even with an early inflationary phase (Gratsias *et al.* 1993), producing results in reasonable agreement with the observations and reviving massive neutrinos for large–scale structure formation.

H.2 Seeded Velocity Field

The seeded perturbation $\delta(\mathbf{r})$ in Eq.(H.1) induces in $\mathbf{r}$ the peculiar velocity $\mathbf{v}(\mathbf{r})$ according to the Poisson equation or, in other words

$$\mathbf{v}(\mathbf{r}) = \int dm\, d\mathbf{x}\; n(m, \mathbf{x})\, \mathbf{v}_{m,\mathbf{x}}(\mathbf{r})\,, \tag{H.7}$$

where $\mathbf{v}_{m,\mathbf{x}}(\mathbf{r})$ is the contribution to $\mathbf{v}$, measured at the point $\mathbf{r}$, due to a single m–seed located at the point $\mathbf{x}$ ie., in comoving coordinates,

$$\nabla \cdot \mathbf{v}_{m,\mathbf{x}}(\mathbf{r}) = -H\,\Omega^{4/7}\,a\;A(m,|\mathbf{r}-\mathbf{x}|)\;; \tag{H.8}$$

here H is the Hubble constant; Ω is the density parameter; a is the scale factor. In practice, $A(m,|\mathbf{r}-\mathbf{x}|)$ acts exactly as a density perturbation source for the single seed–velocity contribution $\mathbf{v}_{m,\mathbf{x}}(\mathbf{r})$, and the total velocity $\mathbf{v}(\mathbf{r})$ is the superposition, for the entire population of seeds, of any single seed–velocity. To determine $\mathbf{v}_{m,\mathbf{x}}(\mathbf{r})$, we integrate the previous equation on the sphere $V_{\mathbf{x}}$ centered in $\mathbf{x}$ with radius $|\mathbf{x}-\mathbf{r}|$. The Gauss' law gives

$$\mathbf{v}_{m,\mathbf{x}}(\mathbf{r}) = \beta(a)\,\bar{A}(m,|\mathbf{x}-\mathbf{r}|)\,\frac{\mathbf{x}-\mathbf{r}}{|\mathbf{x}-\mathbf{r}|}\;, \tag{H.9}$$

where $\beta(a) \equiv -H\,\Omega^{4/7}\,a$: we see that the m–seed in $\mathbf{x}$ originates a velocity component $\mathbf{v}_{m,\mathbf{x}}(\mathbf{r})$ in $\mathbf{r}$ which points *towards* the seed location ie. each seed tends to create a spherical velocity field around it. In Eq.(H.9), we have defined the quantity

$$\bar{A}(m,|\mathbf{x}-\mathbf{r}|) \;\equiv\; \frac{1}{|\mathbf{x}-\mathbf{r}|^2}\int_0^{|\mathbf{x}-\mathbf{r}|} dr'\,r'^2\,A(m,r')\;, \tag{H.10}$$

which represents the integrated density perturbation due to the seed in $\mathbf{x}$, enclosed in a sphere of radius $|\mathbf{x}-\mathbf{r}|$ centered on the seed. From Eqs.(H.7) and (H.9) we obtain the total velocity $\mathbf{v}$ in term of the accretion pattern,

$$\mathbf{v}(\mathbf{r}) = \beta(a)\int dm\,d\mathbf{x}\;n(m,\mathbf{x})\;\bar{A}(m,|\mathbf{x}-\mathbf{r}|)\,\frac{\mathbf{x}-\mathbf{r}}{|\mathbf{x}-\mathbf{r}|}. \tag{H.11}$$

We stress that these equations, in particular Eqs.(H.9) and (H.10), are more general than those in (Scherrer 1992), in that the location of the seed is arbitrarily chosen.

We analyze now the *statistical* properties of the seeded velocity field $\mathbf{v}$. If the seeds are randomly distributed, the probability distribution of the value $\mathbf{v}$ of the total velocity, $p(\mathbf{v})$, may be obtained applying the Poisson model (Peebles 1980; Fry 1985). For doing this, let us introduce the stochastic Poissonian variables ϵ_h in such a way that

$$\epsilon_h = \begin{cases} 1 & \text{if a seed} \in d\mathbf{x}_h \\ 0 & \text{otherwise}\;, \end{cases} \tag{H.12}$$

with mean

$$\langle \epsilon_h \rangle = n(m_h)\, dm_h\, dx_h \ . \tag{H.13}$$

From Eq.(H.7), we know that $\mathbf{v}(\mathbf{r})$ is the superposition of all the single seed contributions; in the discrete–case notation,

$$\mathbf{v}(\mathbf{r}) = \sum_h \mathbf{v}_{m_h,\mathbf{x}_h}(\mathbf{r}) \equiv \sum_h \mathbf{v}_{(h)} \ , \tag{H.14}$$

and, to remember the stochastic information ie. presence or absence of a seed in dx_h, we define the variables $\hat{\mathbf{v}}_{(h)}(\mathbf{r}) \equiv \mathbf{v}_{(h)}(\mathbf{r})\, \epsilon_h$ and $\hat{\mathbf{v}}(\mathbf{r}) \equiv \sum_h \hat{\mathbf{v}}_{(h)}(\mathbf{r})$.

The probability distribution function $p(\mathbf{v})$ may be calculated according to the definition (see, e.g., Ma 1985)

$$p(\mathbf{v}) = \langle\, \delta_D[\hat{\mathbf{v}}(\mathbf{r}) - \mathbf{v}(\mathbf{r})] \,\rangle = \frac{1}{(2\pi)^3} \int_{-\infty}^{+\infty} d\mathbf{S}\ \mathrm{e}^{-i\,\mathbf{S}\cdot\mathbf{v}(\mathbf{r})} \prod_h \mathcal{Z}_{\epsilon_h}[\mathbf{S}] \ , \tag{H.15}$$

where δ_D is the Dirac function and $\mathcal{Z}_{\epsilon_h}[\mathbf{S}]$ is the moment generating function for the *single* seed discrete process (Peebles 1980; Fry 1985)

$$\mathcal{Z}_{\epsilon_h}[\mathbf{S}] \equiv \langle\, \mathrm{e}^{-i\,\mathbf{S}\cdot\mathbf{v}_{(h)}(\mathbf{r})\,\epsilon_h} \,\rangle = \exp n(m_h)\, dm_h\, dx_h \left(\mathrm{e}^{i\,\mathbf{S}\cdot\mathbf{v}_{(h)}(\mathbf{r})} - 1 \right) \tag{H.16}$$

Therefore the overall moment generating function is the product of the individual $\mathcal{Z}_{\epsilon_h}$

$$\mathcal{Z}[\mathbf{S}] = \prod_h \mathcal{Z}_{\epsilon_h}[\mathbf{S}] \longrightarrow \exp \int n(m)\, dm\, dx \left(\mathrm{e}^{i\,\mathbf{S}\cdot\mathbf{v}_{m,\mathbf{x}}(\mathbf{r})} - 1 \right) \tag{H.17}$$

in the continuum limit $dm_h \to 0$ and $dx_h \to 0$. Finally, the velocity pdf $p(\mathbf{v})$ may be written as

$$p(\mathbf{v}) = \frac{1}{(2\pi)^3} \int_{-\infty}^{+\infty} d\mathbf{S}\, \mathrm{e}^{-i\,\mathbf{S}\cdot\mathbf{v}(\mathbf{r})} \exp \int n(m)\, dm\, dx \left(\mathrm{e}^{i\,\mathbf{S}\cdot\mathbf{v}_{m,\mathbf{x}}(\mathbf{r})} - 1 \right) \ . \tag{H.18}$$

Scherrer (1992) showed that the one–point velocity distribution $p(\mathbf{v})$ is a rather poor indicator of non–Gaussian behaviour for seed models with randomly distributed seeds. In particular, for the seeded HDM model, a non–Gaussian velocity field requires an extremely low seed density, while the texture model with CDM has a velocity field which is nearly indistinguishable from a Gaussian. Smoothing tends to make the velocity field more Gaussian. Here we test for the non–Gaussian character of the large–scale matter distribution, by looking at the *two*–point probability distribution of velocity field $\mathbf{v}$ and related statistics.

Taking advantage of the previous results, it is straightforward to show that the the 2–point probability distribution function is given by

$$p(\mathbf{v}_1, \mathbf{v}_2) = \langle\, \delta_D[\widehat{\mathbf{v}}(\mathbf{r}_1) - \mathbf{v}(\mathbf{r}_1)]\, \delta_D[\widehat{\mathbf{v}}(\mathbf{r}_2) - \mathbf{v}(\mathbf{r}_2)]\,\rangle$$

$$= \frac{1}{(2\pi)^6} \int_{-\infty}^{+\infty} d\mathbf{S}_1\, d\mathbf{S}_2\ \mathrm{e}^{-i\,\mathbf{S}_1\cdot\mathbf{v}(\mathbf{r}_1) - i\,\mathbf{S}_2\cdot\mathbf{v}(\mathbf{r}_2)}\ \mathcal{Z}[\mathbf{S}_1, \mathbf{S}_2]\ , \tag{H.19}$$

where

$$\mathcal{Z}[\mathbf{S}_1, \mathbf{S}_2] \equiv \exp \int n(m)\, dm\, d\mathbf{x} \left(\mathrm{e}^{i\,\mathbf{S}_1\cdot\mathbf{v}_{m,\mathbf{x}}(\mathbf{r}_1) + i\,\mathbf{S}_2\cdot\mathbf{v}_{m,\mathbf{x}}(\mathbf{r}_2)} - 1\right)\ , \tag{H.20}$$

is the 2–point moment generating function for the discrete seed process: it generates the 2–point velocity correlation tensor component defined by (Groth, Juzskievicz and Ostriker 1989) $\xi_{\alpha\beta}(r_{12}) \equiv \langle\, v_\alpha(\mathbf{r}_1)\, v_\beta(\mathbf{r}_2)\,\rangle$, $\alpha,\ \beta = 1,\ 2,\ 3$, through partial derivation. In particular, one can recover the velocity variance

$$\sigma_{\mathbf{v}}^2 = \beta(a)^2 \int dm\, d\mathbf{x}\, n(m)\, [\bar{A}(m, |\mathbf{x}|)]^2. \tag{H.21}$$

The statistical properties of the large–scale peculiar velocity field, as described by the correlation tensor, are extensively examined e.g. in Gorski *et al.* (1989) and Landy and Szalay (1992).

From Eq.(H.19), one can in particular obtain the probability distribution of the *velocity difference*

$$p(\mathbf{v}_1 - \mathbf{v}_2) = \frac{1}{(2\pi)^3} \int_{-\infty}^{+\infty} d\mathbf{S}\ \mathrm{e}^{-i\,\mathbf{S}\cdot(\mathbf{v}(\mathbf{r}_1) - \mathbf{v}(\mathbf{r}_2))}\ \mathcal{Z}[\mathbf{S}] \tag{H.22}$$

where now

$$\mathcal{Z}[\mathbf{S}] \ \equiv\ \exp \int n(m)\, dm\, d\mathbf{x} \left(\mathrm{e}^{i\,\mathbf{S}\cdot(\mathbf{v}_{m,\mathbf{x}}(\mathbf{r}_1) - \mathbf{v}_{m,\mathbf{x}}(\mathbf{r}_2))} - 1\right)\ . \tag{H.23}$$

Starting from this, we have numerically evaluated the *skewness* (ie. the third central moment) of the distribution of the component of the velocity difference along the separation $\mathbf{r}_1 - \mathbf{r}_2$, $v_{\|}(\mathbf{r}_1) - v_{\|}(\mathbf{r}_2)$, as a function of separation distance for the $\Omega = 1$ CDM global texture model. The texture accretion function may be found e.g. in Gooding, Spergel and Turok (1991). It results that the skewness of the parallel component of velocity difference (normalized to the velocity variance $\sigma_{\mathbf{v}}$) is a decreasing function of the separation distance of the observation

points; in particular, it changes from 3.75 at 1 Mpc to 0.75 at 50 Mpc, the statistic being useful up to about a 10–50 Mpc separation (for $h = 1/2$). Thus, we see that, for relatively small separations, the difference of velocities *is* a good tracer of the non–Gaussian behaviour. It is trivial to extend these techniques to the case of a smoothed density field.

Applications and extensions of this formalism and analyses of higher order moments of the velocity distribution in the seeded HDM and texture model are in progress (Catelan & Scherrer 1993).

References of Appendix H

Bertschinger, E., & Watts., P.N. 1988, *Ap. J.*, **328**, 23.

Carr, B.J., & Rees, M.J. 1984, *M.N.R.A.S.*, **206**, 801.

Catelan, P., & Scherrer, R. 1993, in preparation.

Cen, R.Y., Ostriker, J.P., Spergel, D.N., & Turok, N. 1991, *Ap. J.*, **383**, 1.

Fry, J.N. 1985, *Ap. J.*, **289**, L53.

Gooding, A.K., Spergel, D.N., & Turok, N. 1991, *Ap. J.*, **372**, L5.

Gorski, K.M., *et al.* 1989, *Ap. J.*, **344**, 1.

Gratsias, J., Scherrer, R.J., & Steigman, G. 1993, *Ap. J.*, **405**, 30.

Griest, K., & Kolb, E.W. 1989, *Phys. Rev. D*, **40**, 3231.

Groth, E.J., Juszkievicz, R., & Ostriker, J.P. 1989, *Ap. J.*, **346**, 558.

Hill, C.T., Schramm, D.N., & Fry, J.N. 1989, *Comm. Nucl. Part. Phys.*, **19**, 25.

Holman, R., Hsu, S., Vachaspati, T., & Watkins, R. 1992, *Phys. Rev. D*, **46**, 5352.

Landy, S.D., & Szalay, A.S., 1992, *Ap. J.*, **394**, 25.

Ma, S.–K. 1985, *Statistical Mechanics*, World Scientific, Singapore.

Park, C., Spergel, D.N., & Turok, N. 1991, *Ap. J.*, **372**, L53.

Peebles, P.J.E. 1980, *The Large–Scale Structure of the Universe*, Princeton University Press, Princeton.

Scherrer, R.J. 1992, *Ap. J.*, **390**, 330.

Scherrer, R.J., & Bertschinger E. 1991, *Ap. J.*, **381**, 349.

Scherrer, R.J., Melott, A.L.,& Bertschinger E. 1991, *Phys. Rev. Lett.*, **62**, 379.

Turok, N. 1989, *Phys. Rev. Lett.*, **63**, 2625.

Turok, N., & Spergel, D.N. 1990, *Phys. Rev. Lett.*, **64**, 2736.

van Dalen, A., & Villumsen, J.V. 1991, *Ap. J.*, **376**, 371.

Vilenkin, A. 1985, *Phys. Rep.*, **121**, 263.

Villumsen, J.V., Scherrer, R.J., & Bertschinger E. 1991, *Ap. J.*, **367**, 37.

References

Aaronson M., 1983, ApJ, **266**, L11.

Aaronson M. *et al.* 1986, ApJ, **302**, 536.

Aaronson M. & Olszewski E.W., 1988, in *Large Scale Structure of the Universe*, IAU Symposium 130, eds. Audouze J., Pelletan M.-C. & Szalay A. (Dordrecht: Kluwer).

Abbott L.F. & Wise M.B., 1984, ApJ, **282**, L47.

Abbott L.F. & Wise M.B., 1984, Nuc. Phys., **B244**, 541.

Adams F.C., Bond J.R., Freese K., Frieman J.A. & Olinto A.V., 1992, Phys. Rev., **D47**, 426.

Adler R.J., 1981, *The Geometry of Random Fields*, Chichester: Wiley.

Allen T.J., Grinstein B. & Wise M., Phys. Lett., **B197**, 66.

Albrecht A. & Stebbins A., 1992, Phys. Rev. Lett., **68**, 2121.

Babul A. & White S.D.M., 1991, MNRaS, **253**, 1P.

Bagla J.S. & Padmanabhan T., 1993, MNRaS, in press.

Bahcall N., 1988, in *Large Scale Structures of the Universe*, eds. Audouze J. *et al.*, IAU Symposium.

Bahcall N. & Burgett W.S., 1986, ApJ, **300**, L35.

Bahcall N. & Soneira R., 1983, ApJ, **276**, 20.

Bahcall N. & Soneira R., 1984, ApJ, **277**, 27.

Bardeen J.R., 1980, Phys. Rev., **D22**, 1882.

Bardeen J.R., 1986, in *Inner Space/Outer Space*, eds. Kolb E.W. *et al.*, University of Chicago Press.

Bardeen J.R., Bond J.R., Kaiser N. & Szalay A.S., 1986, ApJ, **304**, 15 (BBKS).

Bardeen J.R., Steinhardt P.J. & Turner M.S., 1983, Phys. Rev., **D28**, 679.

Barnes A. & Rowlingson R.R., 1989, Class. Quantum Grav., **6**, 949.

Barrow J.D. & Coles P., 1990, MNRaS, **244**, 188.

Barrow J.D. & Turner M.S., 1981, Nature, **292**, 37.

Batuski D.J., Bahcall N.A., Olowin R.P., & Burns J.O., 1989, ApJ, **341**, 599.

Baumgart D.J. & Fry J.N., 1991, ApJ, **375**, 25.

Bean A.J., Efstathiou G., Ellis R.S., Peterson B.A. & Shanks T., 1983, MNRaS, **205**, 605.

Bernardeau F., 1992a, ApJ, **390**, L61.

Bernardeau F., 1992b, ApJ, **392**, 1.

Bernardeau F. 1993, in preparation.

Bertschinger E., 1988, ApJ, **323**, L103.

Bertschinger E., 1990, in *Particle Astrophysics: The Early Universe and Cosmic Structures*, eds Alimi, J.M., *et al.* , Editions Frontières, Gif sur Yvette.

Bertschinger E., 1992, in *New Insights into the Universe*, Proc. UIMP Summer School, eds. Martinez V.J., Portilla M. & Saez D., in press.

Bertschinger E. & Dekel A., 1989, ApJ, **336**, L5.

Bertschinger E., Dekel A., Faber S.M., Dressler A. & Burstein D., 1990, ApJ, **364**, 370.

Bertschinger E. & Jain B., 1993, MIT preprint.

Bertschinger E. & Juszkiewicz R., 1988, ApJ, **334**, L59.

Blumenthal G.R., Faber S.M., Primack J.R. & Rees M.J., 1984, Nature, **311**, 517.

Bond J.R. & Efstathiou G., 1984, ApJ, **285**, L45.

Bond J.R. & Efstathiou G., 1991, Phys. Lett., B**265**, 245.

Bond J.R., Efstathiou G. & Silk J., 1980, Phys. Rev. Lett., **45**, 1980.

Bond J.R., Kolb E.W. & Silk J., 1982, ApJ, **274**, 443.

Bond J.R. & Szalay, 1984, ApJ, **274**, 443.

Bonometto S.A. & Lucchin F., 1978, Astron. Astrophys., **67**, L7.

Borgani S., Jing Y.P. & Plionis M., 1992, ApJ, **395**, 339.

Bosma A., 1981, Astron. J., **86**, 1825.

Bouchet F.R. & Hernquist L., 1992, ApJ, **400**, 25.

Bouchet F.R., Juszkiewicz R., Colombi S. & Pellat R., 1992, ApJ, **394**, L5.

Bouchet F.R., Strauss M. & Davis M., 1991,Proc. of the 2^{nd} DAEC Workshop, eds. Mamon G. & Gerbal D., Meudon Observatory, Paris.

Bouchet, F.R., Strauss, M., Davis, M., Fisher, K.B., Yahil, A., & Huchra, J.P. 1993, ApJ, in press

Bower R.G., Coles P., Frenk C.S. & White S.D.M., 1993, ApJ, **403**, 405.

Brainerd T.G., Scherrer R.J. & Villumsen J.V., 1993, ApJ, in press.

Brandenberger R., 1985, Rev. Mod. Phys., **57**, 1.

Brandenberger R., 1990, in: *Physics of the Early Universe*, eds. Peacock J., Heavens A. & Davies A. (Thirty-Sixth Scottish Universities Summer School in Physics 1989, Edinburgh).

Buchert T., 1989, Astron. Astrophys., **233**, 9.

Buchert T., 1992, MNRaS, **254**, 729.

Burgers J.M., 1974, *The Nonlinear Diffusion Equation*, Reidel, Dordrecht.

Burstein D., 1990, Rep. Prog. in Phys., **53**, 421.

Carignan C. & Freeman K.C., 1985, ApJ, **294**, 494.

Carr B.J., 1978, Comments on Astrophys., **7**, 161.

Cartwright D.E. & Longuet-Higgins M.S., 1956, Proc. Roy. Soc., **A237**, 212.

Catelan P., Coles P., Matarrese S. & Moscardini L., 1993, MNRaS, submitted.

Catelan P., Lucchin F. & Matarrese S., 1988a, Phys. Rev. Lett., **61**, 267.

Catelan P., Lucchin F. & Matarrese S., 1988b, Phys. Rev. Lett., **61**, 2627.

Catelan P., Lucchin F., Matarrese S. & Moscardini L., 1993a, in preparation (LFA).

Catelan P., Lucchin F., Matarrese S. & Moscardini L., 1993b, in preparation (HJ).

Catelan P. & Moscardini L., 1993, ApJ, in press.

Catelan P., & Moscardini L., 1993, in preparation.

Cen R.Y., Gnedin N.Y., Kofman L. & Ostriker J.P., 1992, ApJ, **399**, L11.

Cen R.Y. & Ostriker J.P., 1992, ApJ, **399**, L113.

Cen R.Y., Ostriker J.P., Spergel D.N. & Turok N., 1991, ApJ, **383**, 1.

Centrella J. & Melott A., 1983, Nature, **305**, 196.

Chambers K.C., Miley G.K. & van Breugel W., 1990, ApJ, **363** , 21.

Chandrasekhar S., 1943, Rev. Mod. Phys., **15**, 1.

Cline J.M., Politzer H.D., Rey S.-J. & Wise M.B., 1987, Commun. Math. Phys., **112**, 217.

Coles P., 1986, MNRaS, **222**, 9P.

Coles P., 1988, Phys. Rev. Lett., **61**, 2626.

Coles P., 1989, MNRaS, **238**, 319.

Coles P., 1990, MNRaS, **243**, 171.

Coles P., 1993, MNRaS, **262**, 1065.

Coles P. & Barrow J.D., 1987, MNRaS, **228**, 407.

Coles P. & Frenk C.S., 1991, MNRaS, **253**, 727.

Coles P. & Jones B., 1991, MNRaS, **248**, 1.

Coles P., Melott A.L. & Shandarin S.F., 1993, MNRAS, **260**, 765.

Coles P., Moscardini L., Lucchin F., Matarrese S. & Messina, A., 1993, MNRAS, **264**, 749.

Couchman H.M.P., 1987a, MNRaS, **225**, 777.

Couchman H.M.P., 1987b, MNRaS, **225**, 795.

Croudace K.M., Parry J., Salopek D.S. & Stewart J.M., ApJ, in press.

Daly R.A., 1987, ApJ, **322**, 20.

Daly R.A., 1988, MNRaS, **232**, 853.

Dalton G.B., Efstathiou G., Maddox S.J. & Sutherland W.J., 1992, ApJ Lett., **390**, L1.

Davis M., Efstathiou G., Frenk C.S. & White S.D.M., 1985, ApJ, **292**, 371.

Davis M., Efstathiou G., Frenk C.S. & White S.D.M., 1992, Nature, **356**, 489.

Davis M. & Peebles P.J.E., 1983, Ann. Rev. Astron. Astrophys., **21**, 109.

Davis M. & Peebles P.J.E., 1983, ApJ, **267**, 465.

Davis M., Summers F.J. & Schlegel D., 1992, Nature, **359**, 393.

De Lapparent V., Geller M. & Huchra J., 1986, ApJ, **302**, L1.

Dekel A., 1983, ApJ, **264**, 373.

Dekel A. & Aarseth S.J., 1984, ApJ, **283**, 1.

Dekel A., Bertschinger E. & Faber S.M., 1990, ApJ, **364**, 349.

Dekel A., Blumenthal G.R., Primack J.R. & Olivier S., 1989, **338**, L5.

Dekel A. & Rees M., 1986, Nature, **326**, 455.

Dekel A. & Silk J., 1986, ApJ, **303**, 39.

Dicke R.H., Peebles P.J.E., Roll P.G. & Wilkinson D.T., 1965, ApJ, **142**, 414.

Doroshkevich A.G., 1970, Astrophysica, **6**, 320.

Doroshkevich A.G. & Kotok T.V., 1990, MNRaS, **246**, 10.

Doroshkevich A.G. & Shandarin S., 1978a, Soviet Ast., **22**, 653.

Doroshkevich A.G. & Shandarin S., 1978b, MNRAS, **182**, 27.

Dmitriev N.A. & Zel'dovich Ya.B., 1964, Sov. Phys. JETP, **18**, 793.

Dressler A., 1980, ApJ, **236**, 351.

Dressler A., 1991, Nature, **350**, 391.

Dressler A. *et al.* , 1987a, ApJ, **313**, L37.

Dressler A. *et al.* , 1987b, ApJ, **313**, 42.

Eder J.A., Schombert J.M., Dekel A. & Oemler A., 1989, ApJ, **340**, 29.

Efstathiou G., 1985, MNRaS, **213**, 29.

Efstathiou G. *et al.*, 1985, ApJ Supp., **57**, 241.

Efstathiou G., 1990, in: *Physics of the Early Universe*, eds. Peacock J., Heavens A. & Davies A. (Thirty-Sixth Scottish Universities Summer School in Physics 1989, Edinburgh).

Efstathiou G., Dalton G.B., Sutherland W.J. & Maddox S.J., 1992, MNRaS, **257**, 125.

Efstathiou G., Kaiser N., Saunders W., Lawrence A., Rowan-Robinson M., Ellis R.S. & Frenk C.S., 1990, MNRaS, **247**, 10P.

Efstathiou G. & Silk J., 1983, Fund. Cos. Phys., **9**, 1.

Efstathiou G., Sutherland W.J. & Maddox S.J., 1990, Nature, **348**, 705.

Einasto J., Koasik A. & Sear E., 1974, Nature, **250**, 309.

Einstein A., 1917, S-B Preuss Akad Wiss, 142.

Ellis G.F.R., 1988, Class. Quantum Grav., **5**, 891.

Ellis J., 1991, Phys. Scripta, **T36**, 145.

Ellis J. *et al.*, 1984, Nucl. Phys., **B238**, 453.

Fabbri R., Guidi I., Melchiorri F. & Natale V., 1980, Phys. Rev. Lett., 44, 1563.

Faber S.M., 1984, in *Large-Scale Structure of the Universe, Cosmology and Fundamental Physics*, First ESO-CERN Symposium, eds. Setti G. & Van Hove (Cern: Geneva).

Faber S.M. & Burstein D., 1988, in *Large Scale Motions in the Universe*, eds. Rubin, V.C., & Coyne, G., Princeton University Press, Princeton.

Faber S.M. & Gallagher J.S., 1979, Ann. Rev. Astron. Astrophys., **17**, 135.

Faber S.M. & Lin D.N.C., 1983, ApJ, **266**, L17.

Fall S.M., 1979, Rev. Mod. Phys., **51**, 21.

Fall S.D. & Tremaine S., 1977, ApJ, **216**, 682.

Feller W., 1971, *An Introduction to Probability Theory and Its Applications*, voll. I, II, (New York: Wiley).

Feynman R.P. & Hibbs A.R., 1965, *Quantum Mechanics and Path Integrals*, Mc Graw-Hill, N.Y.

Flores R., Blumenthal G.R., Dekel A. & Primack J.R., 1986, Nature, **323**, 781.

Freese K., Price R. & Schramm D.N., 1983, ApJ, **275**, 405.

Frenk C.S., 1986, Phil. Trans. R. Soc. London, **A330**, 517.

Frenk C.S., White S.D.M. & Davis M., 1983, ApJ, **271**, 417.

Frenk C.S., White S.D.M., Davis M. & Efstathiou G., 1988, ApJ, **327**, 507.

Fry J.N., 1984, ApJ, **279**, 499.

Fry J.N., 1985a, ApJ, **289**, 10.

Fry J.N., 1985b, Phys. Lett., **158B**, 211.

Fry J.N., 1986, ApJ, **308**, L71.

Fry, J.N. & Gaztañaga, E., 1993, preprint

Fry J.N. & Peebles P.J.E., 1978, ApJ, **221**, 19.

Fry J.N. & Seldner M., 1982, ApJ, **259**, 474.

Fry J.N. & Scherrer R.J., 1993, preprint.

Gamow G., 1946, Phys. Rev., **70**, 527.

Gaztañaga, E., 1992, ApJ, **398**, L17.

Geller M., 1987, in: *Observational Cosmology*, IAU Symposium, No. 124.

Gelmini G., Schramm D.N., & Valle J.W.F., 1984, Phys. Lett., **146B**, 311.

Gerhard O.E. & Spergel D.N., 1992, ApJ, **389**, L9.

Gershtein S.S. & Zel'dovich Ya.B., 1966, JETP Lett., 4, 120.

Giavalisco M., Mancinelli B., Mancinelli P.J. & Yahil A., 1993, ApJ, **411**, 9.

Giovanelli R. & Haynes M.P., 1985, ApJ, **292**, 404.

Giovanelli R. & Haynes M.P. & Chincarini G.L., 1986, ApJ, **300**, 77.

Goldberg H., 1983, Phys. Rev. Lett., **50**, 1419.

Gooding A.K., Park C., Spergel D.N., Turok N. & Gott III J.R., 1991, ApJ, **393**, 42.

Goroff M.H., Grinstein B., Rey S.-J. & Wise M.B., 1986, ApJ, **311**, 6.

Gorski K., Davis M., Strauss M.A., White S.D.M. & Yahil, A., 1989, ApJ, **344**, 1.

Gott III J.R., Gao B. & Park C., 1991, ApJ, **383**, 90.

Gramann, M., 1993a, ApJ, **405**, 449.

Gramann, M., 1993b, ApJ, **405**, L47.

Grinstein B. *et al.*, 1987, ApJ, **314**, 431.

Grinstein B. & Wise M., 1987, ApJ, **314**, 448.

Groth E.J., Juszkiewicz R. & Ostriker J.P., 1989, ApJ, **346**, 558.

Groth E.J. & Peebles P.J.E., 1975, Astr. Ap., **41**, 143.

Groth E.J. & Peebles P.J.E., 1977, ApJ, **217**, 385.

Guiderdoni B., A&A, 1987, **172**, 27.

Gunn, J.E., 1989, in *The Extragalactic Distance Scale*, 4, A.S.P. Conference Series, eds Pritchet, C., & van den Bergh, Brigham Young University, Provo.

Gurbatov S.N. & Saichev A.I., 1981, Sov. Phys. JETP, **53**, 347.

Gurbatov S.N., Saichev A.I. & Yakushkin I.G., 1983, Sov. Phys. Usp., **26**, 857.

Gurbatov S.N., Saichev A.I. & Shandarin S.F., 1989, MNRaS, **236**, 385.

Gush H.P., Halpern M. & Wishnow E.H., 1990, Phys. Rev. Letter, **65**, 537.

Guth A.H., 1981, Phys. Rev., D**23**, 347.

Guth A.H. & Pi S-Y., 1982, Phys. Rev. Lett., **49**, 1110.

Guth A.H., 1984, Ann. N.Y. Acad. Sci., **422**, 1.

Guzzo L., Iovino A., Chincarini G., Giovanelli R. & Haynes M., 1991, ApJ, **382**, L5.

Hamilton A.J.S., 1988, ApJ, **331**, L59.

Hamilton A.J.S., Kumar P., Lu E. & Matthews A., ApJ, 1991, **374**, L1.

Harrison E.R., 1970, Phys. Rev., **D1**, 2726.

Hauser M. & Peebles P.J.E., 1973, ApJ, **185**, 757.

Haynes M.P., Giovanelli R., Starosta B. & Magni C., 1988, AJ, **95**, 607.

Hawking S.W., 1982, Phys. Lett., **B115**, 95.

Hill C.T., Schramm D.N. & Fry J.N., 1989, Comm. Nucl. Part. Phys., **19**, 25.

Hime A. & Jelley N.A., 1991, Phys. Lett., B**257**, 441.

Hoffman G.L., Salpeter E.E. & Wasserman I., ApJ, **263**, 485.

Huang K., 1963, *Statistical Mechanics*, Cambridge.

Hubble E., 1934, ApJ, **79**, 8.

Hubble E., 1936, *The realm of the Nebulae*, Yale Observatory Press, Yale.

Huchra J.P., 1992, Science, **256**, 321.

Huchra J.P., Davis M., Latham D.W. & Tonry J., 1983, ApJ Suppl., **53**, 89.

Hunter L., 1964, ApJ, **139**, 570.

Ichimaru S., 1973, *Basic Principles of Plasma Physics*, Reading, Mass., Benjamin.

Ipser J. & Sikivie P., 1983, Phys. Rev. Lett., **50**, 925.

Irvine W.M., 1965, Ann. Phys. N.Y., **32**, 322.

Jacoby G.H., Ciardullo R. & Ford H.C., 1990, ApJ, **356**, 332.

Jeans J., 1928, *Astronomy and Cosmogony*, Cambridge University Press, Cambridge.

Jensen L.G. & Szalay A.S., 1986, ApJ, **305**, L5.

Jing Y.P. & Valdarnini R., 1991, Astron. Astrophys., **250**, 1.

Jing Y.P. & Zhang J.L., 1988, A&A, **190**, L21.

Jing Y.P. & Zhang J.L., 1989, ApJ, **342**, 639.

Juszkiewicz R., 1981, MNRaS, **197**, 931.

Juszkiewicz R., Bouchet F.R. & Colombi S., 1993, ApJ, **412**, L9.

Juszkiewicz R. & Bouchet F.R., 1991, Proc. of the 2^{nd} DAEC Workshop, eds. Mamon G. & Gerbal D., Meudon Observatory, Paris.

Juszkiewicz R., Sonoda D.H. & Barrow J.D., 1984, MNRaS, **209**, 139.

Juszkiewicz R., Vittorio N. & Wise R.F.G., 1990, ApJ, **349**, 408.

Juszkiewicz R., Weinberg D.H., Amsterdamsky P., Chodorowsky M. & Bouchet F.R., 1993, preprint.

Kac M. & Logan J., 1979, in: *Fluctuation Phenomena*, eds. Montroll E.W. & Lebowitz J.L., New York: North Holland.

Kaiser N., 1983, ApJ, **273**, L17.

Kaiser N., 1984, ApJ, **284**, L9.

Kaiser N., 1986, in *Inner Space/Outer Space*, eds. Kolb E.W. *et al.*, University of Chicago Press.

Kaiser N., 1987, MNRaS, **227**, 1.

Kaiser N., 1990a, Contemporary Physics, **31**, 113.

Kaiser N., 1990b, MNRaS, **219**, 785.

Kaiser N., 1991, in: *After the First Three Minutes*, eds. Holt S. *et al.*, pag. 248.

Kaiser N. & Lahav O., 1989, MNRaS, **237**, 129.

Kendall M. & Stuart A., 1977, *The Advanced Theory of Statistics*, vol. 1, Griffin, London.

Kida S., 1979, J. Fluid Mech., **93**, 337.

Klypin A.A., Holtzmann J.R., Primack J.R. & Regos E., 1993, ApJ, **416**, 1.

Klypin A.A. & Kopilov A.I., 1983, Soviet Astr. Lett., **9**, 41.

Kodama H. & Sasaki M., 1986, Int. J. Mod. Phys., **A1**, 265.

Kolb E.W. & Turner M.S., 1990, *The Early Universe*, Addison-Wesley.

Kofman L., Bertschinger E., Gelb J.M., Nusser A. & Dekel A., 1993, ApJ, submitted.

Kofman L., Blumenthal G.R., Hodges H. & Primack J.R., 1989, in *Large–Scale Structures and Peculiar Motions in the Universe*, eds Latham, D.W., & da Costa, L.A.N. (San Francisco, Astronomical Society of the Pacific).

Kofman L.A., Gnedin N. & Bahcall N.A., 1993, ApJ, **413**, 1.

Kofman L.A. & Linde A.D., 1987, Nuc. Phys., **B282**, 555.

Kofman L., 1991, in Proc. IUPAP Conference *Primordial Nucleosynthesis and Evolution of the Early Universe*, K. Sato ed., Kluwer Academic, Dordrecht.

Kofman L., Melott A., Pogosyan D. & Shandarin S., 1992, ApJ, **393**, 437.

Kofman L.A., Pogosyan D. & Shandarin S., 1990, MNRaS, **242**, 200.

Kofman L.A. & Shandarin S.F., 1988, Nature, **334**, 132.

Lachièze–Rey, M., 1993a, ApJ, **407**, 1.

Lachièze–Rey, M., 1993b, ApJ, **408**, 403.

Lahav O., Itoh M., Inagaki S. & Suto Y., 1993, ApJ, **402**, 387.

Landau L.D. & Lifshitz E.M., 1979, *Classical Theory of Fields*, 4th ed. London, Pergamon.

Layzer D., 1963, ApJ, **138**, 174.

Layzer D., 1964, Ann. Rev. Astron. Astrophys., **2**, 341.

Lee B.W. & Weinberg S., 1977, Phys. Rev. Lett., **39**, 165.

Lemaitre G., 1933a, CR, **196**, 903; 1085.

Lemaitre G., 1933b, Ann. Soc. Sci. Bruxelles, **A53**, 51.

Lemaitre G., 1934, Proc NAS, **20**, 12.

Lifshitz E.M., 1946a, ZhETF, **16**, 587.

Lifshitz E.M., 1946b, J Phys., **10**, 116.

Lightman A. & Schecter P., 1990, ApJ.

Lilje P.D. & Efstathiou G., 1988, MNRaS, **231**, 635.

Lilly S.J., 1988, ApJ, **333**, 161.

Limber D.N., 1953, ApJ, **117**, 134.

Lin D.N.C. & Faber S.M., 1983, **266**, L21.

Ling E.N., Frenk C.S. & Barrow J.D., 1986, MNRaS, **223**, 21P.

Lucchin F., Matarrese S., Melott A.L. & Moscardini L., 1993, ApJ, in press.

Lucchin F., Matarrese S. & Mollerach S., 1992, ApJ, **401**, L49.

Lucchin F., Matarrese S. & Vittorio N., 1988, ApJ, **330**, L21.

Lucey J., 1983, MNRaS, **204**, 33.

Luo X.C. & Schramm D.N., 1993, ApJ, **408**, 33.

Lynden–Bell D. *et al.* , 1988, ApJ, **326**, 19.

Ma, S.-K., 1985, *Statistical Mechanics*, (Philadelphia: World Scientific).

Mac Gibbon J.H., 1987, Nature, **329**, 308.

Maddox S.J., Sutherland W.J., Efstathiou G. & Loveday J., 1990, MNRaS, **243**, 692.

Madsen M.S. & Ellis G.F.R., 1988, MNRaS, **234**, 67.

Madsen M.S., Mimoso J.P., Butcher J.A. & Ellis G.F.R., 1992, Phys. Rev., **D46**, 1399.

Maia M.A.G. & da Costa L.N., 1990, ApJ, **349**, 477.

Makino N., Sasaki M. & Suto Y., 1992, Phys. Rev., D**46**, 585.

Martel H. & Freudling W., 1991, ApJ, **371**, 1.

Matarrese S., Lucchin F. & Bonometto S., 1986, ApJ, **310**, L21.

Matarrese S., Lucchin F., Messina A. & Moscardini L., 1991, MNRaS, **253**, 35.

Matarrese S., Lucchin F., Moscardini L. & Saez D., 1992, MNRaS, **259**, 437.

Matarrese S., Ortolan A., & Lucchin F., 1989, Phys. Rev., **D40**, 290.

Matarrese S., Pantano O. & Saez D., 1993a, Phys. Rev., **D47**, 1311.

Matarrese S., Pantano O. & Saez D., 1993b, Phys. Rev. Lett., in press.

Mather J.C. *et al.*, 1990, ApJ, **354**, L37.

Mc Gill C., 1990, MNRaS, **242**, 428.

Mc Gill C. & Couchman H., 1989, MNRaS, **236**, 51P.

Melott A.L. & Fry J.N., 1986, ApJ, **305**, 1.

Melott A.L., Lucchin F., Matarrese S. & Moscardini L., 1993, MNRaS, in press.

Melott A.L., Pellman T.F. & Shandarin S.F., 1993, MNRaS, submitted.

Messina A., Lucchin F., Matarrese S. & Moscardini L., 1992, Astroparticle Phys., **1**, 99.

Messina A., Moscardini L., Lucchin F. & Matarrese S., 1990, MNRaS, **245**, 244.

Meszaros P., 1974, Astr. Ap., **37**, 225.

Mollerach S., Matarrese S., Ortolan A. & Lucchin F., Phys. Rev., **D44**, 1670.

Monin A.S. & Yaglom A.M., 1971, *Statistical Fluid Mechanics*, vols. 1 & 2 (Cambridge: MIT Press).

Moscardini L., Matarrese S., Lucchin F. & Messina A., 1991, MNRaS, **248**, 424.

Moutarde F., Alimi J.-M., Bouchet F.R., Pellat R. & Ramani A., 1991, ApJ, **382**, 377.

Mukhanov V.F., Feldman H.A. & Brandenberger R., 1992, Phys. Rep., **215**, Nos. 5 & 6, 203.

Negele J.W. & Orland H., 1988, *Quantum Many-Particle Systems*, (Redwood City: Addison-Wesley).

Novikov I.D., 1964a, ZhETF, **46**, 686.

Novikov I.D., 1964b, Soviet Phys. JETP, **19**, 467.

Nusser A. & Dekel A., 1990, ApJ, **362**, 14.

Nusser A., Dekel A., Bertschinger E. & Blumenthal G.R., 1991, ApJ, **379**, 6.

Oemler A., 1987, in : *Nearly Normal Galaxies*, ed. Faber S., Springer-Verlag.

Olive K., Seckel D. & Vishniac E., 1985, ApJ, **292**, 1.

Olivier S., Blumenthal G.R., Dekel A., Primack J.R. & Stanhill D., 1990, ApJ, **356**, 1.

Otto S., Politzer H.D. & Wise M.B., 1986a, Phys. Rev. Lett., **56**, 1878.

Otto S., Politzer H.D. & Wise M.B., 1986b, Phys. Rev. Lett., **56**, 2772.

Park C., 1991, ApJ, **382**, L59.

Peacock J.A., 1990, MNRaS, **243**, 517.

Peacock J.A., 1991, MNRaS, **253**, 1P.

Peacock J.A. & Heavens A.F., 1985, MNRaS, **217**, 805.

Peacock J.A. & Nicholson D., 1991, MNRaS, **253**, 307.

Peebles P.J.E., 1980, *The Large Scale Structure of the Universe*, Princeton University Press, Princeton.

Peebles P.J.E., 1982a, ApJ, **258**, 415.

Peebles P.J.E., 1982b, ApJ, **263**, L1.

Peebles P.J.E., 1983, ApJ, **274**, 1.

Peebles P.J.E., 1986, Nature, **321**, 27.

Peebles P.J.E., 1987, ApJ, **317**, 576.

Peebles P.J.E. & Yu J.T., 1970, ApJ, **162**, 815.

Penzias A.A. & Wilson R.W., 1965, ApJ, **142**, 419.

Persic M. & Salucci P., 1991, ApJ, **368**, 60.

Plionis M. & Borgani S., 1991, MNRaS.

Plionis M, Coles P. & Catelan P., 1992, MNRaS, *submitted.*

Politzer H.D. & Wise M.B., 1984, ApJ, **285**, L1.

Postman M., Huchra J.P. & Geller M.J., 1992, ApJ, **384**, 404.

Primack J. & Blumenthal G.R., 1983, in *Formation and Evolution of Galaxies and Large Scale Structures in the Universe*, eds. Audouze J. & Tran Tranh Van J., (Reidel, Dordrecht).

Primack J., 1984, Proc. of International School of Physics *Enrico Fermi*, Varenna, SLAC-PUB 3387.

Ramella M., Geller M.J. & Huchra J.P., 1990, ApJ, **353**, 51.

Ramond P., 1989, *Field Theory: A Modern Primer*, (Redwood City: Addison-Wesley).

Reed M. & Simon B., 1980, *Methods of Modern Mathematical Physics I: Functional Analysis*, (New York: Academic Press).

Rees M., 1985, MNRaS, **213**, 75P.

Reichl L.E., 1980, *A Modern Course in Statistical Physics*, University of Texas Press.

Rice S.O., 1954, in: *Selected Papers on Noise and Stochastic Processes*, ed. Wax N., (New York: Dover).

Rice S.O. & Gray P., 1965, *The Statistical Mechanics of Simple Liquids*, (New York: Wiley Interscience).

Rowan-Robinson M. *et al.*, 1990, MNRaS, **247**, 1.

Ruamsuwan L. & Fry J.N., 1992, ApJ, **396**, 416.

Salopek D.S., 1992, Phys. Rev., **D45**, 1135.

Salopek D.S. & Bond J.R., 1991, Phys. Rev., **D43**, 1005.

Salopek D.S., Bond J.R. & Bardeen J.M., 1989, Phys. Rev., **D43**, 1753.

Saunders W. *et al.*, 1991, Nature, **349**, 32.

Scaramella R. *et al.*, 1989, Nature, **338**, 562.

Scaramella R., Vettolani G. & Zamorani G., 1991, ApJ Lett., **376**, L1.

Schaeffer R. & Silk J., 1985, ApJ, **292**, 319.

Schectman S., 1985, ApJ, **57**, 77.

Scherrer R.J., 1992, ApJ, **390**, 330.

Scherrer R.J. & Bertschinger E., 1991, ApJ, **381**, 349.

Scherrer R.J., Melott A.L. & Bertschinger E., 1989, Phys. Rev. Lett., **62**, 379.

Schramm D.N. & Steigman G., 1981, ApJ, **241**, 1.

Sciama D.W., 1990a, Phys. Rev. Lett., **65**, 2839.

Sciama D.W., 1990b, ApJ, **364**, 549.

Shandarin S.F. & Zel'dovich Ya.B., 1989, Rev. Mod. Phys., **61**, 185.

Shanks T., Bean A.J., Efstathiou G., Ellis R.S., Fong R. & Peterson B.A., 1983, ApJ, **274**, 529.

Sharp N.A., Bonometto S.A. & Lucchin F., 1984, Astron. Astrophys., **130**, 79.

Silk J., 1968, ApJ., **151**, 459.

Silk J., 1985, ApJ, **297**, 1.

Silk J. & Juszkiewicz R., 1991, Nature, **353**, 386.

Sikivie P., 1983, Phys. Rev. Lett., **51**, 1415.

Simpson J.J., 1985, Phys. Rev. Lett., **54**, 1891.

Smith P.F., 1988, Contemp. Phys., **29**, 159.

Smoot G.F. *et al.*, 1991, ApJ, **371**, L1.

Smoot G.F. *et al.*, 1992, ApJ, **396**, L1.

Splinter R.J. & Melott A.L., 1992, ApJ, **394**, 7.

Starobinsky A.A., 1982, Phys. Lett., **b117**, 175.

Staveley-Smith L. & Davies R.D., 1987, MNRaS, **224**, 953.

Staveley-Smith L. & Davies R.D., 1988, MNRaS, **231**, 833.

Stecker F.W. & Shafi Q., 1983, Phys. Rev. Lett., **50**, 928.

Strauss M.A., Davis M., Yahil A. & Huchra J.P., 1991, ApJ, **361**, 49.

Strauss M.A., Yahil A., Davis M., Huchra J.P. & Fisher K., 1992, ApJ, **397**, 395.

Struble M.F. & Rood H.J., 1987, ApJ Supp., **63**, 543.

Suginohara T., Suto Y., Bouchet F.R. & Hernquist L., 1991, ApJ Supp., **75**, 631.

Sutherland W.J., 1988, MNRaS, **234**, 159.

Sutherland W.J. & Efstathiou G., 1991, MNRaS, **248**, 159.

Suto Y. & Sasaki M., 1991, Phys. Rev. Lett., **66**, 264.

Suto Y., Sato K. & Kodama H., 1985, Prog. Theor. Phys., **73**, 1151.

Szalay A., 1988, ApJ, **333**, 21.

Szekeres P., 1975., Commun. Math. Phys., **141**, 55.

Tomita K., 1967, Progr. Theor. Phys., **37**, 831.

Tomita K., 1971, Progr. Theor. Phys., **45**, 1747.

Tomita K., 1972, Progr. Theor. Phys., **47**, 416.

Tonry J.L., 1991, ApJ, **373**, L1.

Tormen G., Moscardini L., Lucchin F. & Matarrese S., 1993, ApJ, **411**, 16.

Toth G., Hollosi J. & Szalay A., 1989, ApJ, **344**, 75.

Totsuji M. & Kihara T., 1969, Publ. Astron. Soc. Japan, **21**, 221.

Tremaine S.D. & Gunn J.E., 1979, Phys. Rev. Lett. **42**, 407.

Turner M.S., 1985, Phys. Rev., **D31**, 1212.

Turner M.S., 1991, Physica Scripta, **36**, 167.

Turner M.S., Steigman G. & Krauss L.M., 1984, Phys. Rev. Lett., **52**, 2090.

Turok N., 1984, Nucl. Phys., **B242**, 520.

Turok N., 1989, Phys. Rev. Lett., **63**, 2625.

Turok N., 1991, Phys. Scripta, **T36**, 135.

Turok N. & Spergel D., 1990, Phys. Rev. Lett., **64**, 2736.

Turok N. & Spergel D., 1991, Phys. Rev. Lett., **66**, 3093.

Uson J.M., Bagri D.S. & Cornwell T.J., 1991, Phys. Rev. Lett., **67**, 3328.

Uson J.M. & Wilkinson D.T., 1984, ApJ, **277**, L1.

Valdarnini R. & Bonometto S., 1985, Astron. Astrophys., **146**, 235.

Valls–Gabaud D., Alimi J.–M. & Blanchard A., 1989, Nature, **341**, 215.

Vanmarcke E., 1983, *Random Fields: Analysis and Synthesis*, MIT Press.

Vilenkin A., 1981, Phys. Rev., **D24**, 2082.

Vilenkin A. 1985, Phys. Rep., **121**, 263.

Villumsen J.V., Scherrer R.J. & Bertschinger E., 1991, ApJ, **367**, 37.

Villumsen J.S. & Strauss M., 1987, ApJ, **322**, 37.

Vishniac E., 1983, MNRaS, **203**, 345.

Vittorio N., Juszkiewicz R. & Davis M., 1986, Nature, **323**, 132.

Vittorio N. & Silk J., 1984, ApJ, **285**, L39.

Wagoner R.V., 1973, ApJ, **179**, 343.

Walker T.P., Steigman G., Schramm D.N., Olive K.A. & Kang H-S., 1991, **376**, 51.

Warren S.J., Hewett P.C., Osmer P.S. & Irwin M.J., 1987, Nature, **330**, 453.

Weinberg S., 1972, *Gravitation and Cosmology*, (New York: Wiley)

Weinberg S., 1978, Phys. Rev. Lett., **40**, 223.

Weinberg D.H. & Cole, S., 1992, MNRaS, **259**, 652.

Weinberg D.H. & Gunn, J.E., 1990a, MNRaS, **247**, 260.

Weinberg D.H. & Gunn J.E., 1990b, ApJ, **352**, L25.

White S.D.M., 1986, in *Inner Space/Outer Space*, eds. Kolb E.W. *et al.*, University of Chicago Press.

White S.D.M. *et al.*, 1987a, Nature, **330**, 451.

White S.D.M., Frenk C.S. & Davis M., 1983, ApJ, **274**, L1.

White S.D.M., Tully R.B. & Davis M., 1988, ApJ, **333**, L45.

White S.D.M., Frenk C.S., Davis M. & Efstathiou G., 1987b, ApJ, **313**, 505.

Williams B.G., Heavens A.F., Peacock J.A. & Shandarin S.F., 1991, MNRaS, **250**, 458.

Wilczek F., 1978, Phys, Rev. Lett., **40**, 279.

Wise M.B., 1988, in *The Early Universe*, eds. W.G. Unruh & G.W. Semenoff, Reidel Pub., p.215.

Yahil A., Tamman G. & Sandage A., 1977, ApJ, **217**, 903.

Yang J., Turner M.S., Steigman G., Schramm D.N. & Olive K.A., 1984, ApJ, **281**, 493.

Zaidi M.H., 1983, Fort. Phys., **7**, 409.

Zel'dovich Ya.B., 1970, Astron. Astrophys., **5**, 160.

Zel'dovich Ya.B., 1972, MNRaS, **160**, 1P.

Zel'dovich Ya.B., 1980, MNRaS, **192**, 663.

Zwicky F., 1933, Helv. Phys. Acta, **6**, 110.

Zwicky F., 1937, ApJ, **86**, 217.